Mechanisms of human RAD51 regulation by RAD52 and BRCA2

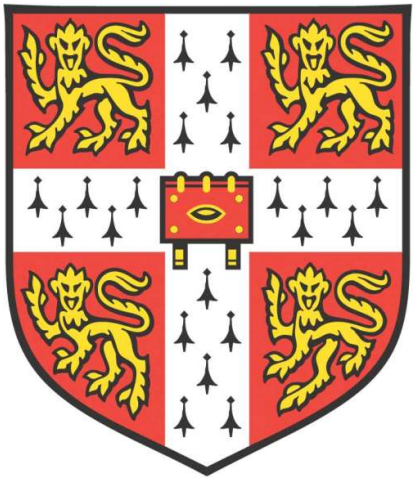

Stephanie Constantinou

Downing College

MRC Cancer Unit

University of Cambridge

This dissertation is submitted for the degree of Doctor of Philosophy

September 2019

DECLARATION

This thesis is the result of my own work and includes nothing which is the outcome of work done in collaboration except as declared in the Preface and specified in the text. It is not substantially the same as any that I have submitted, or, is being concurrently submitted for a degree or diploma or other qualification at the University of Cambridge or any other University or similar institution except as declared in the Preface and specified in the text. I further state that no substantial part of my dissertation has already been submitted, or, is being concurrently submitted for any such degree, diploma or other qualification at the University of Cambridge or any other University or similar institution except as declared in the Preface and specified in the text. It does not exceed the prescribed word limit for the relevant Degree Committee.

ABSTRACT

Stephanie Constantinou

Mechanisms of human RAD51 regulation by RAD52 and BRCA2

The RAD51 recombinase assembles as helical nucleoprotein filaments on single-stranded (ss)DNA substrates to mediate homologous DNA recombination (HR) and replication fork protection, processes vital in human cells for the maintenance of genome stability. RAD51 assembly is controlled by two key mediator proteins in eukaryotic organisms – the tumour suppressor, BRCA2, and RAD52. Recent evidence suggests that human RAD52 becomes essential for viability in cancer cells lacking BRCA2, making its activity an attractive target for potential therapeutic strategies. However, the mechanisms by which RAD52 and BRCA2 coordinate RAD51 regulation during HR or replication fork protection remain unclear. Therefore, I sought to elucidate these mechanisms and determine the functional redundancy, if any, between the two proteins. Here, I show that human RAD52 co-localises with the ssDNA-binding protein RPA and RAD51 following ionising radiation (IR)-induced damage. Moreover, RAD52 controls the chromatin recruitment and DNA assembly of RAD51, as well as subsequent HR-mediated DNA repair in BRCA2-deficient cells, but is dispensable for these processes in cells that are heterozygous or wild-type for *BRCA2*. In contrast, RAD52 protects nascent DNA at reversed replication forks from excessive degradation by the MRE11 endonuclease, not only in BRCA2-deficient cells, but also in cells that are heterozygous or wild-type for *BRCA2*. Mechanistically, RAD52 affects RAD51 recruitment to perturbed replication forks, and its depletion enhances the formation of DNA double-strand breaks (DSBs) and cell death following replication stress induced by hydroxyurea. Thus, these findings suggest divergent requirements for BRCA2 and RAD52 in the regulation of RAD51 during HR versus replication protection. RAD52 is redundant for RAD51-mediated HR in cells that are heterozygous or wild-type for *BRCA2*, but becomes an essential recombination mediator in cells lacking BRCA2. On the contrary, during replication protection, RAD52 activity is essential for RAD51 regulation regardless of BRCA2 function. Lastly, I describe preliminary results from collaborative experiments deploying electron cryo-microscopy to determine structural mechanisms underlying the regulation of RAD51 filament assembly by BRCA2. A high-resolution structure from a complex of RAD51, ssDNA and the BRC repeats of BRCA2 suggests that BRCA2 BRC repeats may promote conformational changes assisting in homologous DNA strand-pairing. Collectively, the research reported in my thesis provides new insight into the mechanisms by which BRCA2 and RAD52 regulate the RAD51 recombinase during reactions that lead to HR and replication fork protection.

ACKNOWLEDGEMENTS

I would like to express my gratitude to Prof. Ashok Venkitaraman for the stimulating and provocative discussions we've had over the last four years. These have undoubtedly shaped my scientific and intellectual thinking. I'd also like to thank Dr. Kalina Haas for the super resolution training, support and inspiring conversations we've had. Furthermore, I'd like to express my appreciation to Dr. Mahmud Shivji for providing the recombinant RAD51 protein, as well as my gratefulness to Dr. Judith Short and Dr. Shaoxia Chen (MRC Laboratory of Molecular Biology) for our successful collaboration in sample preparation, image acquisition and data processing for electron cryo-microscopy structure determination. I would also like to thank the lab members of the Venkitaraman lab for both the scientific and non-scientific support that certainly brightened my PhD journey up. I'm tremendously obligated to my family and friends for helping me see it through the toughest of times over the past years. To conclude, I'd like to thank the Medical Research Council (MRC), UK for funding me and giving me the opportunity to undertake my doctoral research at the University of Cambridge.

TABLE OF CONTENTS

LIST OF ABBREVIATIONS

53BP1	p53-binding protein 1
ALT	Alternative Lengthening of Telomeres pathway
Alt-NHEJ	Alternative Non-Homologous End-Joining
aniPOND	accelerated native iPOND
AP	apurinic/apyrimidinic
AP-1	Activator Protein 1
ATM	Ataxia-Telangiectasia Mutated kinase
ATR	Ataxia-Telangiectasia Mutated (ATM)- and Rad3-related kinase
ATRIP	ATR Interacting Protein
BARD1	BRCA1-Associated associated Ring domain 1
BER	Base Excision Repair
BIC	Breast Cancer Information Core
BIR	Break-induced Replication
BRCA1	Breast cancer type 1 susceptibility protein
BRCA2	Breast cancer type 2 susceptibility protein
CDK	Cyclin-Dependent Kinase
CDT1	CDC10-Dependent Transcript 1
CFS	Common Fragile Site
CHK1	Checkpoint protein Kinase 1

CHK2	Checkpoint protein Kinase 2
CIN	Chromosomal Instability
C-NHEJ	Classical Non-Homologous End-Joining
Cryo-EM	Cryogenic Electron Microscopy
CSA	Cockayne Syndrome protein A
CSB	Cockayne Syndrome protein B
CTF	Contrast Transfer Function
DDK	DBF4-Dependent Kinase
DDR	DNA-Damage Response
DNA2	DNA replication helicase/nuclease 2
DNA-PK	DNA-dependent Protein Kinase
DSBR	Double-Strand Break Repair
DSBs	Double Strand Breaks
ECL	Enhanced chemiluminescence
EdU	5-ethynyl-2'-deoxyuridine
ES	Embryonic Stem
EXO1	Exonuclease-1
EZH2	Enhancer of Zeste Homologue 2
FA	Fanconi Anaemia
HR	Homologous Recombination

HRP	Horseradish phosphatase
HU	Hydroxyurea
ICLs	Interstrand Crosslinks
IdU	5-Iodo-2’-deoxyuridine
IEX	Ion Exchange Chromatography
IHRSR	Iterative Helical Real Space Reconstruction
IMAC	Immobilised Metal Affinity Chromatography
iPOND	Isolation of Proteins On Nascent DNA
IPTG	Isopropyl β-D-1-thiogalactopyranoside
IR	Ionising Radiation
LOH	Loss Of Heterozygosity
MCM	Mini Chromosome Maintenance
MiDAS	Mitotic DNA Synthesis
MIN	Microsatellite Instability
MMEJ	Microhomology Mediated End-Joining
MMS	Methyl Methanesulfonate
MOI	Multiplicity Of Infection
MRE11	Meiotic Recombination 11 homologue 1
MUS81	Methyl methanesulfonate UV-sensitive clone 81
MWCO	Molecular Weight Cut-Off

NAD+	Nicotinamide Adenine Dinucleotide
NBS1	Nibrin
NER	Nucleotide Excision Repair
NES	Nuclear export signals
NHEJ	Non-homologous End Joining
NLS	Nuclear Localisation Signal
NTA	Nitrilotriacetic Acid
NTD	N-terminal domain
OIRS	Oncogene-Induced Replication Stress
ORC	Origin Recognition Complex
PAF1	RNAPII-associated factor 1
PALB2	Partner and localiser of BRCA2
PAR	Polymers of ADP-Ribose
PARP	Poly (ADP-ribose) Polymerase
PARPi	PARP inhibitors
PCAF	P300/CBP-associated factor
PCNA	Proliferating Cell Nuclear Antigen
pI	Isoelectric Point
PIKK	Phosphatidylinositol 3-kinase-related Kinase
Pre-IC	Pre-Initiation Complex

Pre-LC	Pre-Loading Complex
Pre-RC	Pre-Replication Complex
PTMs	Post-translational modifications
RAD51	Radiation repair protein 51 recombinase
RAD52	Radiation repair protein 52
RF	Replication Fork
RFC	Replication Factor C
RNAPII	RNA Polymerase II
ROS	Reactive Oxygen Species
RPA	Replication Protein A
RS	Replication Stress
RSR	Replication Stress Response
SAC	Spindle Assembly Checkpoint
SAM	S-adenosylmethionine
SDSA	Synthesis-dependent strand annealing
SSA	Single-strand annealing
ssDNA	Single-stranded DNA
TA-HRR	Transcription Associated Homologous Recombination Repair
TC-HR	Transcription-Coupled Homologous Recombination
TEM	Transmission Electron Microscopy

TLS	Translesion Synthesis
TOPBP1	DNA topoisomerase-2 binding protein 1
UR-DNA	Under-Replicated DNA
USP1	Ubiquitin carboxy-terminal hydrolase 1
UV	Ultraviolet
WRN	The Werner's syndrome helicase
XLF	XRCC4-Like factor
γH2AX	Phosphorylated histone 2A family member X

PREFACE

DNA: structure and types of damage

Deoxyribonucleic acid (DNA) is a vital macromolecule encoding the genetic information for gene transcription and protein expression, which in turn instruct biological function, cell growth and development. The functional units of DNA are nucleotides, where each nucleotide consists of a nitrogenous base (Cytosine, Adenine, Guanine or Thymine), a deoxyribose sugar and a phosphate group. Within DNA, nucleotides are linked together by phosphodiester bonds to form polynucleotide strands, whereby a DNA molecule is made of two such polynucleotide strands interwound around each other, forming a double helix with a pitch of 34 Å in the canonical B-DNA conformation (Franklin and Gosling, 1953a, 1953b; Watson and Crick, 1953). The helix consists of a sugar-phosphate backbone while the nitrogenous bases of each strand face the interior of the DNA molecule (Franklin and Gosling, 1953b; Watson and Crick, 1953). Hydrogen bonds stabilise the interaction between complementary bases on opposing strands according to the Watson-Crick base pairing, where A pairs with T and G with C (Watson and Crick, 1953). This canonical base pairing enables the formation of a helical molecule of uniform diameter, since a purine base (A or G) made of two rings always pairs with a pyrimidine (T or C), which is only made of a single ring. However, non-canonical base pairs can also occur (Chou and Chin, 2001; Das *et al.*, 2006), thus altering the helical parameters of the DNA molecule.

DNA damage can occur following exposure to either endogenous or exogenous mutagens, with estimates of tens of thousands of lesions being generated in a cell every day (Lindahl, 1993; Ciccia and Elledge, 2010). Different changes can be introduced to the chemical structure of DNA depending on the source of the damage, the majority of which are incurred by endogenous sources due to the inherent instability of the DNA molecule making it susceptible to attack. Spontaneous nucleotide hydrolysis can create abasic sites, also known as apurinic/apyrimidinic sites, at a rate of ~10,000 events per cell daily (Dexheimer, 2013).

Hydrolytic deamination of DNA bases can also occur, converting cytosine to uracil and, less commonly, adenine and guanine to hypoxanthine and xanthine, respectively (Barnes and Lindahl, 2004; Dexheimer, 2013). Base modifications, sugar oxidations and protein-DNA crosslinks can also arise due to oxidation by reactive oxygen- or nitrogen- species derived from normal cellular metabolism, with the example of 8-hydroxyguanine being the most relevant in mammalian cells (Lindahl, 1993). Endogenously reactive molecules like methyl radicals and S-adenosylmethionine (SAM) can also promote the addition of methyl moieties that lead to base alkylation of purine residues (Lindahl, 1993; Barnes and Lindahl, 2004). Finally, endogenous DNA base substitutions can arise during DNA replication at an estimated rate of 10^{-8} to 10^{-10} due to mis-incorporation of dNTPs as a result of DNA polymerase infidelity, with two thirds of all mutations found in cancers estimated to be caused by DNA replication errors (Drake *et al.*, 1998; Dexheimer, 2013; Tomasetti, Li and Vogelstein, 2017).

DNA damage can also be caused by exogenous or environmental sources. Exposure to cigarette smoke and ultraviolet (UV) light can create aromatic adducts, pyrimidine dimers and bulky lesions that cause big structural distortions to DNA (Friedberg, 2003; Ciccia and Elledge, 2010). More hazardously, ionising radiation (IR) can induce a variety of DNA lesions, including single-strand or double-strand DNA breaks (SSBs or DSBs, respectively), the latter being the most troublesome to repair. This is because, in a DSB, there is loss of genetic information from both DNA strands and hence no intact template is available for repair. As a result, DSBs can initiate chromosomal rearrangements and translocations, ultimately causing cell death or mutagenesis (Hoeijmakers, 2001).

Genome instability in cancers

Cancers are characterised by genomic instability, which is increasingly being recognised as an enabling hallmark that allows tumour cells to evolve and adapt rapidly (Negrini, Gorgoulis and Halazonetis, 2010; Hanahan and Weinberg, 2011). Genomic instability primarily arises as a result of replication and repair errors, although it can also occur due to genotoxic stresses, and can lead to mutations, deletions, gene copy number variations and gross chromosomal rearrangements such as translocations (Luo, Solimini and Elledge, 2009; Aguilera and García-

Muse, 2013). In addition, telomere erosion with successive replication cycles and defective chromosome segregation during mitosis can both contribute to genomic instability by causing chromosome translocations and gene amplifications (Luo, Solimini and Elledge, 2009; Aguilera and García-Muse, 2013). There are various types of genetic instability, namely chromosomal instability (CIN) and microsatellite instability (MIN) (Negrini, Gorgoulis and Halazonetis, 2010). CIN is characterised by frequent changes in chromosome number and structure, whereas MIN is caused by the contraction and expansion of nucleotide repeats within microsatellites. Two models have been proposed to explain the source of chromosomal instability in cancers. In hereditary cancers, genomic instability in the form of CIN is thought to arise due to mutations in DNA repair genes, such as the tumour suppressor Breast cancer type 2 susceptibility protein (*BRCA2*), which further enhance the rate of spontaneous mutations and favours tumorigenesis according to the mutator model (Negrini, Gorgoulis and Halazonetis, 2010). In fact, whole genome sequencing of BRCA2-deficient tumours revealed a mutational signature characterised by large insertions/deletions of up to 50 base-pairs with microhomology found at the breakpoints (Nik-Zainal *et al.*, 2012; Alexandrov *et al.*, 2013). However, this is not the case for sporadic cancers, where no mutations in caretaker genes have been identified (Negrini, Gorgoulis and Halazonetis, 2010). Instead, the oncogene-induced hypothesis predicts that replication stress ultimately leads to fork collapse and DSB formation (covered in detail in chapter 2), thus driving tumorigenesis in non-familial cancers (Negrini, Gorgoulis and Halazonetis, 2010). In accordance with this model, pre-neoplastic lesions lacking gross chromosomal rearrangements suffer from aberrant cell proliferation and replication stress (Gorgoulis *et al.*, 2005). This in turn elicits a DNA damage response (Gorgoulis *et al.*, 2005; Lukas *et al.*, 2005), thus suggesting that tumour progression occurs only in cells with deficiencies in DNA damage response components. Hence, replication stress-induced DNA damage is envisioned to cause genomic instability in sporadic cancers, which subsequently enables the selection of cells that can evade cell cycle checkpoints and ultimately drives tumour progression.

DNA-damage signalling and cell-cycle checkpoints

DNA lesions that occur within gene encoding regions and are left un-repaired can lead to permanent damage in the form of DNA mutations, which can trigger tumorigenesis and other diseases. Hence, multiple DNA repair pathways exist to resolve each of the different DNA lesion types, thus maintaining genomic integrity and stability for the accurate transmission of genetic material to subsequent cell generations (reviewed in Jackson and Bartek, 2010).

These repair mechanisms are collectively known as the DNA-damage response (DDR), and act to signal the presence and promote the repair of DNA lesions. Key to DDR signalling are sensor proteins that detect and transduce the damage, which include the phosphatidylinositol 3-kinase-related kinases (PIKKs) and members of the poly(ADP-ribose) polymerase (PARP) family (see chapter 1). PIKK family members are Ser/Thr kinases and include ataxia-telangiectasia mutated (ATM), ATM- and Rad3-related (ATR) and DNA-dependent protein kinase (DNA-PK). ATM and DNA-PK are recruited to and activated by DSBs, whereas ATR is involved in the recognition of RPA-coated ssDNA and stalled replication forks (RFs) through recruitment by its interacting partner, ATR-interacting protein (ATRIP) (reviewed in Tichy *et al.*, 2012). One of the best characterised targets downstream of ATM/ATR are the checkpoint kinases 2 and 1 (CHK2 and CHK1), respectively, which act to reduce cyclin-dependent kinase (CDK) activity by several mechanisms, including ones mediated by p53 activation (Summers *et al.*, 2011). The transcription factor subsequently stimulates repair pathways and responses that determine cell fate directly, or indirectly through the transactivation of target genes. For example, when DNA damage is present before S phase, p53 promotes a G1 arrest by inducing activation of p21 - a CDK inhibitor - whilst the damage is being repaired (reviewed in Gasco, Shami and Crook, 2002; Tichy *et al.*, 2012; Christmann and Kaina, 2013; Schumacher, 2016). Furthermore, CHK1 and CHK2 induce the destabilisation and sub-cellular re-localisation of the activating CDC25 phosphatases, thus maintaining the inhibitory phosphorylation of CDKs by WEE1 (Forment and O'Connor, 2018). CDK inhibition is in fact the molecular basis for the G1-S, intra-S and G2-M cell cycle checkpoints, which allow time for DNA repair before proceeding further into replication or mitosis. Eventually normal cell function can resume if the signalling

cascade activated downstream of ATM/ATR allows effective DNA repair, however, if the damage is too extensive, cell death or senescence ensue to ensure maintenance of genomic stability (Tichy *et al.*, 2012).

DNA repair pathways

Following detection of DNA damage, ATM/ATR signalling encourages DNA repair. Multiple DNA repair pathways exist for the dedicated repair of each of the different lesions that can occur. ATM/ATR stimulation leads to phosphorylation and activation of transcription factors such as p53 and activator protein 1 (AP-1), which in turn promote the upregulation of specific DNA repair proteins both at the transcriptional and post-transcriptional level (Ciccia and Elledge, 2010; Forrester *et al.*, 2012; Christmann and Kaina, 2013). Furthermore, phosphorylation of ATM/ATR substrates promotes the recruitment of DNA repair factors, bringing proteins in close proximity and facilitating their activation through post-translational modifications (reviewed in Ciccia and Elledge, 2010; Jackson and Bartek, 2010).

Repair of SSBs

The main pathways utilised in mammalian cells to repair lesions that affect a single strand are mismatch repair (MMR), base excision repair (BER) and nucleotide excision repair (NER), all of which use the intact complementary strand as a template for repair (figure 1). MMR is required to replace any bases incorrectly incorporated during DNA replication that have escaped the proofreading activity of the replication polymerases, whilst also ensuring the fidelity of homologous recombination by preventing heteroduplex formation between slightly divergent DNA sequences (Heyer, Ehmsen and Liu, 2010; Dexheimer, 2013). BER is involved in removing damaged bases that do not cause major structural rearrangements within the DNA helix, whereas NER removes bulky lesions (i.e. pyrimidine dimers) that cause helix distortions through the excision of a 30-base oligonucleotide containing the lesion (Jackson and Bartek, 2010). In these two pathways, specific proteins recognise and remove the damage, with subsequent DNA synthesis and ligation completing the repair process. Remarkably, some lesions are just bypassed during DNA replication in a process called

translesion synthesis (TLS) involving a distinct class of DNA polymerases (ζ to κ) which have increased base-pairing flexibility and are thus more error-prone (Hoeijmakers, 2001).

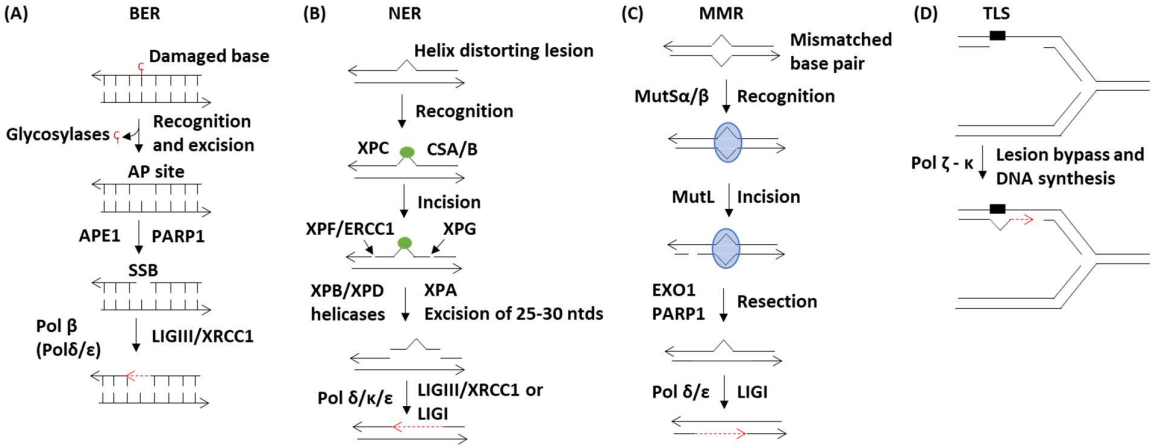

Figure 1: Pathways involved in the repair of single-strand DNA breaks. (A) BER repairs damaged bases resulting from base oxidation, alkylation or deamination. During the repair process, glycosylases remove the damaged base forming an apurinic/apyrimidinic (AP) site, followed by DNA backbone nicking by the AP endonuclease (APE1). DNA synthesis during BER is mainly executed by DNA polymerase β, although long-patch BER can also be catalysed by the more processive polymerases, Pol δ and Pol ε. Strand re-ligation eventually completes the repair process. **(B)** NER is involved in the repair of bulky DNA lesions, which are recognized by XPC or Cockayne syndrome proteins A/B (CSA/B) during global genome NER or transcription-coupled NER, respectively. An incision is made on either side of the lesion, with XPF/ERCC1 and XPG incising 5' and 3' to the damage, respectively, resulting in the excision of 25-30 nucleotides upon DNA unwinding by the XPB/XPD helicases. DNA synthesis is performed by Pol δ and Pol κ or Pol ε, followed by gap sealing by DNA ligases. **(C)** MMR repairs mismatched base pairs that arise during DNA replication. DNA mismatches are recognised by MutSα/β, with subsequent stand nicking by the MutL endonuclease enabling extensive resection in the 5'-3' direction by EXO1. The single-stranded break is then filled in and sealed by Polδ/ε and DNA ligase I. **(D)** DNA damage encountered by an ongoing replication fork causes replication fork stalling and the recruitment of error-prone DNA polymerases (Pol ζ – κ). The TLS polymerases traverse the damage by enabling nucleotide misincorporation opposite the lesion, with subsequent DNA extension by the replicative DNA polymerases completing replication. AP, apurinic/apyrimidinic; BER, Base excision repair; MMR, mismatch repair; NER, nucleotide excision repair; ntd, nucleotide; TLS, translesion synthesis. **Adapted from Heyer, Ehmsen and Liu, 2010 and Nickoloff *et al.*, 2017.**

Repair of DSBs

The repair of DSBs occurs via two pathways: non-homologous end joining (NHEJ) or homologous recombination (HR) (figure 2), with pathway choice depending on the extend of resection at the 5' end of the DSB. NHEJ functions throughout the entire cell cycle and hence is the primary pathway used for the repair of DSBs, whereas HR functions only during the late S and G2 phases of the cell cycle. The two pathways also differ in that NHEJ is error-prone due to the simple ligation of DSB ends for repair, whereas HR provides accurate repair using a homologous chromatid as a template to provide the sequencing information required for filling in the break.

NHEJ is sub-divided into classical-NHEJ (c-NHEJ) and alternative-NHEJ (alt-NHEJ), with the former being the dominant pathway. C-NHEJ involves the Ku heterodimer (Ku70 and Ku80) and p53-binding protein 1 (53BP1), which bind to the free DNA ends and prevent their resection. This recruits DNA-dependent Protein Kinases (DNA-PKs), the XRCC4/Ligase IV heterodimer, XLF (XRCC4-Like factor), and polymerase μ or λ to complete repair (Nickoloff *et al.*, 2017). The single-strand overhangs at the ends of a DSB are aligned and used to guide repair, leading to small indels once the two ends are ligated together in cases where the overhangs are not completely compatible. In cases where the ends are perfectly compatible, then c-NHEJ leads to accurate DSB repair. Alt-NHEJ, also known as microhomology-mediated end-joining (MMEJ), involves limited resection of the ends to create short 3' single-stranded overhangs of up to 25 nucleotides which contain microhomologies and are used to align the broken ends before ligation. Flaps on either side of the aligned sequences are removed and random nucleotides are incorporated by polymerase θ, with XRCC1/Ligase 3 sealing the gap and leading to large deletions and making alt-NHEJ more mutagenic (Mateos-Gomez *et al.*, 2015). Nevertheless, the mutagenicity of both c-NHEJ and alt-NHEJ is beneficial in maximising immune response diversity during antibody class switching and immunoglobulin or T-cell receptor maturation by class switch recombination and V(D)J recombination, respectively (O'Driscoll and Jeggo, 2002; Zan *et al.*, 2017). In addition, albeit error-prone, alt-NHEJ can be

used as a backup mechanism for resected DSBs and stalled replication forks in the absence of functional HR (Ceccaldi *et al.*, 2015; Mateos-Gomez *et al.*, 2015; Hromas *et al.*, 2017).

HR, on the other hand, acts on extensively resected DNA ends that have 3' single-stranded tails. With the help of mediator proteins such as BRCA2, the tails are coated by the RAD51 recombinase which ultimately assembles into nucleoprotein filaments. Such filaments are crucial for homology search and subsequent strand invasion of a sister chromatid. The invading 3' strand is then extended by a DNA polymerase, which incorporates new nucleotides using the homologous chromosome as a template and thus permits the error-free repair of the DSB. Following synthesis of the first DSB end, DNA synthesis of the second one can occur via double-strand break repair (DSBR) or synthesis-dependent strand annealing (SDSA), which will be covered in greater detail in chapter 1.

As a sub-pathway of HR, single-strand annealing (SSA) repairs DSBs between two repeat sequences and involves extensive DNA end-resection to expose long homologous single-strand regions on either side of the break. The homologous sequences in the ssDNA tails are aligned, annealed in a RAD52-dependent manner (Reddy, Golub and Radding, 1997) and subsequently ligated. Any intervening sequences are cleaved, resulting in nucleotide(s) loss and hence leading to inaccurate repair. Since SSA does not require a strand invasion step, this pathway is independent of RAD51 activity.

Lastly, when a one-ended DSB arises following fork collapse and loss of one of the two branches, break-induced replication (BIR) can be used for repair and encouraging fork restart. Moreover, since BIR acts on single-ended DSBs (seDSBs), it can be also used for telomere lengthening and maintenance. This is an HR-based pathway in which DNA end-resection creates a single-stranded tail that enables strand invasion of a homologous sequence. The strand invasion step in this pathway can occur both in the presence and absence of RAD51 (Malkova, Ivanov and Haber, 1996; Ira and Haber, 2002; Malkova *et al.*, 2005; Payen *et al.*, 2008; Sotiriou *et al.*, 2016). Subsequent to strand invasion, replication fork assembly occurs followed by extensive DNA synthesis using the homologous sequence as a template. DNA

synthesis during BIR is conservative (Donnianni and Symington, 2013), thus distinguishing it from canonical DNA replication which is semi-conservative (to be covered in chapter 2).

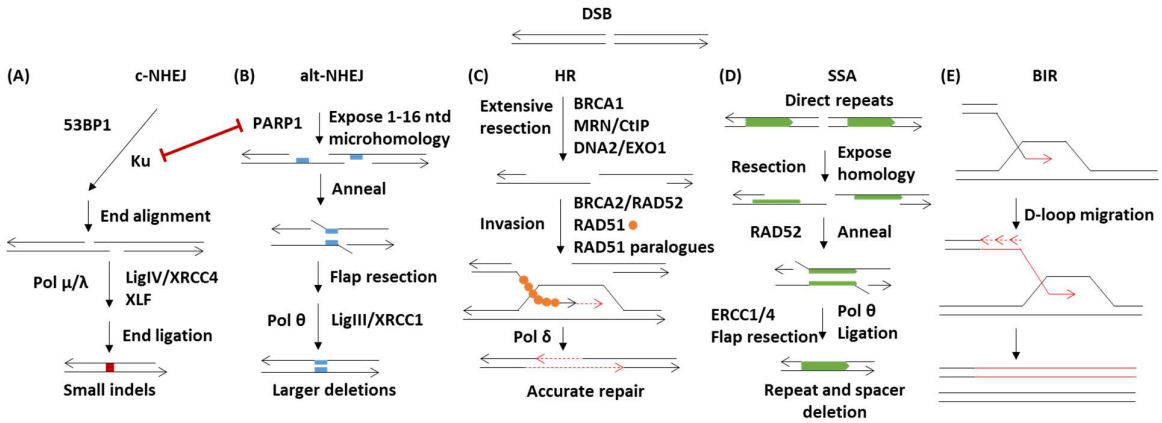

Figure 2: Pathways involved in the repair of double-strand DNA breaks. NHEJ and HR are the main repair mechanisms for double-strand breaks (DSBs), with pathway choice dictated by the extent of end resection. **(A)** Binding of 53BP1 and Ku to DSBs limits end resection and encourages c-NHEJ. **(B)** Binding of DSB ends by PARP1 promotes limited end resection that in turn stimulates the alt-NHEJ sub-pathway. Both of the aforementioned processes involve the alignment and ligation of broken ends, thus leading to error-prone repair. **(C)** During HR, limited end resection mediated by BRCA1, the MRN complex and CtIP is followed by extensive DNA resection by DNA2 and EXO1. This leads to the formation of 3' overhangs that are coated by RAD51, which in turn invades a homologous DNA strand. DNA synthesis using the invaded strand as a template enables the error-free repair of the DSB. **(D)** In the SSA sub-pathway of HR, extensive end resection is followed by the alignment and annealing of repeat sequences, leading to inaccurate repair. **(E)** BIR functions as another HR sub-pathway to repair single-end DSBs through a strand invasion step and conservative DNA synthesis across the break. Alt-NHEJ, alternative nonhomologous end joining; BIR, break-induced replication; c-NHEJ, classical nonhomologous end joining; DSB, double-strand break; HR, homologous recombination; ntd, nucleotide; SSA, single-strand annealing. **Adapted from Donnianni and Symington, 2013; Nickoloff *et al.*, 2017.**

CHAPTER 1

Regulation of RAD51-dependent homologous DNA repair by human RAD52

INTRODUCTION

Homologous Recombination (HR) in focus

HR functions in both meiotic and mitotic cells and depends on the presence of sequence homology on a homologous chromatid to accurately repair DSBs (Hendrickson, 1997). In meiosis, recombination is necessary to allow the exchange of genetic information between alleles on homologous maternal and paternal chromosomes, as well as to ensure faithful chromosome segregation at the first meiotic division of gametes (San Filippo, Sung and Klein, 2008). The recombinases involved during meiosis are DMC1 and RAD51, with the latter being the only one involved in the mitotic recombination process. In mitotic cells, HR functions to repair DSBs formed by assault from DNA mutagens, promote telomere maintenance, as well as enable the repair of one-ended DSBs caused by RF collapse.

As discussed in preface, HR in mitotic cells occurs largely during the late S and G2 phases of the cell cycle, when the homologous chromatid becomes available as a template for repair. Several mechanisms exist to prevent un-scheduled HR at other phases of the cell cycle, which primarily rely on the fact that the process requires resected DNA ends. During G1, 53BP1 (p53 binding protein protein 1) binds to broken DNA ends and DNA-PKcs block the recruitment of the EXO1 (exonuclease-1) nuclease, thus suppressing end resection and HR whilst promoting NHEJ (reviewed in Lavin *et al.*, 2015; Her and Bunting, 2018). Furthermore, factors required for DSB resection, such as CtIP and NBS1, are activated through phosphorylation by S/G2 specific CDKs (Brandsma and Gent, 2012; Falck *et al.*, 2012). Additional suppression of HR in G1 is achieved by PALB2 ubiquitylation during this phase, thus preventing the BRCA1-PALB2 interaction and subsequent complex assembly with BRCA2, which is essential for repair by HR (Orthwein *et al.*, 2015).

Biochemical steps in HR are sub-divided into three phases: pre-synapsis, synapsis and post-synapsis (figure 3). During pre-synapsis, recognition of the DSB occurs by the MRN complex, consisting of MRE11 (meiotic recombination 11 homologue 1), RAD50 and NBS1 (Nibrin). Two hetero-tetramers formed of two MRE11 protomers, RAD50 and NBS1 bind to and tether the two DNA ends together and recruit the ATM kinase to the site (Lavin *et al.*, 2015). ATM in turn phosphorylates histone H2AX at Ser139 to form γH2AX, thus marking the DNA damage site and recruiting repair proteins to the break. Amongst these are BRCA1-BARD1 (BRCA1-Associated associated Ring domain 1), which trigger DNA end resection by the MRN complex. End resection occurs bidirectionally in a two-step process to produce 3'-OH single stranded tails (Himmels and Sartori, 2016). At the first step, the MRN complex together with CtIP are accountable for removing the first 50-100 nucleotides from the 5' terminated end of the break, where MRE11 makes the initial nick via its ssDNA endonuclease activity and then utilises its 3' to 5' exonuclease activity to degrade DNA moving towards the DSB and creating a short 3' ended tail (Himmels and Sartori, 2016; Liu and Huang, 2016). In the second step, EXO1 and/or DNA2 come into play and degrade DNA in the 5' to 3' direction to form extensively resected 3' single strand overhangs (Liu and Huang, 2016).

Following DSB end resection, the single-stranded tail is immediately coated by the trimeric single-stranded binding protein, Replication Protein A (RPA), to prevent further degradation and secondary structure formation (Wold, 1997). RAD51 is then loaded on the single-stranded ends with the help of mediator proteins, which enable the eukaryotic recombinase to displace RPA. Human RAD51 has five paralogues – RAD51B, RAD51C, RAD51D, XRCC2 and XRCC3 – which also facilitate recombinase recruitment to ssDNA (Hatanaka *et al.*, 2005; Van Veelen *et al.*, 2005; Chun, Buechelmaier and Powell, 2013). Following initial binding, RAD51 oligomerises to form a helical filament on ssDNA, creating a RAD51-ssDNA nucleoprotein filament in which the ssDNA is extended to facilitate with homology search. Assembly of the RAD51 filament consists of a slow, rate-limiting step involving the nucleation of protein monomers, followed by rapid elongation of RAD51 multimers (San Filippo, Sung and Klein, 2008). Being the rate-limiting step, RAD51 nucleation requires mediator proteins, such as BRCA2 and RAD52 (Liu *et al.*, 2010; R B Jensen, Carreira and Kowalczykowski, 2010). The

mediator proteins are required to overcome the inhibition imposed by RPA, since RPA has a stronger affinity for ssDNA than RAD51 and thus prevents downstream filament assembly by the recombinase (New and Kowalczykowski, 2002). During synapsis, the RAD51 filament invades an intact homologous DNA duplex, where alignment between the ssDNA and the complementary sister chromatid displaces one of the two sister strands in a strand exchange step. RAD54, an ATP-dependent translocase, acts at this step to stabilise the formed RAD51 filament on ssDNA, potentially unwinding dsDNA to aid homology search within the sister chromatid as well (Liu *et al.*, 2011). Strand invasion forms a heteroduplex, or D-loop, between the ssDNA tail to be repaired and the complementary sister DNA strand.

Eventually, during post-synapsis, the RAD51 filament disassembles following ATP hydrolysis by the ATPase domain of the recombinase protein, with RAD54 aiding in the disassembly process and promoting branch migration by its translocase activity (Bugreev, Mazina and Mazin, 2006). RAD54 is also responsible for exposing the 3'-OH group required by DNA polymerase δ to synthesise DNA and recover the lost genetic information in the first strand (Liu *et al.*, 2011). DNA synthesis of the second DSB end can occur via two separate pathways: synthesis-dependent strand annealing (SDSA) or via the formation a double Holliday Junction (dHJ) during DSBR. In fact, pathway choice determines whether crossover or non-crossover products are formed following completion of DNA repair. In SDSA, the invading strand is displaced, thus resolving the heteroduplex and enabling its annealing to the original complementary strand within the resected DSB (reviewed in San Filippo, Sung, and Klein 2008; McVey et al. 2016). Following gap filling and ligation, this process leads to non-crossover products that lack any genetic information from the sister chromatid. Alternatively, a dHJ is formed by capturing the second DSB end on the displaced strand. Resolution of the dHJ following gap-filling and DNA ligation requires specific nucleases, such as MUS81-EME1, GEN1, SLX1-SLX4 or XPF-ERCC1, which can produce either crossover or non-crossover products depending on the site of the nick, as shown in figure 3 (reviewed in Heyer, Ehmsen and Liu, 2010; Krejci *et al.*, 2012; McVey *et al.*, 2016). In contrast, dissolution of the dHJ by the action of BLM helicase and Topoisomerase III leads to non-crossover products (reviewed in Krejci *et al.*, 2012). Meiotic recombination requires crossovers for appropriate

chromosome segregation during the first meiotic division, and hence most probably occurs via DSBR. Mitotic HR, however, is rarely associated with crossover recombinants, thus suggesting that the major repair pathway for DSB repair is via SDSA rather than DSBR.

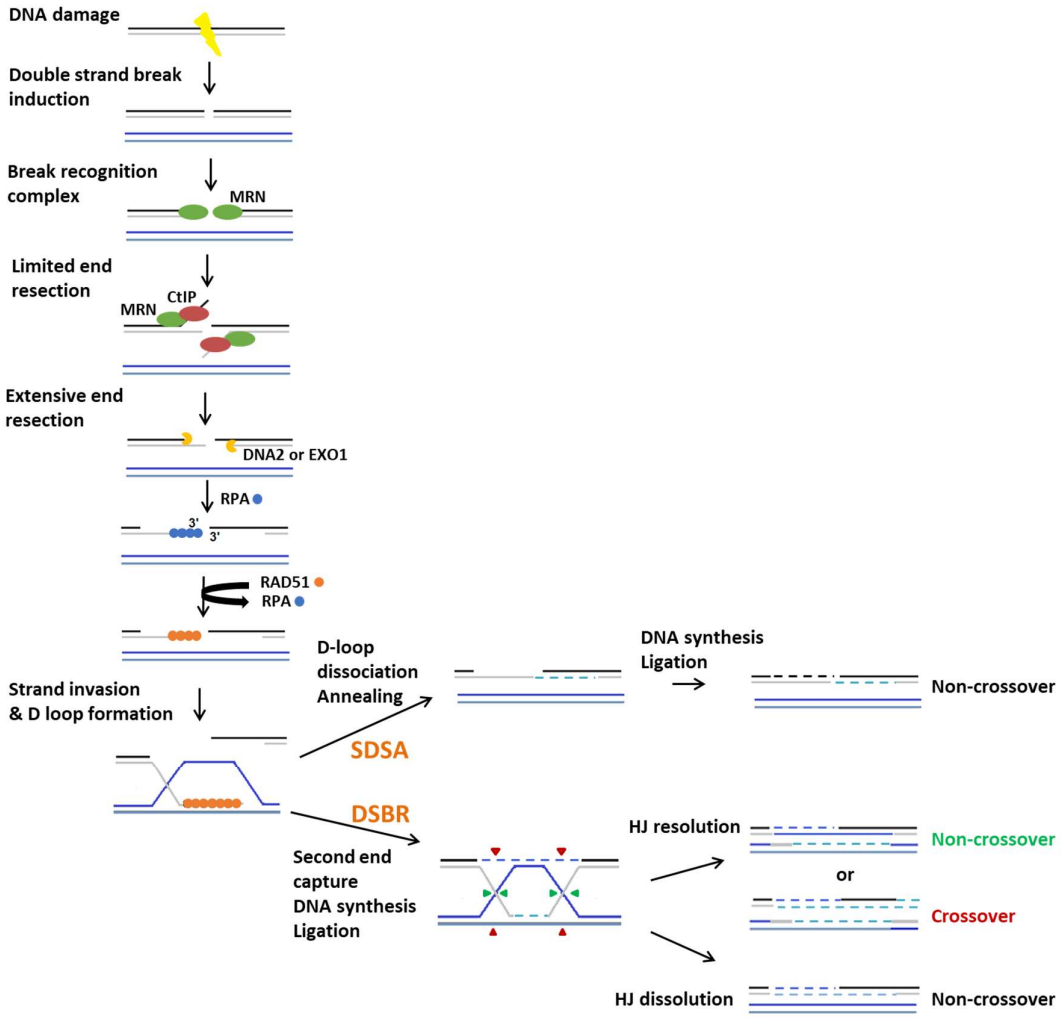

Figure 3: Homologous recombination outline. Following formation of a DSB, the break is recognised and processed by the MRN complex (green oval), which mediates limited DNA end resection with CtIP (red oval). Extensive resection then follows by DNA2 or EXO1 (shown in yellow) to form 3' overhangs. The single-stranded tails generated by DSB processing are coated by RPA (blue circle). Mediator proteins then facilitate recombinase loading on RPA-coated ssDNA, where RAD51 (orange circle) assembles into a nucleoprotein filament. The filament invades an intact homologous DNA (blue) to form a D-loop. The 3' end of the invading strand acts as the primer for DNA synthesis by the DNA polymerase, where branch migration powered by ATP hydrolysis enables heteroduplex extension. Following this step, two routes can follow: SDSA or DSBR. During SDSA, the invading strand is displaced and annealed with the second end of the double strand break, leading to non-crossover products (outcome on top panel). In DSBR, a double Holliday Junction is formed by second end capture, which is dissolved or resolved by nucleases (arrowheads) to form crossover and non-crossover products (outcome on bottom panel). **Adapted from Mladenov and Iliakis, 2011.**

RAD51: recombinase activity and regulation in human HR

The human recombinase protein, RAD51, is a 339 amino acid protein which shares over 50% homology and 30% identity with the bacterial RecA protein (figure 4) (Shinohara *et al.*, 1993; Benson, et *al.*, 1994). The conserved ATPase core is responsible for binding ATP and subsequent nucleotide hydrolysis (Yoshimura *et al.*, 1993). ATP binding is critical for the recombination and repair functions of RAD51, since it enables the recombinase to bind ss- and ds- DNA for subsequent assembly into helical filaments (Shinohara, Ogawa and Ogawa, 1992; Sung, 1995; Namsaraev and Berg, 1998; Chen, Yang and Pavletich, 2008). DNA binding has been shown to stimulate the ATPase activity of RAD51, with consequent ATP hydrolysis promoting RAD51 dissociation from DNA (Namsaraev and Berg, 1998). However, this seems to be incomplete on dsDNA and hence additional motor proteins, such as RAD54, might be required for complete RAD51 filament disassembly (Hilario *et al.*, 2009)

Upon DNA binding, RAD51 forms right-handed helical nucleoprotein filaments, where filament assembly occurs in two steps: a rate-limiting nucleation step by 2-3 RAD51 monomers followed by fast filament extension by protein multimers (Heijden *et al.*, 2007; Hilario *et al.*, 2009). Within the filament, DNA is extended to facilitate homology search within a homologous chromatid (Benson, Stasiak and West, 1994; Chen, Yang and Pavletich, 2008). As previously mentioned, RAD51 loading and subsequent filament assembly on DNA requires mediator proteins to facilitate RPA displacement and enable the subsequent strand exchange step for HR. Furthermore, since RAD51 binds with similar affinities to both ss- and ds- DNA, with dsDNA binding prior to ssDNA known to inhibit strand exchange (Benson, Stasiak and West, 1994; Baumann, Benson and West, 1996; Baumann and West, 1997), regulation RAD51 activity during HR is essential.

The major mediator protein in humans is BRCA2 (covered in greater detail in the next section), which not only delivers RAD51 to sites of DNA damage, but also regulates nucleoprotein filament assembly by the recombinase. In fact, mutations within exon 11 of BRCA2, which is responsible for RAD51 interaction, lead to chromosomal instability and predispose people to cancer (Gayther *et al.*, 1997; Patel *et al.*, 1998; Risch *et al.*, 2001). Within BRCA2, RAD51-

binding motifs called BRC repeats promote RAD51 nucleation and filament assembly on RPA-coated ssDNA as well as strand exchange when present at sub-stoichiometric concentrations *in vitro*, whilst the C-terminal domain of the protein allows the stabilisation of elongated filaments (Davies *et al.*, 2001; Shivji *et al.*, 2006, 2009; Davies and Pellegrini, 2007; Esashi *et al.*, 2007; Carreira *et al.*, 2009; Liu *et al.*, 2010; R B Jensen, Carreira and Kowalczykowski, 2010; Carreira and Kowalczykowski, 2011). When present in excess, however, BRC repeats disrupt RAD51 filaments both *in vitro* and *in vivo* (Chen *et al.*, 1999; Davies *et al.*, 2001). Work by Pellegrini et. al revealed a BRC4-RAD51 crystal structure in which the BRC repeat mimics the oligomerisation interface found between RAD51 monomers, thus proposing a molecular mechanism by which BRCA2 can promote RAD51 filament disassembly (Pellegrini *et al.*, 2002). Additionally, BRCA2 has been described to regulate the DNA-binding ability of RAD51, with the BRC repeats directing protein binding to ssDNA over dsDNA by blocking its loading and nucleation on duplex DNA (Carreira *et al.*, 2009; Shivji *et al.*, 2009; Thorslund *et al.*, 2010). These opposing activities are thought to coordinate RAD51 activity during HR, where BRCA2 can be initially envisioned of sequestering the recombinase away from intact dsDNA, but following DNA damage, the mediator enables RAD51 pre-synaptic filament assembly and stabilisation on ssDNA for strand invasion, and eventually triggers filament disassembly from the repaired dsDNA in a stepwise reaction. Finally, BRCA2 has been shown to allow the appropriate intracellular localisation of RAD51 by preventing its cytoplasmic export, thus ensuring its nuclear retention and function in response to DNA damage (Jeyasekharan *et al.*, 2013).

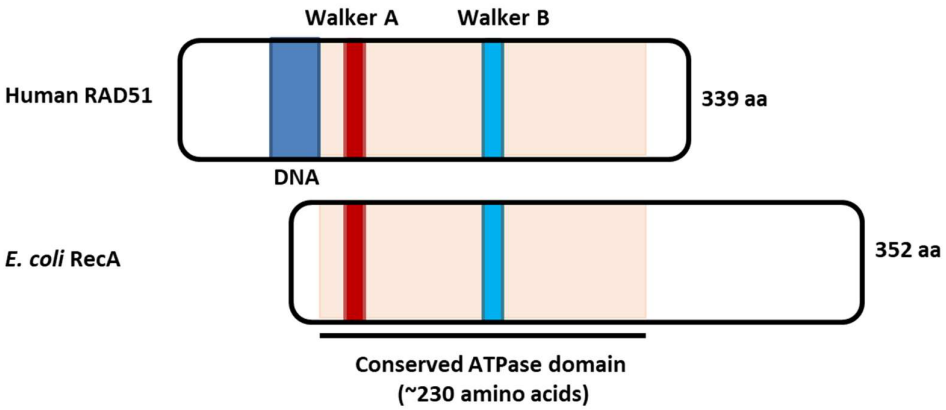

Figure 4: Protein domain structure of human RAD51 aligned to bacterial RecA. The human recombinase, RAD51, and its bacterial counterpart, RecA, share homology across the conserved ATPase domain. The ATPase core is responsible for ATP binding and hydrolysis through the Walker A (red) and Walker B (light blue) motifs, respectively. A DNA-binding motif (dark blue) is found within the N-terminal domain of human RAD51, whilst bacterial RecA utilises its C-terminal domain for DNA binding. aa, amino acids.

BRCA2: protein structure and RAD51 regulation

Breast cancer type 2 susceptibility protein (*BRCA2*) was originally identified as a breast cancer predisposition gene in 1994, with inheritance of a mutant allele predisposing people to early-onset breast, ovarian, prostate and pancreatic cancers (Wooster *et al.*, 1994, 1995). Although the protein is expressed throughout all the cell cycle phases, its expression is maximal during S and G2 – when HR is happening (Vaughn *et al.*, 1996).

BRCA2 is a protein of 3,418 amino acids made of both structural domains and disordered segments (figure 5), responsible of providing multiple protein interaction domains (Tavtigian *et al.*, 1996; Yang *et al.*, 2002). Within the protein, the extreme N-terminal 40 amino acids are responsible for binding to PALB2 (partner and localiser of BRCA2), with this interaction supporting the localisation and stabilisation of BRCA2 in nuclear foci for recombinational repair (Xia *et al.*, 2006).

Interaction with RAD51 is mediated through the central region (exon 11) of BRCA2 containing eight BRC repeats, as well as through an un-related C-terminal region (exon 27). Each of the BRC repeat motifs is 30-40 amino acids in length, and these are found to be evolutionary conserved both in sequence and spacing (Bork, P., Blomberg, N., 1996; Wong *et al.*, 1997). The BRC repeats are sub-divided in two classes, where BRC1-4 are proposed to promote nucleation by binding to monomeric RAD51, whereas BRC5-8 allow the extension of RAD51 filaments by preferentially binding to RAD51-ssDNA instead (Carreira and Kowalczykowski, 2011). Additionally, these domains promote RAD51 loading on ssDNA while inhibiting binding to dsDNA (Carreira *et al.*, 2009; Shivji *et al.*, 2009; Thorslund *et al.*, 2010). The fact that RAD51 can bind to both ssDNA and dsDNA, with filament formation on dsDNA being inhibitory for strand exchange (Baumann, Benson and West, 1996; Sigurdsson *et al.*, 2001), highlights the critical function of the BRC repeats in dictating the DNA binding selectivity of the recombinase (Carreira *et al.*, 2009; Shivji *et al.*, 2009; Ryan B. Jensen, Carreira and Kowalczykowski, 2010). Within each BRC motif, there are two modules suggested to finetune RAD51 interaction and assembly on DNA. The N-terminal motif has a consensus sequence of FxxA and mimics the oligomerisation interface of RAD51, thus binding to this and preventing RAD51 assembly (Pellegrini *et al.*, 2002; Rajendra and Venkitaraman, 2009). In contrast, the C-terminal motif, which has the sequence LFDE in BRC4, binds to the N-terminal domain of RAD51 and is suggested to have a stabilising role in RAD51 assembly (Rajendra and Venkitaraman, 2009). The second RAD51-interacting domain in BRCA2 lies within the conserved C-terminal region of the protein, with RAD51 binding at this domain being independent of BRC repeats (Mizuta *et al.*, 1997). This domain binds to oligomerised RAD51 and is hence necessary for the extension and stabilisation of RAD51 filaments on DNA (Davies and Pellegrini, 2007; Esashi *et al.*, 2007; Haas *et al.*, 2018). Contact between the two proteins at this region is regulated throughout the cell cycle, with CDK-mediated phosphorylation of BRCA2 at Ser3291 during the G2/M transition inhibiting RAD51 interaction and promoting filament disassembly for mitotic entry (Esashi *et al.*, 2005, 2007; Davies and Pellegrini, 2007; Ayoub *et al.*, 2009). Regulation of this interaction is critical for coordinating DNA repair and enabling efficient RAD51-dependent HR. This is further supported by the fact that truncating mutations within

the C-terminal domain abrogate the formation of damage induced RAD51 foci and subsequent HR, even when the BRC repeats are intact within BRCA2 (Moynahan, Pierce and Jasin, 2001; Tutt *et al.*, 2001), thus highlighting the indispensable nature of this domain in executing HR. Together, the two RAD51-interaction domains confer BRCA2 with the ability to support RAD51-mediated strand exchange at multiple steps, including facilitating RAD51 nucleation on single stranded DNA regions and stabilising RAD51-ssDNA filaments by inhibiting RAD51 ATPase activity (Carreira *et al.*, 2009; Shivji *et al.*, 2009; Liu *et al.*, 2010; R B Jensen, Carreira and Kowalczykowski, 2010). However, a precise model of how the BRC repeats and the C-terminal domain of BRCA2 coordinate RAD51 activity and filament dynamics during HR has still not been defined.

Following the BRC repeat region is a ~1,000 amino acid C-terminal DNA-binding domain, which is the most highly conserved region within BRCA2 (Yang *et al.*, 2002). This domain is implicated in DNA binding and is responsible of targeting BRCA2 to the nucleus. Nearly a third of the tumour-derived missense mutations found in BRCA2 lie within this DNA-binding region, emphasising the indispensable role it bears for BRCA2 function (Yang *et al.*, 2002). The domain can be sub-divided into five sections: a helical region, three OB-fold (oligonucleotide/oligosaccharide binding-fold) domains and a tower domain which projects from the second OB-fold domain (Yang et al. 2002). OB folds are widely conserved in prokaryotic and eukaryotic proteins implicated in ssDNA binding, and hence are thought to permit BRCA2 binding to single stranded DNA regions (Yang *et al.*, 2002; Shamoo, 2003). Furthermore, the tower domain has a three-helix bundle (3HB) located at its apex, which contains putative dsDNA-binding folds and is thought to enable dsDNA binding (Yang *et al.*, 2002; Shamoo, 2003; Siaud *et al.*, 2011). A second DNA-binding domain within the N-terminal domain of BRCA2 has also been described to interact with dsDNA (Martin *et al.*, 2016). These observations suggests a mechanism where binding to both ssDNA and dsDNA enables BRCA2 recruitment to dsDNA-ssDNA junctions, as has been previously reported for the BRCA2 orthologue, Brh2, thus supporting RAD51 nucleation at resected DSBs (Yang *et al.*, 2005). In fact, BRCA2 has been shown to preferentially bind tailed DNA substrates over ssDNA, to stimulate RAD51 strand exchange in *in vitro* assays (Liu *et al.*, 2010; Ryan B. Jensen, Carreira

and Kowalczykowski, 2010). The C-terminal domain of BRCA2 also interacts with DSS1, which enhances BRCA2-mediated loading of RAD51 on RPA-coated ssDNA (Marston *et al.*, 1999; Yang *et al.*, 2002). In the absence of DSS1 association, BRCA2 is excluded from the nucleus and, consequently, renders RAD51 cytosolic too, as a result of nuclear export signals (NES) being exposed that would otherwise be masked by the protein interactions (Jeyasekharan *et al.*, 2013). Finally, the extreme C-terminus of BRCA2 contains three nuclear-localisation signals (NLSs), and hence mutations affecting these render the protein cytoplasmic (Spain *et al.*, 1999).

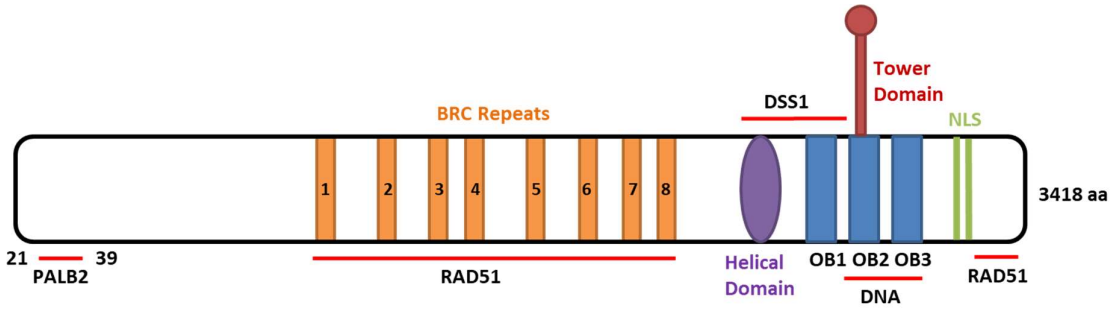

Figure 5: Domain structure of the human BRCA2 protein. The extreme N-terminus of BRCA2 (residues 21-39) interacts with PALB2, with this interaction aiding in protein localisation within nuclear foci during HR-mediated repair. The central part of BRCA2 contains eight BRC repeats (depicted in orange and labelled 1-8), which are responsible for binding and regulating RAD51 activity. A DNA-binding domain lies within the C-terminus of the protein and is made of five sections: a helical region (purple), three oligonucleotide/oligosaccharide binding-folds (OB-folds, dark blue) and a tower domain (red) projecting from OB2. The helical domain and OB1 create a DSS1-binding region, with DSS1 enabling the appropriate nuclear localisation of BRCA2. Within the extreme C-terminal region of the protein lie nuclear localisation signals (NLS, green) and another RAD51-binding domain, which enables a cell cycle-regulated interaction with the recombinase. aa, amino acids.

BRCA2 roles in cells: HR and beyond

Human BRCA2 is essential for the maintenance of chromosome integrity, through functions in homology-directed DNA repair, in stabilizing stalled DNA replication forks, or in mitotic cell division (reviewed in Venkitaraman, 2014). Due to the protein's critical role in the

aforementioned activities, BRCA2 deficiency leads to chromosomal instability and chromosomal aberrations in both structure and copy number (Patel *et al.*, 1998; Tutt *et al.*, 1999; Yu *et al.*, 2000).

BRCA2 is the principal mediator protein in human cells, as shown by its ability to displace RPA from ssDNA to stimulate RAD51-mediated strand exchange (Shivji *et al.*, 2006; R B Jensen, Carreira and Kowalczykowski, 2010). As mentioned in previous sections, following RPA displacement, BRCA2 facilitates the nucleation, elongation and stabilisation of RAD51 filaments on ssDNA while inhibiting recombinase binding to dsDNA (Yang *et al.*, 2002; Carreira *et al.*, 2009; Shivji *et al.*, 2009). All these activities ensure the precise regulation of RAD51 assembly into nucleoprotein filaments, in order to direct the orderly execution of homology-directed repair during HR. The vital function of BRCA2 in human HR is highlighted by the fact that people carrying mutations within this gene have an increased risk of developing breast, pancreatic, ovarian and prostate cancers (The Breast Cancer Linkage Consortium, 1999; Thompson and Easton, 2001).

However, BRCA2 has HR-independent roles as well. One of these is fork protection and will be covered in greater detail in chapter 2. Briefly, this activity is mediated by the C-terminal segment of BRCA2, which is essential for binding to and stabilising oligomerised assemblies of RAD51 (Esashi *et al.*, 2007; Schlacher *et al.*, 2011). Following replication fork stalling by HU treatment, BRCA2 protects nascent DNA at arrested forks from nucleolytic digestion by the MRE11 endonuclease (Lomonosov *et al.*, 2003; Schlacher *et al.*, 2011). Stabilisation of RAD51 filaments by BRCA2 is essential for this fork protection activity, which is consistent with the requirement for the BRCA2 C-terminal domain and its interaction with RAD51 during the process. This is also demonstrated by the fact that RAD51 mutants devoid of ATPase activity do not exhibit DNA degradation following fork stalling (Schlacher *et al.*, 2011). Furthermore, the BRCA2 C-terminal domain is required for the efficient restart of stalled forks, which is in agreement with previously reported functions of RAD51 in promoting fork restart following short HU exposures (Petermann *et al.*, 2010; Kim *et al.*, 2014). In BRCA2 absence, stalled forks

collapse into DSBs and can eventually contribute to the genomic instability observed in BRCA2-deficient cells.

BRCA2, along with PALB2, acts in an HR-independent pathway to maintain the G2 checkpoint following DNA damage (Menzel *et al.*, 2011). It is also responsible of controlling mitotic entry during G2 checkpoint recovery following DNA damage, through a C-terminal motif that regulates RAD51 disassembly (Ayoub *et al.*, 2009; Menzel *et al.*, 2011). BRCA2 mutations that enhance or weaken RAD51 binding to this motif cause delayed or earlier mitotic entry, respectively (Ayoub *et al.*, 2009). Furthermore, BRCA2 has been implicated in the mitotic spindle assembly checkpoint (SAC) and hence directs accurate chromosome segregation (Choi *et al.*, 2012). This activity is performed by the recruitment of the P300/CBP-associated factor (PCAF) acetyltransferase by BRCA2 for subsequent BUBR1 acetylation. This prevents BUBR1 degradation and reinforces the mitotic checkpoint by allowing appropriate microtubule attachment to the kinetochore of metaphase chromosomes (Choi *et al.*, 2012). BRCA2 also plays roles in cell division by localising to the cytokinetic midbody and ensuring the subsequent recruitment of midbody components required for daughter cell abscission (Daniels, 2004; Lee *et al.*, 2011; Mondal *et al.*, 2012). Therefore, BRCA2 inactivation leads to chromosomal abnormalities in the form of polyploidy due to defects in SAC and mitotic exit without prior cytokinetic division (Daniels *et al.*, 2004; Choi *et al.*, 2012).

In addition to regulating cell cycle progression, BRCA2 has been recently reported to prevent R-loop formation independently of its RAD51-dependent HR function (Bhatia *et al.*, 2014; Shivji *et al.*, 2018). R-loops are RNA-DNA hybrids that are formed between the mRNA transcript and the template DNA strand following the displacement of the complementary strand. BRCA2 depletion results to R-loop accumulation owing to reduced RNA Polymerase II (RNAPII)-associated factor 1 (PAF1) recruitment and consequent enhancement of RNAPII pausing close to transcription start sites, eventually impeding nascent transcript synthesis (Bhatia *et al.*, 2014; Shivji *et al.*, 2018). R-loops are a main cause of replication stress (chapter 2) and can provide another source of genomic instability following BRCA2 inactivation or deficiency.

BRCA2 mutations

Around 5% of all breast and ovarian cancers in women are due to a hereditary genetic predisposition syndrome, of which inherited mutations in BRCA2, along with BRCA1, make up around ~17% and 45% of these cancers, respectively (Miki *et al.*, 1994; Easton, Ford and Bishop, 1995; Wooster *et al.*, 1995; Phelan *et al.*, 1996).

The *BRCA2* gene was originally identified as a breast cancer susceptibility locus on chromosome 13 (Wooster *et al.*, 1994, 1995). In fact, further studies have indicated that heterozygous germline mutations in *BRCA2* are linked to enhanced lifetime risk of cancers in organs of epithelial origin, including the breast, ovaries, pancreas and prostate, thus highlighting the vital role of this protein in DNA repair (Tavtigian *et al.*, 1996; Consortium, 1999; Thompson and Easton, 2001; Mersch *et al.*, 2015). Carriers of *BRCA2* mutations have an average cumulative risk of 45-55% and 20% for developing breast and ovarian cancers, respectively, by the age of 70 (Antoniou *et al.*, 2003). The majority of breast, ovarian and pancreatic cancers are sporadic, but 10-19% of familial cases have been reported to have a genetic component in *BRCA2* (Ford *et al.*, 1998; Hahn *et al.*, 2003). Germline *BRCA2* mutations are inherited in an autosomal dominant fashion and are thought to act in dominant-negative manner (Thompson and Easton, 2001; Jeyasekharan *et al.*, 2013), although the somatic wild-type allele might eventually be lost by loss of heterozygosity (LOH) in cancers (Maxwell *et al.*, 2017). Aberrations in chromosome structure and increased sensitivity to genotoxic agents typically occur after biallelic BRCA2 disruption in murine or human cells, rather than with mutations affecting a single allele, thus suggesting that BRCA2 functions as a classical tumour suppressor (Connor *et al.*, 1997; Patel *et al.*, 1998). However, *BRCA2* LOH does not always seem to be necessary for tumorigenesis, such as in the case of $Kras^{G12D}$-driven pancreatic ductal adenocarcinomas which represent the majority of human pancreatic cancers (Skoulidis *et al.*, 2010). Nonetheless, loss of checkpoint mechanisms, such as those mediated by p53, is required for driving tumorigenesis triggered by BRCA2 deficiency (Lee *et al.*, 1999; Jonkers *et al.*, 2001; Skoulidis *et al.*, 2010). This is because biallelic inactivation of BRCA2 can cause cell cycle arrest or apoptosis due to sustained DNA damage triggering DDR and checkpoint

activation. In fact, the homozygous knockout of murine *BRCA2* is embryonic lethal (Ludwig, Chapman and Papaioannou, 1997; Sharan S. K *et al.*, 1997). Hence, for tumorigenesis to occur, BRCA2 loss must be accompanied by the inactivation of checkpoint mechanisms in order to enable the uncontrolled proliferation and invasive growth characteristic of cancers. Actually, tumours in patients with germline BRCA2 mutations often carry somatic mutations in p53 as well (Crook *et al.*, 1998; Rhei *et al.*, 1998).

According to the Breast Cancer Information Core (BIC) database, the majority of *BRCA2* mutations are missense or frameshift and cause premature protein truncation (https://research.nhgri.nih.gov/bic/). Amongst these, around a quarter of the tumour-derived missense mutations lie within the highly conserved C-terminal region of BRCA2, highlighting the essential function of the DNA-binding domain for BRCA2 activity in suppressing tumorigenesis (Yang *et al.*, 2002). The most commonly reported frameshift *BRCA2* mutation is found amongst Ashkenazi Jews and occurs with a population frequency of 1-2% (Neuhausen *et al.*, 1996). This is the founder 6174delT mutation, a deletion mutation within exon 11 that creates a premature stop codon at amino acid 2002, within BRC7 of BRCA2 (figure 56), and predisposes people to early-onset breast, ovarian, pancreatic and prostate cancers (Oddoux C *et al.*, 1996; Levy-Lahad *et al.*, 1997; Szabo and King, 1997). The second most common cancer-associated frameshift mutation is 3036delACAA, a 4-nucleotide deletion within exon 11 that truncates BRCA2 at amino acid 958 before the first BRC repeat, as indicated in figure 56 (Caporale D, 2014; Sotiriou *et al.*, 2016). This is also known to enhance predisposition to breast and ovarian cancer (Infante *et al.*, 2013). With HeLa Kyoto cells used as a parental cell line, cells heterozygous for these two clinically relevant BRCA2 truncating mutations, i.e. +/6174delT and +/3036del4, had been previously developed in our lab. These cell lines were used as part of my work to test whether DNA repair deficiency exists in BRCA2 heterozygous settings.

While biallelic mutations lead to embryonic lethality in mice (Ludwig, Chapman and Papaioannou, 1997; Sharan S. K *et al.*, 1997; Patel *et al.*, 1998), inheritance of two hypomorphic *BRCA2* alleles can occur in a rare syndrome known as Fanconi anaemia (FA)

(Howlett *et al.*, 2002). This syndrome is characterised by congenital defects, progressive bone marrow failure, hypersensitivity to DNA mutagens and susceptibility to cancer (Howlett *et al.*, 2002; D'Andrea, 2010). These clinical features arise due to abrogation of the FA pathway, which is a specialised mechanism that functions during S phase to repair DNA interstrand crosslinks (ICLs). Such lesions covalently link the two DNA strands and are highly troublesome due to their ability to impede processes like DNA replication and transcription. To date, the pathway is known to be mediated by at least 22 proteins (reviewed in Niraj, Färkkilä and D'Andrea, 2019). These proteins are involved in three separate repair pathways, namely NER, HR and translesion synthesis, thus highlighting the complexity of ICL repair. Homozygous or compound heterozygous mutation of any of the genes involved causes Fanconi anaemia, with various different sub-types or complementation groups arising depending on which gene is inactivated (Howlett *et al.*, 2002; D'Andrea, 2010; Niraj, Färkkilä and D'Andrea, 2019). Complementation group D1 contains two distinct frameshift *BRCA2* mutations: 7691insAT within exon 15 and 9900insA within exon 27 (Howlett *et al.*, 2002), which encode C-terminally truncated versions of the protein. The EUFA423 cell line, used as a *BRCA2* deficient model in this work, belongs to the D1 FA sub-type.

Another common cancer-associated mutation within *BRCA2* is a point mutation that replaces the conserved Aspartic acid residue at position 2723 by a Histidine (D2723H) (Goldgar DE1, Easton DF, Deffenbaugh AM, Monteiro AN, Tavtigian SV, 2004; Wu *et al.*, 2005). This variant is predominantly cytoplasmic, due to the mutation abrogating the BRCA2-DSS1 interaction and revealing a NES within BRCA2 that would be otherwise masked by DSS1 binding (Wu *et al.*, 2005; Jeyasekharan *et al.*, 2013). BRCA2 mis-localisation in turn abrogates the nuclear retention of RAD51 due to exposure of a similar NES on RAD51 (Jeyasekharan *et al.*, 2013). As a result, the D2723H mutation is functionally deleterious, and two HeLa Kyoto cell lines that are heterozygous or homozygous for this mutation were used as a *BRCA2* deficient model in my work.

Rad52: yeast and human proteins

Rad52 is conserved in eukaryotes and belongs to the Rad52 epistasis group of proteins including Rad50, Rad51, Rad54, Rad55, Rad57, Rad59, Mre11 and Xrs2. This group is widely conserved across eukaryotic organisms and was originally identified in *Saccharomyces cerevisiae* as part of a genetic screen analysing proteins that, when mutated, conferred hyper-sensitivity to damage induced by ionising radiation (Game and Mortimer, 1974).

The Saccharomyces cerevisiae Rad52 (ScRad52) gene encodes a protein of 471 amino acids, consisting of a conserved N-terminal domain and a non-conserved C-terminal one. The N-terminal domain carries the catalytic activity for homologous recombination and provides the ssDNA binding, oligomerisation and annealing activities (Mortensen *et al.*, 1996; Shinohara *et al.*, 1998; Sugiyama *et al.*, 1998). Self-oligomerisation of Rad52 monomers creates multimeric ring structures with a basic groove at their outer surface, which forms the DNA binding domain (Shinohara *et al.*, 1998; Singleton *et al.*, 2002; San Filippo, Sung and Klein, 2008). Another critical function that lies within the N-terminal domain of yeast Rad52 is its annealing activity which allows second end capture and single-strand annealing (SSA) (Mortensen *et al.*, 1996; Sugiyama *et al.*, 2006). The less conserved C-terminal part of Rad52 enables interaction with Rad51 and RPA in a species-specific manner, whilst also providing an additional DNA-binding domain (Park *et al.*, 1996; Shen *et al.*, 1996; Kagawa *et al.*, 2002; Khade and Sugiyama, 2016). This domain is responsible for conferring the mediator activity during homologous recombination, where an acidic region binds to and displaces RPA for subsequent Rad51 filament formation on ssDNA (Plate *et al.*, 2008). Analogous to BRCA2, two motifs found in yeast Rad52, FVTA and YEKF at amino acid residue positions 316-319 and 376-379, respectively, are essential for Rad51 binding and hence for the mediator activity of the protein (Krejci *et al.*, 2002; Kagawa *et al.*, 2014). The FVTA motif fits in the consensus FxxA sequence that has been reported in human BRCA2 and other Rad51 homologues, thus suggesting a similar mechanism of Rad51 regulation between human BRCA2 and yeast Rad52. In fact, yeast Rad52 is comparable to human BRCA2 in terms of conferring the critical mediator function that is essential for Rad51 loading onto RPA-coated ssDNA whilst preventing Rad51 binding

to dsDNA during recombination (New *et al.*, 1998; New and Kowalczykowski, 2002; Kagawa *et al.*, 2014). As already mentioned, mediator proteins are vital for enabling Rad51-dependent HR, through overcoming the inhibition imposed by RPA to Rad51 filament assembly and subsequent strand exchange (Sung, 1997; Shinohara and Ogawa, 1998; New and Kowalczykowski, 2002). This indispensable function explains why yeast Rad52 mutants exhibit hypersensitivity to γ-radiation, UV light and methyl methanesulfonate (MMS), as well as display severe defects in both meiotic and mitotic recombination (Prakash, 1976; Prakash *et al.*, 1980); phenotypes also characteristic of BRCA2-deficient cells (Patel *et al.*, 1998). Another parallel exists between human BRCA2 and yeast Rad52, in that the two proteins stimulate the strand exchange activity of Rad51 at sub-stoichiometric but not stoichiometric concentrations, thus further supporting the possibility of a conserved mechanism of DSB repair across eukaryotic organisms (Davies *et al.*, 2001; Shivji *et al.*, 2006, 2009; Davies and Pellegrini, 2007; Carreira *et al.*, 2009; Kagawa *et al.*, 2014). Unlike yeast Rad52 and its fungal orthologue Brh2, however, human BRCA2 cannot anneal ssDNA in the presence of RPA (R B Jensen, Carreira and Kowalczykowski, 2010), thus signifying that fundamental differences might exist between DNA repair pathways in yeast and humans.

The human RAD52 gene encodes a protein of 418 amino acids (figure 6), which shares homology with the yeast counterpart within its N-terminal half (Muris *et al.*, 1994; Jackson *et al.*, 2002). The full-length protein forms heptameric rings, whereas crystal structures of the N-terminal homologous pairing domain reveal the formation of undecameric rings instead, with both ring structures having a diameter of 9-13 nm (Stasiak *et al.*, 2000; Jackson *et al.*, 2002; Kagawa *et al.*, 2002; Singleton *et al.*, 2002). A positively charged channel made of basic and aromatic bases forms the outer rim of the rings and is responsible for binding the DNA phosphodiester backbone with the bases facing outwards from the oligomeric protein ring (Singleton *et al.*, 2002; Grimme *et al.*, 2010; Liu *et al.*, 2011). This observation suggests a mechanism whereby RAD52 binding to ssDNA promotes conformational changes in the DNA that can disrupt RPA-ssDNA contacts while promoting RAD51-ssDNA interactions, thus facilitating the displacement of RPA by RAD51 (Grimme *et al.*, 2010; Liu *et al.*, 2011). Furthermore, RAD52 binding to DNA exposes the nucleotide bases by inducing and stabilising

a stretched B-form-like conformation, hence encouraging subsequent annealing to a complementary strand (Singleton *et al.*, 2002; Grimme *et al.*, 2010; Saotome *et al.*, 2018). This conformation is similar to the one induced in ssDNA bound by bacterial RecA and human RAD51, and is thought to assist in homology search and base pair formation (Chen, Yang and Pavletich, 2008; Saotome *et al.*, 2018). Biochemical work by Kagawa *et al.*, 2008 revealed a second DNA-binding site within the human RAD52 protein, which lies outside the groove and displays dsDNA binding activity, thus accommodating duplex DNA once annealing has occurred (Saotome *et al.*, 2018). Extension of RAD52-mediated annealing has been suggested to promote branch migration, thus encouraging DNA unwinding of the invaded dsDNA molecule and stabilising the structure of the recombination intermediate (Sugiyama *et al.*, 2006). Despite human RAD52 exhibiting annealing and strand exchange activities as well as showing preferential binding to resected DSBs at ssDNA-dsDNA junctions like BRCA2 (Van Dyck *et al.*, 1999; Parsons *et al.*, 2000), it lacks a recombination mediator activity *in vitro* due to its inability to replace RPA from ssDNA (Mcilwraith *et al.*, 2000; Bi *et al.*, 2004; Grimme *et al.*, 2010; Ryan B. Jensen, Carreira and Kowalczykowski, 2010). This can potentially explain why Rad52 knockout in eukaryotic organisms such as mice and chicken is viable and exhibits normal levels of DNA repair and minimal HR defects, in contrast to the severe phenotypes observed in yeast (Rijkers *et al.*, 1998; Yamaguchi-iwai *et al.*, 1998). While yeast lack a BRCA2 homologue, higher eukaryotes contain both Brca2 and Rad52, thus suggesting that the functions of yeast Rad52 have been sub-divided to several proteins during evolution. For this reason, BRCA2 and RAD52 are thought of having divergent functions in human cells, with RAD52 performing annealing and BRCA2 stimulating strand exchange by RAD51 (R B Jensen, Carreira and Kowalczykowski, 2010). This in turn implies that BRCA2 has acquired the vital recombination mediator activity in higher eukaryotic organisms like mice and humans, and is thus serving as the functional orthologue of yeast Rad52.

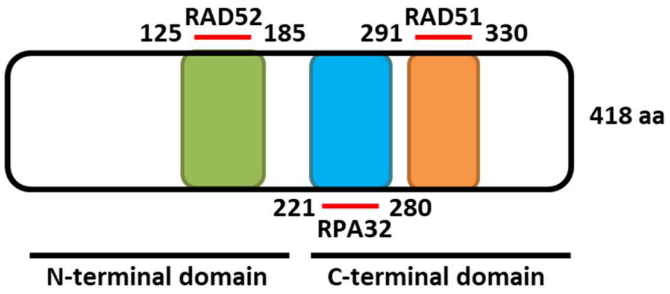

Figure 6: Domain structure of the human RAD52 protein. Within the conserved N-terminal domain (212 amino acids) of the protein lie two DNA binding domains (residues 25-65 and 102-173) and an oligomerisation domain (green, residues 125-185) that mediates the formation of oligomeric ring structures. The C-terminal part of RAD52 is responsible for the species-specific interaction with human RAD51 (orange, residues 291-330) and RPA (light blue, residues 221-280). aa, amino acids.

RAD52 roles in human cells

Even though Rad52 is critical for DNA repair in yeast, it is not yet clear what functions the protein might catalyse in human cells. Thus far, RAD52 has been shown experimentally to facilitate annealing of complementary ssDNA strands *in vitro* (Reddy, Golub and Radding, 1997; Singleton *et al.*, 2002). This function is conserved from simple eukaryotic organisms like yeast (Mortensen *et al.*, 1996; Shinohara *et al.*, 1998; Sugiyama *et al.*, 1998), to higher vertebrates such as mice (Stark *et al.*, 2004), and is thought to involve the formation of RAD52 ring aggregates on ssDNA (Shinohara *et al.*, 1998; Saotome *et al.*, 2018). The DNA annealing activity is postulated to be important in RAD51-independent pathways and might potentially be irrelevant to human HR. This activity has been reported to depend on the physical interaction between RAD52 and RPA (Wu *et al.*, 2008; Grimme *et al.*, 2010), thus proposing that RPA binding by RAD52 is necessary for displacing RPA and enabling subsequent DNA annealing efficiently.

Furthermore, human RAD52 has been reported to stimulate homologous pairing by human RAD51 (Benson, Baumann and West, 1998; Baumann and West, 1999), but this activity is only

effective for DNA that is not complexed by RPA and is not sufficient to overcome the inhibitory effect of RPA coating on RAD51-mediated strand exchange (Mcilwraith *et al.*, 2000; R B Jensen, Carreira and Kowalczykowski, 2010). Therefore, human RAD52 is not thought to function as a mediator protein in HR, even if organisms like the fungus *Ustilago maydis* contain a Rad52 protein with both annealing and mediator functionalities, despite the presence of a BRCA2 homologue in this (Kojic *et al.*, 2012). However, in human cells deficient in BRCA2, RAD52 is thought to play an alternative mediator protein that promotes RAD51-dependent HR when the predominant repair pathway is compromised (Feng *et al.*, 2011; Lok *et al.*, 2013). More recently, RAD52 was also reported of mediating the initial RAD51-ssDNA nucleofilament formation at one ended DSBs formed at collapsed forks, while BRCA2 is required for guiding the RAD51 recombinase activity during later stages (Whelan *et al.*, 2018). In RAD52 absence, BRCA2 can overtake this role in the early recruitment of RAD51 and perform the subsequent steps for repair. Thus, these observations propose a mechanism where RAD52 and BRCA2 act in a sequential manner to regulate RAD51 activity at seDSBs, with the initial nucleation step being performed by either protein.

Human RAD52 has also been described to be implicated in replication stress responses in cells. Sotiriou *et al.*, 2016 proposed a protein role in break-induced replication (BIR), a homologous recombination (HR)-based pathway that repairs one-ended DNA DSBs. Such DSBs can form as a result of replication fork (RF) collapse (covered in greater detail in chapter 2), and RAD52 has been proposed to cooperate with the non-catalytic subunit of mammalian polymerase δ, POLD3, to promote DNA synthesis in response to replication stress and facilitate fork restart (Ciccia and Symington, 2016; Sotiriou *et al.*, 2016). These observations were extended by Bhowmick, Minocherhomji and Hickson, 2016, who reported a role for human RAD52 in mitotic DNA synthesis (MiDAS), a pathway that occurs during prophase to repair DNA that has been under-replicated as a result of replication stress. MiDAS is a process that enables replication completion of difficult-to-replicate genomic loci and is thought to be a form of microhomology-mediated BIR due to its requirement for POLD3 (Minocherhomji *et al.*, 2015). In this work, the pathway was found to be independent of RAD51 and BRCA2 but reliant on RAD52, which was required for the subsequent recruitment of the MUS81 endonuclease and

POLD3 to mitotic chromosomes (Bhowmick, Minocherhomji and Hickson, 2016). In the absence of RAD52, mitotic defects occur due to chromosomal mis-segregation, resulting to the formation of ultra-fine anaphase DNA bridges. The aberrant dissolution of such bridges leads to DNA lesions, the inheritance of which causes chromosomal instability in subsequent cell generations (Lukas *et al.*, 2011; Bhowmick, Minocherhomji and Hickson, 2016). More precisely, under-replicated DNA (UR-DNA) that escapes MiDAS is propagated to daughter cells as 53BP1 nuclear bodies in the ensuing G1 (Lukas *et al.*, 2011). Upon re-entering the cell cycle, 53BP1 nuclear bodies have been described to confine the replication of any embedded DNA to late S phase, in order to enable a RAD52-dependent mechanism that provides a second chance for the repair of UR-DNA lesions (Spies *et al.*, 2019). In response to replication stress, MiDAS has also been described to enable telomere maintenance in a MUS81-independent but RAD52-dependent pathway known as alternative lengthening of telomeres (ALT) (Özer *et al.*, 2018; Verma *et al.*, 2019). Collectively, these reports highlight multiple roles for human RAD52 in maintaining genomic stability in cells undergoing replication stress.

Finally, human RAD52 has been implicated in RNA-directed DNA repair of DSBs (Xue and Greene, 2018). The protein was initially reported by Mazina *et al.*, 2017 to have an *in vitro* 'inverse strand exchange' activity, which is responsible of generating a heteroduplex between a homologous dsDNA sequence and its RNA transcript, also known as an R-loop. Within the heteroduplex, the RNA molecule can act as a template to guide end joining or gap filling for repairing the DSB in the absence of a DNA donor (Mazina *et al.*, 2017). Supporting these observations were *in vivo* data by Yasuhara *et al.*, 2018, showing RAD52 recruitment to R-loops formed at DSBs within transcriptionally active loci. RAD52 was responsible for the downstream recruitment of RAD51 and the XPG endonuclease at these sites, thus promoting RNA-DNA hybrid processing at the 3' end of R-loops, creating ssDNA overhangs for transcription associated homologous recombination repair (TA-HRR) induction and NHEJ prevention in S/G2 (Yasuhara *et al.*, 2018). In a similar mechanism, R-loops induced by reactive oxygen species (ROS) are sensed by Cockayne Syndrome protein B (CSB), which in turn recruits RAD52 to promote the subsequent localisation of RAD51 at these regions. This triggers transcription-coupled homologous recombination (TC-HR), a BRCA1/2-independent

process that acts to protect the actively transcribed genome against DNA damage (Teng *et al.*, 2018). However, since RAD52 has been shown to have an affinity for both single-stranded and double-stranded DNA and RNA substrates, as well as RNA-DNA hybrids (Welty *et al.*, 2018), further research is required to characterise the mechanism by which the protein interacts with R-loops and hence guides RNA-mediated repair.

Therefore, human RAD52 is increasingly being recognised for its importance in maintaining genome integrity in a variety of repair pathways, but the roles necessary for the survival of HR-deficient cells are yet to be elucidated.

Concept of synthetic lethality

The concept of synthetic lethality was originally described in 1922 by Calvin Bridges in *Drosophila melanogaster*. He reported that certain combinations of genes resulted in non-viable offspring when crossing parental fruit flies that were homozygous for only one of the genes (Bridges, 1922). The same observations were noted in *Drosophila pseudoobscura,* when the term 'synthetic lethality' was eventually coined (Dobzhansky, 1946) to describe the phenomenon where a mutation in either of two genes has no effect on viability but a combined perturbation leads to cellular or organismal death. This is true for genes that encode proteins that can compensate for each other if wild-type activity is lost in one of these due to mutations, epigenetic changes or exposure to chemical inhibitors. Synthetic lethality can arise either when ablation of the two proteins has an additive negative effect on one pathway or when the two have overlapping functions within different pathways.

Most of human cancers, as mentioned in preface, are characterised by genomic instability. This generates random mutations that inactivate or suppress apoptotic, senescence and DNA damage responses to enable the acquisition of the so-called 'hallmarks of cancer', including resisting death, sustaining proliferation and achieving replicative immortality (Hanahan and Weinberg, 2011). This implies that cancer cell survival and proliferation can become dependent on specific signalling and repair pathways. This addiction represents the 'Achille's heel' of cancer cells and offers the ability to exploit the approach of synthetic lethality to

develop anti-cancer treatments (figure 7). Inhibition of such pathways will essentially target cancer cells while leaving normal cells unaffected, thus minimising potential off-target and toxic side-effects. Furthermore, the identification of synthetic lethal partners can be used to indirectly target otherwise non-druggable cancer mutations, thus increasing the range of proteins that can be targeted for anti-cancer treatments (Hartwell, 1997).

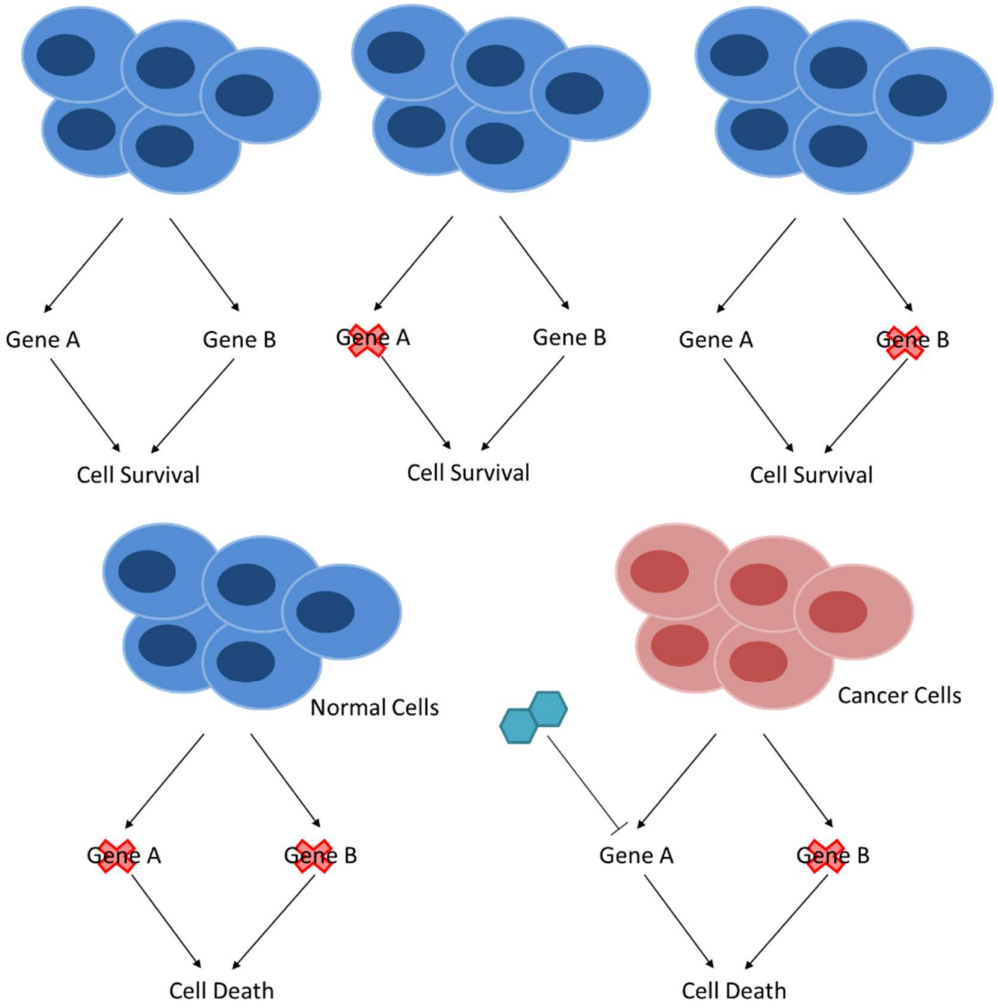

Figure 7: Concept of synthetic lethality. Loss or inhibition of gene A or B alone does not impact cell survival, but concomitant ablation of both results to cell death in normal cells. Similarly, death can be induced in cancer cells with a cancer-specific mutation in gene B upon pharmacological inhibition of gene A (and vice-versa).

BRCA2 and PARP-1

A well-known paradigm where synthetic lethality is currently being exploited in anti-cancer treatment is the use of poly (ADP-ribose) polymerase (PARP) inhibitors (PARPi) in BRCA1/2-deficient cancers (Bryant et al. 2005; Farmer et al. 2005). Amongst the PARP family of proteins, the PARP-1 enzyme is the one specifically targeted in HR-deficient cancers.

PARP-1 belongs to the PARP superfamily, consisting of eighteen proteins. These share a catalytic domain encoding for the poly (ADP-ribose) polymerase activity, which catalyses the addition of ADP-ribose moieties to Glu residues on acceptor proteins (reviewed in Amé, Spenlehauer and De Murcia, 2004; Schreiber *et al.*, 2006). PARP-1 and PARP-2 are the best-studied members of the superfamily and the only ones whose activity has been reported to be induced in response to DNA breaks (Doucet-Chabeaud *et al.*, 2001; Ménissier de Murcia *et al.*, 2003). They have been shown to participate in the repair of single-stranded breaks and BER, with knockout mice models of either protein exhibiting increased DNA repair deficiency and enhanced sensitivity to DNA damaging agents, whilst a double knockout causes embryonic lethality (De Murcia *et al.*, 1997; Trucco *et al.*, 1998; Schreiber *et al.*, 2002; Ménissier de Murcia *et al.*, 2003). The two enzymes consist of an N-terminal DNA binding domain and a C-terminal catalytic domain, although PARP-1 also contains a BRCT motif that is involved in protein interactions. Upon DNA damage, the catalytic domain binds nicotinamide adenine dinucleotide (NAD+) to form a linear or branched polymer of ADP-ribose (PAR) (de Murcia *et al.*, 1983; Amé, Spenlehauer and De Murcia, 2004). The average chain length consists of 20-30 ADP-ribose units, which build up a negatively charged moiety that promotes chromatin opening at the DNA lesion (Poirier *et al.*, 1982; Aubin *et al.*, 1983; Amé, Spenlehauer and De Murcia, 2004). This chromatin reorganisation enables the recruitment of DNA repair effectors to mediate DNA damage responses, but PARP-1 eventually auto-PARylates leading to its dissociation from DNA and ending the response (Yoshihara *et al.*, 1981; de Murcia *et al.*, 1983).

PARP-1 is the predominant enzyme responsible for PARylation in cells, accounting for 80-90% poly(ADP-ribose) synthesis while PARP-2 contributes the rest (Shieh *et al.*, 1998; Amé *et al.*,

1999). PARP-1 acts as a general sensor of DNA damage, with its zinc fingers recognising a multitude of DNA lesions, including SSBs, DSBs, as well as DNA crosslinks and stalled forks. At arrested replication forks, PARP-1 has been shown to mediate fork protection against MRE11-dependent degradation, as well as prevent premature fork restart by inhibiting the regression activity of the RECQ1 helicase (S Ying, Hamdy and Helleday, 2012; Berti *et al.*, 2013). Furthermore, the enzyme has been recently recognised for its role in alt-NHEJ, which functions in the absence of HR as a back-up mechanism for the repair of resected DSBs, in which PARP-1 is responsible of recruiting polymerase θ to DSBs (Audebert, Salles and Calsou, 2004; Wang *et al.*, 2006; Ceccaldi *et al.*, 2015; Mateos-Gomez *et al.*, 2015; Sharma *et al.*, 2015).

Since PARP-1 activity is essential for detecting DNA damage and initiating intracellular cascades that signal DNA repair and/or cell death, the protein was originally suggested as an anticancer drug target whose inhibition would sensitise cancer cells to DNA-damaging agents. The first PARP inhibitor to be approved for the treatment of BRCA1/2 mutated cancers was olaparib in 2014, followed by rucaparib and niraparib in 2016 and 2017, respectively (reviewed in Hengel, Spies and Spies, 2017). These are nicotinamide derivatives which prevent NAD+ binding to the catalytic domain of PARP-1 and PARP-2, although they potentially inhibit other members of the PARP superfamily as well as other NAD+ binding enzymes. PARP inhibitors have been mainly approved for the treatment of ovarian and breast cancers, but are currently being tested in clinical trials for treating cancers of the lung, pancreas and prostate. Nevertheless, the precise mechanism of PARPi action is still unknown. The original thinking behind PARPi development was that catalytic inhibition of PARP-1 would lead to SSB accumulation, which would eventually collapse into single-stranded DSBs during replication. Such DSBs would be un-repairable because of HR deficiency in BRCA1/2 mutated cells, whilst they would not pose a problem to healthy ones. As proof of concept, PARP inhibition by olaparib treatment has been shown to enhance replication fork stalling and degradation in BRCA1/2-deficient cells, owing to the requirement of PARP-1 recruitment to arrested forks to protect them from excessive nucleolytic processing (S Ying, Hamdy and Helleday, 2012; Chaudhuri *et al.*, 2016). Mechanistically, some compounds have been shown to act by

inhibiting PARP enzyme dissociation and encouraging protein trapping on DNA, thus causing cytotoxic protein-DNA complexes that enhance replication fork stalling and potentially block the recruitment of repair proteins (Murai *et al.*, 2012, 2014). Moreover, PARP-1 has recently been implicated in the repair of DSBs via alt-NHEJ (Audebert, Salles and Calsou, 2004; Wang *et al.*, 2006; Ceccaldi *et al.*, 2015; Mateos-Gomez *et al.*, 2015; Sharma *et al.*, 2015), thus proposing that PARP inhibitors might also function by suppressing this mechanism to enhance the number of toxic DSBs in cells.

However, despite promising results, resistance to these compounds arises quite rapidly. This occurs through enhanced efflux and reduced uptake of the drug, loss of PARP expression, as well as through restoration of HR by numerous mechanisms. Such mechanisms include the reversion of mutant BRCA2 to wild-type, enhanced RAD51 expression and/or abrogation of NHEJ through suppression of 53BP1 (reviewed in Pommier, Connor, and Bono 2016; Hengel, Spies, and Spies 2017). Moreover, since PARP-1 modulates the nucleolytic processing and restart of stalled forks, PARPi resistance in cells that do not develop BRCA2 revertant mutations has been attributed to fork protection (Berti *et al.*, 2013; Chaudhuri *et al.*, 2016; Rondinelli *et al.*, 2017). Preventing the formation of DSBs downstream of stalled replication forks, through the inhibition of nucleases such as MUS81, has also been reported to cause fork protection and lead to PARPi resistance in BRCA2-deficient tumours (Rondinelli *et al.*, 2017; Schlacher, 2017). Therefore, understanding the roles of PARP enzymes in DNA repair is fundamental for elucidating the mechanisms of PARPi action and potential resistance pathways. Such insights will consequently enable the identification of biomarkers, thus permitting a more accurate prediction of PARPi response and improved patient stratification.

BRCA2 and RAD52

In the context of DNA repair, a more recent example of a synthetic lethal relationship comes from the observation that BRCA2-deficient cells require human RAD52 for viability (Feng *et al.*, 2011). In this report, the authors proposed an *in vivo* function for human RAD52 in enabling RAD51-dependent HR when BRCA2 function is compromised. Low levels or depletion of RAD52 were found to correlate with reduced RAD51 foci, HR efficiency and growth rate in

BRCA2-deficient cells. Conversely, depleting RAD52 in cells that had been complemented with wild-type BRCA2 had minimal effect. These data suggested that RAD52 is required for the proliferation of cells with no or low BRCA2 activity to maintain RAD51-dependent repair of DSBs via HR. In fact, the simultaneous abrogation of Rad52 and that of proteins supporting Rad51 activity, like Xrcc3, has been previously shown to lead to cell death in chickens as a result of enhanced chromosomal aberrations (Fujimori *et al.*, 2001). Since then, synthetic lethality with RAD52 has been expanded to proteins like BRCA1 and PALB2, which also function to support RAD51-dependent HR (Lok *et al.*, 2013), thus demonstrating that human RAD52 provides an alternative repair pathway when the predominant pathway for RAD51-mediated HR is compromised. This has been actually demonstrated in the fungus *Ustilago maydis,* where Rad52 can compensate for the deletion of the DNA binding motif of Brh2, the fungal BRCA2 homologue, thus unveiling a conserved mediator role for Rad52 in eukaryotic organisms (Kojic *et al.*, 2012). Collectively, these findings have revealed that human RAD52 is synthetic lethal in cells with HR deficiency due to the lack of wild-type BRCA1, PALB2 or BRCA2 activities (Feng *et al.*, 2011; Lok *et al.*, 2013).

Owing to the fact that synthetic lethality between RAD52 and HR proteins has been described in breast, ovarian and pancreatic cancer cells (Feng *et al.*, 2011; Lok *et al.*, 2013), rigorous research is underway to develop RAD52 inhibitors for the targeted treatment of cancers with BRCA1/BRCA2 mutations or deficiencies in HR. Moreover, there are no currently known mutations within *RAD52* that confer an enhanced predisposition to breast, ovarian or leukemic cancers (Bell *et al.*, 1999; Beesley *et al.*, 2007), which can often be associated with BRCA1/2 mutations. The facts that RAD52 is not frequently mutated or lost in human cancers whilst its abrogation does not affect BRCA1/2-proficient cells, therefore, make the protein an even more attractive target for cancer therapy. For this reason, a variety of inhibitors have been recently developed, targeting the DNA binding, oligomerisation and/or annealing functions of human RAD52. The first ones to prove the concept of synthetic lethality between RAD52 and BRCA1/2 using a RAD52 inhibitor were Cramer-Morales et al, who developed a peptide aptamer targeting the F79 residue within the DNA binding domain of RAD52 to exert synthetic lethality in leukemic, breast, pancreatic and ovarian cancer cells (Cramer-Morales

et al., 2013). Following this, the small molecule 6-hydroxy-DL-dopa was found to act as an allosteric inhibitor of RAD52, which acts to prevent its ssDNA binding activity as well as its oligomerisation into rings and higher-order molecular assemblies (Chandramouly *et al.*, 2015). Subsequently, an *in silico* molecular docking screen by Sullivan et al identified 5-Aminoimidazole-4-carboxamide ribonucleotide (AICAR) 5' phosphate (ZMP) as an inhibitor of RAD52-ssDNA binding that prevented the SSA activity of the protein (Sullivan *et al.*, 2016). Another high-throughput screen combined with computational modelling described epigallocatechin (EGC) and corilagin as additional inhibitors of the ssDNA- binding and annealing of activities of RAD52 (Hengel *et al.*, 2016). Finally, Huang et al. reported that D-I03 inhibits both the annealing and DNA strand exchange activities of RAD52 in BRCA-deficient cancer cell lines (Huang *et al.*, 2016). These chemicals undoubtedly provide a good starting point as lead compounds for the development of potent RAD52 inhibitors, however such studies should now be extended to *in vivo* models to monitor the efficacy and any potential off-target effects of such inhibitors.

Project Aim

Despite Rad52 protein conservation across eukaryotic organisms and its essential role as a recombination mediator in yeast, the original report by Feng et al. was received with surprise, since mammalian Rad52 was previously thought of being dispensable for viability, fertility and DNA repair. In fact, mouse and chicken knockouts of Rad52 exhibit minimal sensitivity to DNA damaging-agents and mild defects in HR (Rijkers *et al.*, 1998; Yamaguchi-iwai *et al.*, 1998). These observations could be partly explained by the fact that, regardless of the high degree of sequence homology with yeast Rad52, the human protein lacks a recombination mediator activity *in vitro* due to its inability to displace RPA from ssDNA, suggesting species-specific activities (Kagawa et al. 2002; Park et al. 1996; San Filippo et al. 2008; Liu & Heyer 2011). Instead, human BRCA2 was believed to have acquired the recombination mediator function of the yeast Rad52 protein. Therefore, BRCA2 and RAD52 were originally thought of having assumed divergent functions in human cells, with RAD52 performing annealing activities and BRCA2 stimulating strand exchange by human RAD51 (R B Jensen, Carreira and Kowalczykowski, 2010). Nevertheless, as discussed earlier, the precise cellular roles of RAD52 are not known, thus obscuring our understanding of the molecular mechanisms that can mediate synthetic lethality between RAD52 and BRCA2 in human cells.

Hence, the work described in my thesis is focussed on exploring and characterising the activities mediated by RAD52 that make its presence critical for the survival of BRCA2-deficient cells. BRCA2 has established roles in numerous cellular functions, including homologous DNA repair, stalled fork protection, spindle assembly and mitotic checkpoint reinforcement, as well as cytokinesis and R-loop prevention. In an attempt to elucidate the role(s) of RAD52 in human cells, and hence establish whether BRCA2 and human RAD52 carry divergent or redundant roles in humans, the ability of RAD52 to replace for established BRCA2 activities was assessed in cells wild-type, heterozygous or biallelic mutant for *BRCA2*. More specifically, as part of this work I investigated the involvement of human RAD52 in DSB repair by HR and replication fork protection, both of which rely on the formation of elongated RAD51 filaments on single-stranded DNA for homology search and replication fork stability,

respectively. In humans, BRCA2 has an established role in mediating RAD51 filament initiation, elongation and stabilisation needed for recombinase functions in HR and replication fork protection. Therefore, I hypothesised that in the absence of a functional BRCA2 protein, RAD52 will take over this recombination mediator function to enable RAD51 activity and viability of BRCA2-deficient cells. Furthermore, since BRCA2 mutations occur in breast, ovarian, pancreatic and prostate cancers, establishing the relationship between BRCA2 and RAD52 will not only provide further insights into the mechanisms of homologous recombination and genome maintenance in human cells, but also offer the scientific basis for new approaches to the therapy of BRCA2-deficient cancers. As aforementioned, such cancers are currently being treated with PARPi, but resistance to such treatment is not unusual. Therefore, BRCA2-mutated cancers that are not responsive to PARPi can be alternatively treated with RAD52 inhibitors. Importantly, a synergistic effect has been recently described between RAD52i with PARPi in tumours deficient in HR, with RAD52 inhibitors improving the therapeutic outcome of such malignancies (Sullivan-Reed *et al.*, 2018). Therefore, elucidating the mechanisms by which RAD52 and BRCA2 are synthetically lethal will not only enable the identification of therapeutic approaches for the targeted treatment of BRCA1/2 cancers, but will also broaden our understanding of the cellular functions of human RAD52 that can in turn provide the molecular basis for combating resistance pathways to either PARP or RAD52 inhibition.

Finally, in order to determine the structural mechanisms directing homologous DNA repair and define the steps permitting RAD51-mediated strand invasion, biochemical work was undertaken to structurally characterise the regulation of RAD51 nucleofilament assembly by BRCA2 using electron cryo-microscopy. Despite a number of RAD51 structures bound to different DNA substrates and nucleotides having been described (Yu *et al.*, 2001; Pellegrini *et al.*, 2002; Conway *et al.*, 2004; Short *et al.*, 2016; J. Xu *et al.*, 2017; Brouwer *et al.*, 2018), the field lacks a high-resolution structure of a RAD51 protein filament interacting with BRCA2 on DNA. Such a structure will broaden our understanding of the protein interactions coordinating RAD51 loading and/or assembly on ssDNA, as well as elucidate the mechanism by which

BRCA2 might dictate filament dynamics for fine-tuning recombinase activities necessary for DNA repair by HR.

Collectively, the research reported in my thesis aims to provide new insight into the mechanisms by which BRCA2 and RAD52 regulate RAD51 during reactions that lead to HR and replication fork protection (figure 8).

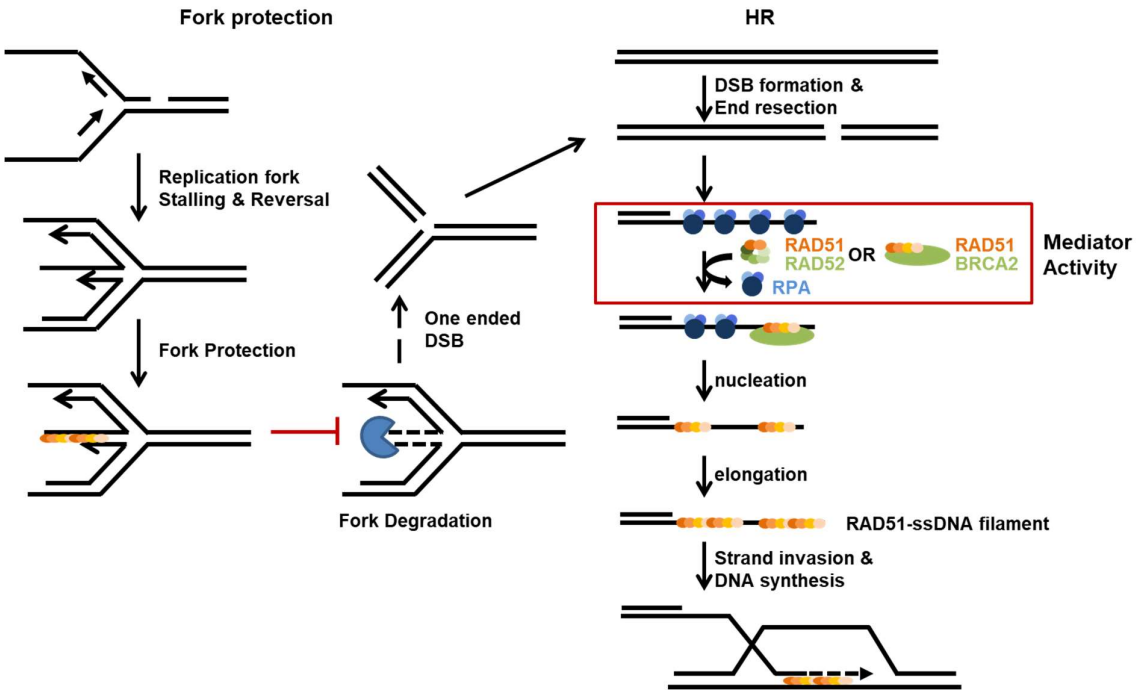

Figure 8: Thesis focus. The RAD51 recombination enzyme assembles as helical nucleoprotein filaments on single-stranded DNA substrates to mediate homologous DNA recombination (HR) and replication fork protection. Filament assembly across eukaryotic organisms is controlled by two key mediators – the tumour suppressor protein Brca2 and Rad52. Elucidating the functional interplay between RAD52 and BRCA2 during HR and replication fork protection in human cells is the aim of the work outlined in my thesis.

In this chapter, I will be assessing the role of human RAD52 in RAD51-dependent homologous DNA repair. Previous work in our lab using super resolution microscopy to characterise homologous recombination reactions in cells has shown that extended RAD51 filaments are formed in cells wild-type for BRCA2 after DNA damage (Haas *et al.*, 2018). In contrast, cells carrying inactivating mutations in BRCA2 nucleate small, focal RAD51 accumulations without elongated filamentous structures, a phenotypic distinction that would otherwise not be possible using confocal microscopy. These observations suggest that RAD51 nucleation may be necessary to sustain the growth of BRCA2-deficient cells, since homologous recombination is essential for viability. Although these results do not rule out the possibility that residual BRCA2 activity supports RAD51 nucleation but not elongation, it is also possible that nucleation may be BRCA2-independent (at least in BRCA2-deficient cells). Indeed, the well-established role of Rad52 as a mediator protein in yeast and the reported synthetic lethality of human RAD52 with BRCA2, BRCA1 or PALB2, combined with our own observations, raise the possibility that RAD52 enables RAD51 nucleation in human cells with BRCA2 deficiencies. This would imply that cells wild-type for RAD52 but mutant for BRCA2 would be proficient in minimal RAD51 nucleation to sustain viability; nonetheless, full-length BRCA2 would be required for the assembly of extended RAD51 filaments. This hypothesis is further supported by the fact that RAD51-null cells undergo immediate cell death in contrast to the proliferative defect observed in BRCA2-null cells, thus suggesting that RAD51 can mediate HR independent of BRCA2 in vertebrates (Qing *et al.*, 2011). For these reasons, a potential function of the human RAD52 protein in mediating RAD51 filament nucleation and/or assembly for homologous DNA repair was examined.

RESULTS

1.1 Depletion of RAD52 leads to proliferation defects in cells with BRCA2 deficiency

Following observations by Feng *et al.*, 2011 reporting that RAD52 is synthetically lethal with BRCA2 deficiency in human cells, a panel of cell lines with different BRCA2 status was used to assess cell proliferation upon RAD52 depletion. HeLa Kyoto cells, which carry two wild-type *BRCA2* alleles, were used as a parental cell line to develop cells heterozygous or homozygous for cancer-associated BRCA2 mutations. In the heterozygous models that we currently have in the lab, one allele was maintained WT for BRCA2 whilst the other was genetically modified by CrispR-Cas9 to carry either the 6174delT or the 3036del4 mutation. These heterozygous models have been previously described to be BRCA2 haploinsufficient upon exposure to aldehydes (Tan *et al.*, 2017). The homozygote model used was the one carrying the D2723H mutation within *BRCA2*, which ultimately leads to the cytoplasmic mis-localisation of both BRCA2 and RAD51 (Jeyasekharan *et al.*, 2013). Additionally, the Fanconi anaemia cell line which bears biallelic truncations in BRCA2, EUFA423 (EUFA-), was used along with its Flag-BRCA2 complemented derivative (EUFA+) as an additional model system.

1.1.1 Generation and validation RAD52-depleted cell lines

RAD52 depletion was performed by virally transducing cells to develop stable cell lines expressing a doxycycline-inducible shRNA against human RAD52. An inducible lentiviral system was chosen to permit the regulated manipulation of RAD52 expression in cells, and more specifically in BRCA2-deficient backgrounds where RAD52 depletion is expected to lead to cell death. Notably, a cell line stably expressing shRAD52 could not be developed in the homozygous D2723H BRCA2 background, suggesting a more severe effect of this variant in compromising protein functionality when compared to the other BRCA2 mutation models used.

Viral transduction was performed at a multiplicity of infection (MOI) of 0.3 and transduced cells were selected 48 hours post-transduction using puromycin. A non-targeting (NT) shRNA

was used as negative control, and RAD52 knockdown was subsequently validated by qPCR and western blotting (figure 9). Currently available antibodies against endogenous RAD52 are non-specific, with the tested reagents yielding multiple bands at the expected molecular weight that are not diminished by RNA interference, thus making endogenous protein detection technically challenging. Nonetheless, a RAD52 antibody that runs as a protein band doublet on a 4-12% gradient gel and exhibits protein band depletion (indicated by the arrow in figure 9) upon shRAD52 expression was identified and used for the purpose of knockdown confirmation.

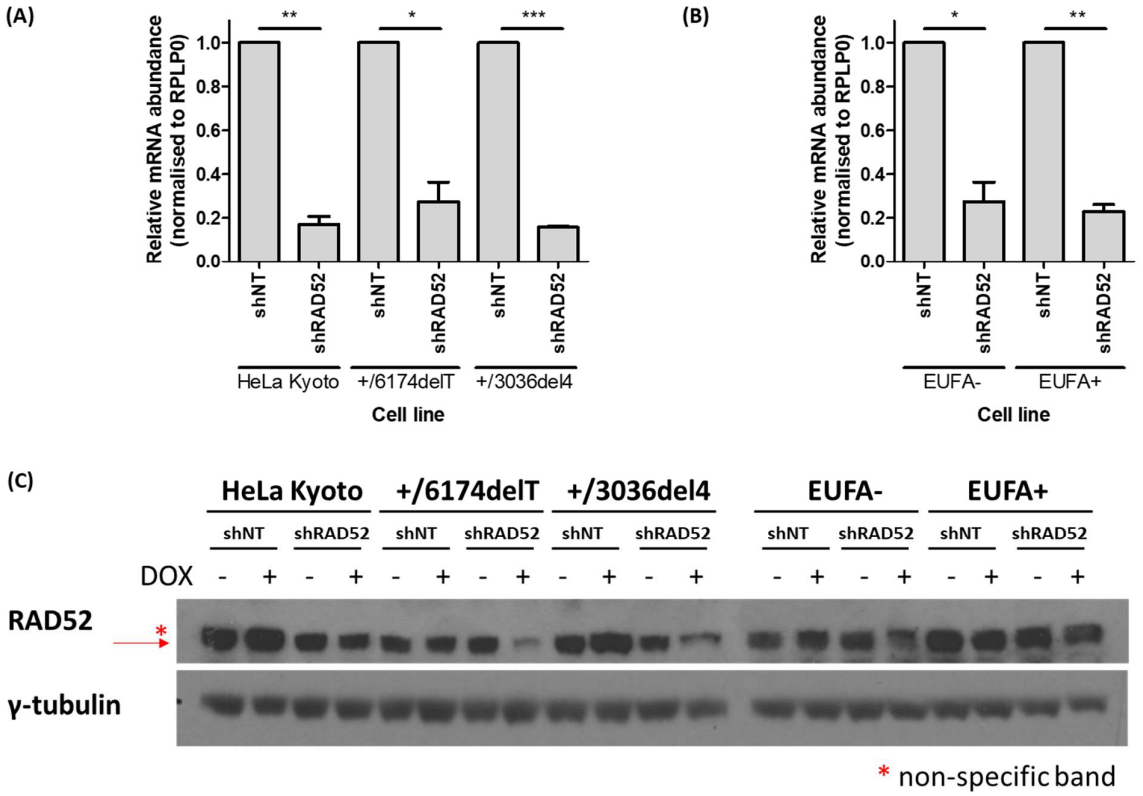

Figure 9: Validation of RAD52 depletion in transduced cell lines. Quantitative PCR (qPCR) was performed on transduced cells to assess RAD52 expression. The relative abundance of RAD52 mRNA levels was calculated in each cell line by normalising to the RPLP0 housekeeping gene and the respective shNT control in the parental HeLa Kyoto **(A)** or EUFA423 **(B)** cell line. The bars presented show the mean ± SEM of three biological repeats. **(C)** Western blot analysis prior to and following doxycycline induction (1 µg/ml, 48 hours) of the shRNA constructs was performed to assess leakiness of the pTRIPZ system and determine RAD52 protein levels in cells. RAD52 runs as a doublet due to an upper non-specific band, as indicated by the asterisk (*).

1.1.2 RAD52 depletion in cells leads to reduced proliferative capacity, which is exacerbated in BRCA2-deficient backgrounds

Cell viability and growth were assessed using the colony forming assay and live cell imaging by the Incucyte microplate reader, respectively. For the colony forming assay, cells were plated at a low density and allowed to grow for 7-10 days, after which colonies were fixed and counted. Cell proliferation was followed for a week by the Incucyte by monitoring red fluorescence in cells due to the turboRFP reporter in the shRNA constructs used for transduction. RAD52 depletion does not significantly reduce the survival of HeLa Kyoto cells that are wild-type or heterozygous for *BRCA2* mutations (figure 10), but a reduction in their proliferation rate is observed over time in comparison to the respective shNT controls (figure 11). This observation might be due to the clonogenic potential of cells differing from their proliferative capacity, in instances where not all viable cells are able to actively divide. In the EUFA423 cell line model, similar observations are made in the Flag-BRCA2 complemented counterpart, EUFA+, in which RAD52 depletion only modestly affects the survival and proliferation of the cells. However, loss of RAD52 in EUFA- cells, which are biallelically mutated for *BRCA2*, causes a marked reduction in both the survival and proliferative capacity of the cells even in the absence of exogenous DNA damage. These observations suggest a role for human RAD52 in supporting the proliferation of cells, which becomes essential for cell survival in BRCA2-deficient backgrounds.

Remarkably, amongst the two *BRCA2* heterozygous cell lines used, RAD52 depletion causes a more severe proliferation rate defect in the model carrying the 3036del4 mutation when compared to the respective shNT control (figure 11). This might be owing to the lack of BRC repeats within the mutated *BRCA2* allele in these cells, in contrast to the 6174delT mutation in which 6 of the 8 BRC repeats are preserved. These findings further suggest that RAD52 activity becomes increasingly essential or is unveiled upon loss of BRC repeats, which would otherwise facilitate RAD51 loading on ssDNA.

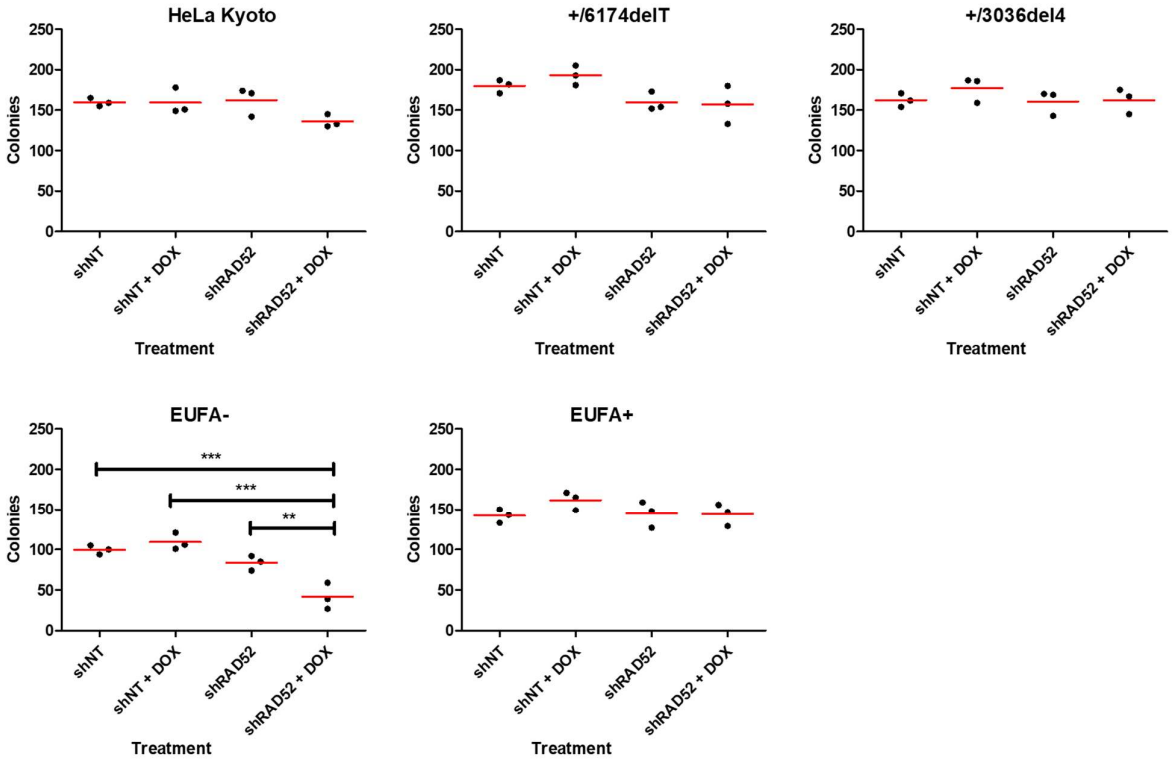

Figure 10: Cell viability is reduced following RAD52 depletion in BRCA2-deficient cells. A colony forming assay was performed in the absence and presence of doxycycline induction (1 µg/ml) of the shRNA constructs in cells. Doxycycline induction was performed for 48 hours prior to cell seeding and maintained for the duration of the experiment. Colonies formed at the end of a 7-10 day duration were quantified from duplicate wells for each condition. Graphs are representative of three independent experiments, with the mean indicated by a red line. Statistical analysis performed by a one-way ANOVA test and a Tukey post-test to compare all pairs of columns.

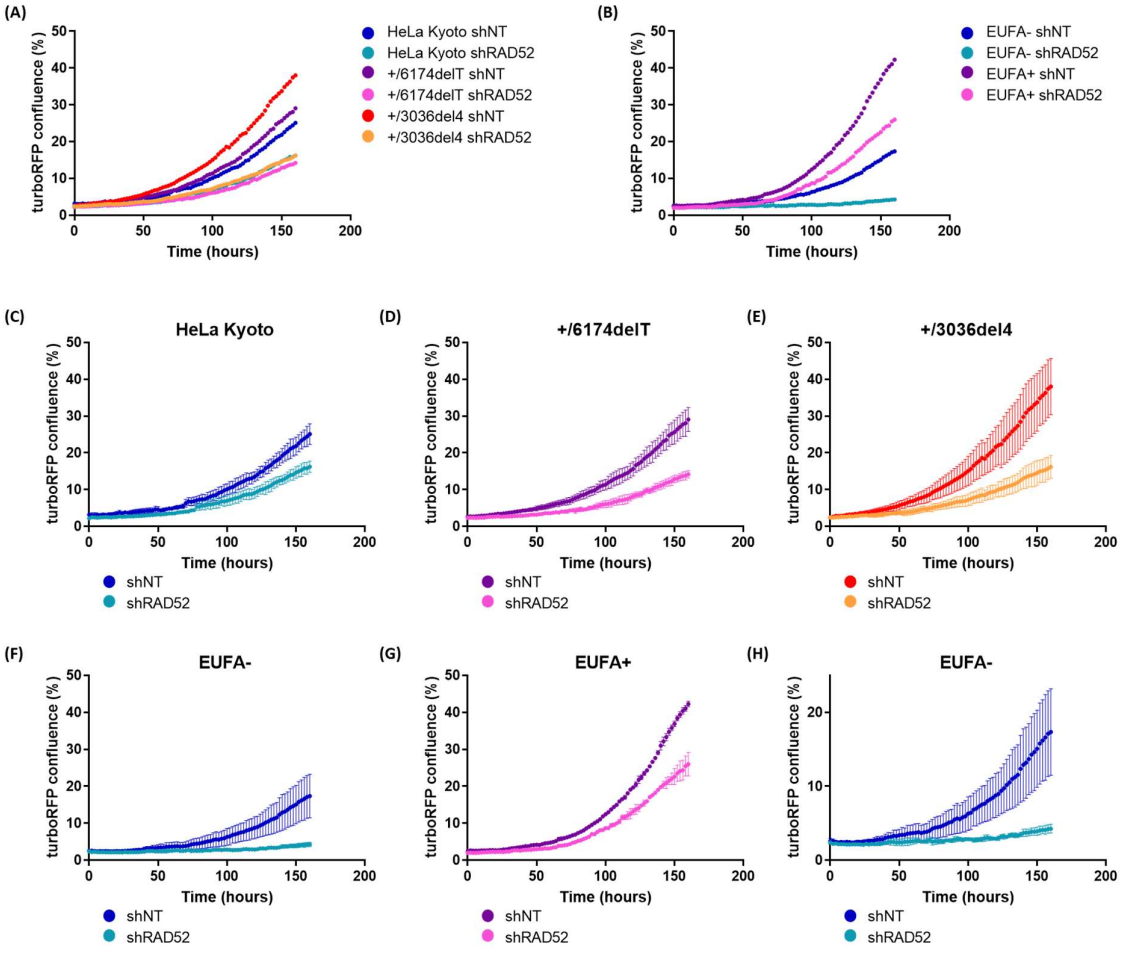

Figure 11: Depletion of RAD52 reduces the proliferation rate of cells. Cells expressing turboRFP-shRNA were monitored using the IncuCyte ZOOM cell imaging system and percentage confluence was measured throughout the week-long culture period. An overlay of the HeLa Kyoto and EUFA423 cell lines is shown in **(A)** and **(B)**, respectively, with graphs of the individual cell lines comparing shNT- and shRAD52- transduced cells shown in **(C-G).** A zoomed in version of the proliferation curves of EUFA- cells is shown in **(H)** to demonstrate the gradual proliferation of shRAD52-transduced cells. The graphs are representative of at least two biological repeats and error bars indicate standard deviation.

A technical limitation in assessing cell proliferation following RAD52 depletion was the variation in the transduction efficiency between different cell lines. This implies that a better transduced cell line will appear to have a faster growth curve due to enhanced multiplication of turboRFP-carrying cells, thus making it difficult to directly compare the effect of RAD52 depletion on the proliferation rate of each cell line. For this reason, each cell line was normalised to its respective shNT control to obtain a ratio that allows a direct comparison between the different cell lines and hence better represents the effect of RAD2 depletion in each genetic background.

In general, shRAD52 cell lines proliferate slower than their respective shNT controls since the ratio falls below 1 soon after the beginning of the experiment (figure 12). At the end of the week-long culture period, RAD52 depletion causes a ~20% reduction in the proliferation rate of HeLa Kyoto and EUFA+ cells, both of which are BRCA2 proficient. This decrease is more pronounced in the BRCA2 heterozygous cell lines, with 50% and 60% reduction in the proliferation rate of the +/6147delT and +/3036del4 cells, respectively. The most severe effect, however, is observed in the BRCA2-deficient EUFA- cells, with RAD52 depletion causing a 70% reduction in their proliferation rate at the end of the experiment. Importantly, EUFA- cells expressing turboRFP-labelled shRAD52 can be seen dividing over the course of the experiment (figure 13), albeit very slowly. This observation contradicts the previously reported synthetic lethal relationship between BRCA2 and RAD52 in human cells and suggests a synthetic sick relationship instead. This further implies that RAD52 depletion delays the proliferation of BRCA2-deficient cells, potentially to enable the efficient repair of endogenous DNA damage, but does not kill them.

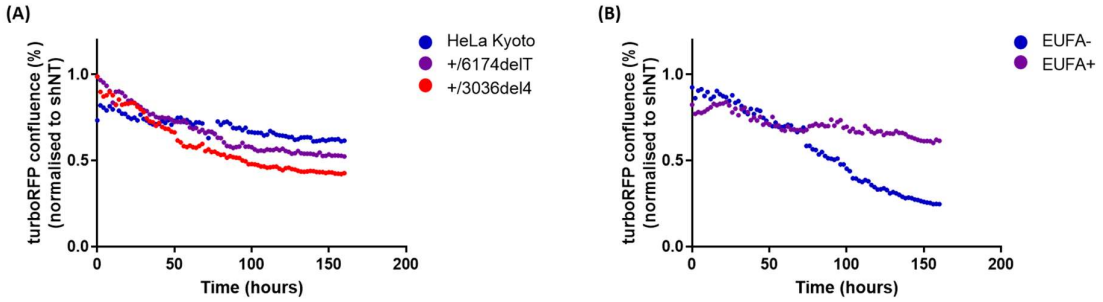

Figure 12: Depletion of RAD52 leads to a reduced proliferative capacity in cells. Proliferation curves for each of the cell lines normalised to their respective shNT control are shown for HeLa Kyoto **(A)** and EUFA423 **(B)** cell lines.

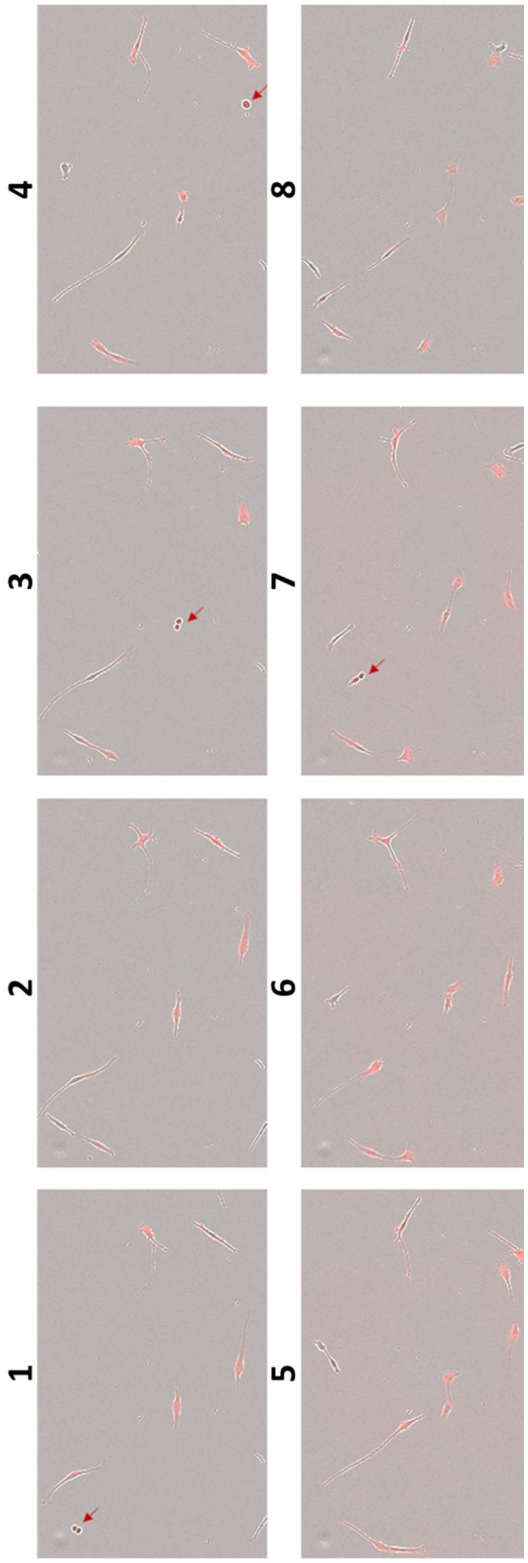

Figure 13: Depletion of RAD52 in EUFA- cells leads to reduced proliferative capacity, but not death. Representative images of a culture of EUFA- cells expressing turboRFP-shRAD52 (depicted red) undergoing healthy cell divisions at 5 days post-seeding. Dividing cells are indicated by red arrows. Cell growth was monitored and live cell images were acquired every 3 hours by the IncuCyte ZOOM cell imaging system, with successive image acquisitions over a 24-hour period indicated by increasing number labels.

1.2 Human RAD52 co-localises with RAD51 and RPA upon DNA damage

The fact that RAD52 depletion caused noticeable proliferation defects in cells heterozygous or homozygous for *BRCA2* mutations led me to investigate the functions that RAD52 might be playing in BRCA2-deficient cells. BRCA2 is the predominant mediator protein in human cells, facilitating RPA displacement from ssDNA for RAD51-dependent HR, while Rad52 plays the equivalent role in yeast, which lack a BRCA2 homologue (Benson, Baumann and West, 1998; Miyazaki *et al.*, 2004; Shivji *et al.*, 2006; Liu *et al.*, 2010; Ryan B. Jensen, Carreira and Kowalczykowski, 2010; Thorslund *et al.*, 2010). ScRad52 interacts with Rad51 and enables Rad51 focus formation (Miyazaki *et al.*, 2004), where foci are sub-nuclear aggregates of proteins involved in DNA repair formed following DNA damage. Such foci represent sites of ongoing repair, although some also exist in un-damaged cells, presumably indicating the attempted repair of stalled or broken replication forks. The ability of human cells to form RAD51 foci following DNA damage correlates with their capacity to repair DSBs via HR, and hence can be used as a surrogate measure of HR efficiency. Upon DNA damage, yeast Rad51 and Rad52 have been shown to form co-localised nuclear foci (Shinohara, Ogawa and Ogawa, 1992; Miyazaki *et al.*, 2004). This observation has been further extended to higher eukaryotes, including hamster and mouse cells (Liu and Maizels, 2000; Van Veelen *et al.*, 2005). Since the human homologue of ScRad52, RAD52, has been shown to bind the human RAD51 protein and stimulate *in vitro* homologous pairing reactions, I next questioned whether the two proteins would co-localise following DNA damage in human cells.

As previously mentioned, commercially available antibodies against human RAD52 are not specific, thus hindering studies on the endogenous protein and its activity following DNA damage. To overcome this problem, an HA-tagged RAD52 construct was created to allow monitoring of RAD52 activity preceding and following DNA damage in cells wild-type or deficient for *BRCA2*. Successful construct cloning and protein expression was verified by restriction digest, sequencing and transient cell transfection experiments (figure 14).

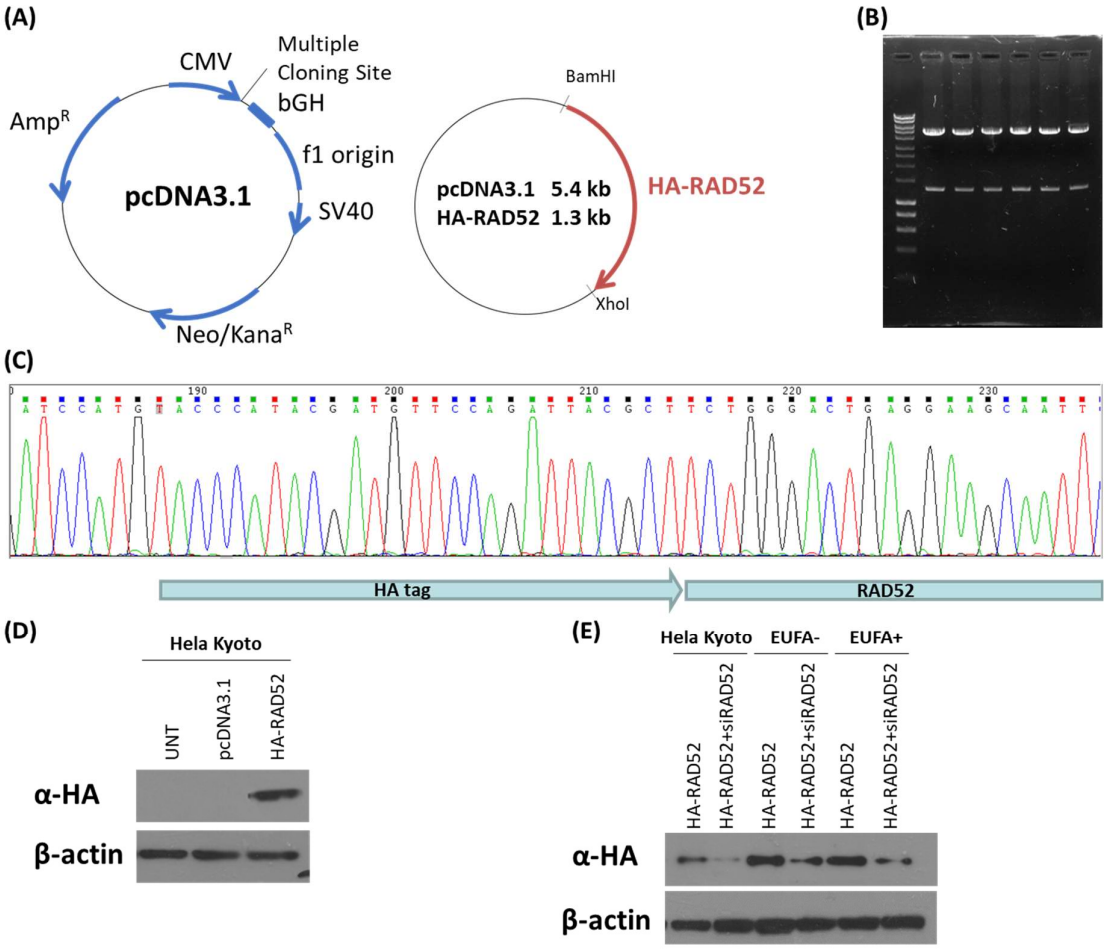

Figure 14: HA-RAD52 construct design and validation. (A) Schematic of the plasmid construct used for transfection, indicating the restriction enzyme cloning sites used for pcDNA3.1-HA-RAD52 recombinant plasmid design. **(B)** Following mini prep, double digest of the plasmid was performed using BamHI and XhoI for insert verification. **(C)** Sequence chromatogram verifying the presence of the HA tag in the construct. **(D)** HeLa Kyoto cells were transfected with 1µg of empty-vector control (pcDNA3.1) or the HA-RAD52 plasmid and protein expression of HA-RAD52 was assessed after 48 hours. **(E)** Verification of RAD52 knockdown in HeLa Kyoto, EUFA- and EUFA+ cells by transient co-transfection of HA-RAD52 and siRAD52 for a duration of 48 hours.

Following construct verification, HeLa Kyoto, EUFA- and EUFA+ cells were transiently transfected with HA-RAD52. Forty-eight hours following transfection, an asynchronous population of cells was exposed to 5 Gy of ionising radiation and RAD52 protein localisation and focalisation was assessed by confocal microscopy at various time points before and after damage.

Prior to IR exposure, HA-RAD52 was found to be diffuse throughout the nucleus of cells (figure 15). In response to DNA damage, however, the protein began accumulating in nuclear foci in the three cell lines used, irrespective of their BRCA2 status. Notably, HA-RAD52 focalisation in the BRCA2-deficient EUFA- cells was much more remarkable compared to cells wild-type for BRCA2. By 30 minutes to an hour following DNA damage, the BRCA2-deficient cells were found to contain HA-RAD52 foci, which persisted for up to 5 hours (figure 15). In contrast, HA-RAD52 focalisation became apparent at later time-points in the two BRCA2-proficient cell lines used, HeLa Kyoto and EUFA+, with focus accumulation peaking at 3-5 hours following damage. This observation could potentially underline a greater degree of RAD52 dependence for RAD51 focus formation early following DNA damage in cells like EUFA423, which are BRCA2 deficient.

Co-localisation of nuclear HA-RAD52, RPA and RAD51 foci following DNA damage was subsequently assessed. Cells were transiently transfected with HA-RAD52 for 48 hours, as before, and exposed to 5 Gy of IR for 5 hours. Focalisation by HA-RAD52, RPA and RAD51 was monitored by immunostaining with fluorescent secondary antibodies conjugated to the 488, 568 and 647 fluorophores, respectively. Image acquisition was performed by sequential laser excitation of the sample to eliminate the possibility of fluorescence emission bleed-through between the different detection channels. Remarkably, the nuclear foci formed by the three proteins were found to co-localise, as shown in the bottom panel of figure 16, thus suggesting the recruitment of HA-RAD52 to sites of damage and the cooperation of RAD52, RPA and RAD51 during DNA repair in human cells. However, HA-RAD52 showed better co-localisation with RPA than RAD51 (quantification in top and middle panels of figure 16), potentially indicating a mediator role for RAD52, which has not been previously acknowledged in

mammalian organisms. At 5 hours following IR exposure, co-localisation between HA-RAD52 and RPA was nearly 100% in all three cell lines. In EUFA- cells, co-localisation between HA-RAD52 and RAD51 reached a maximum of 47% foci at 5 hours post-damage, potentially owing to the reduced capacity of this BRCA2-deficient cell line to form RAD51 foci and perform RAD51-mediated HR. This is in comparison to the other two BRCA2-proficient cell lines used, EUFA+ and HeLa Kyoto, which are competent in RAD51 focus formation and in which co-localisation between HA-RAD52 and RAD51 foci reached 71% and 78%, respectively. These values are consistent with previous reports of RAD51 co-localisation with RPA following IR damage (Haas *et al.*, 2018), considering that HA-RAD52 and RPA have an almost identical localisation within foci in cells and hence RPA foci can be used to make inferences about the extent of co-localisation between RAD51 and HA-RAD52. Of interest is the fact that not all RAD51 foci co-localise with HA-RAD52 and RPA, implying additional roles for HA-RAD52 and RPA other than RAD51-dependent repair, as already suggested for yeast Rad52 (Tuskamoto *et al.*, 2003).

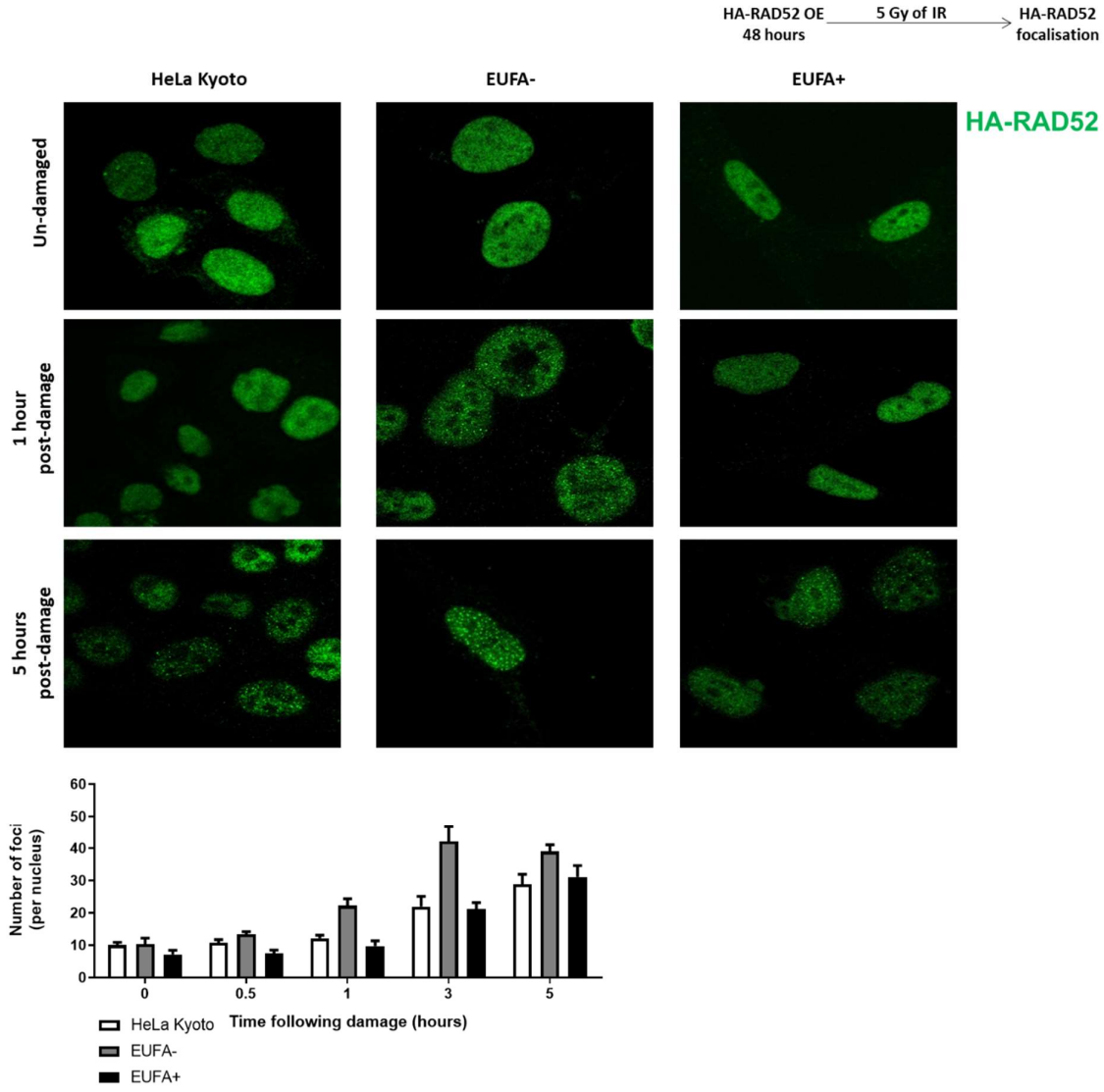

Figure 15: Human RAD52 assembles into sub-nuclear foci upon IR-induced damage in cells. HeLa Kyoto, EUFA- and EUFA+ cells were transfected with a plasmid encoding for HA-RAD52 and exposed to 5 Gy of ionising radiation 48 hours later. The formation of nuclear HA-RAD52 foci, detected by immunolabelling with a 488 fluorophore, was monitored at the indicated time-points. Quantification of HA-RAD52 foci was done using ImageJ and the bars represent mean ± SEM of three biological repeats.

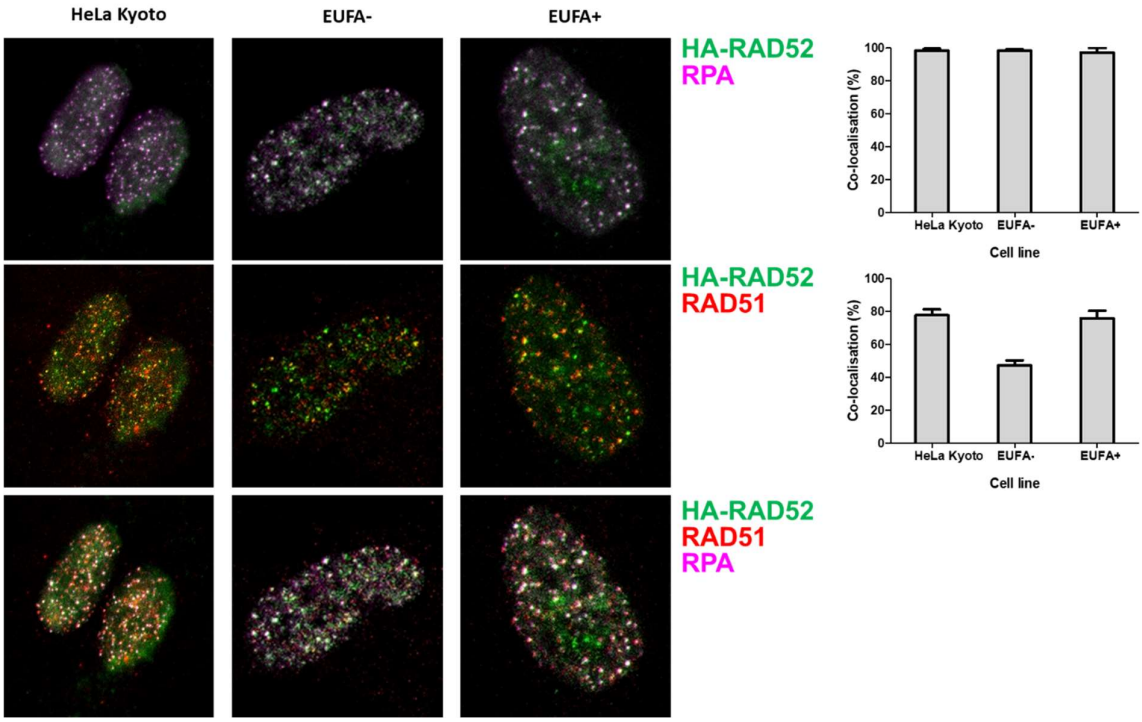

Figure 16: RAD52 exhibits co-localisation with RPA and RAD51 in human cells following IR-induced damage. HeLa Kyoto, EUFA- and EUFA+ cells were transfected with a plasmid encoding for HA-RAD52 and exposed to 5 Gy of ionising radiation 48 hours later. The formation of nuclear HA-RAD52, RPA and RAD51 foci, detected by immunolabelling with the 488, 568 and 647 fluorophores, respectively, was monitored 5 hours post IR-induced damage. The co-localisation of HA-RAD52 and RPA (upper panel) or HA-RAD52 and RAD51 (middle panel) in cells is shown. Quantification of the extent of co-localisation between the proteins was performed in ImageJ and is indicated on the right, with the bars representing mean ± SEM of three biological repeats. A merge of all three channels is shown in the bottom panel, with regions of protein co-localisation indicated by white foci.

1.3 Human RAD52 regulates RAD51 assembly on DNA in BRCA2-deficient cells

1.3.1 RAD51 assembly on DNA is enhanced in BRCA2-deficient cells following ectopic expression of RAD52

The observation that RAD52 co-localises with RAD51 and RPA following DNA damage, combined with previous reports showing that human RAD52 physically interacts with RAD51 both *in vitro* and *in vivo* (Shen *et al.*, 1996), suggests a role for RAD52 in regulating RAD51-dependent repair. Therefore, I chose to study RAD51 nucleoprotein filament assembly and its regulation by RAD52 through analysis of RAD51 foci numbers following DNA damage by IR in a panel of BRCA2- proficient and deficient cell lines.

As a general trend, nuclear RAD51 foci formation was enhanced upon ectopic expression of HA-RAD52 in the cell lines tested (figure 17). However, the only statistically significant increase in the number of RAD51 foci per cell was in the BRCA2-deficient cell line, EUFA-, with an enhancement observed for both spontaneous and irradiation-induced RAD51 foci. Empty-vector transfected cells contained 4 ± 1 and 8 ± 1 foci per cell, whereas cells ectopically expressing HA-RAD52 contained 13 ± 2 and 27 ± 2 foci per cell, before and 5 hours post-damage respectively. These observations are in agreement with a previously reported increase in spontaneous and damage-induced RAD51 foci upon RAD52 over-expression in another BRCA2-defective cell line, Capan-1 (Feng *et al.*, 2011). On the contrary, the two BRCA2-proficient cell lines, HeLa Kyoto and EUFA+, do not exhibit a consistent, statistically significant increase in the number of RAD51 foci at all the tested time-points following RAD52 over-expression. Similar observations have been reported for MCF-7 cells, which is a cell line that contains wild-type BRCA2 (Feng *et al.*, 2011).

These observations thus suggest that RAD52 can potentially mediate RAD51 focus formation both in wild-type and defective *BRCA2* backgrounds, but becomes an essential recombination mediator in cells lacking BRCA2.

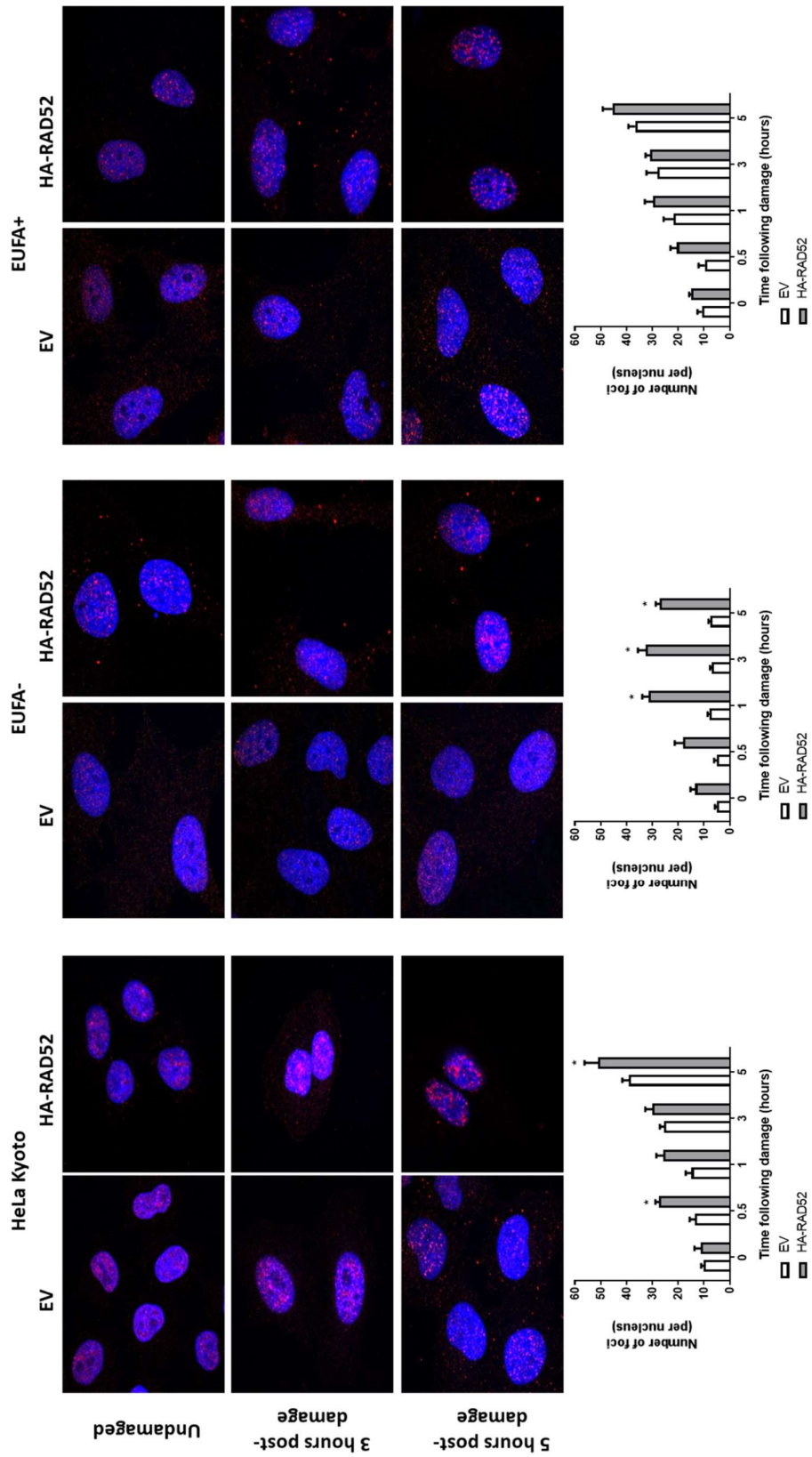

Figure 17: Ectopic expression of HA-RAD52 induces the formation of nuclear RAD51 foci in BRCA2-deficient cells. Cells were transfected with a plasmid encoding for HA-RAD52 or an empty-vector (EV) control, and exposed to 5 Gy of ionising radiation 48 hours later. The formation of nuclear RAD51 foci, shown in red, was monitored at the indicated time-points and quantified using ImageJ. The bars represent mean ± SEM of three independent biological repeats (n=3).

To date, confocal microscopy has provided some insights into the mechanism of homologous recombination and RAD51 nucleofilament formation, by enabling the visualisation of microscopic protein aggregates of RAD51, also known as foci, in cells following exposure to DNA damaging agents. However, the resolution of confocal microscopy is limited by a diffraction limit, and hence super resolution microscopy has been developed to monitor the molecular interactions between specific proteins at the nanometer resolution. Previous work in our lab using super resolution microscopy by *d*STORM described the formation of extended RAD51 filaments in cells wild-type for *BRCA2* following DNA damage (Haas *et al.*, 2018). Cells carrying inactivating mutations in *BRCA2*, by contrast, nucleate small focal accumulations of RAD51 that cannot extend into elongated filamentous structures. This highlights the invaluable nature of super resolution microscopy in elucidating HR, since such phenotypic distinctions would not have been possible using confocal microscopy.

Super resolution microscopy was therefore used to further characterise homologous recombination reactions in BRCA2-deficient cells and assess if filament nucleation and/or extension is controlled by human RAD52. In these experiments, RAD52 was hypothesised to be an alternative mediator protein that enables minimal RAD51 nucleation but cannot support filament extension in human cells with BRCA2 deficiencies. Data obtained in HA-RAD52 over-expressing cells showed an enhancement of RAD51 nucleation in EUFA- cells (figure 18), with multiple discrete RAD51 nuclei arranged linearly, possibly on the same DNA molecule. In support with our hypothesis, no elongated filaments are observed in these cells, confirming that RAD52 has a potential role in RAD51 nucleation but not extension. Therefore, the data suggest that the C-terminal domain of BRCA2 is essential for filament elongation and/or stabilisation (Haas *et al.*, 2018). Furthermore, ectopic expression of HA-RAD52 did not have an effect on RAD51 nucleofilaments in EUFA+ cells, and thus RAD52 does not appear to influence RAD51 filament length.

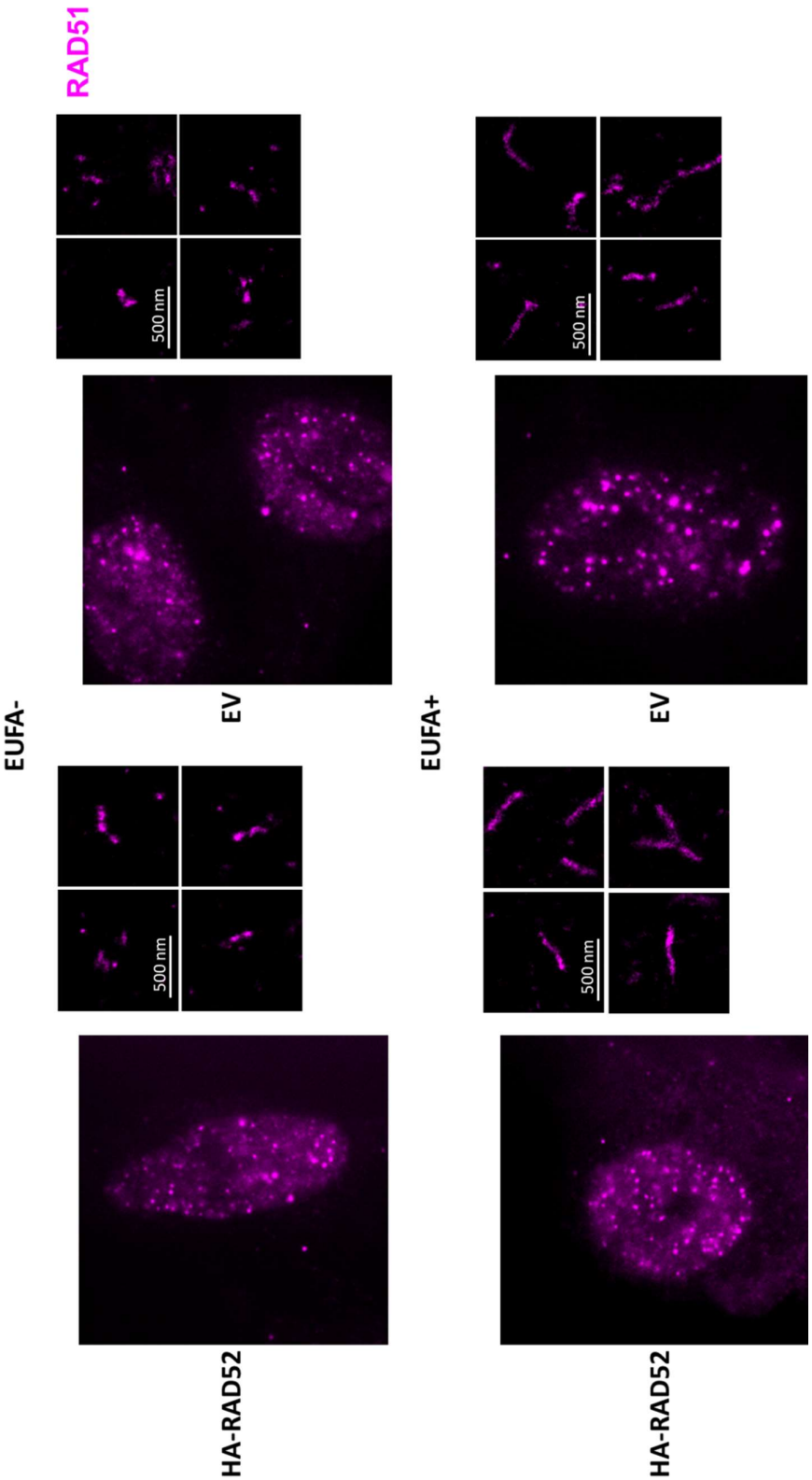

Figure 18: Ectopic expression of HA-RAD52 does not promote filament extension in BRCA2-deficient cells. Immunofluorescence images of EUFA423 cells transfected with a plasmid encoding for HA-RAD52 or an empty-vector (EV) control. Cells were exposed to 5 Gy of ionising radiation 48 hours post-transfection. The formation of nuclear RAD51 foci, shown in magenta, was monitored by *d*STORM at 3 hours following IR-induced damage.

1.3.2 RAD51 assembly on DNA is compromised following RAD52 depletion in cells deficient in BRCA2

My observations thus far suggest that RAD52 has a regulatory role on the assembly of RAD51 foci in cells, both in the presence and absence of a functional BRCA2 protein. Since my hypothesis proposes that RAD52 regulates the activity of RAD51 in the absence or deficiency of *BRCA2*, I then proceeded to RAD52 knockdown by siRNA in the three cell lines with wild-type or mutant *BRCA2*. Cells were then exposed to 5 Gy of IR and RAD51 focalisation was followed before and after IR damage, as before. RAD52 depletion did not affect RAD51 foci formation in cells containing wild-type *BRCA2*, as exemplified by HeLa Kyoto and EUFA+ cells, which contained 42 ± 5 and 38 ± 4 of RAD51 foci per cell, respectively, in both siRAD52 and control siRNA transfected cells at 5 hours following damage (figure 19). In contrast, RAD52 depletion in EUFA- cells led to a reduction in the number of damage-induced RAD51 foci, with the same number of nuclear foci observed before and after exposure to IR. Five hours following IR exposure, the number of damage-induced foci was found to decrease from 9 ± 1 to 4 ± 1 foci per cell, with an average of 4 ± 1 RAD51 foci also found in un-irradiated cells that had been depleted of RAD52. This suggests that reducing RAD52 levels in BRCA2-deficient cells minimises focus formation by RAD51 and hence RAD51-dependent DNA repair. Furthermore, any RAD51 foci observed in EUFA- cells following RAD52 knockdown could be as a result of a residual BRCA2 activity exhibited by the truncated protein in these cells.

To further describe the role of RAD52 in cells with differing *BRCA2* status, I assessed RAD51 focalisation in HeLa Kyoto cells heterozygous for the 6174delT or 3036del4 mutation in *BRCA2*. To this end, the stable cell lines expressing shRAD52 were treated with 5 Gy of IR and RAD51 focus formation was followed at the pre-determined timepoints before and after DNA damage (figure 20). RAD51 focalisation is comparable between the parental HeLa Kyoto cells and the +/6174delT and +/3036del4 cell lines, as indicated by the similar numbers of foci formed in the three cell lines pre- and post- DNA damage. This suggests that BRCA2 heterozygosity does not compromise the ability of cells to form RAD51 foci. Furthermore,

RAD52 depletion in these does not seem to affect RAD51 functionality in terms of foci formation.

In summary, these observations suggest that BRCA2 is the primary HR mediator in human cells, and a single wild-type copy of the protein is sufficient to maintain RAD51 focalisation in heterozygous settings. In the absence of a functional copy of BRCA2, however, my data propose that RAD52 takes over to mediate RAD51 loading and/or assembly on DNA. More precisely, RAD52 seems to facilitate the nucleation of RAD51 assemblies but does not support filament extension to the lengths previously observed in the presence of BRCA2, as suggested by the *d*STORM data obtained following HA-RAD52 over-expression in EUFA- cells.

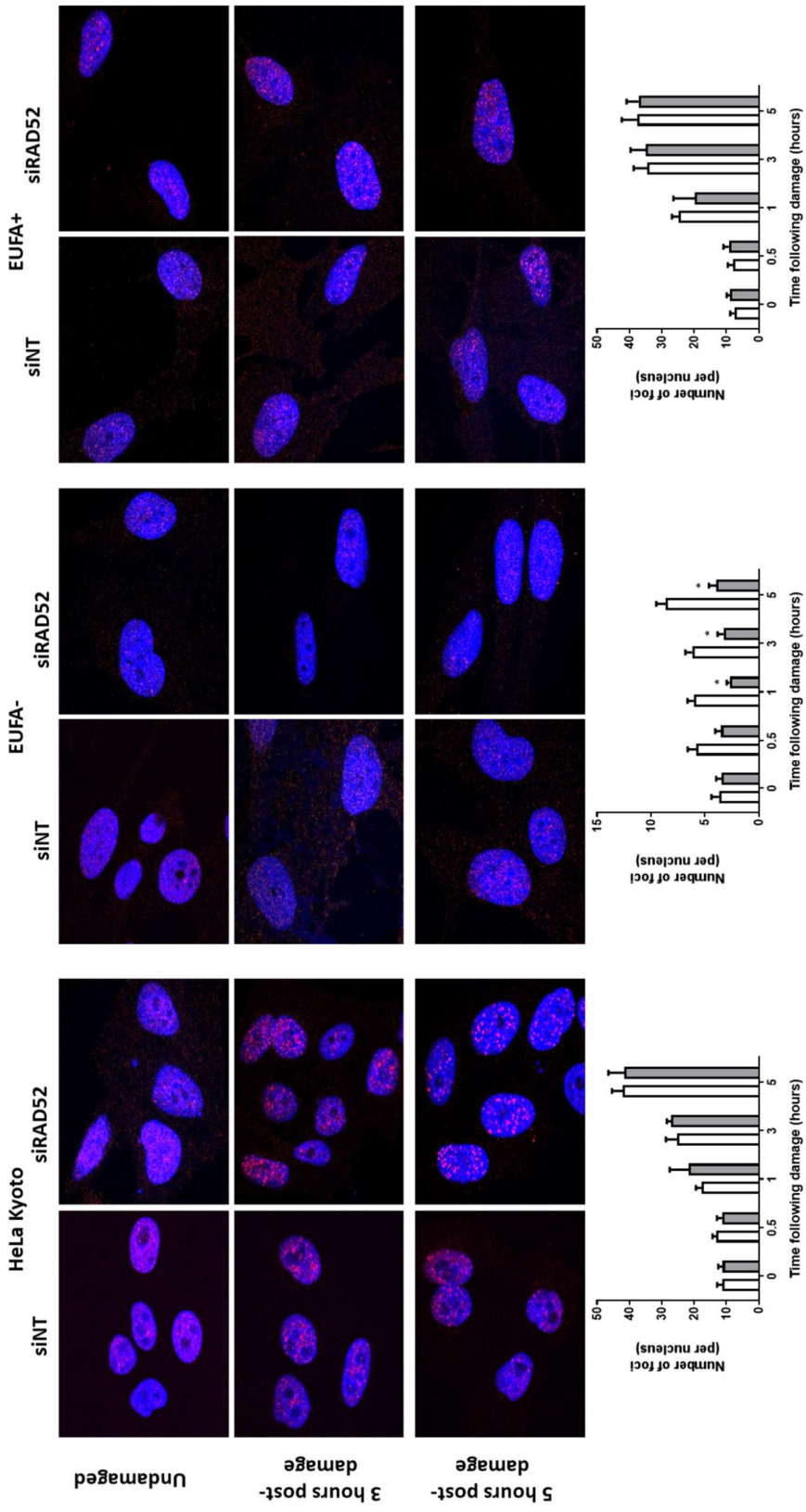

Figure 19: Depletion of RAD52 causes decreased formation of nuclear RAD51 foci in BRCA2-deficient cells. Cells were transiently transfected with siRAD52 or non-targeting control siRNA (siNT), and exposed to 5 Gy of ionising radiation 48 hours later. The formation of nuclear RAD51 foci, shown in red, was monitored at the indicated time-points and quantified using ImageJ. The bars represent mean ± SEM of three independent biological repeats (n=3).

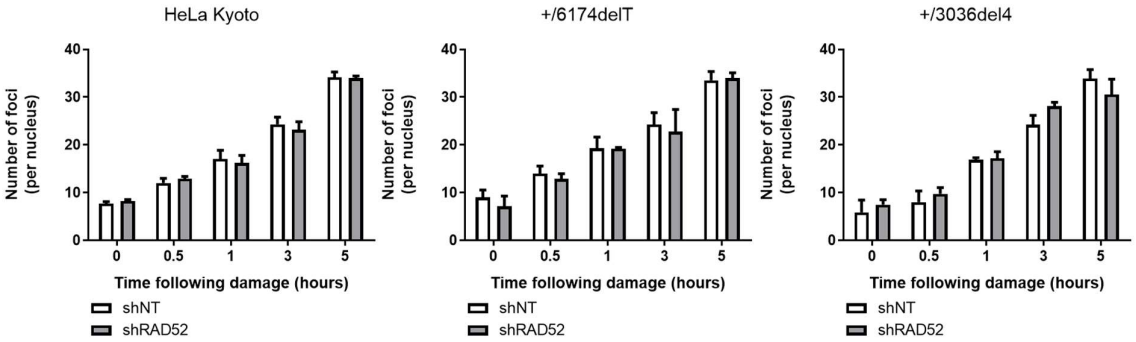

Figure 20: Depletion of RAD52 does not affect the formation of nuclear RAD51 foci in cells heterozygous for BRCA2. Cells stably expressing shNT or shRAD52 were exposed to 5 Gy of ionising radiation. The formation of nuclear RAD51 foci was monitored and quantified at the indicated time-points using ImageJ. The bars represent mean ± SEM of two biological repeats (n=2).

1.4 HR efficiency is further reduced following RAD52 depletion in cells lacking BRCA2

Since RAD52 was found to regulate RAD51 focalisation in BRCA2 deficient cells, I then wanted to assess the HR proficiency of RAD52-depleted cells using the Cas9/mClover assay. This method was developed by Pinder, Salsman and Dellaire, 2015, and measures the HR-dependent repair of a Cas9-generated DSB generated within the LaminA gene, using a homologous template plasmid carrying an mClover tag. Cells proficient in HR hence express green fluorescent LaminA and can be detected by immunofluorescence. For this assay, the cell lines stably expressing shRAD52 were co-transfected with a plasmid encoding Cas9-sgRNA and the mClover-containing template for 72 hours before assessing green fluorescence in these.

RAD52 depletion causes a reduction in the number of mClover-positive cells in comparison to the respective shNT control in all the cell lines used (figure 21). These observations thus confirm that RAD52 is important for HR in cells irrespective of their *BRCA2* status. However, cells that are wild-type or heterozygous for *BRCA2* do not exhibit a statistically significant decrease in HR proficiency following RAD52 depletion, with an observed reduction of up to 13% in these. On the other hand, the observed decrease in HR proficiency following RAD52 depletion in the BRCA2-deficient EUFA- cells is remarkable, owing to their lack of a fully functional *BRCA2* allele and their dependence on RAD52 to execute HR. Of note, the BRCA2 heterozygous cell lines are not compromised in HR functionality, as the population of mClover-positive cells is comparable to that of the parental HeLa Kyoto cell line that bears two wild-type copies of *BRCA2*.

Overall, these results indicate that BRCA2 is the predominant mediator protein for HR, a function that is compensated for by human RAD52 in the absence of a wild-type BRCA2 allele, as in the case of EUFA- cells.

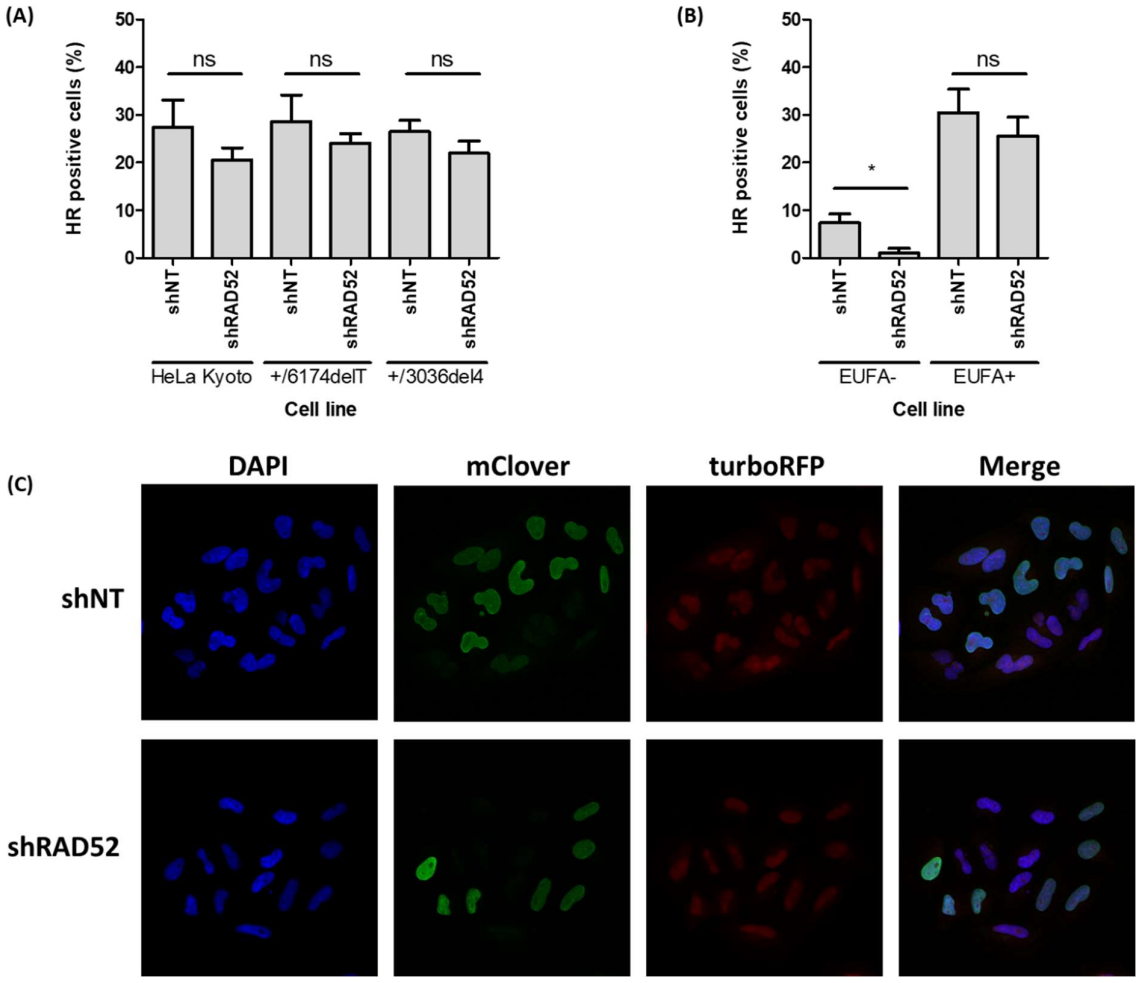

Figure 21: Depletion of RAD52 leads to a reduction in HR-proficiency in BRCA2-deficient cells. The mClover-LMNA assay was used to assess HR proficiency in the HeLa Kyoto **(A)** and EUFA423 **(B)** cell lines following stable depletion of endogenous RAD52. The repair of a Cas9-induced DSB was determined by monitoring expression of the mClover reporter three days following cell transfection. Quantification of mClover-positive cells indicates the percentage of cells that are proficient in HR-mediated DNA repair within a specific cell population. The graphs are representative of at least two independent experiments. **(C)** Representative immunofluorescence images of the HeLa Kyoto +/3036del4 cell line in control- and RAD52-depleted cells.

1.5 RAD52 regulates the sub-cellular distribution of RAD51 in cells

The observation that RAD52 affects RAD51 focalisation in BRCA2-deficient cells led me to investigate the mechanism by which this happens. BRCA2 has been previously shown to direct the nucleo-cytoplasmic distribution of RAD51 (Jeyasekharan *et al.*, 2013), and hence I wanted to test whether RAD52 similarly affects the sub-cellular localisation of RAD51 to facilitate recombinase loading on DNA for subsequent DNA repair. In order to examine this possibility, I assessed the total protein levels and the sub-cellular localisation of RAD51 and BRCA2 in RAD52-depleted cells using the cell line panel stably expressing shNT or shRAD52.

As shown in figure 22, RAD52 depletion does not affect the total protein levels of RAD51. However, RAD52 appears to promote the appropriate sub-cellular localisation of RAD51, as demonstrated by the fact that the recombinase shows reduced chromatin localisation in cells that are deficient in both RAD52 and BRCA2 under un-damaged conditions (figure 23). This phenotype is not apparent in the +/6174delT cell line, potentially owing to the presence of BRC repeats within both *BRCA2* allele products in these cells. However, in the +/3036del4 cells where no BRC repeats are retained on the mutated BRCA2 protein, RAD51 localisation to chromatin is severely compromised following RAD52 depletion. This observation is analogous in EUFA- cells which contain two mutant *BRCA2* alleles. Interestingly, in cells where BRCA2 is intact, such as the HeLa Kyoto and EUFA+ cells, the protein exhibits enhanced recruitment to chromatin upon RAD52 depletion, which is accompanied by improved chromatin loading of RAD51 in comparison to the respective shNT control. Upon exposure to IR, however, RAD52 depletion diminishes RAD51 localisation to chromatin in all the cell lines used, irrespective of their BRCA2 status (figure 24).

Overall, these data suggest that RAD52 has a BRCA2-independent function in facilitating RAD51 localisation on chromatin in cells. Requirement for this RAD51-loading activity of RAD52 differ in cells depending on their BRCA2 status and/or exposure to DNA damage.

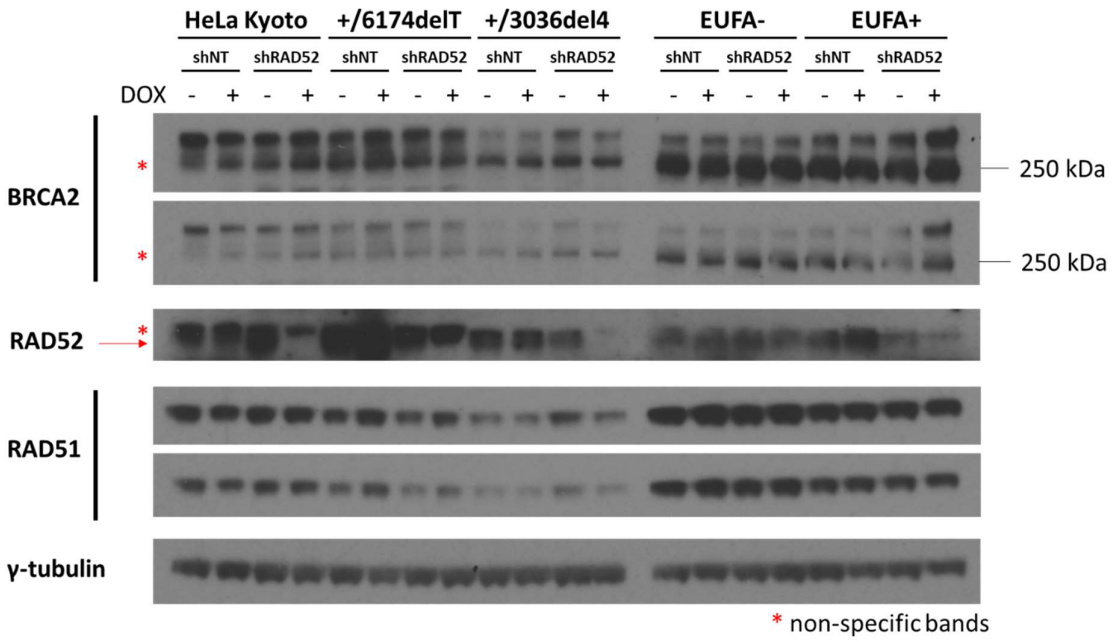

Figure 22: RAD52 depletion does not affect the total protein levels of BRCA2 and RAD51 in cells. Whole protein extracts were obtained from transduced cells prior to and following doxycycline induction (1 µg/ml, 48 hours) of the shRNA constructs. Western blot analysis was then performed to assess the total protein levels of BRCA2 and RAD51 in cells. RAD52 runs as a doublet due to an upper non-specific band, as indicated by the star. Asterisks (*) denote non-specific bands.

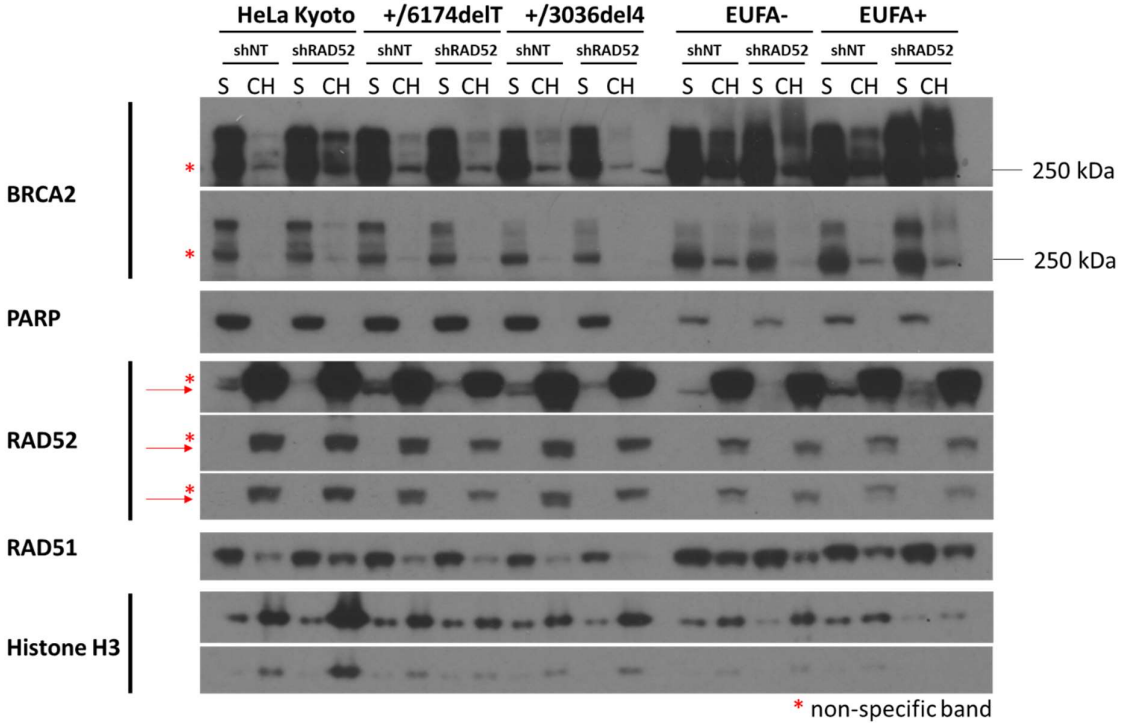

Figure 23: RAD52 controls the sub-cellular localisation of RAD51 in cells. Sub-cellular fractionation was performed in un-treated cells to obtain soluble (S) and chromatin (CH) bound protein fractions. PARP and Histone H3 were used as loading controls for the soluble and chromatin fractions, respectively. RAD52 runs as a doublet due to an upper non-specific band, as indicated by the star. Asterisks (*) denote non-specific bands.

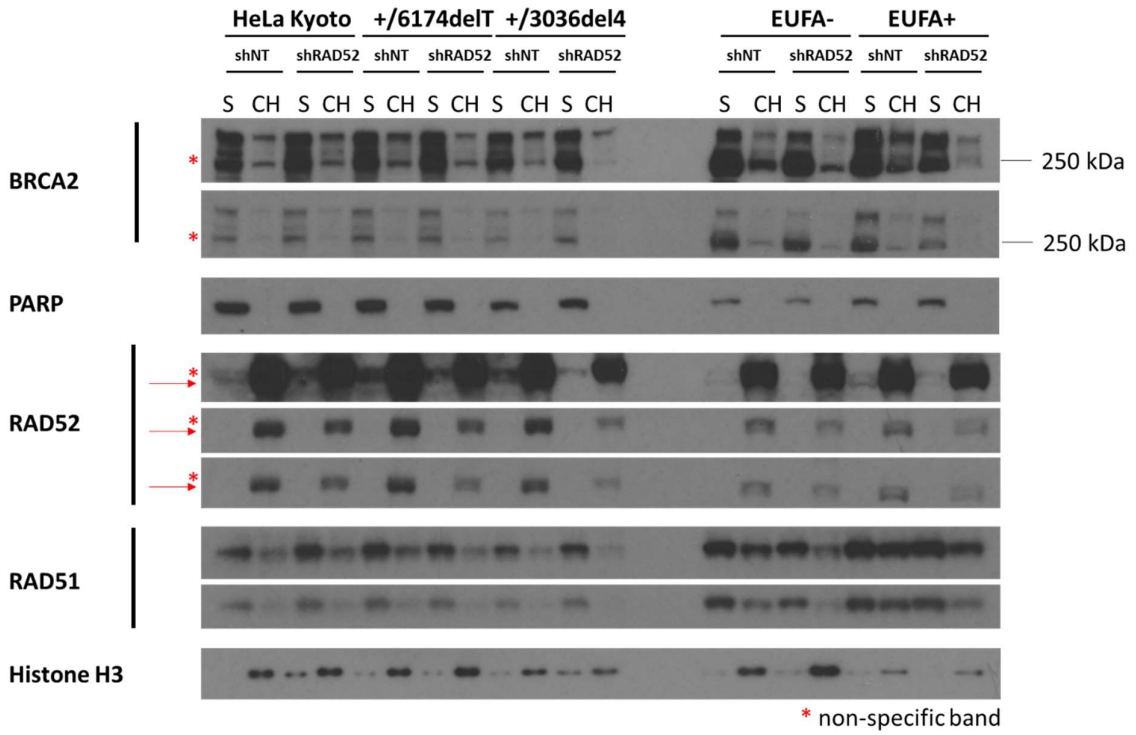

Figure 24: RAD52 controls the sub-cellular localisation of RAD51 in cells after 5 hours of IR treatment. Sub-cellular fractionation was performed in cells to obtain soluble (S) an chromatin (CH) bound protein fractions. PARP and Histone H3 were used as loading controls for the soluble and chromatin fractions, respectively. RAD52 runs as a doublet due to an upper non-specific band, as indicated by the star. Asterisks (*) denote non-specific bands.

DISCUSSION

RAD52 has been described to be synthetically lethal with HR deficiency in a variety of cancers, ranging from breast, ovarian, pancreatic and leukemic cell models (Feng *et al.*, 2011; Cramer-Morales *et al.*, 2013; Lok *et al.*, 2013). These observations were reported following depletion or biallelic mutation of BRCA2, where the protein function was severely abrogated. Therefore, the molecular mechanism of this described synthetic lethality was examined in a panel of cell lines with different genetic backgrounds in *BRCA2*.

To first validate the reported synthetic lethal relationship between RAD52 and BRCA2 in human cells, I evaluated the effect of RAD52 depletion in cells in terms of proliferation rate and survival. Loss of RAD52 only modestly affects the survival of cells that are wild-type or heterozygous for *BRCA2* mutations, while causing an evident decrease in the colony forming capacity of cells that are biallelic mutant for BRCA2. Abrogation of RAD52 activity causes a proliferation rate reduction, even in cells that are wild-type or heterozygous for *BRCA2.* This observation suggests that that the protein is required for supporting the proliferation of normal cells. Cells heterozygous for the 6174delT mutation, which truncates BRCA2 within the BRC7 repeat, experienced an enhanced reduction following RAD52 loss, when compared to the parental cell line carrying two wild-type copies of *BRCA2*. Cells heterozygous for the 3036del4 mutation that truncates BRCA2 before the first BRC repeat, exhibited an even more pronounced proliferation defect following RAD52 depletion. The observed defect is likely more severe in these cells owing to the complete lack of a BRC repeat in the truncated *BRCA2* allele, in contrast to the +/6174delT cells which retain seven out of the eight BRC repeats on the truncated protein product. These observations suggest that with increasing loss of BRCA2 BRC repeats, there is an enhanced compromise in protein functionality coupled to an augmented reliance on RAD52 for supporting cellular proliferation. This difference between the two heterozygous cell lines suggests a role of RAD52 in supporting the proliferation of cells, which is more pronounced upon loss of BRC repeats in the expressed BRCA2 protein. Overall, the two BRCA2 heterozygous cell lines exhibit a similar proliferation defect relative to their parental HeLa Kyoto cell lines. For instance, the heterozygous cells initially proliferate

as rapidly as the BRCA2 wild-type counterparts, as indicated by the overlapping proliferation curves up until two days of growth (50 hours, figure 11). However, with successive divisions, cells bearing an allele of truncated BRCA2 become progressively more impaired in terms of proliferation rate. Such a phenotype has been previously described for truncating BRCA2 mutations in mice (Patel *et al.*, 1998), and indicates that loss of one wild-type *BRCA2* allele is sufficient to limit BRCA2 function and activity to a quantitively significant extent. In fact, loss of one *BRCA2* allele has been reported to be sufficient for driving carcinogenesis (Skoulidis *et al.*, 2010; Tan *et al.*, 2017). These observations have led to the hypothesis that BRCA2 mutants have a dominant-negative nature or alternatively lead to a decrease in BRCA2 expression levels that induces protein haploinsufficiency (Jeyasekharan *et al.*, 2013; Tan *et al.*, 2017). Notably, EUFA- cells which harbour biallelic mutations of *BRCA2*, exhibit the most severe growth defect following abrogation of RAD52 activity. The growth curve of EUFA- cells is flat, with the cells exhibiting a 70% decrease in proliferation rate in comparison to the shNT control. This observation is in line with Feng *et al.*, 2011, who originally reported that RAD52 depletion is synthetically lethal with BRCA2 deficiency in human cells. However, EUFA- cells harbouring shRAD52 can be seen dividing during the experiment, owing to the trackable turboRFP reporter found within the shRNA construct (figure 13). In fact, live cell monitoring by Incucyte indicated that fluorescently red cells do not exhibit any morphological features characteristic of cell death, such as shrinking and blebbing. This observation creates two non-exclusive implications. Firstly, concomitant loss of both RAD52 and BRCA2 might not actually be synthetic lethal, according to the strict definition of synthetic lethality, but induces synthetic sickness associated with a severe proliferation defect in cells instead. Secondly, deficiency in both proteins possibly allows cells to eventually bypass the induced proliferation block through pathways that potentially lead to genomic instability. Reports of enhanced chromosomal instability in cells that are doubly deficient in BRCA2 and RAD52 are in line with this hypothesis (Feng *et al.*, 2011).

These observations collectively indicate a role for RAD52 in supporting the proliferation of cells, which is uncovered upon loss of one wild-type BRCA2 allele but ultimately becomes essential following loss of the second wild-type allele. In the BRCA2 heterozygous settings,

the role of RAD52 becomes more pronounced when the truncating mutation leads to loss of all BRC repeats within the protein product of BRCA2. Since BRC repeats are responsible for RAD51 loading on ssDNA and, thus, conferring the mediator activity of BRCA2 (Shivji et al., 2006, 2009; Carreira et al., 2009), this observation suggests that RAD52 has a recombination mediator role in human cells. Such a function for the Rad52 protein has not been described in organisms containing BRCA2 homologues thus far, with the two proteins thought of having separate functions in humans, whereby RAD52 is solely an annealer protein whereas BRCA2 acts as a mediator stimulating strand exchange by RAD51 instead. Interestingly, the BRCA2 homologue in *U. maydis*, Brh2, appears to bear both mediator and annealing functions, thus being capable of assembling Rad51 filaments and capturing the second DNA end to enable completion of DSB repair. However, deletion of the DNA binding domain of Brh2 can be partially compensated for by Rad52, thus providing evidence that Rad52 might be required for homologous directed-DNA repair in organisms carrying a BRCA2 homologue (Kojic et al., 2012). The fact that the N-terminal domain of Rad52, which contains the DNA annealing activity of the protein, cannot fully compensate for the loss of the DNA binding domain of Brh2, further supports the idea that Rad52 can play both annealing and mediator roles in a Brh2-defective background (Kojic et al., 2012). In fact, *U. maydis* lacking the DNA-binding domain of Brh2 rely on Rad52 for repair and survival following UV-induced damage (Kojic, Milisavljevic and Holloman, 2018). Therefore, organisms containing BRCA2 homologues with Rad51-interacting BRC elements appear to have a back-up recombination mediator function served by Rad52. Remarkably, both Brh2 and Rad52 contain F(P/T)P motifs in *U. maydis*, elements that were originally identified for mediating Rad51 interaction and enabling DNA repair proficiency (Thorslund, Esashi and West, 2007; Kojic et al., 2012). Importantly, BRCA2 also bears such a motif which is accountable for the protein's interaction with the meiosis-specific DMC1 recombinase, a RAD51 paralogue (Thorslund, Esashi and West, 2007). Altogether, these lines of evidence further consolidate a potential recombination mediator role for the human RAD52 protein, which only becomes apparent when BRCA2 is defective.

Although still far from characterising the role of human RAD52 in homologous recombination and how this regulates RAD51 filament assembly, this work indicates that RAD52 plays a

mediator role and induces RAD51-dependent repair following ionising damage in human cells. Firstly, the fact that HA-RAD52 is diffuse throughout the nucleus of un-irradiated cells but forms discrete nuclear foci following IR exposure indicates its involvement in mammalian DNA repair. Formation of distinct HA-RAD52 foci in all the cell lines used indicates that RAD52 focalisation and possibly activity is independent of the BRCA2 status of the cells, as has been previously suggested by Feng et al. 2011. In addition, the co-localisation observed between HA-RAD52, RAD51 and RPA, provides molecular evidence that these proteins cooperate in DNA damage responses to IR to attempt repair via HR (figure 16). Despite co-localisation between the three proteins at nuclear foci, HA-RAD52 co-localised to a greater extent with RPA than RAD51 in the tested cell lines. The two proteins reached almost complete co-localisation at 5 hours following IR exposure, potentially indicating a mediator role for RAD52 in promoting RPA displacement from ssDNA, which had not been previously identified in mammalian organisms. Although this function has not been verified biochemically by *in vitro* assays (Mcilwraith *et al.*, 2000; R B Jensen, Carreira and Kowalczykowski, 2010), structures of the DNA-binding domain of human RAD52 revealed a positively charged groove that binds and distorts DNA in a conformation that disrupts RPA-ssDNA contacts (Singleton *et al.*, 2002; Grimme *et al.*, 2010). Therefore, the displacement of RPA from ssDNA by RAD52 to encourage RAD51 loading seems to be plausible by a hand-off mechanism in which RAD52 and RAD51 compete for RPA binding (Jackson *et al.*, 2002). Furthermore, deleting the RPA binding domain of RAD52 has been shown to reduce recombination frequency in monkey cells, thus suggesting that DSB repair by homologous recombination in mammalian cells actually depends on the *in vivo* interaction between RAD52 and RPA (Park *et al.*, 1996). Interestingly, not all RAD51 foci co-localise with HA-RAD52 and RPA, implying additional roles for HA-RAD52 and RPA other than RAD51-dependent repair, as already suggested for yeast Rad52 (Tuskamoto *et al.*, 2003). In a similar manner, the human RAD52 protein might perform RAD51-independent functions at IR-induced foci.

Importantly, in contrast to BRCA2-proficient cells, HA-RAD52 focalisation in EUFA- cells is more prominent and occurs earlier following DNA damage by IR. This could either indicate the resolution of damage in cells with wild-type *BRCA2*, or highlight the greater degree of

dependence on HA-RAD52, and hence endogenous RAD52, upon DNA damage induction in BRCA2-deficient cells. If the latter is true, this would further support the idea that RAD52 promotes RAD51 foci formation in mammalian cells that lack wild-type BRCA2 functionality. Moreover, both HeLa Kyoto and EUFA+ cells, which serve as our models for wild-type BRCA2, contained less damage-induced HA-RAD52 foci compared to EUFA- cells. This implies that RAD52 is not an absolute requirement for RAD51-dependent HR in BRCA2-proficient cells, or that low protein levels that are not detectable as foci by confocal microscopy are involved in DNA repair processes in such cells. Nevertheless, HA-RAD52 focalisation occurs in these cell lines, both of which contain fully functional BRCA2, thus indicating that RAD52 potentially serves additional functions in cells that are wild-type for *BRCA2*. The later focalisation observed in BRCA2-proficeint backgrounds suggests that RAD52 might have a more significant post-synaptic role in cells which are wild-type for *BRCA2*, but might serve additional roles earlier during synapsis in BRCA2-deficient cells, like the yeast Rad52 protein (Miyazaki *et al.*, 2004).

Genetic manipulation of the protein levels of RAD52 revealed that the protein regulates RAD51 assembly on DNA in BRCA2-deficient cells, but not in cells that are wild-type or heterozygous for *BRCA2*. Briefly, ectopic over-expression of HA-RAD52 consistently enhanced RAD51 foci numbers in the BRCA2-deficient EUFA- cells, whereas a slight but non-significant increase was observed in BRCA2-proficient cells (figure 17). Conversely, depleting endogenous RAD52 by either siRNA or shRNA caused a decrease in the assembly of IR-induced RAD51 foci in the EUFA- cell line, whilst cells that are either wild-type or heterozygous for *BRCA2* did not exhibit such a defect (figures 19 and 20) . The fact that the BRCA2 heterozygous cell lines are not compromised in RAD51 focalisation, suggests that one wild-type copy of *BRCA2* is sufficient to enable RAD51 assembly on DNA and subsequent recombinase activity following IR-induced DNA damage. Notably, EUFA- cells depleted of RAD52 contained the same number of RAD51 foci pre- and post- irradiation. This observation suggests that cells doubly deficient in BRCA2 and RAD52 are incapable of eliciting a RAD51-dependent DNA damage response, therefore implying that the truncated protein products of BRCA2 exhibit little residual activity in EUFA- cells. These data are in agreement with previous reports, where

human RAD52 was shown to regulate RAD51 focus formation in BRCA1- or BRCA2-deficient backgrounds (Feng *et al.*, 2011; Lok *et al.*, 2013). Cells have actually been previously described of being capable to form BRCA2-independent RAD51 foci (Tarsounas, Davies and West, 2003; Haas *et al.*, 2018). The study by Feng *et al.*, 2011 was, however, the first one to propose that RAD52 has functions in human HR, by showing that low levels of RAD52 correlate with reduced RAD51 foci, HR and growth rate in cells that lack full BRCA2 functionality. Importantly, RAD52 focalisation was not found to be affected by the BRCA1/2 status of cells (Feng *et al.*, 2011; Lok *et al.*, 2013), thus suggesting that RAD52 acts as an independent mediator protein that drives an alternative repair pathway of RAD51-mediated HR. Furthermore, RAD52 depletion was described to have a small effect on RAD51-dependent HR in the presence of wild-type BRCA2, but instead had a big impact in cells upon loss of BRCA2. Therefore, RAD52 was dubbed to be essential for the proliferation of cells with no or low BRCA2 function, due to its role in maintaining the minimum required threshold of RAD51 activity in these.

As suggested by the observations in *U. maydis*, Rad52 is required to act both as a mediator and an annealer upon loss of the DNA binding domain in Brh2, which is the major mediator protein in this eukaryotic organism. This could also be the case in EUFA423 cells, in which RAD52 appears to be essential for RAD51 foci formation owing to the loss of the DNA-binding domain in one of the two BRCA2 alleles. This is further supported by the later focalisation of HA-RAD52 in EUFA+ cells in comparison to EUFA- cells, with the latter appearing to rely on RAD52 both early and late after damage, as suggested by HA-RAD52 focalisation that can be detected from 30 minutes up to 5 hours following damage. This dependence on RAD52 that is observed early after damage in BRCA2- defective but not proficient cells could be as a result of the more extensively truncated version of BRCA2, lacking the DNA binding domain, acting in a dominant negative manner in EUFA423 cells. Recently, a study revealed that BRCA2 dimerises to recruit two sets of RAD51 molecules in opposing directions. Upon ssDNA binding by the C-terminal domain of BRCA2, which is localised at the outer rim of the dimer, only one of two RAD51 sets is in the correct polarity to form filaments in the 3'-5' direction (Shahid *et al.*, 2014). According to this study, BRCA2 can still dimerise in EUFA- cells, given that the C-

terminus of the protein does not contribute to dimerisation and is localised at the outer surface of the dimer. However, this model creates an important implication, where C-terminal truncations of BRCA2 can result to inactive dimers if the set of RAD51 monomers with the correct polarity is bound by the more extensively C-terminally truncated version of BRCA2 that lacks a DNA binding domain. This implication thus provides a potential mechanism by which C-terminal truncations of BRCA2 can act in a dominant-negative manner.

Previous observations in our lab by super-resolution microscopy revealed that RAD51 foci are found in cells following BRCA2 knockdown (Haas *et al.*, 2018), although these are formed away from RPA foci located at sites of DNA damage. This suggests that other mediator proteins, like RAD52, are loading RAD51 on DNA. RAD51 filament formation is proposed to occur in two steps: the rate-limiting nucleation of RAD51 monomers followed by the rapid extension by protein multimers (Heijden *et al.*, 2007; Hilario *et al.*, 2009). To further investigate at which steps of RAD51 assembly RAD52 might be playing a role in, super-resolution microscopy was used to assess RAD51 foci to near atomic resolution and facilitate the discrimination between filament nucleation and elongation. Data obtained with this technique revealed the presence of extended RAD51 filaments in Flag-BRCA2 complemented EUFA+ cells following IR. This contrasts with the BRCA2-deficient EUFA- cell line, which only exhibited clusters or nuclei of RAD51 molecules upon DNA damage. This suggested that the truncated BRCA2 protein products expressed in EUFA- cells are incapable of supporting the extension and/or stabilisation of RAD51, thus preventing the formation of elongated RAD51 filaments. HA-RAD52 over-expression did not alter the length of the RAD51 nuclei observed in EUFA- cells and did not cause any additional extension in the assembled filaments of EUFA+ cells (figure 18). This suggests that RAD52 cannot promote or support the extension of RAD51 nuclei into elongated filaments. However, an enhanced number of discrete RAD51 nuclei was observed in EUFA- cells, suggesting that HA-RAD52 can encourage the primary oligomerisation of RAD51 into small nuclei for promoting repair. In contrary, depletion of RAD52 reduced the number of such nuclei in these cells, whilst not having any observable effect in the EUFA+ cell line. These observations suggest that RAD52 can mediate the initial loading of RAD51 on ssDNA at sites of DNA damage to form nuclei, in an independent

mechanism from BRCA2. However, formation of elongated RAD51 filaments can only be attributed to BRCA2 activity in cells, which is thought to be the only protein capable of orchestrating RAD51 activity during homology search and resolution (Whelan *et al.*, 2018). Nevertheless, when compared to extended RAD51 filaments, the assembly of nuclei as encouraged by RAD52 might not be able to optimally repair DNA damage, but such RAD51 structures seem to suffice in enabling cell viability and/or proliferation of BRCA2-deficient cells.

RAD51 focalisation is very commonly used as a surrogate measure of HR proficiency in cells. Nonetheless, in order to directly address the role of human RAD52 in homologous DNA repair, the Cas9/mClover assay was employed, whereby the repair of a Cas9-induced DSB makes cells become fluorescently green. Therefore, this technique enables cells which are proficient in HR to be recognised, tracked and enumerated owing to their green fluorescence. RAD52 depletion was found to decrease HR efficiency in cells, even those which are BRCA2-proficient. The effect, however, was minimal in cells that contain at least one wild-type allele of *BRCA2*, with up to ~13% reduction observed in cells that are wild-type or heterozygous for *BRCA2*. Such a modest decrease in HR following RAD52 loss had been previously seen in MCF7 cells (Feng *et al.*, 2011), which are also wild-type for *BRCA2*. These data suggest that RAD52 has roles in HR, even when BRCA2 is present and fully functional in cells. Moreover, despite being BRCA2-deficient, the EUFA- cell line exhibits residual levels of HR, as previously observed by Sullivan-Reed *et al.*, 2018 for other BRCA-deficient models. This provides further evidence that additional proteins other than BRCA2, such as RAD52, are responsible for supporting DNA repair via HR in cells. This hypothesis is validated by the fact that RAD52 depletion in EUFA- cells eliminates any residual HR activity in these. Collectively, these observations suggest that RAD52 promotes HR in cells irrespective of their BRCA2 status, but protein activity becomes essential for enabling HR-mediated repair in the absence of a functional BRCA2 protein product.

The main protein responsible of controlling RAD51 loading on DNA and subsequent filament assembly in human cells is BRCA2. However, as revealed by confocal and super-resolution

microscopy, the human RAD52 protein is also accountable for regulating the accumulation of RAD51 at sites of DNA damage. A mechanism by which protein activity can be regulated is through control of its sub-cellular localisation. In fact, BRCA2 has been previously described to control the nuclear localisation of the recombinase, by masking a NES and preventing protein export to the cytoplasm (Jeyasekharan *et al.*, 2013). Nevertheless, the association of RAD51 with chromatin during S-phase has also been shown to occur independently of BRCA2 (Tarsounas, Davies and West, 2003). Hence, to investigate the molecular mechanism by which abrogation of RAD52 activity leads to reduced assembly of RAD51 on DNA and subsequent HR-mediated DNA repair in BRCA2-deficient cells, I assessed if RAD52 plays any roles in directing RAD51 localisation within different sub-cellular compartments. To this end, fractionation of cells was performed to check the soluble and chromatin-bound fractions of the recombinase following stable depletion of RAD52 in these.

RAD52 was found to affect RAD51 sub-cellular localisation under both un-damaged and IR-treated conditions, minimising the chromatin localisation of the recombinase (figures 23 and 24). However, the observed effect was more pronounced following DNA damage, under which RAD52 seems to affect the sub-cellular localisation of RAD51 in all cell lines, irrespective of their BRCA2 status. Therefore, the role of RAD52 in regulating RAD51 localisation and hence activity becomes more critical following IR-induced DNA damage, even in cells that are wild-type for *BRCA2*. Additionally, the fact that the protein levels of full-length BRCA2 are reduced in the +/6174delT and +/3036del4 heterozygous cell lines (figure 22) potentially indicates that these cells exhibit a BRCA2 insufficiency, which in turn renders them more susceptible to RAD52 depletion and further impairs RAD51 localisation to the correct sub-cellular compartments upon RAD52 loss. This observation could also suggest a dominant negative nature for BRCA2 truncating mutations in the heterozygous setting, in terms of dictating accurate RAD51 sub-cellular localisation.

Interestingly, RAD52 depletion in the two BRCA2 wild-type models used, HeLa Kyoto and EUFA+, seems to enhance RAD51 localisation to chromatin. This potentially indicates that cells can sense lack of RAD52 and trigger other RAD52-independent pathways to correct for the

RAD51 mis-localisation observed in the protein's absence. Furthermore, this observation implies that RAD52 is the primary protein involved in loading RAD51 onto chromatin at sites of DNA damage. If the primary mechanism of RAD51 loading on DNA fails, then cells switch to an alternative one that does not rely on RAD52 and likely involves BRCA2. If this holds true, RAD52, thus, lies upstream of BRCA2 in loading RAD51 on DNA. This model is supported by Whelan *et al.*, 2018, where RAD52 has been described to mediate initial RAD51 loading on ssDNA at single-ended DSBs. According to the authors, BRCA2 can functionally substitute RAD52 activity in loading RAD51 on DNA, which can potentially explain the lack of a phenotype in eukaryotic models of RAD52 knockout (Rijkers *et al.*, 1998; Yamaguchi-iwai *et al.*, 1998). As seen in figures 22, 23 and 24, upon RAD52 loss in cells where BRCA2 is intact, there is no change in the total BRCA2 protein levels, but an enhanced chromatin recruitment of the protein enables the improved targeting of RAD51 to sites of DNA damage. The fact that an increased amount of RAD51 is localised on chromatin in BRCA2-proficient settings following RAD52 depletion, as compared to control cells, supports previous biochemical evidence demonstrating that BRCA2 is a more efficient mediator protein in displacing RPA and loading RAD51 on DNA in comparison to RAD52 (R B Jensen, Carreira and Kowalczykowski, 2010).

These results propose a functional redundancy between RAD52 and BRCA2 during HR in human cells, whereby RAD52 is dispensable for RAD51 regulation in cells that are heterozygous or wild-type for *BRCA2*, but becomes an essential recombination mediator in cells lacking BRCA2. In combination with the fact that the C-terminal region of BRCA2 is thought to be necessary for the stabilisation of elongated RAD51 filaments (Haas *et al.*, 2018), these findings potentially uncover a molecular mechanism in which RAD52 acts upstream of BRCA2 to promote initial RAD51 loading and/or nucleation on DNA. However, the fact that RAD51 recruitment to chromatin is not as severely impacted in cells wild-type for *BRCA2*, indicates that BRCA2 can substitute for the early roles of RAD52 in loading the recombinase on DNA. Such a relationship between RAD52 and BRCA2 has been recently described at single-ended DSBs formed at collapsed replication forks (Whelan *et al.*, 2018), where initial loading of RAD51 is mediated by RAD52 or by BRCA2 in the absence of RAD52. Nevertheless,

subsequent RAD51 activity for homology search seems to be entirely regulated by BRCA2. Finally, the fact that RAD51 recruitment to chromatin is severely compromised in the absence of both BRCA2 and RAD52 might explain the observed synthetic lethality between the two proteins, with RAD51 loading to DNA being the limiting factor for cell viability upon exposure to DNA damage. Indeed, RAD51 nucleation on DNA is considered to be the limiting step in filament assembly for subsequent homologous DNA repair (Heijden *et al.*, 2007; Hilario *et al.*, 2009).

Collectively, data presented in this chapter propose a functional interplay between BRCA2 and RAD52 and provide new mechanistic insights into human HR. In the existing model of HR-mediated DNA repair, BRCA2 is the predominant recombination mediator protein, and a role for RAD52 in supporting this pathway is only unveiled in the absence of a fully functional BRCA2 protein product. According to this model, BRCA2 is the primary protein that supports RAD51 focalisation and formation of extended filaments for subsequent repair by HR in human cells. This statement is supported by the observations that RAD51 focalisation, filament extension and HR efficiency are not compromised in cells harbouring at least one wild-type *BRCA2* allele following RAD52 depletion. However, in the absence of the canonical HR pathway involving BRCA2, human RAD52 takes over to enable a minimal level of RAD51 functionality in terms of DNA assembly and subsequent repair via HR in response to DNA damage. Although there appears to be a functional redundancy between BRCA2 and RAD52 in enabling the minimum threshold of RAD51 activity in cells, RAD52 does not fully compensate for the loss of BRCA2, as revealed by the absence of extended RAD51 filaments in BRCA2-deficient cells. In the updated mechanistic model proposed by my findings (figure 25), RAD52 lies upstream of BRCA2, enabling the initial loading and nucleation of RAD51 on ssDNA, supporting the subsequent BRCA2-dependent assembly of extended filaments. In the absence of RAD52, BRCA2 can substitute for these early roles performed by RAD52, thus enabling DNA loading and chromatin localisation of RAD51 for subsequent DNA repair. In the absence of functional BRCA2, however, the proposed limited nucleation of RAD51 by RAD52 mediator activity seems to suffice for the repair of critical DNA damage, which consequently enables the viability of BRCA2-deficient cells. Multiple discrete RAD51 nuclei on the same DNA

molecule might come together with prolonged periods of time in order to attempt repair of extended regions of DNA damage. However, such nuclei never form fully functional elongated filaments, due to the requirement of the C-terminal domain of BRCA2 in filament elongation and/or stabilisation of extended filaments (Haas *et al.*, 2018). For this reason, RAD51 nuclei likely only sub-optimally repair DNA damage, owing to DNA end-resection occurring un-interrupted at DNA damage sites even in the absence of RAD51 filament assembly and appropriate homologous pairing (Haas *et al.*, 2018). Propagation of unrepaired DNA damage to subsequent cell generations therefore implies that RAD52 supports the viability of BRCA2-deficient cells, potentially at the expense of genomic stability. Nevertheless, concomitant loss of BRCA2 and RAD52 has been described to cause an increased level of genomic instability in comparison to cells that are only deficient in BRCA2 activity (Feng *et al.*, 2011), thus proving that RAD52 functions to prevent further genomic instability in BRCA2-deficient cells. Therefore, RAD52 maintains minimal RAD51 activity by promoting its chromatin localisation and ensuing assembly on DNA for the repair of IR-induced DSBs via HR in the absence of BRCA2. These functions provide an alternative pathway for HR, which supports the viability of the intrinsically genetically unstable BRCA2-deficient cells.

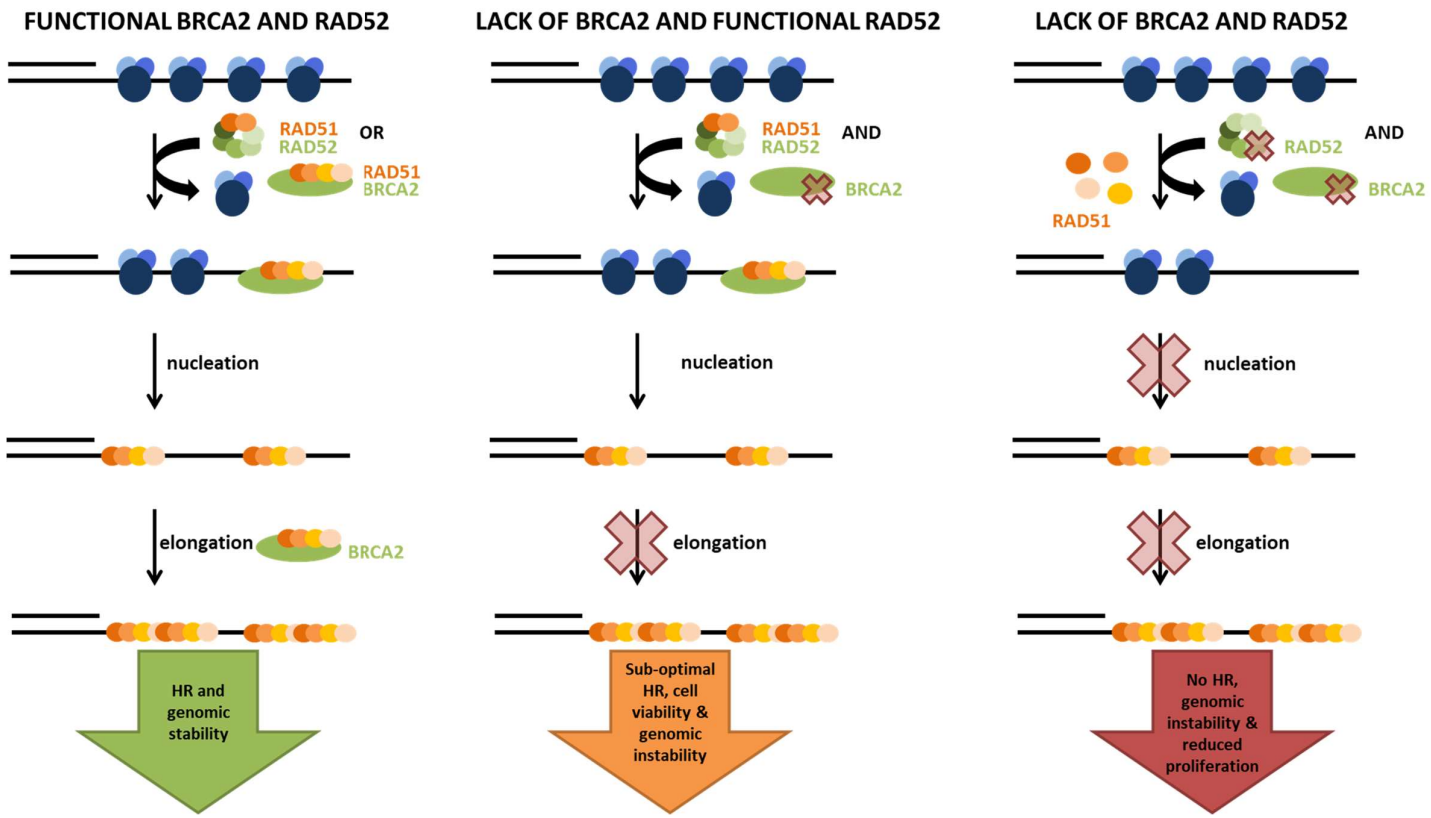

Figure 25: Proposed model of HR-mediated DNA repair. RAD51 loading on DNA and subsequent nucleation and filament elongation takes place as normal in the presence of functional BRCA2 and RAD52 proteins, thus enabling DSB repair by HR and preserving genomic stability. In the absence of BRCA2, RAD52 supports the formation of RAD51 nuclei that cannot assemble into elongated filaments. Such nucleation events enable sub-optimal HR-mediated repair that supports the viability of BRCA2-deficient cells at the expense of genomic stability. In the absence of both BRCA2 and RAD52 proteins, DNA loading of RAD51 is completely abrogated, preventing residual DNA repair by HR, causing further genomic instability and leading to a synthetic sick phenotype characterised by reduced cell proliferation.

The fact that RAD52 inactivation is synthetic lethal with key proteins involved in HR-mediated DNA repair, including BRCA1, PALB2, BRCA2 and paralogues of RAD51 (Fujimori et al., 2001; Feng et al., 2011; Chun, Buechelmaier and Powell, 2013; Lok et al., 2013), suggests that the mediator function has been conserved in the human RAD52 protein, but is only uncovered upon loss of the canonical HR pathway in cells. However, potential post-synaptic roles of RAD52, which can contribute to HR proficiency in cells, have not been investigated as part of this work. Human RAD52 has been reported of re-binding ssDNA following RAD51-dependent strand exchange and dissociation from DNA (Ma *et al.*, 2017), possibly promoting second-end capture and completion of DNA repair (McIlwraith and West, 2008). Collectively, these reports highlight a range of RAD52 activities which might be critical during mammalian HR. Furthermore, they emphasise the intricate nature of homologous DNA repair in human cells, which relies on a complicated array of recombination proteins and associated co-factors to ensure the appropriate regulation of RAD51 activity, as well as safeguard genome stability. Therefore, dissecting the roles of each of the proteins in DSB repair is essential for us to better comprehend the mechanism of human HR and characterise which protein functions can be targeted for anti-cancer therapy in tumours with HR deficiencies.

CHAPTER 2

Regulation of RAD51 activity at stalled replication forks by RAD52

INTRODUCTION

Replication in eukaryotes: An overview

DNA replication requires the faithful duplication of the genetic material. The process occurs in a semi-conservative manner and initiates from regions known as replication origins that are licensed in the G1 phase of the cell cycle (reviewed in Fragkos *et al.*, 2015; Kang *et al.*, 2018). Origin licensing involves the recruitment of the origin recognition complex (ORC), consisting of six subunits (ORC1-6), followed by binding of CDC6 and CDT1 (CDC10-dependent transcript 1). The latter two proteins subsequently recruit two hexameric mini-chromosome maintenance (MCM) complexes, each comprising MCM2-7, thus assembling the pre-replication complex (pre-RC) and concluding the licensing reaction. Each of the hexameric MCM2-7 complexes forms a ring structure with ATPase activity, where ATP hydrolysis is essential for the helicase activity of the complexes. Once origins have been licensed, re-licensing should be prevented to ensure that chromosomes are replicated only once during the cell cycle. For this reason, MCM2-7 helicase loading and activation are temporally separated, with loading occurring in G1 and activation in S phase, respectively (reviewed in Mueller, Keaton and Dutta, 2011). Origin activation, or firing, is achieved by the phosphorylation of the two inactive MCM2-7 complexes by DDK (DBF4-dependent kinase) and CDKs, thus recruiting CDC45 and Treslin (reviewed in Fragkos *et al.*, 2015; Kang *et al.*, 2018). Subsequently, the pre-loading complex (pre-LC), consisting of GINS, RECQL4, DNA topoisomerase-2 binding protein 1 (TOPBP1) and DNA polymerase ε, is recruited to form the CMG complex (CDC45, MCM, GINS) (Kang *et al.*, 2018). Finally, MCM10 triggers the dissociation of the two MCM hexamers, thus leading to their activation with each of them forming an active DNA helicase within the CMG complex. The helicases catalyse DNA

unwinding in the 3’ to 5’ direction to form single-stranded DNA regions which are stabilised by RPA, and establishing two functional replication forks that move in opposite directions at each origin (Fragkos *et al.*, 2015). Since nucleotide incorporation by DNA polymerases and hence DNA synthesis can only occur in the 5’to 3’ direction, one DNA strand is synthesised continuously in the same direction as replication fork progression, known as the leading strand, whereas the lagging strand is synthesised in a discontinuous manner in the direction opposite to that of the growing replication fork. For this reason, lagging strand synthesis occurs by the formation of multiple ~200 base pair DNA segments, known as Okazaki fragments, across the lagging strand template. The primase subunit of DNA polymerase α synthesises small RNA primers, which are then extended by the polymerase subunit that incorporates an additional 20 bases, thus forming RNA-DNA primers for both the leading strand and every Okazaki fragment on the lagging one (Stillman, 2008). The RNA-DNA primers in turn recruit the Replication Factor C (RFC) clamp loader, which subsequently expels DNA polymerase α while promoting proliferating cell nuclear antigen (PCNA) clamp loading and relaying the primers to more processive polymerases with exonuclease activity (Stillman, 2008). These are the DNA polymerase ε and DNA polymerase δ, which catalyse synthesis of the leading and lagging strands, respectively, and are tethered to DNA by the sliding clamp PCNA to ensure processivity (Kang *et al.*, 2018). Once strand replication finishes, the RNA primers are removed and replaced by DNA, at which point the DNA sequences of the Okazaki fragments on the lagging strand are ligated by the DNA ligase to form a continuous replicated DNA strand. As the helicase unwinds parental DNA, the double helix ahead of the replication fork rotates, thus leading to positive super-coiling and torsional build-up. Topoisomerases act to break and re-seal the DNA to relieve this tension by adding negative supercoils to the double helix, thus ensuring that replication fork progression is not affected. Following genome duplication, replication termination occurs upon collision between two converging replication forks. CMG and PCNA rings are disassembled from double-stranded DNA upon Okazaki fragment ligation to safeguard genome integrity (Kang *et al.*, 2018).

Replication stress

Once DNA replication starts, cells need to balance cell metabolism to ensure that the availability of nucleotides and replication factors meet the needs for replication accuracy and speed. For this reason, cells fire origins in a regulated manner, with about 70% of these lying dormant during an unperturbed S phase and being activated only upon exposure to replication stress (RS) (Zeman and Cimprich, 2014; Fragkos *et al.*, 2015).

Replication stress is any condition that slows and stalls normal fork progression and can potentially lead to fork collapse. Replication forks are constantly being challenged by endogenous and exogenous impediments. These include nicks and gaps within dsDNA, which can occur during physiological DNA repair pathways and can physically block the replication machinery, thus creating replication stress and forming single-stranded DSBs upon collapse. In addition, mis-incorporation of ribonucleotides during DNA synthesis by Polymerase δ and Polymerase ε can also stall RFs and generate replication stress (Dalgaard, 2012). Difficult to replicate genomic regions, including common fragile sites (CFSs) and other repetitive sequences that can form secondary structures, such as G-quadruplexes, also slow RFs down and contribute to stress induction. Collisions between replication and transcription machineries, as well as R-loop formation between the nascent transcript and its DNA template can both interfere with RF progression and are sources of RS (Hoffman *et al.*, 2015; Özer and Hickson, 2018). DNA unwinding during replication or gene transcription creates topological stress, which also contributes to fork stress and stalling. Finally, since replication relies on the availability of dNTPs, nucleotide deficiencies can also cause stalling of forks and decrease fork speed (Halazonetis, Gorgoulis and Bartek, 2008; Bester *et al.*, 2011; Venkitaraman, 2011). The latter scenario is commonly observed early during oncogenesis and is termed oncogene-induced replication stress. Oncogene activation promotes cell proliferation by altering CDK activity in the G1 and S phases, thus leading to cell cycle deregulation and aberrant S-phase entry. This consequently enhances origin firing and replication initiation, which in turn depletes dNTP pools. Reduced dNTP availability increases the likelihood of fork collision with the transcription machinery, thus inducing replication

stress that can potentially lead to fork collapse, DSB formation and genomic instability. Similarly, treatment with chemicals such as hydroxyurea (HU) and aphidicolin, cause depletion of dNTPs. Finally, DNA-protein complexes and crosslinks (DPCs) formed during DNA repair and replication processes can block replisome movement and cause stalling.

Replication stress response

Persistent replication stress and fork stalling triggers a signal transduction pathway that protects arrested forks and ensures the faithful completion of DNA replication before cell division, thus avoiding genomic instability. During replicative stress, the activities of the MCM helicase and the DNA polymerases become uncoupled, whereby the polymerases stall while the helicase progresses, consequently leading to the accumulation of unwound DNA at the arrested fork (Byun *et al.*, 2005; Forment and O'Connor, 2018). The persistent presence of long stretches of RPA-coated ssDNA at the fork in turn encourages ATRIP binding, hence signalling the presence of replication stress and activating the replication stress response (RSR). Subsequent recruitment and activation of ATR triggers a cascade that is primarily mediated by CHK1, which promotes cell cycle arrest, as in the case of DDR (covered in preface), and suppresses further origin firing (Zeman and Cimprich, 2014; Forment and O'Connor, 2018). Although the ATR-CHK1 axis is shared by both the DDR and the RSR, the latter has additional roles in protecting stalled replication forks and permitting a sufficient supply of dNTPs under replicative stress conditions. More specifically, ATR-CHK1 activation enhances the levels of ribonucleotide reductase, a key enzyme for dNTP generation, to ensure replication stress tolerance, cell survival and eventually efficient fork restart following stress removal (Forment and O'Connor, 2018).

Restart pathways exist to restore replication fork progression once the stress is released, or even when this persists (reviewed in Marians, Pasero and Yeeles, 2013; Zeman and Cimprich, 2014). Firing of a neighbouring dormant origin is the most common mechanism of fork rescue, but converging RFs can also allow completion of DNA synthesis by merging with the stalled fork. Re-priming of the replication machinery is also used as a fork restart mechanism, where

the replisome re-initiates DNA synthesis downstream of the lesion and leaves behind a ssDNA gap that is subsequently filled in by specialised polymerases involved in lesion bypass pathways. Such processes include the error-free template switching mechanism, in which the undamaged sister chromatid is used as the template for DNA synthesis, or the mutagenic translesion synthesis pathway performed by the DNA polymerases ζ, η, θ, ι and κ (reviewed in Lehmann, 2005). These polymerases can accommodate damaged bases within their active site, and hence these enzymes can replace the replicative polymerase at the stalled fork in real-time to allow DNA replication past the lesion. Finally, fork remodelling by regression or reversal, to be discussed in greater detail in the next sections, is a key mechanism for enabling fork repair and restart for DNA synthesis to resume without chromosomal breakage (Quinet, Lemaçon and Vindigni, 2017).

Despite the presence of restart mechanisms, forks might fail to restart and eventually collapse into single-ended DSBs by the action of endonucleases. In fact, fork collapse is a major source of endogenous DSBs (Saleh-Gohari *et al.*, 2005; Halazonetis, Gorgoulis and Bartek, 2008), with lesions ahead of the replicon resulting in seDSBs that require HR or other pathways for repair (Bryant *et al.*, 2009; Peng *et al.*, 2012). Upon fork collapse, the CMG helicase loses its GINS subunit, and hence for replication re-start to occur GINS and Pol ε must be re-loaded on DNA in a recombination-mediated mechanism reliant on MRE11-mediated processing and RAD51-dependent strand invasion (Hashimoto, Puddu and Costanzo, 2012). Furthermore, as previously mentioned, BIR can repair seDSBs formed downstream of collapsed DNA replication forks (Costantino *et al.*, 2014). This process is initiated by invasion of the broken end into an intact homologous chromosome, forming a D-loop as in HR, with migration of the D-loop enabling conservative DNA synthesis by DNA polymerase δ (Donnianni and Symington, 2013; Costantino *et al.*, 2014). The enzyme's limited processivity eventually enables fork disengagement and enables the nascently synthesised DNA to be re-ligated to the free DSB end.

Roles and regulation of RAD51 at replication forks

RAD51 has several roles at stalled replication forks, namely fork reversal, protection and restart. These functions need to be tightly regulated to ensure preservation of genome stability.

Replication fork reversal

Following replisome uncoupling, remodelling of the fork structure occurs in a process known as fork reversal or regression. Fork reversal is a physiological global response to replication stresses in human cells, and has recently emerged as a mechanism of protecting stalled forks by limiting replication runoff or endonuclease cleavage, processes that can otherwise lead to DSB formation (Chaudhuri *et al.*, 2012; Zellweger *et al.*, 2015). During fork reversal, the three-way junction at the fork is converted into a four-way one, with this involving the coordinated annealing of the two nascent strands and the re-annealing of the template strands to form a 'chicken foot' structure. The RAD51 recombinase has been found to promote fork reversal following exposure to replication stress (figure 26), in a step that does not require extension and/or stable filament formation and is thus BRCA2-independent (Zellweger *et al.*, 2015; Kolinjivadi *et al.*, 2017; Mijic *et al.*, 2017; Taglialatela *et al.*, 2017). Fork remodelling enzymes, including members of the SNF2 family - namely SMARCAL1, ZRANB3 and HLTF- utilise their ATP-dependent translocase activity to drive fork reversal in cooperation with RAD51 (Kolinjivadi *et al.*, 2017; Taglialatela *et al.*, 2017).

Fork reversal is thought to prevent the genetic instability observed downstream of oncogene-induced RS in various ways (reviewed in Bhat and Cortez, 2018). Initially, reversal can support fork stabilisation until the region is passively replicated by a nearby converging fork. Additionally, formation of a reversed fork re-introduces the DNA lesion within a double-stranded DNA environment to encourage its repair by excision-repair mechanisms. Furthermore, annealing the newly synthesised strands during fork reversal provides an undamaged template that can be utilised in a template-switching mechanism to enable DNA

synthesis past the lesion. Finally, HR-mediated repair can take place following limited reversed fork processing by endonucleases into a DSB, thus preventing chromosomal breakage and supporting genome stability. While fork reversal prevents permanent stalling and encourages replication restart, reversed fork intermediates need to be properly controlled to avoid pathological consequences. This is because unrestrained fork processing and remodelling can also be detrimental in BRCA-deficient settings due to the regressed arm of a reversed fork resembling a one-ended DSB that can be acted upon by structure-specific endonucleases. Unprotected reversed forks are in fact the entry points of nucleases (MRE11, EXO1, MUS81, DNA2 and WRN) in the absence of BRCA2-stabilised RAD51 filaments (Thangavel *et al.*, 2015; Kolinjivadi *et al.*, 2017; Lemaçon *et al.*, 2017; Mijic *et al.*, 2017; Taglialatela *et al.*, 2017). Aberrant nucleolytic processing of reversed forks can thus cause genomic instability as a result of DSB formation and chromosome breakage (Neelsen *et al.*, 2013).

Replication fork protection: combating nucleolytic degradation

The second role of RAD51 at stalled RFs is its fork protection activity, which, in contrast to fork reversal, is BRCA2-dependent (figure 26). As aforementioned, reversed forks are the entry points for nucleolytic degradation, whereby chromatin remodelling enzymes including MLL3/4-PTIP, CDH4 (Chaudhuri *et al.*, 2016) and PARP1 (Bryant *et al.*, 2009) open up the chromatin structure at unprotected stalled forks to recruit the MRE11 nuclease (Lemaçon *et al.*, 2017; Mijic *et al.*, 2017). Fork protection requires RAD51-ssDNA filaments stabilised by BRCA2 to prevent nucleolytic digestion of the reversed nascent DNA strands. This activity necessitates the conserved Ser3291 residue within the C-terminal domain of BRCA2, which is involved in RAD51 interaction and subsequent RAD51 filament stabilisation (Schlacher *et al.*, 2011; Feng and Jasin, 2017). As a result, BRCA2 deficiencies and RAD51 mutants that disable stable nucleofilament formation exhibit enhanced reversal and extensive degradation of stalled forks, accompanied by genomic instability (Schlacher *et al.*, 2011; Wang *et al.*, 2015; Kolinjivadi *et al.*, 2017; Mijic *et al.*, 2017).

In BRCA2-deficient conditions where no stable RAD51 nucleofilaments can be formed, CtIP triggers limited MRE11-dependent resection of the regressed arm, which is then extended by the EXO1 nuclease (Lemaçon *et al.*, 2017). This creates 3'-ssDNA tails at forks, forming substrates that promote the recruitment of the structure-specific endonuclease, MUS81 (methyl methanesulfonate UV-sensitive clone 81). MUS81 localisation to the fork is dependent on the SLX4 scaffold protein (Muñoz *et al.*, 2009), as well as the chromatin modifier EZH2 (enhancer of zeste homologue 2), which methylates H3K27 to open up the chromatin structure at stalled RFs (Rondinelli *et al.*, 2017). Ensuing MUS81-mediated cleavage of forks generates DSBs, that can be subsequently repaired by HR and promote fork restart (Hanada *et al.*, 2007). In addition to the MUS81-driven pathway, numerous other mechanisms involving different nucleases and helicases have been reported to promote stalled fork degradation and restart, with nuclease choice being dictated by the structure of the replication intermediate formed. For instance, a DNA2-depedent pathway has been described to occur downstream of MRE11-mediated resection to encourage processive cleavage into DSBs, where the DNA2 nuclease/helicase acts redundantly to EXO1 due to its ability to resect 5' ends into 3' ssDNA overhangs (Thangavel *et al.*, 2015; Lemaçon *et al.*, 2017), but does not seem to contribute to the fork degradation phenotype seen in BRCA2-deficient cells (Lemaçon *et al.*, 2017). In a different report using cells with intact BRCA2, a DNA2-mediated mechanism has been described to degrade stalled RFs to promote the restart of RAD51-reversed forks, in a process that requires the WRN helicase but is independent of MRE11, EXO1, CtIP and MUS81 (Thangavel *et al.*, 2015). This highlights that in the presence of HR factors, like BRCA2, different replication fork intermediates are formed that are differentially processed by the available nucleases.

While limited nascent DNA degradation can remove end-bound proteins to enable HR-dependent fork repair and restart in BRCA-proficient cells, DSBs formed as a result of extensive degradation can also lead to chromosomal rearrangements and trigger genomic instability and/or cell death in BRCA2 absence. This makes BRCA2 deficient cancer cells exhibit hypersensitivity to replication-stalling agents like PARP inhibitors (Bryant *et al.*, 2005;

Chaudhuri *et al.*, 2016). In fact, protection of stalled forks confers resistance to PARPi and cisplatin treatment (Chaudhuri *et al.*, 2016). In this paper, the authors suggested that nascent fork protection from MRE11-dependent degradation is sufficient to prevent the genomic instability and lethality observed in BRCA2-deficient cells, even in the absence of HR re-instatement. This report hence highlights the importance of replication stress in determining chromosomal stability and responses to chemotherapeutics.

Replication fork restart

Following replication stress removal, regressed forks can resume DNA synthesis by a process known as fork restart. This requires the re-establishment of the replication fork, a step that relies on the RECQ1 helicase for resolving the regressed 4-way structures to restore the fork configuration into a normal three-way junction (Berti *et al.*, 2013; Zellweger *et al.*, 2015).

The nucleolytic pathways mediated by MRE11, MUS81 or DNA2/WRN, outlined in the previous section, are responsible for processing reversed forks and driving HR-mediated fork restart (Hanada *et al.*, 2007; Bryant *et al.*, 2009; Peng *et al.*, 2012; Thangavel *et al.*, 2015). In a similar yet non-redundant, mechanism to that driven by DNA2/WRN, the BLM helicase, which also belongs to the RECQ family of helicases, has been shown to be recruited to arrested forks to encourage fork restart (Davies, North and Hickson, 2007; Sidorova *et al.*, 2013). Additionally, downstream of unscheduled reversed fork processing, fork breakage and DSB formation by MUS81, POLD3-dependent restart of DNA synthesis has been described to occur in an attempt to rescue stalled forks formed in a BRCA2-deficient background (Lemaçon *et al.*, 2017; Rondinelli *et al.*, 2017). This is a BIR-like mechanism that promotes fork restart and enables cell survival at the expense of genomic stability (figure 26). Similarly, human RAD52 has been recently implicated in rescuing seDSBs formed by fork collapse through BIR in a POLD3-dependent mechanism that promotes fork restart (Ciccia and Symington, 2016; Sotiriou *et al.*, 2016). This suggests that RAD52 and MUS81 function in the same fork restart mechanism, which is further supported by the observation that the concomitant loss of both proteins causes death in checkpoint-deficient cells (Murfuni *et al.*, 2013). Whether these fork

restart pathways function redundantly, complementary or compete in different settings, however, is still unknown.

The RAD51 recombinase has also been implicated in the restart of transiently arrested forks following short exposures to replication stress, an activity mediated by strand invasion and facilitated by the RAD51 paralogue, XRCC3 (Petermann *et al.*, 2010). In this work, RAD51 was described to have a distinct role following prolonged HU exposures, which acts to promote HR for the repair of DSBs at collapsed forks, while fork restart is encouraged by new origin firing and is RAD51-independent, instead. In contrast, Hashimoto, Puddu and Costanzo, 2012, defined a pathway in which fork restart of collapsed forks required the reloading of replisome components in a recombination-mediated process that depends on RAD51 and MRE11. Therefore, although RAD51 is suggested to promote fork restart, the precise mechanisms driving this remain to be elucidated. Both WRN and BLM helicases have been described to promote RAD51-dependent fork restart, potentially by generating DNA substrates that enable the invasion of the re-annealed template strands, thus reconstituting an active fork and triggering HR-mediated fork restart by the recombinase enzyme (Hashimoto, Puddu and Costanzo, 2012; Sidorova *et al.*, 2013). Despite evidence implicating RAD51 in fork restart, the role of BRCA2 in this is controversial. Schlacher *et al.*, 2011 originally reported that BRCA2 deficiency does not impair fork restart in cells, an observation that was later confirmed by Songmin Ying, Hamdy and Helleday, 2012. A few years later, however, publications by Kim *et al.*, 2014 and Kolinjivadi *et al.*, 2017 described BRCA2 as being necessary for fork restart, potentially by stabilising RAD51 binding, filament formation and subsequent strand invasion on DNA.

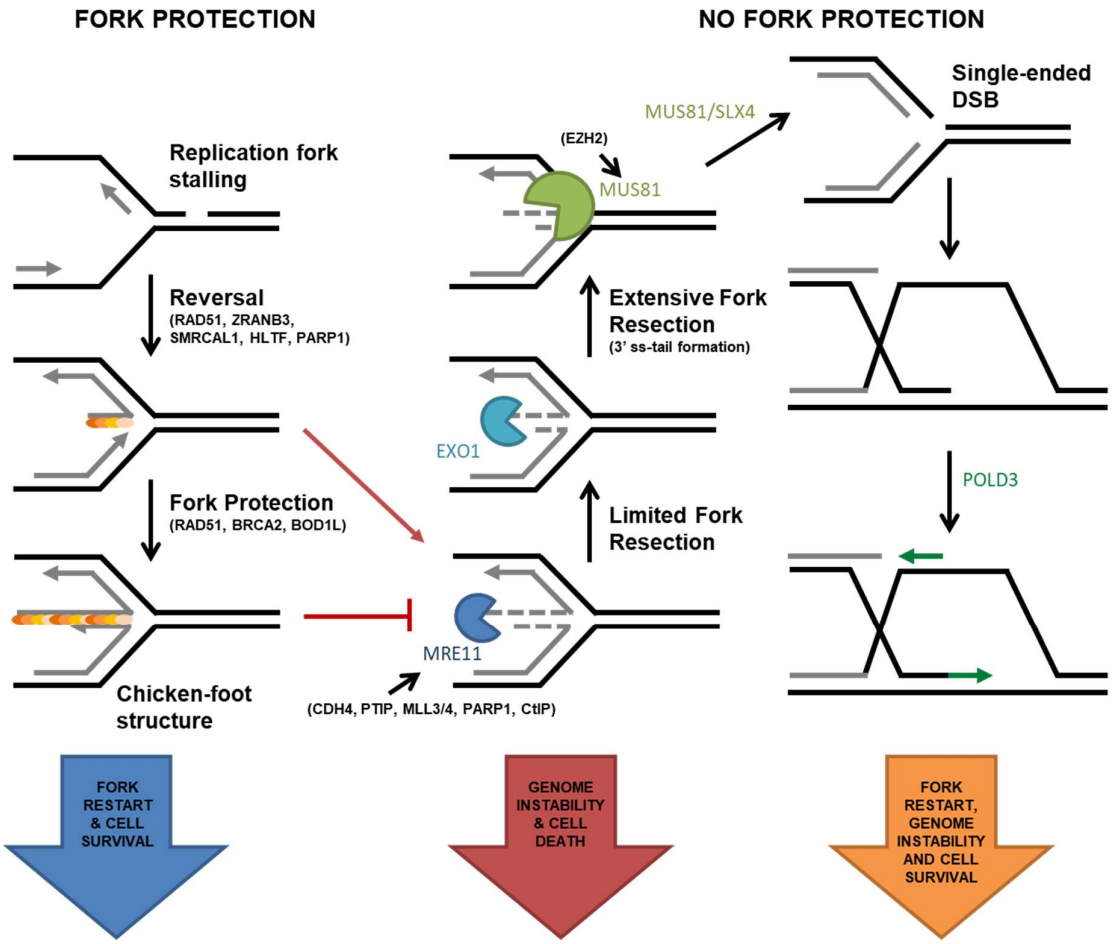

Figure 26: Pathways and proteins involved in preventing or mediating stalled fork degradation. Upon fork stalling, fork reversal is driven by RAD51 and DNA translocases (ZRANB3, SMARCAL1 and HLTF). The activity of PARP-1 keeps stalled forks in the regressed state by preventing resolution of the chicken-foot structure by the RECQ1 helicase. Unprotected reversed forks are the entry points for nucleases, and hence pathways exist to prevent the uncontrolled nucleolytic degradation of stalled forks. In the presence of stable RAD51 nucleoprotein filaments, forks are protected and can be restarted in HR- dependent and independent ways to enable cell survival. In the absence of stable RAD51 filaments, reversed forks are the substrates for nucleases that process fork structures and ultimately lead to extensive fork degradation. Following reversal, the MRE11 nuclease is recruited to the unprotected fork by CDH4, MLL3/4-PTIP, PARP1, and CtIP. MRE11 promotes limited nascent DNA degradation, which is further extended by EXO1 to form 3' ssDNA tails. These overhangs recruit the structure-specific endonuclease MUS81 to the fork, following opening of the chromatin structure by EZH2. Cleavage by MUS81 forms DSBs and promotes fork restart by BIR in a pathway that enables cell survival of BRCA2-deficient cells at the expense of genomic

stability. Other nucleases like DNA2/WRN can also be recruited to reversed forks, but this mechanism does not contribute to the extensive degradation phenotype observed in BRCA2-deficient cells and hence has been omitted for simplicity. For this reason, only the EXO1/MUS81 pathway is shown downstream of MRE11-dependent processing, due to its biological significance in BRCA2-deficient settings. **Adapted from Bhat and Cortez, 2018 and Liao *et al.*, 2018.**

RAD51 regulation at forks

Since fork reversal and subsequent nucleolytic processing can be detrimental to genomic instability, numerous proteins act to regulate and finetune the activities of RAD51 at forks. BOD1L acts downstream of BRCA2 to stabilise RAD51 filaments at stalled RFs, to prevent FBH1- and BLM-mediated displacement of RAD51 whilst inhibiting downstream over-resection by DNA2 (Higgs *et al.*, 2015). In the absence of BOD1L, extensive DNA2-dependent resection of RFs triggers compensatory new origin firing that can lead to genomic instability (Higgs *et al.*, 2015). RADX has also been identified to be important in promoting fork stability by antagonising RAD51 activity (Dungrawala *et al.*, 2017; Schubert *et al.*, 2017; Bhat *et al.*, 2018). It functions at forks to buffer RAD51 activity and define the balance between the fork reversal and protective activities of the recombinase (Dungrawala *et al.*, 2017; Bhat *et al.*, 2018). In addition, RADX prevents fork degradation and collapse downstream of RAD51-mediated reversal to maintain genome stability, and its depletion rescues the fork degradation phenotype seen in BRCA2 deficient cells by preventing RAD51-dependent fork reversal (Dungrawala *et al.*, 2017; Bhat *et al.*, 2018). As a result, RADX inactivation confers resistance to PARP inhibitors in cells with deficiencies in the BRCA2/RAD51 pathway (Dungrawala *et al.*, 2017; Bhat *et al.*, 2018).

Nonetheless, there exist RAD51-independent mechanisms of fork protection. Such a mechanism has been described for Abro1, which inhibits DNA2/WRN-dependent degradation of stalled forks in a pathway that is distinct from the BRCA2-dependent pathway that prevents MRE11-mediated degradation (S. Xu *et al.*, 2017).

Collectively, the multitude of proteins implicated in replication stress responses and the regulation of fork reversal, protection, processing and restart, highlights the intricate nature of the pathways involved. Failure to control RF intermediates is detrimental to genome stability and can lead to cell death (Murfuni *et al.*, 2013), and hence elucidating the mechanisms enabling replication stress tolerance holds great promise for targeting these and enhancing chemotherapeutic response in cancer cells (reviewed in Forment and O'Connor, 2018).

The emerging roles of human RAD52 in repair pathways associated with replication stress (Murfuni *et al.*, 2013; Bhowmick, Minocherhomji and Hickson, 2016; Sotiriou *et al.*, 2016) prompted me to investigate any potential protein functions in regulating fork protection by fine-tuning RAD51 activity at stalled forks, as well as in determining the cellular response to hydroxyurea-induced replication stress. Experiments were performed in a panel of cell lines that are wild-type, heterozygous or biallelic mutant for *BRCA2*, thus enabling me to assess whether RAD52 serves essential or redundant functions to BRCA2 in supporting RAD51 activity at stalled replication forks.

RESULTS

2.1 Human RAD52 is involved in replication stress responses

My observations that RAD52 focalises to form active repair centres following ionising radiation, both in cells that are proficient and deficient in BRCA2 activity, implicates the mammalian protein in recombinational repair of IR–induced DNA damage and highlights one of its potential activities that contribute to the survival of BRCA2-deficient cells. However, BRCA2 is increasingly being recognised for its fork protection functions at stalled RFs (Schlacher *et al.*, 2011; Chaudhuri *et al.*, 2016; Kolinjivadi *et al.*, 2017; Taglialatela *et al.*, 2017), and hence I wanted to assess if RAD52 is similarly implicated in responses following replication stress that can further characterise the observed synthetic lethality between the two proteins in human cells.

As mentioned in this chapter's introduction, replication stress is characterised by any condition that impedes normal fork progression, causing fork slowing and potentially collapse into single-stranded DSBs. During tumorigenesis, aberrant cell proliferation and increased replication driven by oncogene activation not only deplete dNTP pools by enhancing origin firing but also increase collisions with the transcriptional machinery, thus triggering oncogene-induced replication stress (OIRS) (Halazonetis, Gorgoulis and Bartek, 2008; Bester *et al.*, 2011; Venkitaraman, 2011). Treatment with hydroxyurea (HU) likewise causes deoxyribonucleotide depletion by inhibiting the enzyme ribonucleotide reductase and can be used to mimic OIRS in cancer cells.

Human RAD52 has binding sites for both ss- and ds- DNA (Kagawa *et al.*, 2008; Seong *et al.*, 2008) and hence can potentially bind dsDNA-ssDNA junctions found at replication forks. In fact, RAD52 foci have been previously described to be induced to a greater extent in human cells following exposure to 10 mM HU than 8 Gy of IR, thus suggesting a more dominant role for the protein at collapsed RFs, potentially by mediating HR-dependent fork restart (Wray *et al.*, 2008). However, the doses used in this study are either on the higher end or beyond the

limit achieved in the clinic for both agents (Belt *et al.*, 1980; Charache *et al.*, 1992; Hellevik and Martinez-Zubiaurre, 2014; Vesela *et al.*, 2017), and hence caution must be taken during data interpretation regarding RAD52 activities in cells. Regardless, the protein has been recently reported to participate in replication stress responses by facilitating fork restart and repair of UR-DNA though BIR and MiDAS, respectively (Bhowmick, Minocherhomji and Hickson, 2016; Sotiriou *et al.*, 2016). However, a potential role in maintaining the integrity of stalled forks has not been investigated for the protein yet.

To this end, cells transiently transfected with HA-RAD52 were exposed to 4 mM HU either for 5 or 24 hours, as indicated. This drug concentration has been extensively used for studying fork stalling due to the reversible effect of HU on DNA replication that enables cells to restart paused forks following short exposures (Petermann *et al.*, 2010; Schlacher *et al.*, 2011). Upon prolonged exposures (24 hours) to HU, stalled forks eventually collapse into DSBs that require HR for repair (Petermann *et al.*, 2010). Following replication stress induction, immunofluorescence was employed to check for RAD52 and RAD51 focalisation in cells. RAD52 foci were observed in both BRCA2- proficient and deficient cells following HU exposure (figure 27), thus implicating RAD52 in replication stress responses irrespective of the BRCA2 status of cells. Moreover, the fact that Rad52 formed foci following both short and long HU treatments suggests potential roles for the protein at both stalled and collapsed RFs.

RAD51 focalisation, however, proved very difficult to detect, potentially owing to the lack of elongated RAD51 filaments at stalled RFs after 5 hours of HU treatment. In support of this view is the fact that the smallest detectable RAD51 foci have been suggested to cover kilobases of single-stranded DNA (Raderschall, Golub and Haaf, 1999), while stalled RFs are thought to contain ssDNA regions of only ~80 bases (Zellweger *et al.*, 2015). Moreover, forks are expected to have collapsed by 24 hours of HU treatment, thus potentially explaining the lack of RAD51 focalisation at both timepoints tested following replication stress exposure.

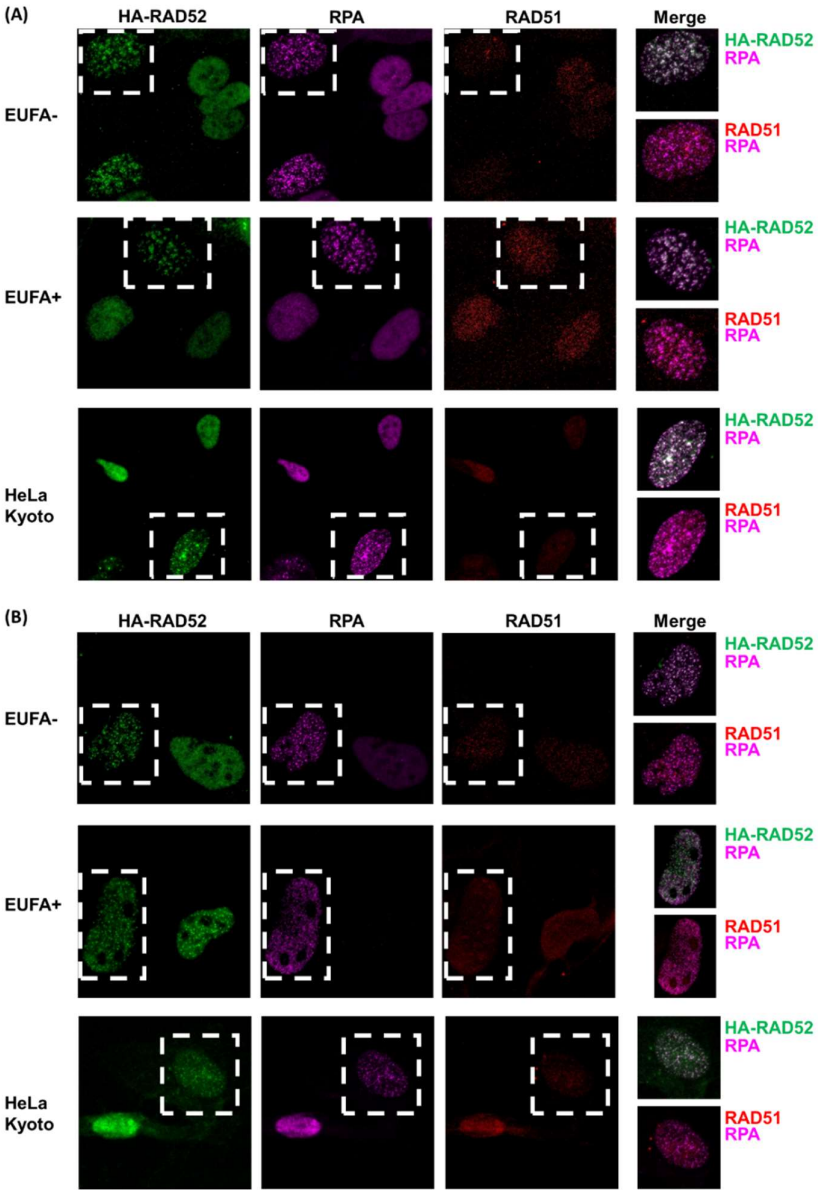

Figure 27: The human RAD52 protein is involved in replication stress responses. HA-RAD52 was over-expressed for 48 hours in EUFA-, EUFA+ and HeLa Kyoto cells before treatment with 4 mM HU for 5 **(A)** or 24 **(B)** hours. Protein focalisation by HA-RAD52, RPA and RAD51 was subsequently assessed by immunolabelling with the 488, 568 and 647 fluorophores, respectively. Immunofluorescence images are representative of three independent biological repeats (n=3).

2.2 Human RAD52 prevents degradation of nascently synthesised DNA at stalled replication forks

Subsequently, to test if RAD52 has a protective role at stalled RFs, the single molecule DNA fibre assay was employed to assess nascent DNA degradation in cells exposed to replication stress in the form of HU. For these experiments, cells were transfected with either non-targeting siRNA control (siNT) or siRNA against human RAD52 (siRAD52) for 48 hours before use in the DNA fibre assay. The HeLa Kyoto and EUFA+ cell lines were used to model cells containing wild-type BRCA2, whilst the HeLa Kyoto D2723H homozygous mutant and EUFA- cells were used to represent BRCA2-deficient cells. Moreover, the +/6174delT and the +/3036del4 BRCA2 heterozygous cell lines were also used to recapitulate BRCA2-deficient backgrounds, from which RAD52 was stably ablated through expression of shRAD52.

Nascently synthesised DNA was labelled with IdU for 20 minutes, before washing off the pyrimidine analogue and treating the cells with 4mM HU for 5 hours. Following replication fork stalling, cells were collected for DNA combing and immunofluorescent staining of the DNA tracts. Retention of the IdU label following HU treatment gives an indication of fork stability, and hence the length of IdU tracts was measured for each condition to determine the corresponding replication fork stability in each genetic background.

Depletion of RAD52 caused a reduction in the median nascent DNA tract length in all the cell lines tested, and surprisingly, that was the case irrespective of the BRCA2 status of the cells (figure 28). Shorter tract lengths were observed following siRAD52 even in the absence of replication stress, although shortening was further enhanced upon exposure to HU in BRCA2-deficient settings. These observations suggest roles for RAD52 both on unperturbed and stalled replication forks, with the protein being more essential under conditions of replication stress in BRCA2-deficient cells. They also propose that cells have endogenous replication stress even in the absence of added HU, with RAD52 protecting forks even under such conditions.

Regarding the BRCA2 heterozygous background, cells do not seem to lack fork stabilisation following HU treatment (figure 29). This suggests that one wild-type copy of BRCA2 is sufficient to protect and stabilise stalled forks induced by HU, since the median tract lengths in BRCA2 heterozygous cells are comparable to that of the parental HeLa Kyoto cell line. However, RAD52 depletion in these resulted in significant shortening of the median IdU tract length when compared to the respective shNT control, both in the absence and the presence of extrinsic replication stress. Hence, RAD52 is required for maintaining replication fork stability irrespective of the BRCA2 background of cells.

A time-course experiment where tract lengths were measured at 0.5, 2.5 and 5 hours following HU treatment displayed progressive DNA tract shortening with increasing time of exposure to replication stress, which was accentuated upon RAD52 depletion in EUFA- cells (figure 30). Reduced nascent DNA tract length can be either due to delayed fork progression or as a result of enhanced degradation by nucleolytic enzymes. However, the first scenario can be disregarded owing to the enhanced shortening with increasing exposure time, which confirms fork resection occurrence.

Collectively, these findings suggest that RAD52 depletion induces replication fork deprotection in cells irrespective of their BRCA2 status, whether that is wild-type, heterozygous or homozygous for a mutation.

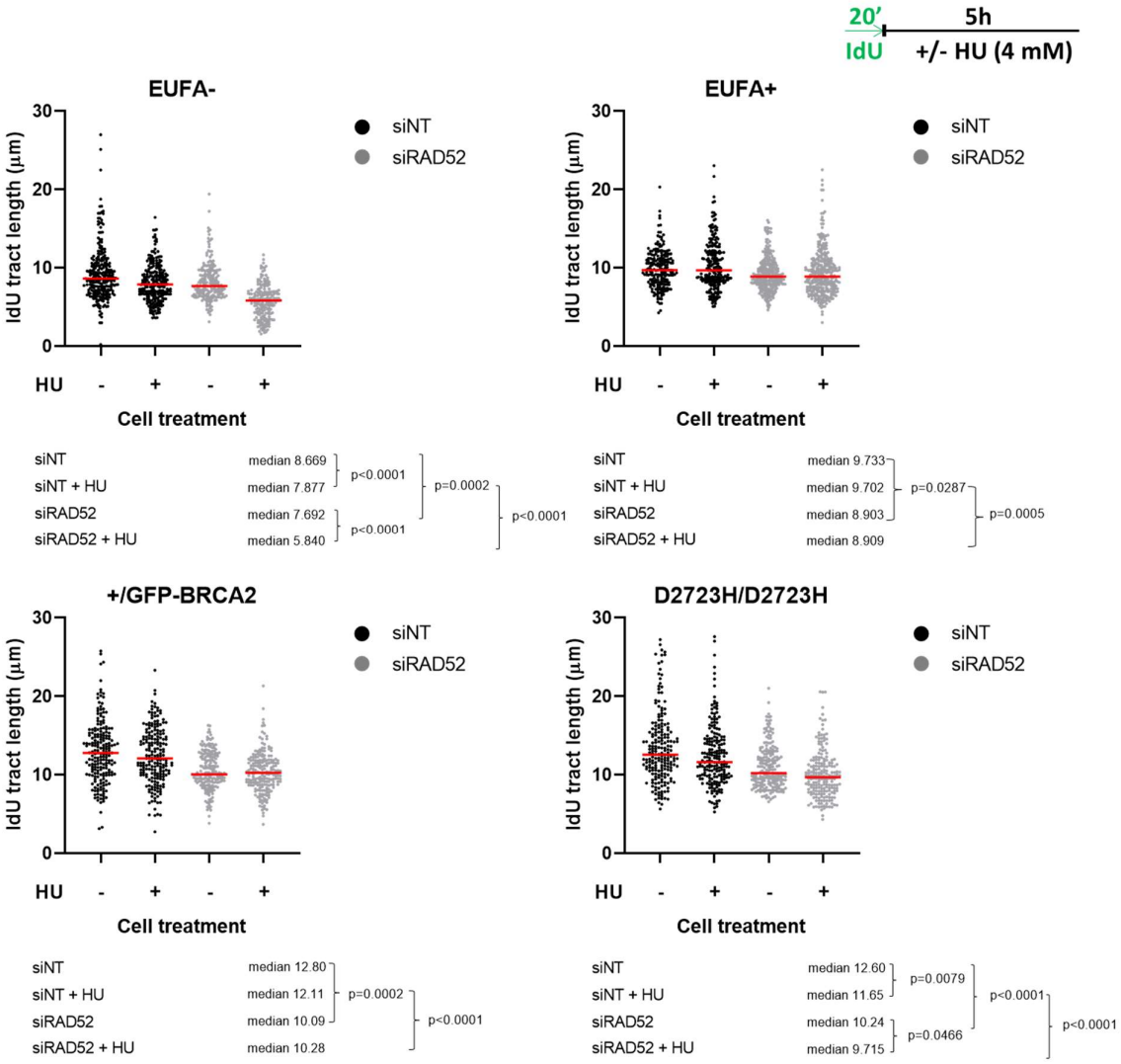

Figure 28: RAD52 depletion by siRNA leads to enhanced degradation of nascent DNA at stalled replication forks in cells. IdU tract lengths of cells following RAD52 knockdown (25 nM siRNA for 48 hours) in the presence and absence of hydroxyurea-induced replication stress (4 mM for 5 hours). The scatter plots are representative of at least two independent experiments, with lengths of at least 200 tracts measured for each condition. Median tract lengths are indicated by a red line, and a Mann-Whitney t-test was used to determine statistical significance between different cell treatments. A schematic of the experimental setup used for the DNA fibre assay is shown in the top right corner. Green tract, IdU; HU, hydroxyurea.

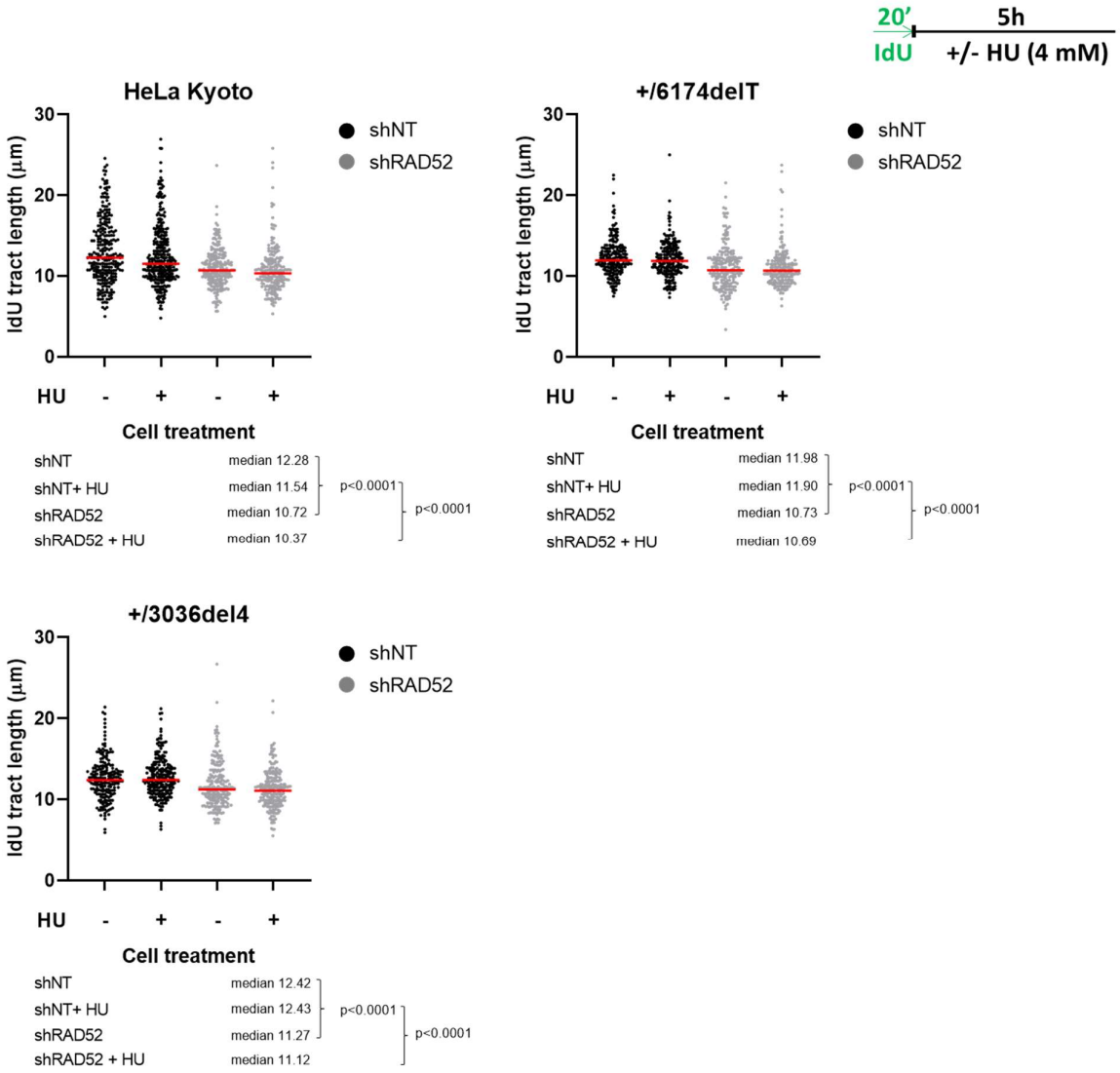

Figure 29: RAD52 depletion by shRNA leads to enhanced degradation of nascent DNA at stalled replication forks in cells. IdU tract lengths of cells following stable depletion of RAD52 by shRAD52 in the presence and absence of hydroxyurea-induced replication stress (4 mM for 5 hours). The scatter plots are representative of at least two independent experiments, with lengths of at least 200 tracts measured for each condition. Median tract lengths are indicated by a red line, and a Mann-Whitney t-test was used to determine statistical significance between different cell treatments. A schematic of the experimental setup used for the DNA fibre assay is shown in the top right corner. Green tract, IdU; HU, hydroxyurea.

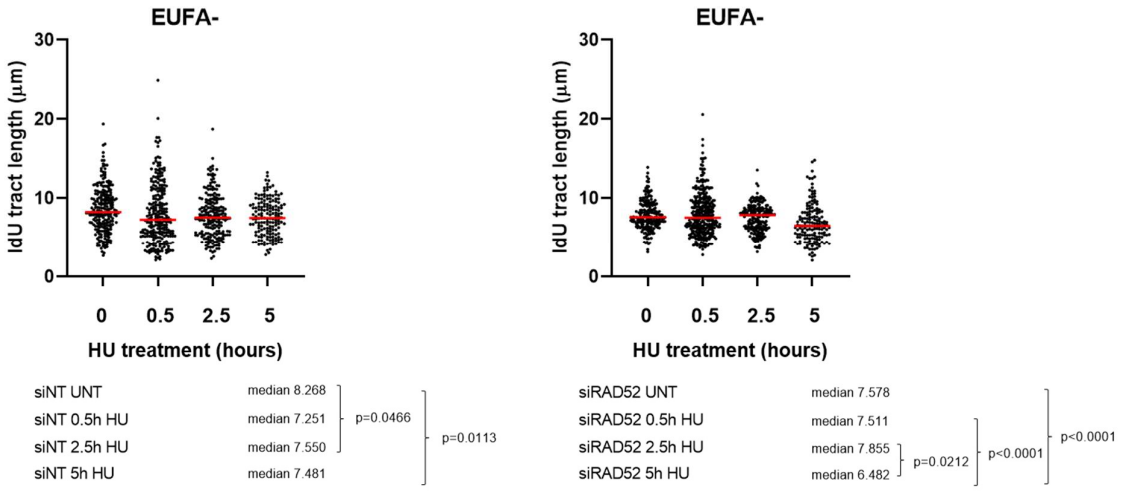

Figure 30: RAD52 depletion by siRNA leads to progressively enhanced degradation of nascent DNA with increasing exposure time to hydroxyurea-induced replication stress. A time-course experiment was performed to assess fork stability in EUFA- cells following RAD52 knockdown and exposure to 4 mM HU for 0.5, 2.5 and 5 hours. IdU tract lengths are shown for each condition. The scatter plots are representative of at least two independent experiments, with lengths of at least 200 tracts measured for each condition. Median tract lengths are indicated by a red line, and a Mann-Whitney t-test was used to determine statistical significance between different cell treatments. UNT, untreated; HU, hydroxyurea.

2.3 Nascent DNA degradation following RAD52 depletion is due to MRE11-dependent degradation

Stable RAD51 filaments are known to protect reversed stalled forks from nucleolytic degradation by MRE11, a nuclease that has both 3'-5' and 5'-3' nucleolytic activities (Schlacher *et al.*, 2011; Lemaçon *et al.*, 2017). Mirin, the chemical inhibitor of MRE11 exonuclease activity, can thus be used to inhibit MRE11-dependent degradation of nascent DNA at stalled replication forks. For this reason, mirin was used in RAD52-depleted cells to test if the nascent strand degradation observed in these is MRE11-dependent. Concomitant exposure to HU and mirin reverses the DNA degradation phenotype observed upon RAD52 depletion in both BRCA2- deficient and proficient cells (figures 31 and 32), thus suggesting that RAD52 protects nascent DNA tracts at stalled forks from nucleolytic degradation by MRE11. This observation holds true for the BRCA2 heterozygous cell lines too, suggesting that RAD52 depletion makes stalled replication forks susceptible to MRE11-dependent degradation, irrespective of the BRCA2 status of cells. These findings potentially indicate that RAD52 and BRCA2 function in distinct pathways to protect cells from replication fork deprotection.

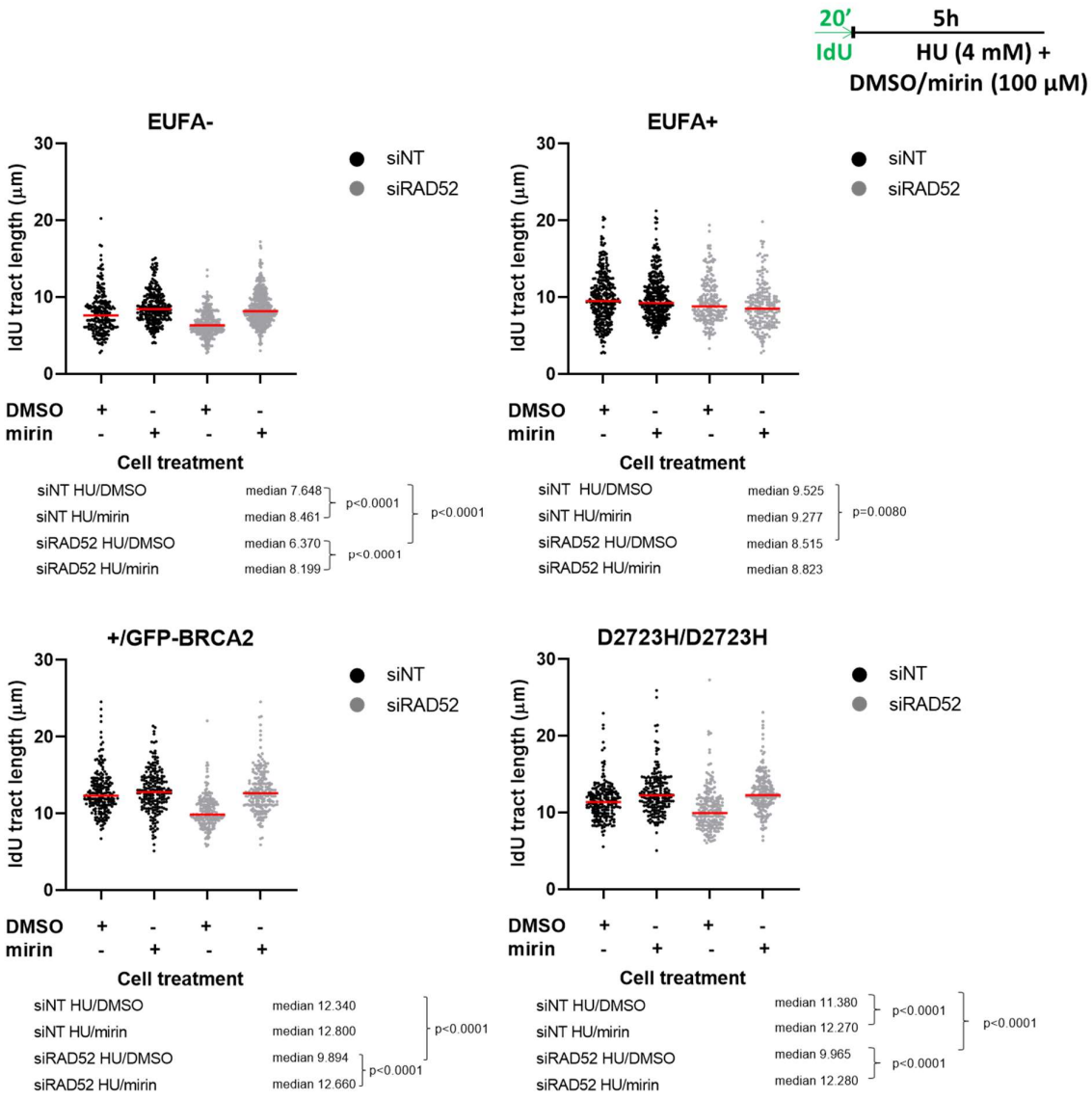

Figure 31: Nascent DNA degradation following siRNA-mediated RAD52 depletion in cells is dependent on nucleolytic degradation by MRE11. IdU tract lengths of RAD52-depleted cells (25 nM siRNA for 48 hours) following HU exposure (4 mM for 5 hours) in the presence or absence of mirin. DMSO was used as a vehicle control for cells that were not treated with mirin. The scatter plots are representative of at least two independent experiments, with lengths of at least 200 tracts measured for each condition. Median tract lengths are indicated by a red line, and a Mann-Whitney t-test was used to determine statistical significance between different cell treatments. A schematic of the experimental setup used for the DNA fibre assay is shown in the top right corner. Green tract, IdU; HU, hydroxyurea.

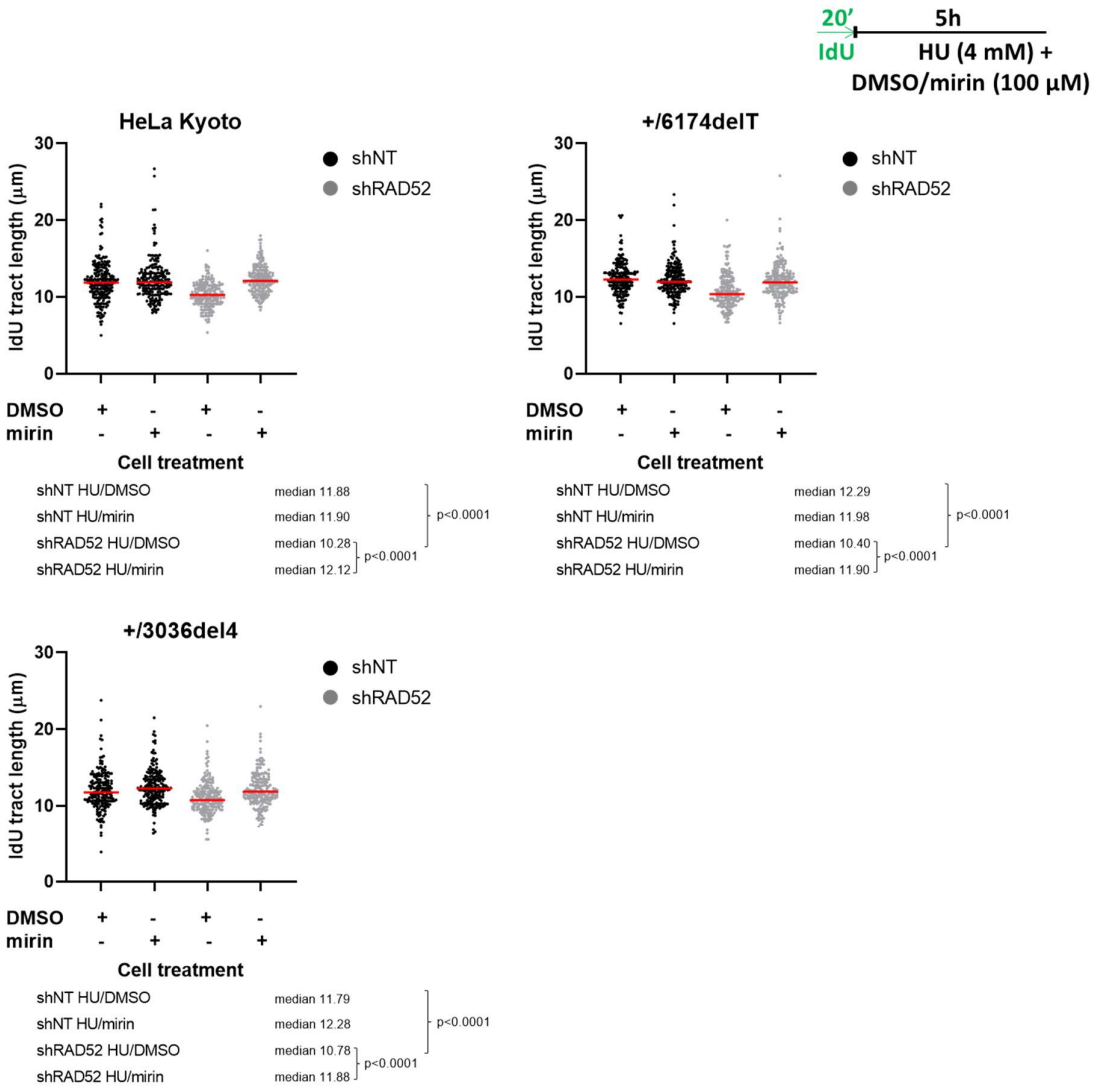

Figure 32: Nascent DNA degradation following shRNA-mediated RAD52 depletion in cells is dependent on nucleolytic degradation by MRE11. IdU tract lengths of RAD52-depleted cells (shRAD52) following HU exposure (4 mM for 5 hours) in the presence or absence of mirin. DMSO was used as a vehicle control for cells that were not treated with mirin. The scatter plots are representative of at least two independent experiments, with lengths of at least 200 tracts measured for each condition. Median tract lengths are indicated by a red line, and a Mann-Whitney t-test was used to determine statistical significance between different cell treatments. A schematic of the experimental setup used for the DNA fibre assay is shown in the top right corner. Green tract, IdU; HU, hydroxyurea.

2.4 RAD52 does not affect the sub-cellular distribution of RAD51 following exposure to replication stress

Stable RAD51 filaments are known to be required for protecting stalled replication forks from nucleolytic digestion by MRE11 (Schlacher *et al.*, 2011). Hence, in order to understand how RAD52 maintains fork stability and if this effect is mediated by regulating RAD51, I assessed the effect of RAD52 depletion on RAD51 sub-cellular localisation following replication stress induction by HU. To test this, the stable cell lines expressing shRAD52 were treated with 4 mM HU for 5 hours, as before, and then harvested for sub-cellular fractionation. As shown in figure 33, RAD52 depletion does not cause RAD51 re-localisation in comparison to the respective shNT control cell lines. Hence, RAD52 depletion does not induce nascent DNA tract shortening by decreasing the chromatin accumulation of RAD51 in cells following HU exposure.

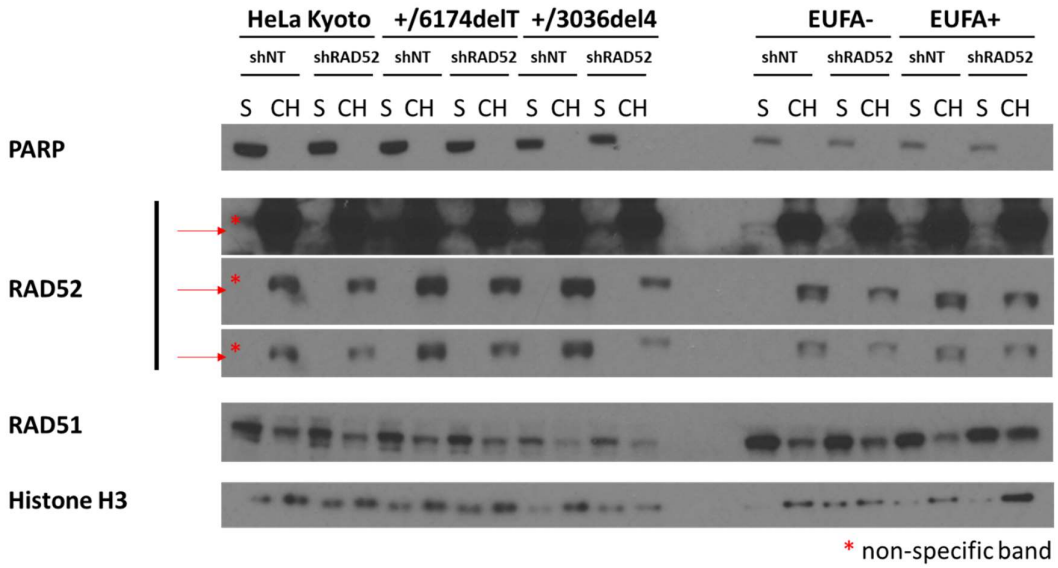

Figure 33: RAD52 depletion does not affect the sub-cellular localisation of RAD51 following exposure to replication stress. Sub-cellular fractionation was performed in cells following treatment with HU (4 mM) for 5 hours to obtain soluble (S) and chromatin (CH) bound protein fractions. PARP and Histone H3 were used as loading controls for the soluble and chromatin fractions, respectively. RAD52 runs as a doublet due to an upper non-specific band, as indicated by the asterisk (*).

2.5 RAD52 is recruited to stalled replication forks and regulates RAD51 loading on these

The iPOND assay was firstly developed by Sirbu *et al.*, 2011 to specifically detect proteins bound to nascent DNA at replication forks. Hence this method is more appropriate for studying protein dynamics at RFs rather than examining the chromatin localisation of RAD51. The technique involves the brief labelling of active replication forks with EdU before the covalent attachment of a biotin tag to the thymidine analogue using biotin azide in a 'click reaction'. This biotinylates any nascently synthesised DNA and enables its purification using streptavidin-coated beads along with any bound proteins. In the 'no-click' or DMSO control reaction, biotin azide is omitted and replaced by DMSO in the click reaction mix, thus serving as a negative control for the pull-down. However, a formaldehyde crosslinking step of DNA-protein complexes prior to cell harvesting interferes with protein detection by western blotting.

For this reason, aniPOND was later advanced (T. Leung, El Hassan and Bremner, 2013) to improve protein yield and detection. This approach omits the formaldehyde crosslinking step following fork labelling, and lyses cells to allow nuclear harvesting in a single step before proceeding to the 'click reaction'. Chromatin is then extracted from nuclei and solubilised by extensive sonication for the subsequent purification of biotin-labelled DNA and its associated proteins via streptavidin capture. This updated technique was therefore used to assess whether the fork protective activity of RAD52 at stalled forks is through controlling RAD51 loading on these, since BRCA2 has been previously shown to contribute to fork protection by stabilising RAD51 filaments (Schlacher *et al.*, 2011). To investigate this possibility, aniPOND was performed in cells stably expressing shRAD52 following a 3-hour treatment with 4 mM HU.

A few test runs were performed using HeLa Kyoto and EUFA- cells (figure 34) to ensure appropriate detection of the proteins in question in the absence and presence of HU. A protein is interpreted to be enriched at the replication fork if it is detected in a 'click reaction'

sample but cannot be detected in the corresponding DMSO control sample. Furthermore, replication stress proteins recruited to damaged forks should only be detectable after a chase into a replication stress reagent such as HU. Purification of proteins at RFs is confirmed by probing for PCNA and histone H3, both of which are used as positive controls for the assay. Histone H3 is used as a loading control and to ensure chromatin capture of EdU labelled samples subjected to the 'click reaction'. The protein levels decrease upon HU treatment, since histones are newly synthesised at nascent DNA (Sirbu *et al.*, 2011). HU-induced stalling of active replisomes stops DNA replication and consequently minimises histone synthesis and capture for subsequent detection. In addition, PCNA is used as a control to ensure isolation of replisome proteins on active replication forks. In the presence of replication stress in the form of HU, the detected levels of PCNA reduce due to protein unloading following RF stalling (Sirbu *et al.*, 2011).

During the test runs, two types of streptavidin beads were used, including magnetic and agarose-coupled, to test purification yield and efficiency for each (figure 34). The background was lower in the pull-down with the magnetic beads, and hence these were used for subsequent runs to minimise non-specific binding. In both cases, however, high background was observed upon probing with the RAD51 antibody, thus making RAD51 detection challenging. Nevertheless, the protein was found to be captured on replication forks both before and after HU treatment. Its recruitment to the fork was enhanced upon exposure to HU, thus suggesting an enhanced affinity of the protein for stalled RFs and classifying RAD51 as a replication stress protein. Despite my initial plan to use EUFA- as my BRCA2-deficient model for aniPOND, detection of RAD51 at RFs could not be fulfilled in this cell line (figure 34D), potentially owing to reduced protein loading and/or assembly as a result of the specific BRCA2 mutations in the cells. For this reason, the +/3036del4 BRCA2 heterozygous cell line was used instead, in which RAD52 depletion was previously found to more severely impact the chromatin localisation of RAD51 (chapter 1, figures 23 and 24).

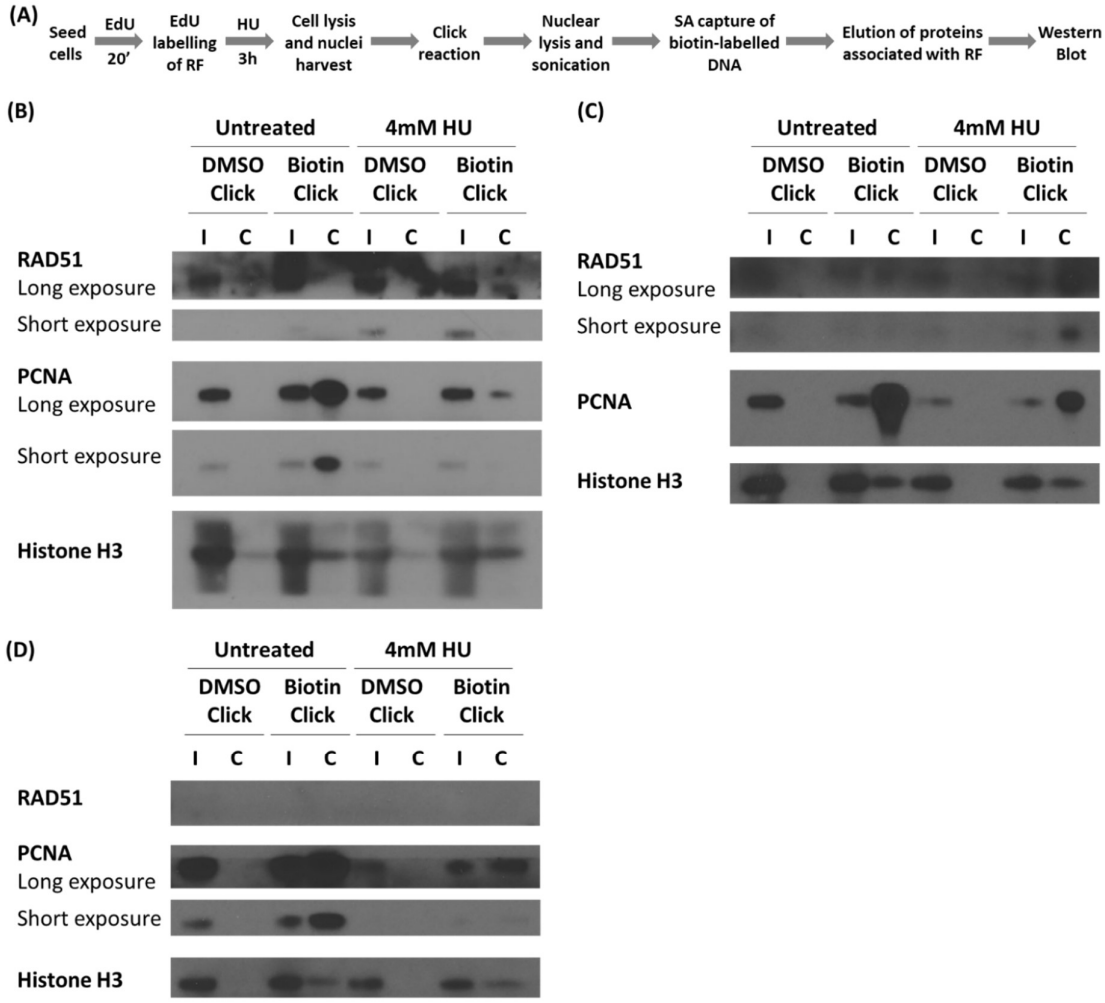

Figure 34: Optimisation of the aniPOND technique. (A) Schematic of the aniPOND technique. Test runs of the aniPOND assay using HeLa Kyoto cell lysates on agarose-coupled beads **(B)**, HeLa Kyoto cell lysates on magnetic beads **(C)** and EUFA- lysates on magnetic beads **(D)** are shown. Cells were either left un-treated or treated with 4 mM HU for 3 hours. PCNA and histone H3 were used as loading controls. Input = 0.25% cell equivalent ($1.5x10^5$) cells. Capture = 25% cell equivalent ($1.5x10^7$) cells. I, input; C, capture.

The results from the aniPOND assay indicate that RAD52 is recruited to stalled RFs, as shown in figure 35. In agreement with this observation, protein detection on perturbed forks is abrogated in cells expressing sRAD52. With respect to RAD51 localisation to HU-stalled forks, capture of RAD51 is diminished in RAD52-depleted cells when compared to the shNT control. These findings suggest that RAD52 is recruited to stalled RFs to either facilitate RAD51 loading or stabilise RAD51 filament formation on these. However, since recombinase loading and subsequent RAD51-mediated fork reversal are very early events following fork stalling, with reversal requiring minimal amounts of RAD51 (Bhat *et al.*, 2018), my experimental conditions of a 3-hour HU treatment are probably capturing the second scenario despite not eliminating the first possibility.

Therefore, the results presented thus far suggest that RAD52 activity is essential for conferring replication fork protection against MRE11-dependent degradation by regulating RAD51 recruitment to stalled forks, regardless of BRCA2 function.

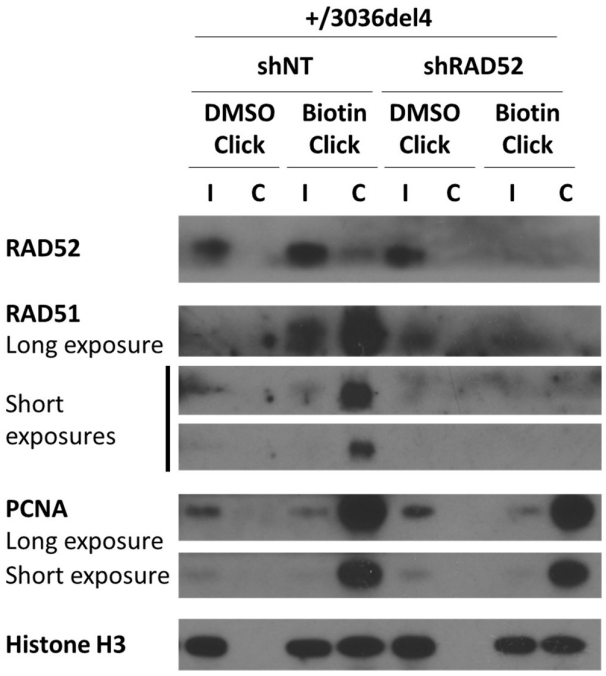

Figure 35: RAD52 is recruited to stalled replication forks and controls RAD51 localisation to these. aniPOND of HeLa Kyoto cells heterozygous for the 3036del4 mutation following a 3-hour treatment with 4 mM HU. PCNA and histone H3 were used as loading controls. The blots are representative of one experiment. Input = 0.25% cell equivalent ($1.5x10^5$) cells. Capture = 25% cell equivalent ($1.5x10^7$) cells. I, input; C, capture.

2.6 RAD52 prevents DSB formation downstream of fork arrest in human cells

Since RAD52 depletion leads to replication fork deprotection in cells irrespective of their BRCA2 status, I next wanted to assess DNA break induction in the form of DSBs following HU treatment. For this, I employed a neutral comet assay via single cell electrophoresis. Briefly, cells were treated with 4 mM HU for 5 hours, embedded in agarose and lysed before being subjected to electrophoresis. Cell lysis forms nucleoids made of supercoiled DNA, which was then allowed to unwind under neutral conditions for an hour before application of an electric field. Electrophoresis causes the negatively charged DNA to move towards the positively charged anode, with damaged DNA migrating out of the nucleoid forming comet tails while un-damaged DNA stays compact within the comet head. Hence, the amount of DNA in the tail is representative of the extent of DNA damage in a cell. After electrophoresis, the DNA was stained using ethidium bromide and at least 100 comets were imaged per condition for analysis.

RAD52 was depleted using siRAD52 in cells that are wild-type for *BRCA2*, HeLa Kyoto and EUFA+, or biallelic mutant for the gene, as in the case of EUFA- and the D2723H homozygote BRCA2 mutant cell line. RAD52 loss caused an increase in the number of DSBs, both in the absence and presence of replication stress, as measured by the neutral comet assay (figure 36). This was true in both BRCA2- proficient and deficient cells, suggesting an independent function of RAD52 in preventing DSB formation downstream of endogenous or exogenous replication stress. As expected, exposure to HU enhanced DSB formation in cells. In addition, S1 nuclease treatment further enhanced DSB formation, suggesting that at 5 hours post-HU exposure not all stalled replication forks have collapsed into DSBs and some single-stranded gaps remain for S1 nuclease-induced DNA breakage (figure 37).

These observations suggest that RAD52 activity prevents collapse of stalled forks into DSBs during conditions of endogenous or exogenous replication stress. This stands true irrespective of the BRCA2 status of cells, thus proposing that RAD52 functions to protect genomic stability in cells by preventing DNA damage downstream of fork stalling and/or collapse.

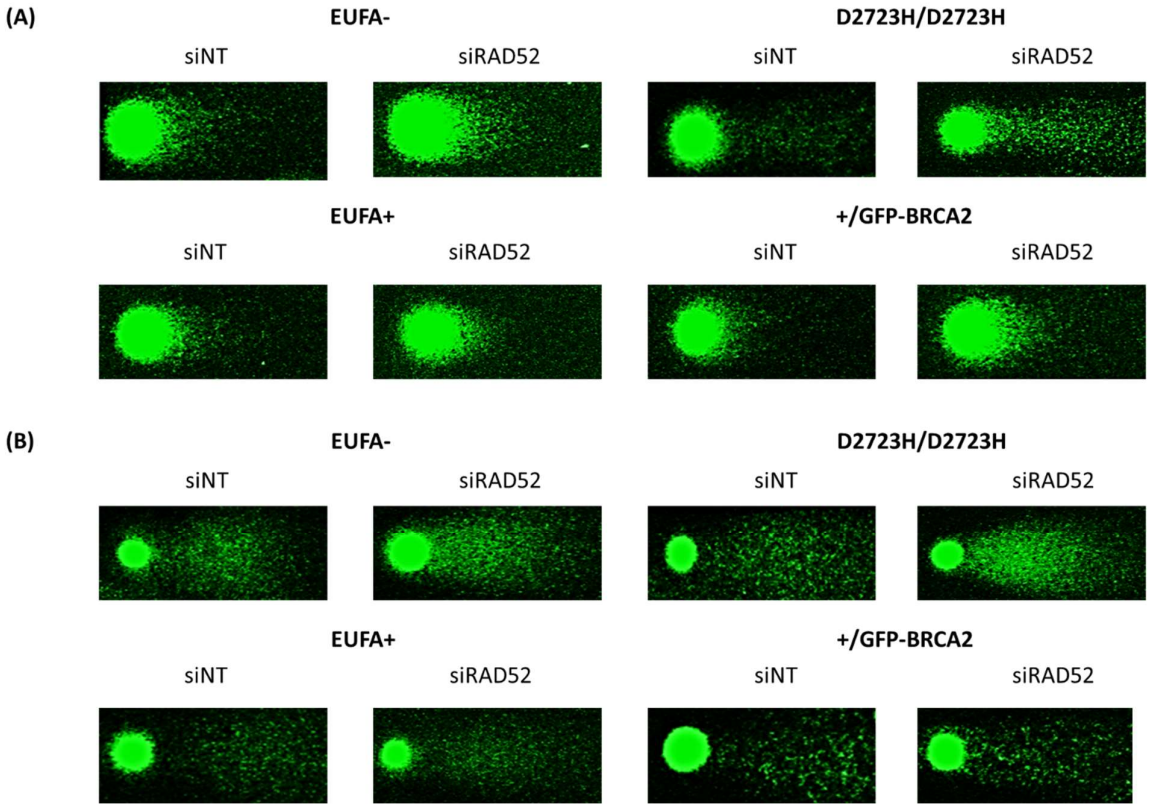

Figure 36: RAD52 depletion enhances DSB formation in cells. A neutral comet assay was performed in un-treated cells **(A)** or following a 5-hour exposure to 4 mM HU **(B)** to determine DSB formation following RAD52 depletion (25 nM siRNA for 48 hours). Cell DNA was stained with ethidium bromide and imaged by confocal microscopy. Immunofluorescence images are representative of three independent experiments (n=3).

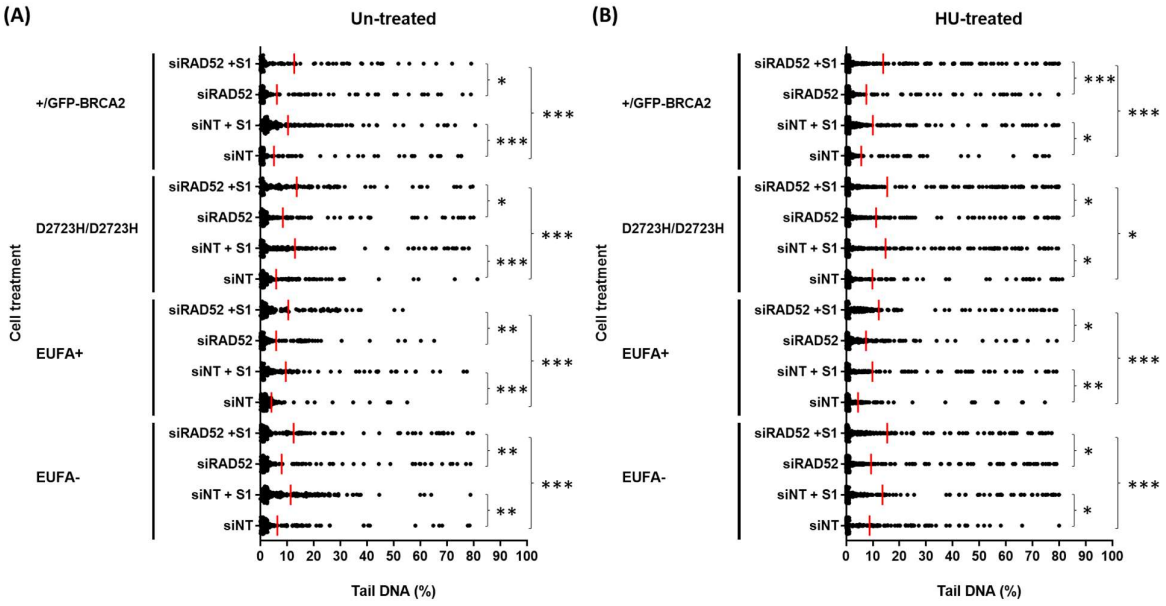

Figure 37: Quantification of DSBs detected by the neutral comet assay. The comet images obtained from the neutral comet assay for un-treated **(A)** and HU-treated **(B)** cells were analysed using the CaspLab software. The percentage of DNA found in comet tails corresponds to the amount of DNA damage found in cells. Mean values are indicated by a red line. The data are representative of three independent experiments (n=3) and statistical significance is indicated by asterisks (*p<0.05, **p≤0.01, ***p≤0.001).

2.7 RAD52 depletion leads to reduced cell viability in response to replication stress

Next, I was interested to find out the consequences of replication stress exposure in cells following RAD52 depletion in terms of cell viability. To test this, I used the cell line panel stably expressing shNT or shRAD52. Cells were treated with 4 mM HU for 5 hours, as in previous experiments, before plating them for a colony forming assay to assess growth and survival. Exposure to HU was found to decrease the clonogenic survival of cells in comparison to the untreated controls (figure 39), irrespective of RAD52 depletion. However, RAD52 depletion further exacerbated cell survival under replicative stress conditions, as observed by the lower number of colonies formed by all the tested cell lines upon doxycycline-induced expression of the shRAD52 construct (figure 38). Since protein loss did not affect the colony forming capacity of cells that are wild-type or heterozygous for *BRCA2* in the absence of exogenous replication stress (chapter 1, figure 10), the experimental results presented here uncover a novel role of RAD52 in supporting cell survival following induction of replication stress, irrespective of BRCA2 function.

In summary, data in this chapter propose that RAD52 protects stalled replication forks from nucleolytic degradation and in turn prevents the downstream collapse of these into DSBs. In RAD52 absence, the resultant excess formation of DSBs leads to reduced viability. Therefore, RAD52 is critical for protecting cells under replication stress conditions, potentially by mediating DNA repair pathways that enable cell survival at the expense of genetic stability.

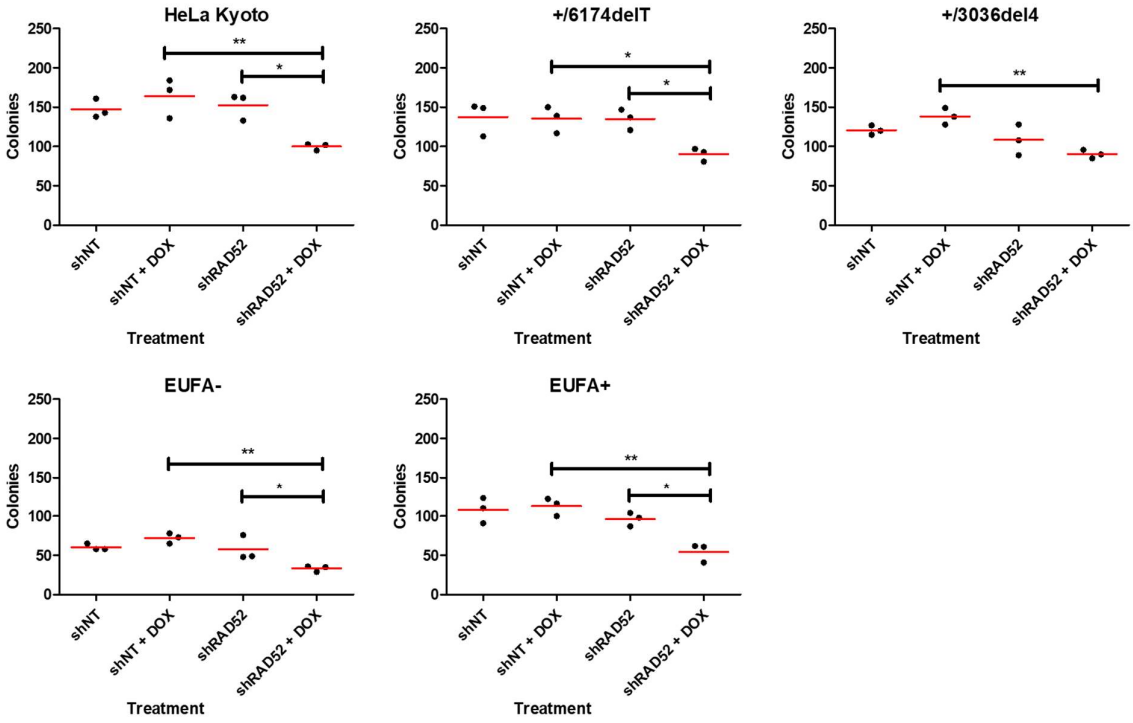

Figure 38: Cell viability is reduced in RAD52-depleted cells under conditions of replicative stress. A colony forming assay was performed in the presence and absence of doxycycline induction (1 µg/ml) of the shRNA constructs. Doxycycline induction was performed for 48 hours prior to cell seeding and maintained for the duration of the experiment. Cells were treated with 4 mM HU for 5 hours, re-plated and allowed to grow for a 7-10 day duration. Colonies formed were quantified from duplicate wells for each condition. Graphs are representative of three independent experiments, with the mean indicated by a red line. Statistical analysis performed by a one-way ANOVA test and a Tukey post-test to compare all pairs of columns.

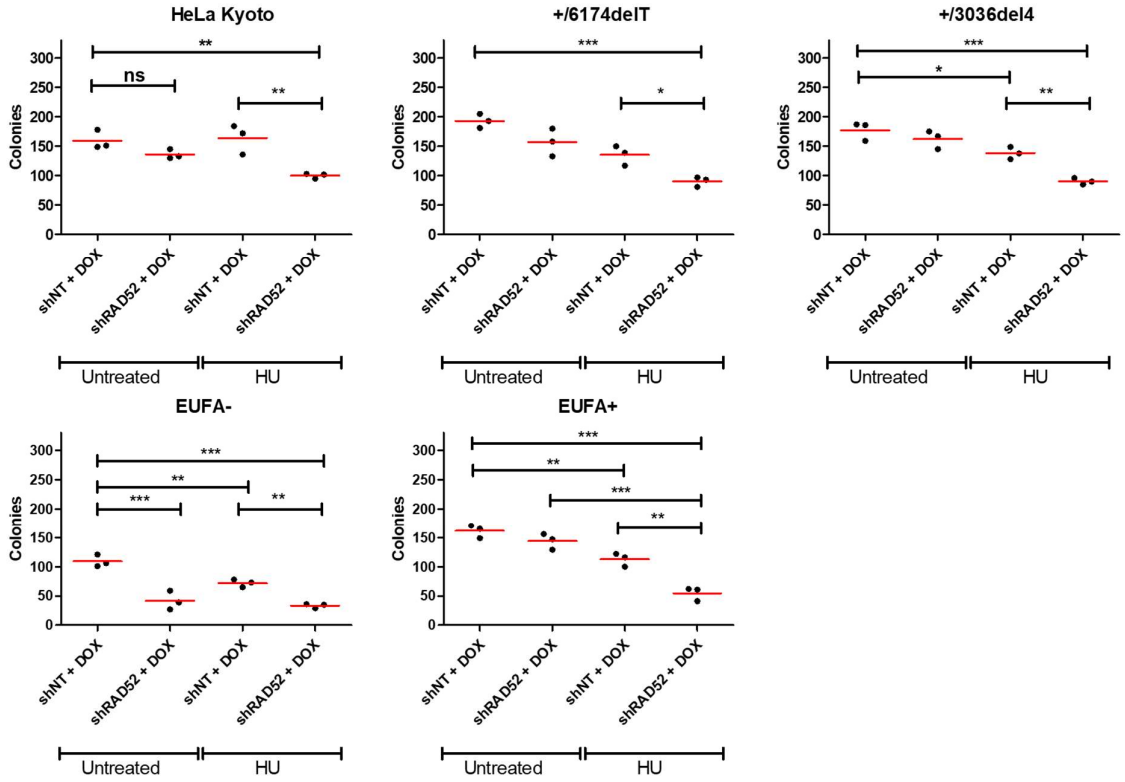

Figure 39: Exposure to HU reduces cell viability. A side-to-side comparison of the colonies formed by un-treated and HU-treated cells is shown for each cell line following doxycycline-induced expression (1 µg/ml) of the shRNA constructs. Graphs are representative of three independent experiments, with the mean indicated by a red line. Statistical analysis performed by a one-way ANOVA test and a Tukey post-test to compare all pairs of columns.

DISCUSSION

Replication stress is the most common source of endogenous damage, since fork stalling can cause fork collapse following prolonged periods of time and subsequently trigger the formation of one-ended DSBs. Such DSBs lack blunt ends and hence can only be repaired by HR or, in HR-deficient settings, by SSA or alt-NHEJ. An HR-independent role for BRCA2 in protecting stalled RFs from nucleolytic degradation has been recently uncovered, which supports the stabilisation of elongated RAD51 filaments (Lomonosov *et al.*, 2003; Schlacher *et al.*, 2011; S Ying, Hamdy and Helleday, 2012). Since RAD51 localisation to chromatin and subsequent focalisation have been shown to also occur independently of BRCA2 during replication (Tarsounas, Davies and West, 2003; Chaudhuri *et al.*, 2016), RAD51 activity during fork arrest might be regulated by other proteins, such as RAD52. In fact, human RAD52 has been shown to promote DNA synthesis for the restart of collapsed RFs via break-induced repair or the replication-stress related process of mitotic DNA synthesis (Bhowmick, Minocherhomji and Hickson, 2016; Sotiriou *et al.*, 2016). However, a role for RAD52 in maintaining the integrity of stalled RFs has not been investigated or documented.

Following exposure to 4 mM HU for 5 or 24 hours, HA-RAD52 was found to form nuclear foci in cells irrespective of their BRCA2 status. Treatment with the stalling agent is thought to reversibly arrest forks following a 5-hour exposure, with stalled forks eventually collapsing into DSBs by 24 hours of treatment. Therefore, the observed focalisation of RAD52 at the two tested time-points proposes functions of the protein at both stalled and collapsed replication forks, in both BRCA2- deficient and proficient settings, as exemplified by EUFA- and EUFA+ cells, respectively. Using a proximity ligation assay, Roy *et al.*, 2018 described RAD52 recruitment to nascently synthesised DNA both at low and high concentrations of HU, thus supporting the suggested roles of the protein equally at stalled and collapsed forks. Moreover, human RAD52 has been shown to interact with components of the MCM complex *in vitro*, thus further implicating the protein in replication stress responses promoting DNA repair (Shukla *et al.*, 2005).

In order to further investigate the proposed function of RAD52 at stalled forks, the stability of arrested RFs was assessed by the single molecule DNA fibre technique following RAD52 depletion in cells with different genetic backgrounds of *BRCA2*. Importantly, the biallelic mutation of *BRCA2* itself led to nascent DNA degradation at stalled forks following exposure to HU, as previously reported by Schlacher *et al.*, 2011. This is indicated by the observed tract shortening in EUFA- and D2723H/D2723H cells on comparison of the siNT and siNT+HU samples in figure 28. Nevertheless, cells depleted of RAD52 exhibited an enhanced nascent tract shortening when compared to control-depleted cells. Intriguingly, tract shortening in cells was observed following RAD52 depletion both in the absence (siNT compared to siRAD52) and presence of added HU (siNT+HU compared to siRAD52+HU). This indicates the presence of endogenous replication stress in cells, which is unveiled upon RAD52 depletion, even in the absence of added replication stress. Notably, this observation holds true for all the cell models used. In BRCA2-proficient cells, in either the wild-type or heterozygous setting, the observed tract shortening occurring following RAD52 depletion is not further exacerbated following added HU exposure (figures 28 and 29, siRAD52 compared to siRAD52+HU). This observation suggests that BRCA2 plays roles downstream of RAD52 in combating replication stress and preventing additional degradation of stalled replication forks. In contrast, in BRCA2-deficient settings where none of the protein alleles are intact, RAD52 depletion leads to excessive nascent tract shortening upon addition of exogenous stress in the form of HU (siRAD52 compared to siRAD52+HU).

In both BRCA2- deficient and proficient cells, tract shortening following RAD52 loss was induced by MRE11-dependent degradation, since concomitant exposure to HU and mirin - an inhibitor of the MRE11 nuclease - restored IdU tract lengths (figures 31 and 32). This observation reveals a role for RAD52 in stabilising stalled forks by protecting these against excessive nucleolytic degradation by MRE11. Importantly, this role is significant both in the presence and absence of functional BRCA2 in cells. Therefore, both RAD52 and BRCA2 have fork protective roles in human cells, which act to prevent the nucleolytic digestion of stalled

replication forks by MRE11, as indicated by the additive tract shortening observed upon loss of both proteins in cells.

A fork protection function has been previously described for BRCA2, which has been shown to prevent excessive MRE11-dependent degradation of stalled forks by stabilising RAD51 filaments (Schlacher *et al.*, 2011). Although the mechanism of RAD51-mediated protection has not been characterised, RAD51 filaments are hypothesised of coating ssDNA at stalled forks, thus preventing access to MRE11 and counteracting degradation mediated by the nuclease (Hashimoto *et al.*, 2010; Petermann *et al.*, 2010). However, upstream of filament formation for fork protection, RAD51 is known to drive fork reversal in response to replication stress, in a step independent of the BRCA2 mediator (Zellweger *et al.*, 2015; Mijic *et al.*, 2017). This differential requirement for BRCA2 in fork protection but not reversal seems to be due to the fact that the latter only requires limited amounts of RAD51, whereas fork protection requires higher concentrations of the recombinase for the formation of extended filaments (Bhat *et al.*, 2018). Therefore, I then wanted to investigate the molecular mechanism by which RAD52 prevents the MRE11-dependent degradation of stalled RFs and assess whether this is by regulating RAD51 activity and at which step. In order to address whether the observed RAD52-mediated protection of nascent DNA is via RAD51, I first evaluated the sub-cellular localisation of RAD51 in cells exposed to replication stress in the presence and absence of RAD52. Unexpectedly, RAD52 depletion did not affect the sub-cellular localisation of RAD51 in cells following HU treatment. This might be because, as already mentioned, RAD51 levels necessary for fork reversal are very minimal and hence any changes in these might not be enough to cause an observable difference in the sub-cellular distribution of RAD51. Reduced protein amounts of RAD51 are required for fork reversal and RF protection in comparison to those necessary for HR (Bhat and Cortez, 2018; Bhat *et al.*, 2018), and hence RAD51 activity at stalled RFs might not be quantitatively sufficient to alter protein levels in different sub-cellular compartments.

In order to more specifically detect RAD51 on stalled RFs, aniPOND was then employed. This technique specifically isolates proteins on replication forks that are either active or stalled by replication stress-inducing agents. Although the cell line model originally planned for this experiment were EUFA- cells, RAD51 detection was technically impossible in these. This suggests that EUFA- cells have inherently reduced levels of RAD51 bound to stalled RFs, which could be as a result of the biallelic truncations they carry in *BRCA2*. This would imply that BRCA2 is the primary protein that facilitates RAD51 loading and filament extension at replication forks, as in the case of DSBs. In absence of BRCA2, other HR mediators can assist recombinase function for ssDNA loading, fork reversal or nucleofilament formation (Bugreev, Rossi and Mazin, 2011; Piwko *et al.*, 2016), but in a less efficient manner. Furthermore, RAD51 protein requirements are thought to be minimal at RFs, especially for fork reversal (Bhat *et al.*, 2018), thus making protein detection difficult in EUFA- cells which lack elongated RAD51 filaments and might potentially only have reversed forks. In fact, short and unstable filaments formed by RAD51 mutants with constitutive ATPase activity have been shown to suffice for fork reversal, even in the absence of efficient RPA displacement or BRCA2 involvement (Mijic *et al.*, 2017). Therefore, the assay was eventually performed in the +/3036del4 cell line, where BRCA2 heterozygosity was hypothesised to be more likely of unveiling a role for RAD52 at forks. RAD52 was found to localise at stalled RFs and promote RAD51 loading to these, as proved by the reduced recruitment of RAD51 in RAD52-depleted cells. RAD52 was recently reported of localising to ssDNA following fork arrest by a proximity ligation assay (Malacaria *et al.*, 2019), thus supporting the protein recruitment I observe by the aniPOND assay.

Human RAD52 has multiple emerging activities, including single-strand annealing, strand exchange and mediator functions (Kagawa *et al.*, 2001, 2008; Bi *et al.*, 2004; Kumar and Gupta, 2004; Feng *et al.*, 2011; Brouwer *et al.*, 2017; Mazina *et al.*, 2017; Yasuhara *et al.*, 2018), which have been described of facilitating DNA repair. Which of these is required for replication fork protection, however, remains to be elucidated. During fork reversal, annealing of the two nascent daughter strands and re-annealing of the parental ones converts the three-way junction at the RF into a four-way Holliday Junction with a ‘chicken-foot’ structure (Higgins,

Kato and Strauss, 1976). RAD52 might therefore be required for this strand annealing step and hence be necessary for fork regression into a reversed fork structure.

Given the numerous functions of RAD51 at stalled forks, namely reversal, protection and restart (Petermann *et al.*, 2010; Schlacher *et al.*, 2011; Mijic *et al.*, 2017), we cannot deduce by aniPOND which RAD51 activity is being dictated by RAD52. Regulation could occur at multiple steps following fork stalling, as well as before and after RAD51-dependent fork reversal. For instance, depleting RAD52 can prevent RAD51-driven fork reversal by reducing recombinase loading on stalled forks. This would hence prevent RF re-modelling to a structure that is accessible to nucleases, preventing nucleolytic degradation and conferring protection to nascent DNA upstream of reversal of stalled RFs. In fact, RAD52 has been recently reported to prevent fork reversal by altering the fork structure into a more compact form that is not as accessible to remodelling enzymes that drive fork regression (Malacaria *et al.*, 2019). Furthermore, both RAD52 and the fork reversal enzyme SMARCAL1 make use of RQK motifs for interacting with RPA (Ciccia *et al.*, 2009; Grimme *et al.*, 2010), and hence can be envisioned of competing for binding to RPA-coated ssDNA at stalled forks. This suggestion implies that RAD52 can potentially restrict SMARCAL1-driven fork reversal, and RAD52 loss would thus lead to enhanced reversal and degradation of stalled replication forks. Alternatively, since reversed forks are the entry points for nucleases (Kolinjivadi *et al.*, 2017; Lemaçon *et al.*, 2017; Mijic *et al.*, 2017; Taglialatela *et al.*, 2017), the MRE11-depedent degradation is expected to be abrogated if RAD51-driven fork reversal is limited consequent to RAD52 loss and lack of RAD51 loading on stalled forks. In line with this hypothesis is a report of RAD52 depletion restoring the frequency of reversed forks being formed in BRCA2-defective cells following HU exposure (Mijic *et al.*, 2017), thus supporting a role for RAD52 in aiding RAD51 loading and subsequent reversal of stalled forks. Furthermore, the same study described that inhibition of RAD52 activity reduces MRE11 recruitment to arrested replication forks (Mijic *et al.*, 2017). However, observations by Mijic *et al.*, 2017, whereby RAD52 depletion was reported to enhance fork protection by preventing MRE11-dependent recruitment and subsequent degradation, are contradictory to my own experimental evidence as well as data published

earlier this year in Malacaria *et al.*, 2019. According to figures 28-30, RAD52 depletion causes tract shortening instead of inducing stabilisation of stalled RFs, thus arguing against the theory developed by Mijic *et al.*, 2017. Therefore, I propose a model (figure 40) in which RAD52 acts downstream of RAD51-mediated fork reversal, stabilising RAD51 filaments on reversed forks and protecting fork structures from MRE11-dependent degradation, in a similar manner to BRCA2. In fact, Malacaria *et al.*, 2019 described RAD52 of being recruited to nascent ssDNA following fork reversal, since SMARCAL1 depletion substantially reduced the interaction between RAD52 and stalled forks.

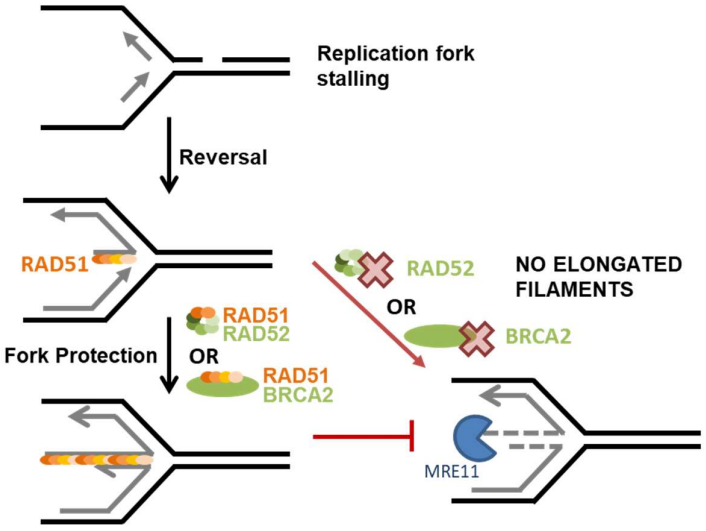

Figure 40: Proposed model for RAD52 activity conferring replication fork protection in cells. Upon fork stalling, replication fork reversal is driven by minimal amounts of RAD51. Subsequent formation of stable elongated RAD51 filaments on reversed forks prevents their nucleolytic degradation. Both BRCA2 and RAD52 confer fork protection against MRE11-dependent degradation in humans, with the protective activity of RAD52 being independent of the BRCA2 status of cells. The two proteins appear to act downstream of fork reversal, and hence confer this fork protective activity by stabilising RAD51 assemblies at reversed stalled replication forks and inhibiting downstream excessive nucleolytic processing. Concomitant loss of both RAD52 and BRCA2 leads to additive nascent DNA degradation, further suggesting that the two proteins protect stalled replication forks from MRE11-dependent degradation in independent pathways.

As part of this work, fork degradation was also shown to occur subsequently to fork reversal in cells devoid of RAD52, thus further supporting the suggestion that RAD52 protects reversed fork structures rather than stalled forks prior to reversal. Furthermore, over-expression of RAD51 in RAD52-inibited cells reverted the observed fork degradation, as a result of enhanced coating of nascent ssDNA by the recombinase (Malacaria *et al.*, 2019). Collectively, these results suggest that protection of reversed forks by RAD52 is through regulating RAD51 activity, potentially by stabilising RAD51 structures on reversed forks. Additionally, as suggested by my aniPOND data, RAD52 seems to control the recruitment of RAD51 on perturbed RFs. In fact, the inappropriate recruitment of RAD51 to parental versus nascent strands, occurring in RAD52 absence, has been described to cause enhanced nascent ssDNA degradation due to the inability of the recombinase to protect all the formed reversed fork structures (Malacaria *et al.*, 2019). Hence, the fork protective activity of RAD52 appears to be two-fold: regulating the appropriate recruitment of RAD51 to nascent ssDNA as well as stabilising RAD51 structures on reversed forks.

Arrested forks, unlike DSBs, do not span extensive regions of ssDNA, and hence limited RAD51 nucleation or extension, like the one observed in EUFA- cells following IR exposure, might be sufficient to confer protection at such structures. In fact, the ssDNA stretches formed at stalled RFs have been reported to extend for less than 100 bases (Zellweger *et al.*, 2015), whereas resection of DSBs can generate ssDNA regions spanning thousands of nucleotides (Chung *et al.*, 2010). However, we cannot deduce from the aniPOND results whether RAD51 localised at arrested forks is elongated and to what extent. Regardless, RAD51 loading on stalled forks is known to be insufficient for fork protection (Schlacher *et al.*, 2011), since -as already mentioned- RAD51 promotes fork regression and reversed forks are actually the entry points for nucleolytic enzymes (Kolinjivadi *et al.*, 2017; Lemaçon *et al.*, 2017; Mijic *et al.*, 2017; Taglialatela *et al.*, 2017). Downstream of fork reversal, BRCA2 is required for fork protection against excessive nucleolytic digestion, presumably by stabilising RAD51 filaments at reversed forks (Schlacher *et al.*, 2011). Nonetheless, RAD52 is found to confer some fork protective activity in cells, even in the absence of BRCA2, thus suggesting that the protein does not solely

regulate RAD51 loading at stalled RFs. RAD52 might be additionally involved in the formation and/or stabilisation of RAD51-dependent structures following recombinase loading at forks. Therefore, the effect of RAD52 depletion on fork structure should be further investigated to derive an accurate model of how the protein regulates replication forks prior to and following arrest, since such mechanistic insights cannot be inferred from the limited information obtained by aniPOND. To address these questions, microscopic techniques of higher resolution, such as *d*STORM or electron microscopy, are required. In fact, EM-based analysis is now being increasingly used to assess the structural architecture of RF intermediates and evaluate fork reversal, degradation and symmetry (Kolinjivadi *et al.*, 2017; Lemaçon *et al.*, 2017; Mijic *et al.*, 2017).

Following fork reversal, replication intermediates are processed by numerous nucleases to initiate fork restart. Currently, the first step in nucleolytic processing is thought to be the controlled MRE11-dependent resection of the regressed arm, due to the limited processivity of the nuclease, which is subsequently extended by EXO1 (Lemaçon *et al.*, 2017). This creates 3'-ssDNA tails at forks, forming substrates for MUS81/SLX4-mediated cleavage into DSBs, that can be subsequently repaired by HR. Others have reported a DNA2-depedent pathway occurring downstream of MRE11-mediated resection to encourage processive cleavage into DSBs, where DNA2 acts redundantly to EXO1 due to its ability to resect 5' ends into 3' ss-overhangs (Thangavel *et al.*, 2015; Lemaçon *et al.*, 2017). However, DNA2 does not seem to contribute to the fork degradation seen in BRCA2-deficient cells (Lemaçon *et al.*, 2017), and has been described of degrading stalled RFs to promote the restart of RAD51-reversed forks in a mechanism that requires WRN but is independent of MRE11, EXO1, CtIP and MUS81 (Thangavel *et al.*, 2015). This suggests that different fork intermediates are formed in the presence or absence of specific recombination factors, that in turn enable access to different nucleases (Hromas *et al.*, 2017; Lemaçon *et al.*, 2017). Nevertheless, the precise mechanism dictating nuclease choice is still unknown, although this is thought to be defined by the structure of the replication intermediate produced, owing to the substrate specificity of the nucleases involved (i.e. GEN1, SLX4, EEPD1). MRE11, for example, is known to preferentially

cleave ssDNA tails found at dsDNA-ssDNA junctions, whereas EXO1 acts on dsDNA substrates with 3'-ssDNA overhangs (Mimitou PE, 2010; Liu and Huang, 2016). MUS81, on the other hand, has a preference for 3' flaps or three-way junctions like those formed at replication forks (Constantinou *et al.*, 2002), and has been shown to act downstream of a RAD52-dependent structure in checkpoint-deficient cells (Murfuni *et al.*, 2013). MUS81-dependent cleavage of stalled forks into DSBs in turn enables the survival of replication-stressed checkpoint-deficient cells. This is potentially through encouraging POLD3-dependent DNA synthesis for fork restart via break-induced repair (Sotiriou *et al.*, 2016; Lemaçon *et al.*, 2017), which appears to be critical for cell rescue and has been shown to be dependent on Rad52 in yeast (Malkova, Ivanov and Haber, 1996). MUS81 seems to cleave RF intermediates in both BRCA2- proficient and deficient settings, but fork stalling is more dramatically exacerbated in BRCA2-deficient settings following MUS81 loss, suggesting its more critical requirement in such genetic backgrounds (Lemaçon *et al.*, 2017). In fact, the simultaneous loss of MUS81 and RAD52 leads to cell death in checkpoint-deficient cells, with lethality being rescued by RAD51 depletion, owing to the formation of RAD51-dependent toxic intermediates downstream of GEN1 cleavage (Murfuni *et al.*, 2013). In an alternative pathway, EEPD1-mediated fork processing has been shown to be detrimental in RAD52-depleted BRCA1 mutant cells (Hromas *et al.*, 2017). In the absence of the RAD52 bypass pathway, the HR deficient cells form toxic EEPD1-dependent fork repair intermediates that lead to cell death. Such intermediates formed in BRCA1-deficient backgrounds cannot be processed by MUS81 and can only be cleaved by EEPD1 (Hromas *et al.*, 2017; Lemaçon *et al.*, 2017). Depleting EEPD1 in this setting promotes restart of stalled RFs, by enabling cells to repair DSBs by alt-NHEJ (Hromas *et al.*, 2017). Alt-NHEJ, however, is not a conservative DNA repair pathway and can lead to enhanced genomic instability (Mateos-Gomez *et al.*, 2015). Collectively, these observations suggest that pathway choice, engagement, outcome and genomic maintenance are all determined by HR mediator protein availability, the structural architecture of fork intermediates and downstream substrate accessibility by the available nucleases (Hromas *et al.*, 2017). RAD52 might be implicated in creating different fork intermediates in the presence or absence of

BRCA1/2, thus determining pathway choice in terms of substrate availability for the multiple nucleases involved in fork processing and degradation. RAD51-independent mechanisms that confer fork protection have also been reported, thus highlighting the complexity and the multi-layered regulation of processes involved in fork protection. This also pinpoints to the fact that targeting HR-deficient cancers in the clinic should be approached differently according to their genetic background and whether these are BRCA1- or BRCA2- deficient. For example, MUS81 depletion has been found to confer fork protection and subsequent chemotherapeutic sensitivity in BRCA2- but not BRCA1-deficient cells (Chaudhuri *et al.*, 2016; Rondinelli *et al.*, 2017). Furthermore, loss of fork stability has been reported of contributing to the genomic instability and embryonic lethality observed in BRCA2-deficient cells (Chaudhuri *et al.*, 2016), thus stressing the importance of RF remodelling and that of fork protection pathways in influencing the pathogenesis of HR-deficient tumours. Intriguingly, several studies have suggested that lack of homologous recombination does not necessarily correlate with drug sensitivity in BRCA-mutated tumours (Chaudhuri *et al.*, 2016; Rondinelli *et al.*, 2017; Taglialatela *et al.*, 2017), as indicated by the fact that not all HR-deficient cancers respond to PARP inhibition. Therefore, assessing fork protection in cancer patients with BRCA mutations could provide a more accurate biomarker for predicting drug response in these, rather than examining their HR proficiency.

Downstream of fork stalling and collapse, RAD52 has been reported to mediate the initial RAD51-ssDNA nucleofilament formation at one ended DSBs, while BRCA2 is required for guiding the RAD51 recombinase activity during later steps in DNA repair (Whelan *et al.*, 2018). This is supported by the fact that RAD52 and RAD51 co-localise early during recovery from camptothecin-induced fork stalling, before BRCA2 recruitment to damage foci. In RAD52 absence, BRCA2 can take over this role of early RAD51 recruitment to RFs, as well as perform the subsequent steps for repair. These observations propose a mechanism where RAD52 and BRCA2 act in a sequential manner to regulate RAD51 activity at stalled RFs, with the initial nucleation step being performed by either protein. Collectively, these papers support a role for RAD52 in cells undergoing replication stress and supporting RAD51 activity at forks. As

discussed earlier, the recombinase has been reported to encourage fork restart at collapsed forks (Hashimoto, Puddu and Costanzo, 2012), although both RAD51- dependent and independent fork restoration pathways have been described (Ira and Haber, 2002). RAD52 might thus be implicated in such restart pathways, whether reliant on RAD51 or not, and hence regulate fork restart mechanisms. In fact, in the absence of RAD51 activity for adequate homology search and strand invasion, as in BRCA2-deficient settings, the strand annealing function of RAD52 has been suggested to come into play, whereby the annealed strands can provide a template that is conductive for fork restart and DNA initiation. Furthermore, depletion or inhibition of RAD52 has been described to decrease the frequency of restarting forks and new origin firing (Hromas *et al.*, 2017; Malacaria *et al.*, 2019), thus implying protein roles in replication stress recovery. These defects observed upon RAD52 abrogation are further exacerbated by mirin treatment (Malacaria *et al.*, 2019), indicative that MRE11-mediated processing of stalled forks provides an alternative pathway for fork restart in RAD52 absence. Actually, fork resection by MRE11 remodels stalled forks into intermediates that facilitate repair and recovery via RAD51-dependent restart, thus preventing subsequent formation of DSBs (Trenz *et al.*, 2006; Bryant *et al.*, 2009; Hashimoto, Puddu and Costanzo, 2012). Additionally, human RAD52 interacts with the WRN helicase, both *in vitro* and *in vivo*, thus proposing that the two proteins cooperate to rescue forks (Baynton *et al.*, 2003). WRN is implicated in fork restart responses in collaboration with the DNA2 nuclease (Thangavel *et al.*, 2015), with the latter not contributing to fork degradation in BRCA2-deficient cells (Lemaçon *et al.*, 2017), thus suggesting that RAD52-dependent fork structures are formed under replicative stress conditions lacking BRCA2, which are subsequently processed and restarted by a DNA2/WRN pathway. Moreover, both WRN and BLM helicases have been linked to RAD51-dependent fork restart (Sidorova *et al.*, 2013), thus suggesting that RAD52 might by mediating such HR-mediated fork restart pathways involving the recombinase enzyme. Lastly, RAD52 has been described to promote the repair of collapsed forks through BIR, a pathway that relies on the MUS81 nuclease and POLD3 for DNA synthesis (Sotiriou *et al.*, 2016). Since MUS81-dependent fork processing and POLD3-mediated fork restart have

been reported to rescue perturbed forks in BRCA2-deficient backgrounds (Lemaçon *et al.*, 2017; Rondinelli *et al.*, 2017), this RAD52-supported pathway potentially provides an escape route for BRCA2-deficient cells to recover following replication stress. This is further supported by the fact that loss of either RAD52 or MUS81 leads to enhanced chromosomal damage, which ultimately leads to cell death upon concomitant depletion of both proteins in checkpoint-deficient settings (Murfuni *et al.*, 2013) that often characterise BRCA2 mutated cancers (Crook *et al.*, 1998; Rhei *et al.*, 1998). These observations suggest another mechanism that contributes to the synthetic lethality seen in cells co-depleted of RAD52 and BRCA2, since RAD52 drives a process that enables the resolution of fork intermediates via MUS81, which in turn enables the cell viability of BRCA2-deficient cells following fork collapse by maintaining sufficient genomic stability.

In order to assess the outcome of replication fork de-protection in RAD52 depleted cells, the neutral comet assay was employed. RAD52 loss was found to enhance DSB formation, both in the absence and presence of replication stress, as measured by the neutral comet assay. This is also the case in cells wild-type for *BRCA2*, suggesting that RAD52 has roles in protecting against DSB formation independently of BRCA2. However, RAD52 depletion exacerbates DSB formation in the presence of HU, thus suggesting that the protein is even more critical for protecting against genomic instability following replication stress in cells, irrespective of their BRCA2 status. Additionally, RAD52 depletion further reduces cell survival following exposure to replication stress, as revealed by a colony formation assay. Hence, RAD52 protects stalled replication forks from nucleolytic degradation to prevent downstream collapse of these into DSBs. In RAD52 absence, the resultant excess formation of DSBs leads to reduced viability and cell death. Consistently, RAD52-deficient cells have been described to exhibit sensitivity to HU (Kan, Batada and Hendrickson, 2017). Therefore, RAD52 is critical for protecting cells in replication stress conditions, irrespective of the BRCA2 status of cells. However, since concomitant loss of BRCA2 and RAD52, as in EUFA- cells, leads to an enhanced level of DSBs and reduced cell viability, the two proteins seem to regulate independent pathways for RF protection following replication stress. This is in line with previous reports suggesting that

human RAD52 has conserved its functions at replication forks to promote repair after replication stress exposure (Wray *et al.*, 2008; Allen *et al.*, 2011; Murfuni *et al.*, 2013; Sotiriou *et al.*, 2016).

The observed correlation between enhanced DSB formation and reduced cell viability following replication stress highlights the fact that DSBs formed downstream of RFs are detrimental for cell survival. Repair of these is critical for maintaining genomic stability and survival, especially in HR-deficient cells. RAD52 might be able to play additional roles in DSB repair, which have not been investigated as part of my work and may be independent of RAD51-mediated HR. For example, single strand annealing functions as a sub-pathway of HR and is thought to be dependent on RAD52 in human cells (Reddy, Golub and Radding, 1997), owing to the lack of an annealer activity in BRCA2 (R B Jensen, Carreira and Kowalczykowski, 2010). Intriguingly, RAD52-mediated SSA has been previously described to occur downstream of replication fork stalling in p53-deficient cells (Roy *et al.*, 2018). However, extensive DNA resection occurs at the DSB during SSA, until complementary sequences are encountered and annealed, and is thus mutagenic. Since the majority of BRCA2-deficient tumours are also mutated in p53 (Crook *et al.*, 1998; Rhei *et al.*, 1998), this RAD52-dependent pathway may be playing biologically relevant roles in the pathogenesis of cancer patients bearing BRCA2 mutations, and hence targeting SSA can potentially improve their outcome. In the absence of both BRCA1/2 and RAD52, alt-NHEJ is used as an escape pathway for the repair of DSBs and enabling cell survival (Mateos-Gomez *et al.*, 2015; Hromas *et al.*, 2017). This pathway requires limited DNA resection of a few nucleotides, and is characterised by microhomology at repair junctions. Alt-NHEJ is mediated by polymerase θ, which has been shown to have RAD51-binding motifs and is thus responsible of sequestering the protein and preventing nucleofilament assembly (Ceccaldi *et al.*, 2015). In the absence of polymerase θ, however, RAD51 forms intermediates that are toxic and lead to the death of HR-deficient cells (Ceccaldi *et al.*, 2015). These observations imply a hierarchy in pathway choice for repairing DSBs formed downstream of collapsed RFs. In the proposed hierarchy, the principal pathway is classical HR, but in the absence of BRCA1 or BRCA2, RAD52-mediated HR and/or SSA would

compensate for this loss. Upon abrogation of both pathways, alt-NHEJ would eventually be employed by cells for DNA repair, but this potentially occurs at the expense of genomic stability.

GENERAL OUTLOOK

The findings described in the preceding chapters suggest divergent requirements for BRCA2 and RAD52 in the regulation of RAD51 during homologous recombination versus replication protection. During HR, RAD52 is redundant for RAD51 regulation in cells that are heterozygous or wild-type for *BRCA2*, but becomes an essential recombination mediator in cells lacking functional BRCA2. However, during replication protection, RAD52 activity is essential for RAD51 regulation regardless of BRCA2 function. Therefore, RAD52 provides a backup pathway for RAD51-mediated homologous DNA repair at DSBs in BRCA2 absence, whilst conferring an independent fork protection mechanism that prevents excessive degradation of reversed forks subsequent to replication stress. The latter activity prevents fork collapse into DSBs and supports the viability of cells, irrespective of their BRCA2 status. However, since only BRCA2-deficient cells are significantly compromised in cell proliferation and/or viability, this highlights that the critical role of RAD52 in enabling the viability of such cells lies in supporting HR. Replication fork de-protection for prolonged periods of time can ultimately lead to collapse and subsequent DSB formation, however, such DSBs can be repaired faithfully by HR in the presence of BRCA2. Nonetheless, enhanced DSB formation in cells lacking both BRCA2 and RAD52, which are thus HR-deficient, eventually leads to compromised viability.

Although PARP inhibitors have been developed on the principle of conferring synthetic lethality to BRCA1/2 mutant cancers, these are only truly effective in a limited number of patients due to inherent and acquired resistance mechanisms (reviewed in Dziadkowiec *et al.*, 2016; Noordermeer and van Attikum, 2019). Therefore, there is an unmet clinical need for identifying targets that can be used in a similar synthetic lethal approach. RAD52 is not mutated or inactivated in human cancers, thus highlighting the therapeutic potential it can offer in BRCA2-deficient tumours. In fact, there are no known RAD52 mutations currently described to enhance predisposition to breast, ovarian and blood cancers (Bell *et al.*, 1999; Beesley *et al.*, 2007). Besides, the fact that RAD52 loss on its own is aphenotypic, illustrates

the clinical importance of this protein in specifically targeting BRCA2-mutated cancers without affecting normal HR-proficient tissues. RAD52 inhibitors targeting different protein activities are currently being developed (Cramer-Morales *et al.*, 2013; Chandramouly *et al.*, 2015; Hengel *et al.*, 2016; Huang *et al.*, 2016; Sullivan *et al.*, 2016), however, it is vital for us to understand the mechanism by which synthetic lethality is conferred by RAD52 abrogation in HR-deficient cells and any backup pathways that may be arise to support cellular proliferation. This knowledge can then be translated into effective therapeutic interventions and aid in drug resistance mechanism evasion. For instance, RAD52 over-expression has been reported to occur following chemotherapeutic treatment in melanoma patients, thus suggesting that a RAD52-dependent pathway is supporting the viability and out-growth of tumour cells subsequent to DNA damage exposure (Jewell *et al.*, 2011). Moreover, loss of human RAD52 enhances chromosome fragility and genomic instability (Feng *et al.*, 2011; Murfuni *et al.*, 2013; Lieberman *et al.*, 2017), thus emphasising that protein functions in DNA lesion repair maintain sufficient genome integrity that in turn enable the viability of BRCA2-deficient tumours. Targeting RAD52 activities in homologous DNA repair and/or replication fork protection, both of which appear to preserve genomic stability and contribute to the survival of BRCA-mutated cancers, will thus be invaluable in the clinic. Importantly, there appears to be a synergistic effect between inhibitors blocking RAD52 and PARP-1 activities (Sullivan-Reed *et al.*, 2018), underscoring the potential of RAD52 inhibitors in improving the therapeutic outcome of HR-deficient cancers being treated with drugs targeting PARP-1.

Synthetic lethal interactions exist between different genes owing to the mechanisms used by cells to maintain homeostasis in the face of genetic or environmental changes. The classical view of synthetic lethality relies on the principle that homozygous loss of either gene is viable whilst the combined loss of both genes leads to cell death (Nijman, 2011). However, in this instance, BRCA2 deficiency is sufficient to drive tumourigenesis while RAD52 seems to be dispensable for viability in humans. Therefore, the synthetic lethal relationship between the two proteins might not arise as a result of deficiency in a single pathway, but due to disruption of multiple DNA repair pathways - including the p53-dependent checkpoints that are

abrogated during loss of BRCA2 function in cells - that have a cumulative detrimental effect on cell viability. RAD52 has recently acquired a lot of emerging roles in human cell biology and further studies are necessary to identify the contexts in which each activity is critical. Elucidating the context-specific functions of human RAD52 will ultimately enable guidance of therapy choice by identifying additional settings where RAD52 abrogation would be beneficial, even in HR-proficient cancers.

CHAPTER 3

Regulation of RAD51 nucleoprotein filament assembly by BRCA2

INTRODUCTION

RAD51: protein and filament structures

The human recombinase RAD51 (hRAD51) is a 339 amino acid protein, consisting of a positively charged N-terminal DNA-binding domain, a β-strand linker and a catalytic ATPase core. The N-terminal domain (NTD) consists of 5 α-helices that form a protruding lobe to allow ss- and ds- DNA binding, and is thought to regulate the activation of the filament (Aihara *et al.*, 1999; Yu *et al.*, 2001; Galkin *et al.*, 2006). The ATPase core, which shows sequence identity to that of bacterial RecA, consists of a β-sheet flanked by α-helices and conserved DNA interacting loops, known as L1 and L2 (Story RM, Weber IT, 1992; Pellegrini *et al.*, 2002; Reymer *et al.*, 2009). Walker A and B motifs found in the core domain are responsible for binding ATP and stimulating nucleotide hydrolysis (Yoshimura *et al.*, 1993). ATP binding by RAD51 is necessary for protein binding to both ss- and ds- DNA for subsequent nucleoprotein filament assembly (Shinohara, Ogawa and Ogawa, 1992; Sung, 1995; Namsaraev and Berg, 1998; Chen, Yang and Pavletich, 2008). Binding to DNA in turn stimulates the ATPase activity of RAD51, thus promoting ATP hydrolysis and dissociation of the recombinase from DNA. Motor proteins are required for complete RAD51 filament disassembly from double-stranded DNA, since protein dissociation seems to be incomplete on dsDNA substrates (Namsaraev and Berg, 1998; Shin *et al.*, 2003; Hilario *et al.*, 2009)

RAD51 forms right-handed helical nucleoprotein filaments following DNA binding. Assembly of such filaments occurs in a rate-limiting nucleation step involving 2-3 RAD51 monomers, followed by a fast filament extension step which engages protein multimers instead (Heijden *et al.*, 2007; Hilario *et al.*, 2009). Structural evidence of filaments has revealed a stoichiometry

of three nucleotides per RAD51 protomer and ~6 protomers per helical turn (Namsaraev and Berg, 1998; Yu *et al.*, 2001; Conway *et al.*, 2004; Chen, Yang and Pavletich, 2008; Short *et al.*, 2016). Within the filament, DNA is underwound and extended to have a 5.1 Å rise per nucleotide from that of 3.4 Å in B-DNA, with the extension thought to facilitate homology search within a homologous chromatid (Benson, Stasiak and West, 1994; Chen, Yang and Pavletich, 2008). Depending on whether the filament is in an inactive or active state, i.e. ADP- or ATP- bound, it can have a pitch ranging from 65-85 Å to 90-130 Å per helical turn, respectively (Ruigrok *et al.*, 1993; Yu *et al.*, 2001; Conway *et al.*, 2004; Spírek *et al.*, 2018). Recently, two conformations of the ATP-bound RAD51-ssDNA filament have been described which have different lengths and are proposed to interconvert between each other during homology search to facilitate disengagement of incorrectly paired sequences (Brouwer *et al.*, 2018).

Within the RAD51 filament, adjacent protomers make contact across three interfaces. The first interface is formed between the N-terminal domain of one protomer and the ATPase core of the next one through aromatic stacking between Tyr54 and Phe195, respectively (Conway *et al.*, 2004; Chen, Yang and Pavletich, 2008; J. Xu *et al.*, 2017). The second interface is created by the packing of a β–strand of the interdomain linker of one protomer against the central β-sheet of the ATPase core in the adjacent protomer (Chen, Yang and Pavletich, 2008; J. Xu *et al.*, 2017). The last one is mediated by ATP juxtaposed between two protomers, thus enabling the ATPase domains of neighbouring RAD51 monomers to be in direct contact (Conway *et al.*, 2004; Chen, Yang and Pavletich, 2008; J. Xu *et al.*, 2017). Hence, the ATP-binding pocket is formed by the interface between two protomers in the filament (Conway *et al.*, 2004; Galkin *et al.*, 2006). Consequently, ATP hydrolysis destabilises this protomer-protomer interface by eliminating this inter-protomer interaction and therefore promotes filament disassembly (Chen, Yang and Pavletich, 2008).

BRCA2 regulation of RAD51 filament assembly: Current biochemical and structural insights

Assembly of RAD51 filaments on ssDNA is critical for homology search, strand exchange and fork protection, as described in the previous chapters. Mutations in RAD51 and failure to form stable elongated filaments are associated with hypersensitivity to DNA damaging agents and carcinogenesis (reviewed in van der Zon, Kanaar and Wyman, 2018). For this reason, the assembly, stability and activity of the nucleoprotein filament is tightly controlled by both positive and negative regulator proteins. RAD51 nucleation and loading on DNA is thought to occur by the mediator proteins BRCA2 and RAD52, with other paralogues acting to remodel and stabilise the filament in specific conformations. In addition, negative regulators act to disassemble or destabilise the filament, and these include helicases and translocases such as RAD54, RECQ5, FBH1 and BLM (reviewed in Heyer, Ehmsen and Liu, 2010). BRCA2 is the principal mediator protein that dictates RAD51 assembly in human cells, however, the structural basis for filament formation is still poorly defined.

As discussed in chapter 1, BRCA2 binds to the recombinase through its BRC repeats that lie in exon 11 and a C-terminal RAD51 interacting-domain that is encoded by exon 27. Within each BRC repeat there are two tetrameric motifs that regulate RAD51 assembly on DNA: an inhibitory N-terminal motif and a permissive C-terminal one. The N-terminal motif, which has a consensus sequence of FxxA, inhibits RAD51 assembly by mimicking its inter-subunit oligomerisation interface (Rajendra and Venkitaraman, 2009). Structural modelling of BRC-RAD51 interactions predicted a clash between the FxxA motif of BRC4 and the protomer-protomer interface of RAD51 (Short *et al.*, 2016). This interface is thought to be buried in active pre-synaptic filaments bound by AMP-PNP, a non-hydrolysable ATP analogue, whereas it is accessible for BRC repeat binding in inactive RAD51 filament states. Thus, regulation of RAD51 filament assembly and disassembly can be envisioned to occur in a mechanism whereby ATP hydrolysis by the recombinase can alter the inter-protomer interface, consequently exposing BRC interaction sites and promoting BRC repeat binding that in turn encourages the conversion of extended ATP-bound filaments to compact ADP-bound ones and eventually triggers filament disassembly. On the other hand, the C-terminal motif found

within BRC repeats, which has the sequence LFDE in BRC4, is expected to bind to the N-terminal domain of RAD51 and has been reported to form a salt bridge that is permissive to RAD51 assembly (Rajendra and Venkitaraman, 2009; Short *et al.*, 2016). In addition, the BRC repeats of BRCA2 have been described to dictate the DNA binding specificity of the recombinase, by directing it to ssDNA and inhibiting its nucleation on dsDNA (Carreira *et al.*, 2009; Shivji *et al.*, 2009; Ryan B. Jensen, Carreira and Kowalczykowski, 2010; Thorslund *et al.*, 2010). This function is critical for enabling the strand exchange reaction during HR, since RAD51 has similar affinities for both ss- and ds- DNA, with dsDNA binding prior to ssDNA preventing heteroduplex formation (Benson, Stasiak and West, 1994; Baumann, Benson and West, 1996; Baumann and West, 1997). These observations emphasise the crucial role of the BRC repeats in finetuning RAD51 loading and assembly on DNA and regulating homologous recombination. Work by Pellegrini et. al, described a BRC4-RAD51 crystal structure in which BRC repeats contain two anti-parallel β strands that form a β-hairpin and pack against the central β-sheet of the ATPase core in RAD51, as shown in figure 41 (Pellegrini *et al.*, 2002; Shin *et al.*, 2003). Since the ATPase core creates the oligomerisation interface between individual RAD51 monomers, BRCA2 mimicry of this inter-subunit interface prevents RAD51 oligomerisation and filament assembly (Pellegrini *et al.*, 2002; J. Xu *et al.*, 2017). The above-mentioned FxxA motif of the BRC4 repeat lies within the β-hairpin, thus providing further proof that this BRC repeat module is inhibitory to filament assembly. Collectively, these remarks suggest a molecular mechanism by which the architecture of the BRC repeats directs RAD51 activity during HR in a stepwise process, which initially enables pre-synaptic filament assembly on ssDNA whilst hindering it on dsDNA, allows the subsequent engagement of dsDNA and eventually encourages filament disassembly following completion of repair. Finally, the C-terminal region of BRCA2 encoded by exon 27 binds to an interface between adjacent RAD51 protomers and is thought to be necessary for the extension and stabilisation of RAD51 filaments on DNA (Davies and Pellegrini, 2007; Esashi *et al.*, 2007; Haas *et al.*, 2018).

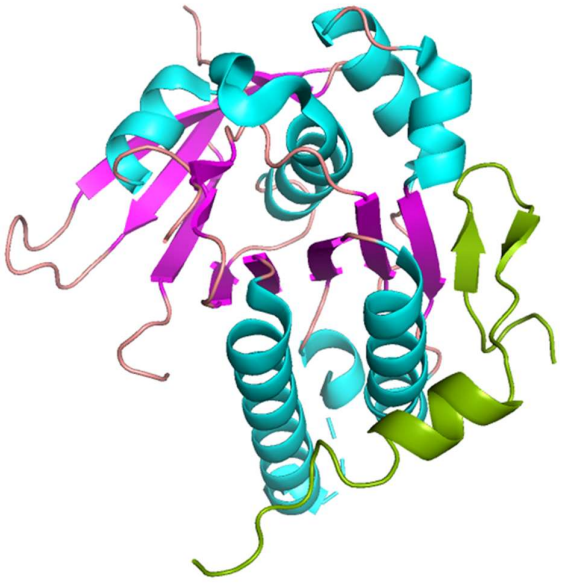

Figure 41: Ribbon representation of the RAD51–BRC4 complex as described by Pellegrini *et al.*, 2002. RAD51 is coloured by secondary structure elements, with β-sheets, α-helices and loops shown in magenta, light blue and peach, respectively. The BRC4 repeat is shown in green. The figure was created on PyMOL by using the PDB coordinates under accession code 1N0W.

Other than the model obtained from the fusion protein between BRC4 and the ATPase core of RAD51 (Pellegrini *et al.*, 2002), no other structural information is available on the regulation of RAD51 filament assembly by BRCA2. This is primarily due to the ability of BRCA2 BRC repeats to promote disassembly of RAD51 filaments at 1:1 molar ratios, whereas they can promote RAD51 nucleation and subsequent strand exchange at sub-stoichiometric concentrations (Davies *et al.*, 2001; Shivji *et al.*, 2006, 2009; Davies and Pellegrini, 2007; Carreira *et al.*, 2009; R B Jensen, Carreira and Kowalczykowski, 2010). In order to elucidate the mechanism of homologous DNA repair and define the steps involved in RAD51-mediated strand exchange, structural work is being undertaken to characterise RAD51 nucleofilament assembly and subsequent homology search. Although there are various structures of RAD51

bound to different DNA substrates and nucleotide analogues, the field is still missing a high-resolution structure of a nucleoprotein filament of RAD51 in complex with BRCA2.

In the scope of determining the structural mechanisms underlying the regulation of RAD51 filament assembly by BRCA2, biochemical assays were performed to obtain a high-resolution structure of a nucleoprotein filament encompassing RAD51, ssDNA and the BRC repeats of BRCA2. Such a structure will not only enable the characterisation of vital protein-protein interactions required for filament assembly, but will also provide structural insights into how the mediator protein modulates the ability of RAD51 to oligomerise on DNA as well as controls filament dynamics to permit downstream recombinational repair. In order to investigate the underlying mechanism, I first expressed and purified a construct encoding for the third and fourth BRC repeats (BRC34) of the human BRCA2 protein. In each of these repeats, the FxxA motif shown to disrupt RAD51 oligomerisation was modified to GxxG, in order to alleviate any potential inhibitory effects on RAD51 filament assembly. The construct was designed to carry an N-terminal 6x His tag to facilitate with the purification process, with the linker between the two repeats consisting of the wild-type intervening sequence. Following purification, complex assembly between the BRC34 fragment and wild-type recombinant human RAD51 protein, previously purified in our lab by Dr. Mahmud Shivji, was assessed. Finally, after confirming an *in vitro* BRC34-RAD51 interaction on ssDNA, electron cryo-microscopy and image processing was performed by Dr. Shaoxia Chen and Dr. Judith Short, respectively, to derive a structure of the RAD51 nucleoprotein filament in complex with the BRC repeats of BRCA2.

RESULTS

The wild-type sequence encompassing the third and fourth BRC repeats (BRC3 and BRC4) is encoded by the amino acid residues 1421-1551 of BRCA2, according to the Uniprot database annotation, and encodes for a peptide with an expected molecular weight of 15 kDa. The sequence is depicted in figure 42, where the wild-type FxxA motifs are highlighted in teal, the mutated GxxG residues are coloured red and the linker between the two repeats is shown in grey. This sequence was converted into cDNA, inserted into the pET-28a vector carrying two 6xHis tags (both an N- and a C- terminal tag), and transformed into the *E. coli* BL21 (DE3) pLysS competent cells for over-expression.

This bacterial strain was chosen due to its suitability in allowing the tightly regulated and inducible expression of the target gene. The bacterial host carries a chromosomal copy of the λ phage DE3 lysogen, which encodes the T7 RNA polymerase required for transcription of the T7-regulated recombinant gene in the pET-28a expression vector. In the absence of an inducer, basal transcription of the T7 RNA polymerase by the *E.coli* RNA polymerase is negatively regulated by the lac repressor, which binds to the *lac*UV5 promoter controlling the T7 polymerase gene. As a result, expression of the T7 RNA polymerase and, in turn, of the recombinant protein are kept to a minimum prior to induction. An added level of target gene repression under basal conditions is introduced by the pLysS plasmid expressed in the bacterial host. This plasmid constitutively expresses low levels of the T7 lysozyme, which binds to and inhibits the T7 RNA polymerase, thus further reducing 'leaky' basal expression of the recombinant gene. These levels of negative control enable basal protein expression pre-induction to be kept low and minimise any potential protein-induced toxicity in bacterial cells expressing the construct. Upon addition of isopropyl β-D-1-thiogalactopyranoside (IPTG), a non-hydrolysable lactose analogue, these two levels of negative control are abolished. IPTG binds to the lac repressor and promotes its dissociation from the *lac*UV5 operator, thus inducing T7 RNA polymerase expression. This leads to T7 polymerase protein accumulation to levels that can now overcome the inhibition presented by low T7 lysozyme levels. Therefore, IPTG addition leads to the elevated expression and activity of the T7 RNA

polymerase, thus enabling high-level transcription of the target gene and recombinant protein production in an inducible manner.

As for the choice of tag, poly-histidine tags were preferred due to their high affinity for transition metal ions, including Ni^{2+} and Co^{2+}, which enables rapid and efficient enrichment of the recombinant protein in a single purification step by immobilised metal affinity chromatography (IMAC). This is owing to the relatively low abundance of Histidine residues in bacterial proteins, while the imidazole rings of the Histidines within the affinity tag can readily form coordination bonds with immobilised metal ion matrices. Nickel-nitrilotriacetic acid (Ni^{2+}-NTA) is an example of such a matrix, where the Ni^{2+} ions are secured through four coordination sites while leaving two available for interaction with the histidine residues in the hexahistidine tag (Bornhorst and Falke, 2000). Elution of His-tagged proteins can occur under mild and non-denaturing conditions by the addition of free imidazole, which competes with the His tag for binding to the positively charged matrix and hence enables the recovery of biologically active recombinant proteins. Furthermore, owing to the small size (0.84 kDa) and charge of hexahistidine tags at physiological pH, these rarely interfere with the function and structure of the protein. As a result, the tag may not be necessary to be removed before use of the recombinant protein in downstream applications (Spriestersbach *et al.*, 2015).

Wild-type

FETSDTFFQTASGKNISVAKESFNKIVNFFDQKPEELHNFSLNSELHSDIRKNKMDILSYEETDIVK
HKILKESVPVGTGNQLVTFQGQPERDEKIKEPTLLGFHTASGKKVKIAKESLDKVKNLFDEKEQ

Mutant

FETSDTFGQTGSGKNISVAKESFNKIVNFFDQKPEELHNFSLNSELHSDIRKNKMDILSYEETDIVK
HKILKESVPVGTGNQLVTFQGQPERDEKIKEPTLLGGHTGSGKKVKIAKESLDKVKNLFDEKEQ

Figure 42: Amino acid sequence encoding for the third and fourth BRC repeats (BRC34) of human BRCA2. The wild-type sequence encoding for BRC34 is shown on top whilst the mutated sequence used for construct design and protein expression is shown below. The FxxA motifs within the wild-type sequence are coloured in teal, the mutated residues within the engineered sequence are in red and any intervening sequence between the two BRC repeats is highlighted in grey.

3.1 Expression condition screening and purification optimisation of the BRCA2 fragment

E. coli BL21 (DE3) pLysS transformed to carry the BRC34 construct were grown at 37°C at 220 rpm. Once the bacterial culture OD_{600} reached a value between 0.4 and 0.8, a pre-induction sample was collected and protein expression was then induced. A concentration of 1 mM IPTG was used for induction and protein expression was subsequently tested at two different temperatures for different durations: bacteria were either allowed to grow at 37°C for up to 3 hours or overnight at 22°C. Post-induction samples were obtained every hour for cultures grown at 37°C and following overnight incubation at 22°C. Pre- and post- induction samples were compared by SDS-PAGE to check for protein expression. As shown by the band observed at 18 kDa in figure 43, the protein is more highly expressed and enriched when bacteria are grown at 37°C following induction with IPTG. Subsequently, protein solubility was tested to ensure that the protein is not aggregating to form insoluble inclusion bodies in bacterial cells. Various bacterial lysing conditions were tested, including sonication and/or lysozyme incubation, to choose the one at which maximal recovery of soluble BRC34 protein occurs. Incubation with lysozyme without any additional sonication seemed to be the best condition for obtaining the greatest protein amount in the soluble fraction, despite the majority remaining in the insoluble fraction under all different extraction conditions tested.

Before proceeding with a large-scale preparation, capture and purification of the recombinant protein using magnetic Ni^{2+} beads was tested to ensure that the 6xHis tag was in a structural conformation that is accessible for purification by IMAC. Elution conditions were also tested with three different imidazole concentrations before automated purification using a commercially available HisTrap column on the ÄKTA Avant 25 system. Elution with 250, 350 or 450 mM imidazole was tested on the magnetic Ni^{2+} beads (figure 44), where the recovered fraction of His-BRC34 was found to be maximal when eluting with the highest imidazole concentration. During automated HisTrap affinity purification, elution was thus performed using a buffer supplemented with 450 mM imidazole and a 0-100% gradient, where the imidazole concentration was increased by 5% in each of the eluted fractions. As

shown in figure 45, His-BRC34 was found to elute across fractions 1-21, thus covering the whole gradient corresponding to 0-450 mM of imidazole. The chromatograph indicated two elution peaks, with fractions 1-5 containing nearly pure His-BRC34 whereas fractions 6-21 comprised of His-BRC34 mixed with other contaminating proteins.

Since His-BRC34 was found to be more highly enriched in the impure fractions, all fractions (1-21) were pooled together and the salt concentration was diluted down to 20 mM for subsequent purification by ion exchange chromatography (IEX). This technique separates proteins based on their total charge, which in turn depends on the environmental pH. This is owing to the chemical groups found on amino acid side chains, which contain many ionizable groups and give an overall positive, negative or neutral charge to the protein. The pH at which a protein has no net charge is called the isoelectric point (pI); with the proteins being positively charged at a pH below the pI and negatively charged above it, respectively. The ProtParam tool on the ExPASy website was used to predict the pI of His-BRC34, which was found to be 6.12. IEX was performed using the commercially available Capto Q column, which is a strong anionic exchanger that binds negatively charged proteins due to its positively charged resin. An anionic exchanger needs to be run at 0.5-1.5 pH units above the pI of the protein of interest, and hence a buffer pH of 8.5 was initially chosen. Elution was performed in 15 column volumes by applying a 0-100% gradient with buffer supplemented with 1 M NaCl, so that the salt concentration would increase by 6.7% at each step. As shown in figure 46, the recombinant protein came out in the flow-through and the washes, and elutes in fractions 5-8 (333-533 mM NaCl), thus indicating that at the chosen pH it wasn't strongly negatively charged to interact stably with the Capto Q resin. This could be because the theoretical pI is different from the actual one, owing to protein folding and charges being unavailable for IEX. Furthermore, the chromatograph elution peak has a shoulder peak which is indicative of the His-BRC34 protein eluting, but as the salt gradient increases contaminants start to elute with the protein of interest (top protein bands in figure 46). For the next CaptoQ run, therefore, the buffer pH was increased to 9.0 and elution was performed in 40 column volumes using a salt gradient of 0-50% to ensure better separation of His-BRC34 from protein

contaminants, with salt concentration increasing by 1.25% at each step. In this case, minimal protein was detected in the flow-through and eluted mainly in fractions 9-16. These fractions correspond to ~10-20% of the salt gradient, thus indicating that ~100-200 mM NaCl is required to elute His-BRC34 from the Capto Q column at pH 9.0 (figure 47). Furthermore, protein impurities were found to elute in separate fractions, as indicated by the upper bands observed from fraction 17 onwards. Thus, this step enabled us to purify the protein of interest to near homogeneity for subsequent EM assays.

Following IEX, fractions containing His-BRC34 (8-16) were pooled together and applied to a molecular weight cut-off (MWCO) filter, under the brand name Vivaspin™, to concentrate the protein. Since the protein was previously found to not be highly recoverable after application to a cut-off filter of 10 kDa, potentially owing to the stickiness of His-BRC34 to the membrane, a 30 kDa centrifugal filter was used instead. The membrane with the 30 kDa cut-off has a more porous filter and hence His-BRC34 should be more easily recoverable from this. The pooled fraction was centrifuged at 4,000 rpm for 10’ at 4°C, which reduced the protein-containing fraction volume from 8 ml to 1 ml. Given that the molecular weight of BRC34 is 18 kDa, the recombinant protein was expected to be found in the flow-through after application to a 30kDa cut-off membrane. However, the protein was found to be in the retained fraction, potentially due to protein oligomerisation or the MWCO not being at least 50% bigger than the molecular size of His-BRC34 (figure 48A). Nevertheless, the protein was recovered from the retained fraction and its concentration was finally determined to be 11 µM.

In summary, the recombinant protein was purified to near homogeneity by a three-step purification process (figure 48B). The affinity of the N-terminal His_6 tag for transition metal ions enabled initial protein purification by Nickel affinity chromatography. The protein-containing fractions were then pooled and applied to an anionic column to further purify His-BRC34 based on the protein’s negative charge and the column’s cationic nature at a pH of 9.0. Lastly, the purified protein was concentrated to a final concentration of 11 µM using a centrifugal filter with a molecular weight cut-off of 30 kDa.

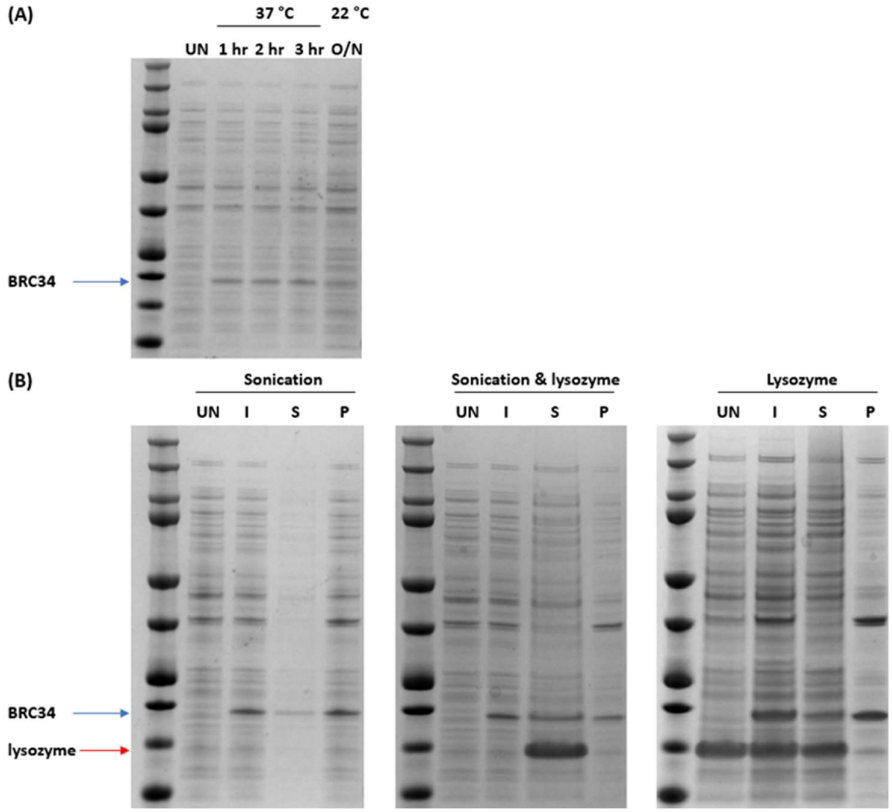

Figure 43: Optimisation of His-BRC34 expression and protein solubility. (A) Protein expression was tested by induction with 1 mM IPTG and allowing bacterial growth for up to 3 hours at 37°C or for overnight at 22°C. Pre- and post- induction samples were compared by SDS-PAGE to assess BRC34 expression. **(B)** Protein solubility was evaluated using sonication and/or lysozyme incubation for bacterial lysis. UN, un-induced sample; I, induced sample; S, soluble; P, pellet; O/N, overnight.

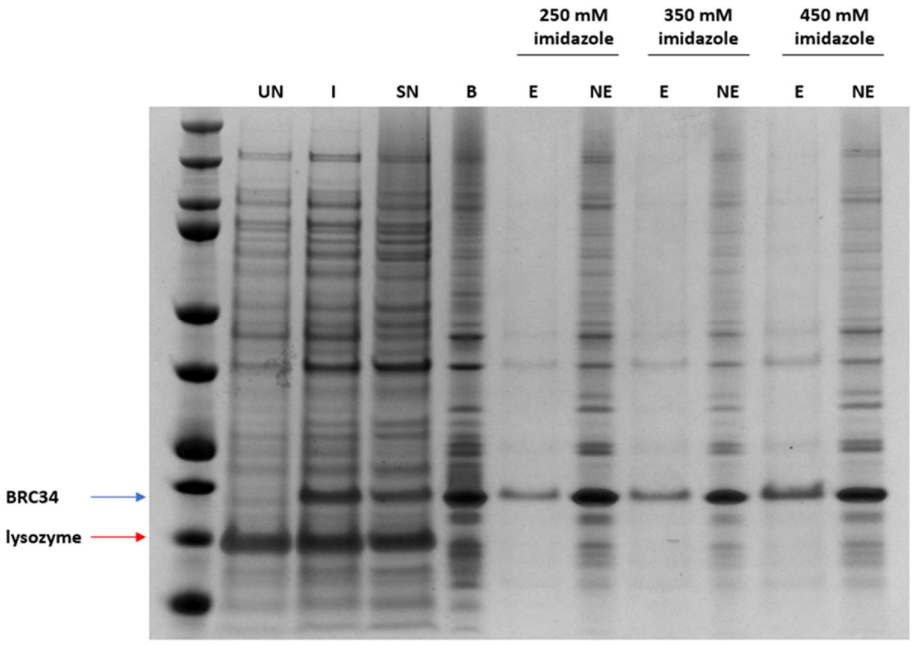

Figure 44: Assessing the suitability of a Ni^{2+}-charged resin for the purification of His-BRC34. Magnetic Ni^{2+} beads were used to assess capture of the His-BRC34 protein and subsequent elution by three different imidazole concentrations. SDS-PAGE was used to assess the amount of BRC34 eluted from the beads (**E**) or remaining bound (**NE**) at each of the tested imidazole concentrations. UN, un-induced sample; I, induced sample; SN, supernatant; B, bound fraction; E, eluate; NE, non-eluted fraction.

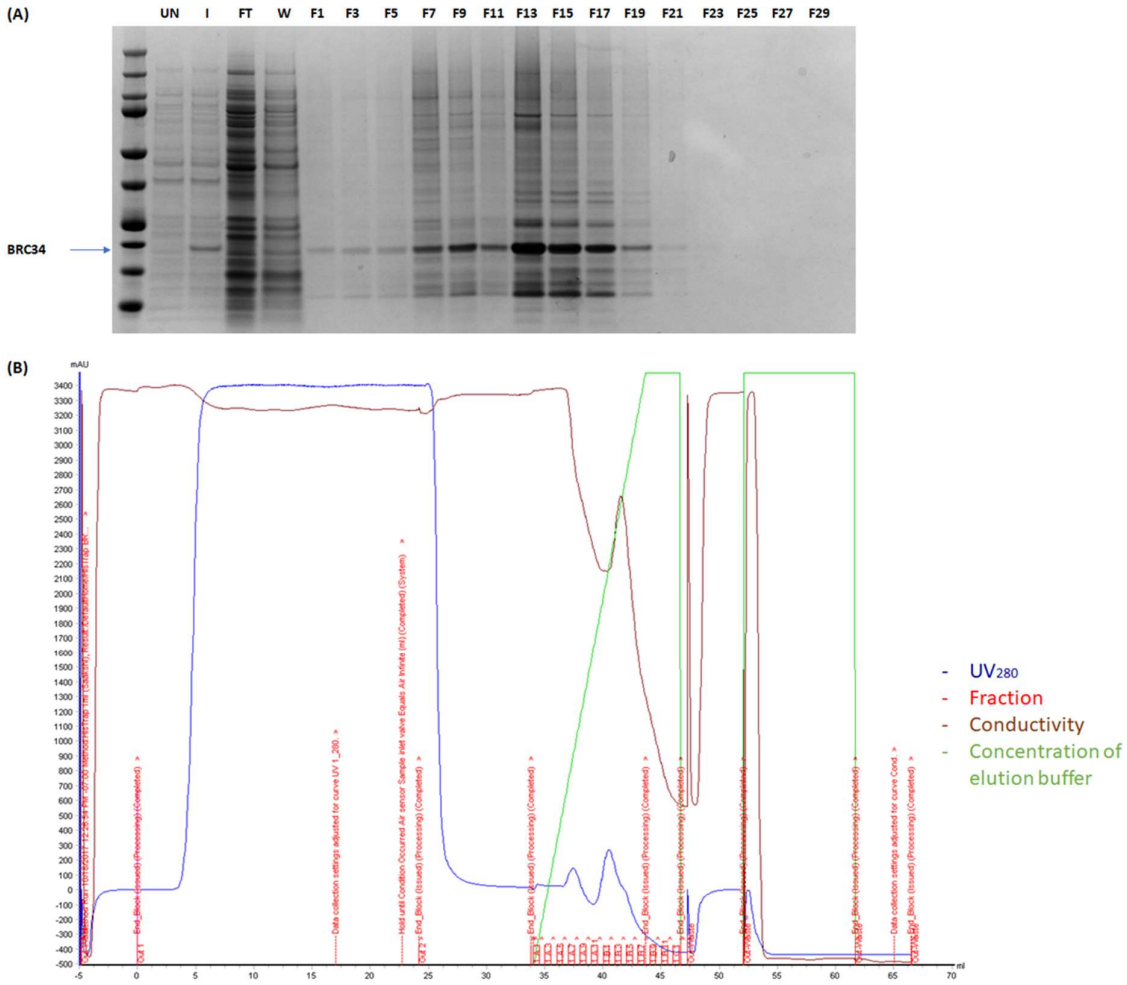

Figure 45: His-BRC34 purification by Nickel chromatography. A commercially available HisTrap column was used to purify His-BRC34 based on the affinity of the hexahistidine tag for Ni^{2+} ions. The presence of His-BRC34 was assessed in the flow-through, wash and in alternating elution fractions following IMAC by SDS-PAGE **(A)**. The chromatogram profile of the purification run is shown in **(B)**. UN, un-induced sample; I, induced sample; FT, flow-through; W, wash; F, fraction number; IMAC, immobilised metal affinity chromatography.

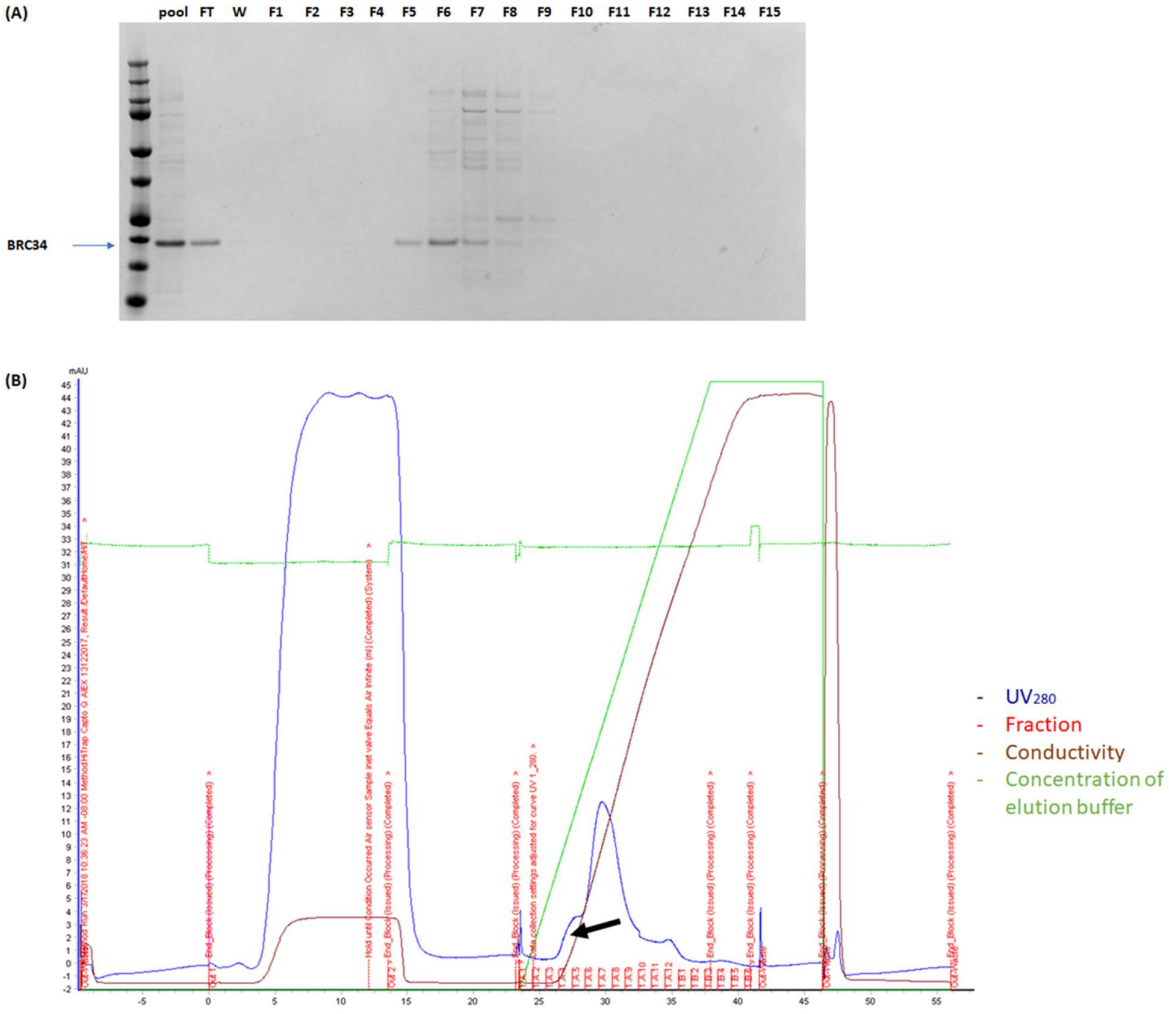

Figure 46: His-BRC34 purification by IEX at pH 8.5. A commercially available CaptoQ column was used to further purify His-BRC34 based on protein charge. Fractions containing His-BRC34 obtained from IMAC were pooled together and applied to a CaptoQ column at a pH of 8.5. The presence of His-BRC34 was assessed in the protein pool, flow-through, wash and in alternating elution fractions by SDS-PAGE **(A)**. The chromatogram profile of the purification run is shown in **(B)**. The arrow is pointing on the shoulder peak signifying protein elution, but as the gradient increases contaminants are also being eluted. FT, flow-through; W, wash; F, fraction number; IEX, ion exchange chromatography; IMAC, immobilised metal affinity chromatography.

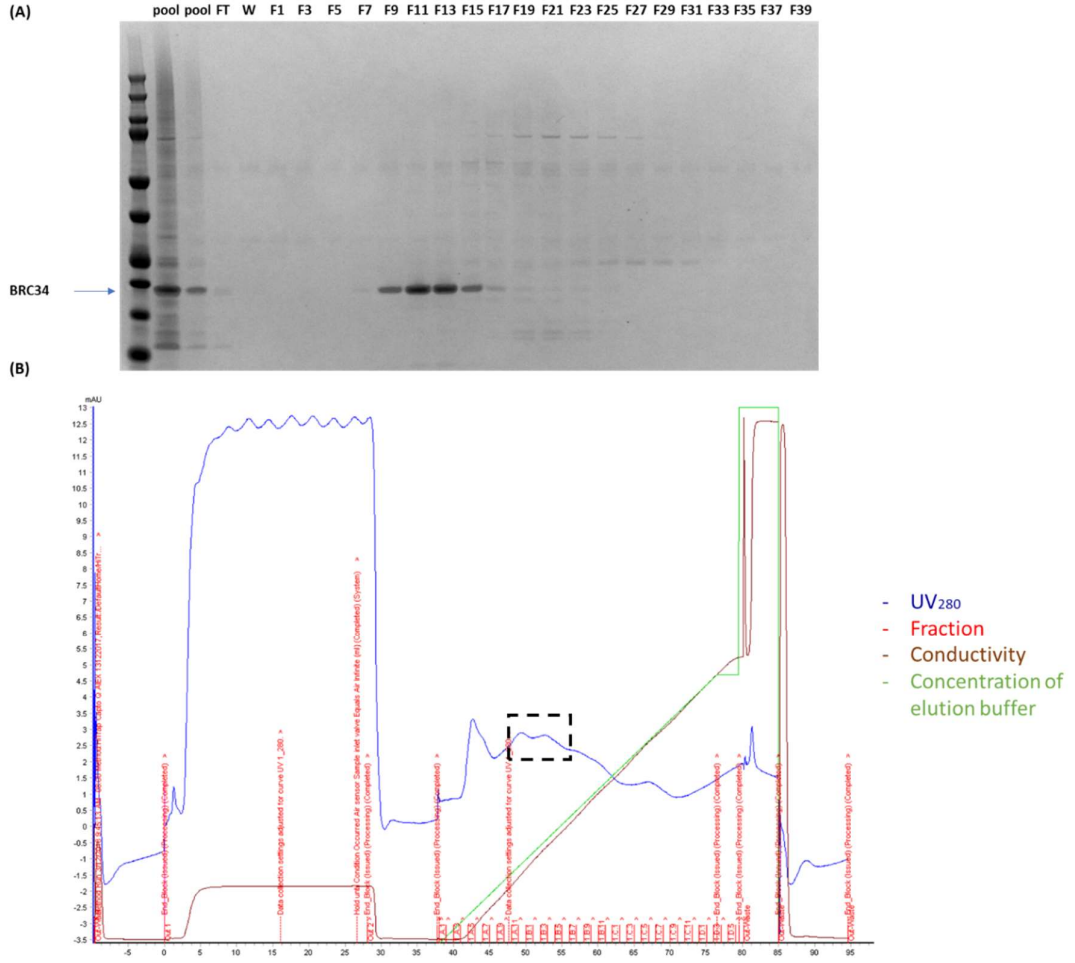

Figure 47: His-BRC34 purification by IEX at pH 9.0. The pH of the CaptoQ run was increased to 9.0 in order to increase protein charge and optimise purification by IEX. Fractions containing His-BRC34 obtained from IMAC were pooled together and diluted in binding buffer to lower the salt content before application to the CaptoQ column. A sample from the diluted pool was kept aside for SDS-PAGE analysis. The presence of His-BRC34 was assessed in the protein pools, flow-through, wash and in alternating elution fractions by SDS-PAGE **(A)**. The chromatogram profile of the purification run is shown in **(B)**. The dashed box indicates the elution peaks in which His-BRC34 comes out. FT, flow-through; W, wash; F, fraction number; IEX, ion exchange chromatography; IMAC, immobilised metal affinity chromatography.

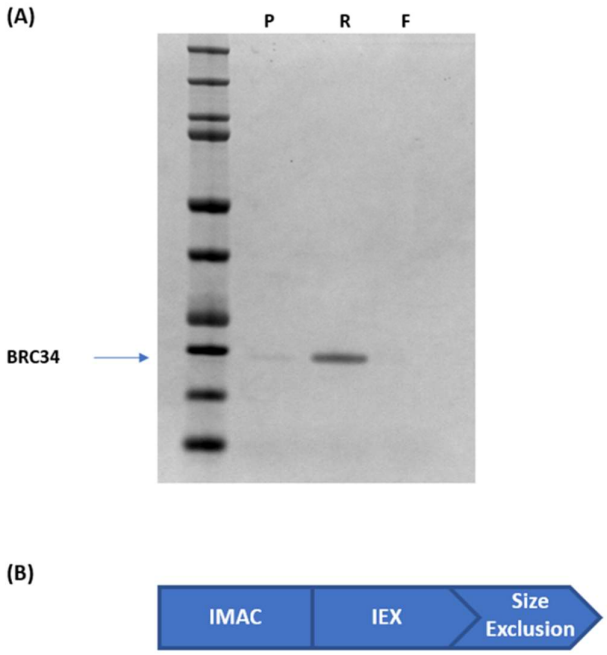

Figure 48: His-BRC34 purification and concentration by size exclusion. Following IEX, fractions containing His-BRC34 were pooled together and applied to a centrifugal concentrator with a molecular weight cut-off (MWCO) membrane of 30 kDa. The protein sample was centrifuged for 10 minutes at 4,000 rpm and 4°C and recovered in the retained fraction from the concentrator **(A)**. A flow diagram indicating the three-step purification process is shown in **(B)**. P, pool; R, retained fraction; F, flow-through; IMAC, immobilised metal affinity chromatography; IEX, ion exchange chromatography.

3.2 Assessing His-BRC34 interaction with RAD51 and complex assembly on ssDNA

Once the His-BRC34 protein fragment was purified to homogeneity, its ability to interact with either the endogenous or recombinant RAD51 protein was assessed.

To this end, magnetic Ni^{2+} beads were incubated with a total protein lysate of HeLa Kyoto cells in the absence or presence of the His-BRC34 peptide. The affinity of the His-tag for Ni^{2+} beads enables its immobilisation on the beads and subsequent capture of any proteins interacting with it. The pull-down assay was performed at two different salt concentrations: 100 and 500 mM NaCl, where 100 mM is closer to the physiological salt concentration while 500 mM is recommended to enhance protein binding to the magnetic beads. After His-BRC34 immobilisation, the whole cell extract - containing endogenous RAD51 - was added and incubated with the beads. Western blotting analysis was subsequently performed using an anti-RAD51 antibody to assess complex formation between His-BRC34 and the endogenous RAD51 protein. Even though endogenous RAD51 was captured by the beads incubated with the purified His-BRC34 peptide (figure 49A, lane 2), the protein could also be detected in the negative control performed in the absence of the recombinant peptide (figure 49A, lane 3). This indicates that endogenous RAD51 can interact non-specifically with the Ni^{2+} beads, potentially through ionic interactions that can be abrogated by increasing the salt concentration to 500 mM NaCl (compare lanes 3 and 5 in figure 49A). However, His-BRC34 binding to the Ni^{2+} beads was remarkably reduced at 500 mM NaCl (right panel of figure 49A, lane 4), and hence a salt concentration of 100 mM was used in subsequent pull-down assays to maximise capture of any proteins interacting with the BRC34 peptide. The experiment was repeated using buffer supplemented with 10 or 20 mM imidazole, in an attempt to reduce non-specific binding of proteins. Unfortunately, including imidazole in the buffer did not prevent non-specific RAD51 binding to the Ni^{2+} beads (figure 49B, lanes 3 and 5). Furthermore, an imidazole concentration of 20 mM abrogated His-BRC34 binding to the Ni^{2+} beads (right panel of figure 49B, compare lanes 2 and 4), and hence if imidazole was to be used in subsequent experiments this was performed at a concentration of 10 mM. As a final attempt to assess His-BRC34 binding to endogenous RAD51, the experiment was performed in the

same way but, instead of using the binding buffer for the washing steps, the beads were washed with buffer containing a high salt concentration to eliminate non-specific interactions (figure 50). Two wash conditions were tested: one where all three washes were performed with buffer containing 500 mM NaCl (first two lanes of each condition), or where an increasing salt concentration was used in each wash such that the first one contained 100 mM, followed by 250 mM and then 500 mM NaCl (last two lanes of each condition). However, non-specific binding of endogenous RAD51 to the beads could not be prevented under any of the conditions tried (figure 50, lanes 3 and 5), and hence I attempted to determine whether there is a physical interaction between RAD51 and recombinant His-BRC34 in the *in vitro* setting, as a cleaner and simpler way of addressing this question.

For the *in vitro* pull-down experiments, recombinant RAD51 protein was purified in our lab as previously described in Baumann *et al.*, 1997 by Dr. Mahmud Shivji. Briefly, a biotinylated 72mer oligodT was immobilised on streptavidin beads, at which point RAD51 was added and incubated with the ssDNA. The His-BRC34 fragment was either added at the same time as RAD51 if co-incubation was performed or added following the 30-minute incubation of RAD51 with ssDNA. Complex assembly between recombinant RAD51, His-BRC34 and ssDNA, which would be indicative of RAD51 filament assembly on ssDNA that is bound by the BRCA2 fragment, was then assessed by western blot analysis. As before, both RAD51 and His-BRC34 were found to be non-specifically pulled-down by the beads even in the absence of a ssDNA substrate (figure 51, lane 5 on the top panel and lane 7 on the bottom panel). Therefore, 0.5% Triton X-100 was added to the buffer to minimise non-specific interactions between the proteins and the beads. This buffer composition was found to reduce non-specific RAD51 binding to the beads whilst significantly diminishing His-BRC34 capture on them (figure 52, lane 5 on the top panel and lane 7 on the bottom panel). The pull-down also revealed complex formation between RAD51 and His-BRC34 upon co-incubation of the two proteins with ssDNA (lane 15 in figure 52). An increased amount of RAD51 was found in the supernatant fraction during component co-incubation (compare lanes 14 and 16 in the top panel of figure 52), thus suggesting that RAD51 interaction with His-BRC34 limits/regulates RAD51 loading, binding

and/or assembly on ssDNA. Furthermore, pre-assembly of the RAD51 filament on the ssDNA by initial incubation of RAD51 with the 72mer oligonucleotide followed by His-BRC34 addition seems to diminish His-BRC34 peptide binding (compare lanes 13 and 15 in the bottom panel of figure 52). This indicates that a BRCA2-RAD51 interaction is required for RAD51 delivery to ssDNA and that pre-coating of ssDNA by RAD51 prevents BRCA2 binding downstream. Therefore, for any subsequent experiments, all reaction components (RAD51, His-BRC34 and ssDNA) were either co-incubated or the two proteins were incubated before ssDNA addition, to ensure BRC34 interaction with RAD51 for nucleoprotein complex assembly.

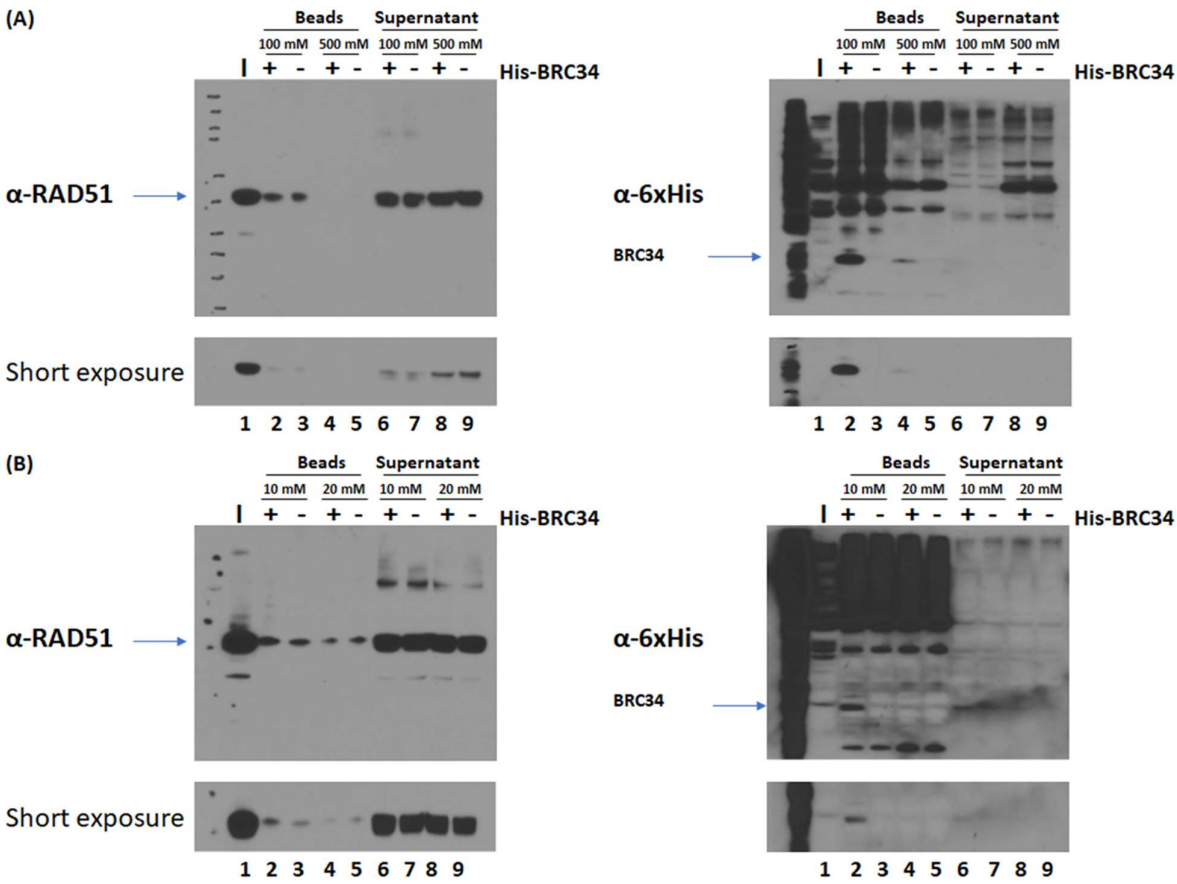

Figure 49: Buffer composition optimisation for assessing the ability of purified His-BRC34 to interact with endogenous RAD51. A whole protein lysate containing endogenous RAD51 protein was obtained from HeLa Kyoto cells. The lysate was incubated with magnetic Ni^{2+} beads with or without the His-BRC34 peptide in buffer containing 50 mM Tris pH 7.4, 0.1% Triton-X100 and 0.25 mM EDTA. **(A)** The pull-down was performed at two different salt concentrations (100 mM or 500 mM NaCl) to maximise protein capture by the beads. **(B)** The pull-down was performed using 100 mM NaCl in the binding buffer and imidazole was added (at 10 mM or 20 mM) to reduce non-specific interactions. For panels **(A)** and **(B)** the first lane for each condition indicates samples obtained in the presence of His-BRC34 **(+)**, whereas samples shown in the second lane were obtained in the absence **(-)** of the peptide. Western blot analysis was used to assess capture of RAD51 and His-BRC34 by the beads in the tested conditions. Input = 10% of cell lysate. I, input.

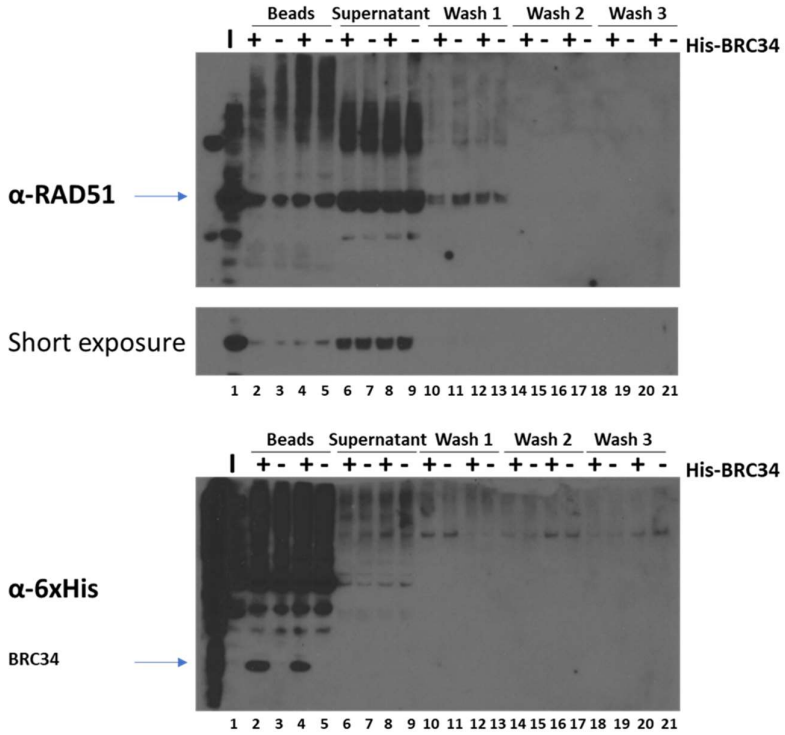

Figure 50: Further buffer composition optimisation for assessing the ability of purified His-BRC34 to interact with endogenous RAD51. The experiment was repeated as before but instead of using the binding buffer for the washing steps, the beads were washed with buffer containing a high salt concentration to eliminate non-specific interactions. Two wash conditions were tested: three washes with buffer containing 500 mM NaCl (first two lanes of each condition), or washes with increasing NaCl concentration at each step (100 mM in wash 1, 250 mM in wash 2 and 500 mM in wash 3 - last two lanes of each condition). The first lane for each condition indicates samples obtained in the presence of His-BRC34 **(+)**, whereas samples shown in the second lane were obtained in the absence **(-)** of the peptide. Western blot analysis was used to assess capture of RAD51 and His-BRC34 by the beads in the tested conditions. Input = 10% of cell lysate. I, input.

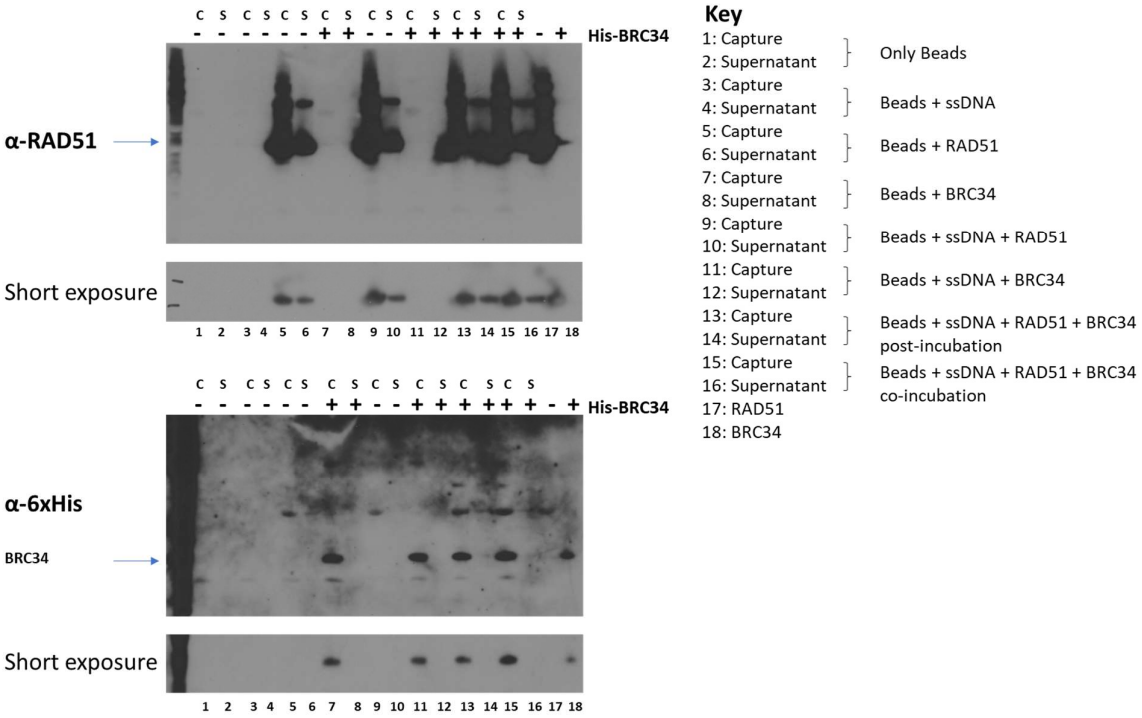

Figure 51: Assessing the *in vitro* interaction between purified His-BRC34 and recombinant RAD51. Streptavidin beads were used to immobilise biotinylated ssDNA (72mer) and subsequently incubated with or without recombinant RAD51 and/or the purified His-BRC34 peptide. The His-BRC34 fragment was either added following the 30-minute incubation of RAD51 with ssDNA (post-incubation) or added at the same time as RAD51 (co-incubation). The pull-down was performed in buffer containing 25 mM Tri-Acetate pH 7.0, 100 mM NaCl, 2 mM $MgCl_2$, 2 mM AMPP-PNP and 1 mM DTT. Complex assembly between recombinant RAD51, His-BRC34 and ssDNA was then assessed by western blot analysis. The identity of the sample loaded in each lane is shown in the figure key. C, capture; S, supernatant.

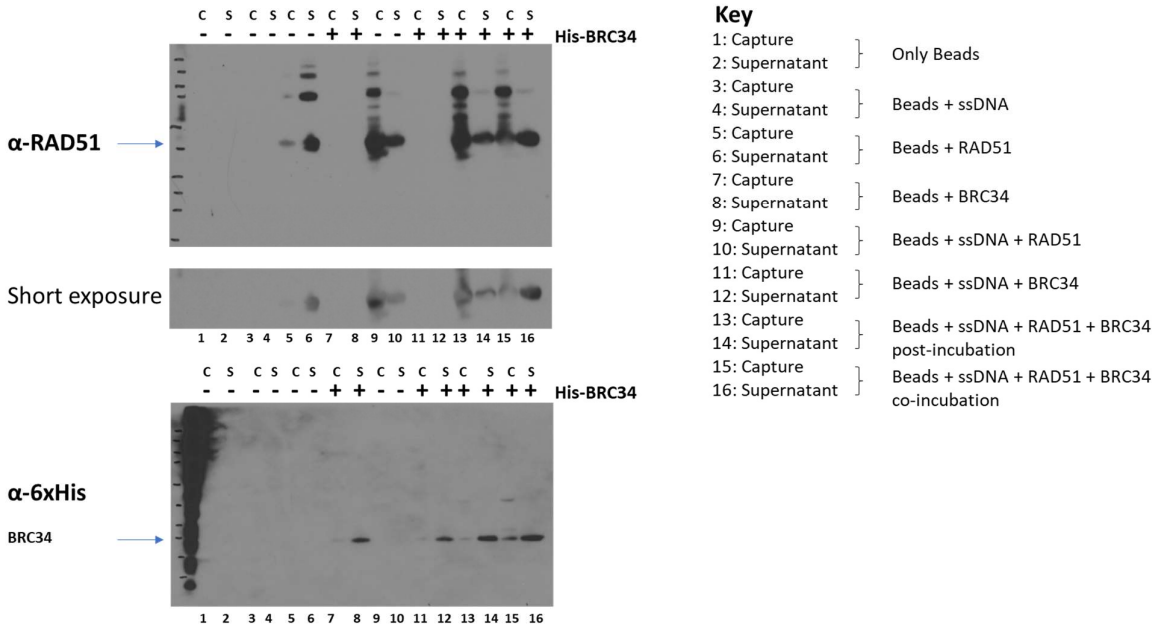

Figure 52: Purified His-BRC34 interacts with recombinant RAD51 *in vitro*. Streptavidin beads were used to immobilise biotinylated ssDNA (72mer) and subsequently incubated with or without recombinant RAD51 and/or the purified His-BRC34 peptide. The His-BRC34 fragment was either added following the 30-minute incubation of RAD51 with ssDNA (post-incubation) or added at the same time as RAD51 (co-incubation). This time the pull-down was performed using buffer containing 25 mM Tri-Acetate pH 7.0, 100 mM NaCl, 2 mM $MgCl_2$, 2 mM AMPP-PNP and 1 mM DTT and supplemented with 0.5% Triton-X100 to eliminate non-specific interactions. Complex assembly between recombinant RAD51, His-BRC34 and ssDNA was then assessed by western blot analysis. The identity of the sample loaded in each lane is shown in the figure key. C, capture; S, supernatant.

3.3 Structural insights into a RAD51 nucleoprotein filament assembled in the presence of BRC34

After confirming His-BRC34 binding to RAD51 in the presence of ssDNA, cryo-electron microscopy (cryo-EM) was employed for data acquisition by Dr. Shaoxia Chen (MRC Laboratory of Molecular Biology). This technique is invaluable for obtaining high-resolution structures of biological molecules, and hence can provide structural insights into the mechanism of pre-synaptic RAD51 filament assembly as dictated by BRCA2 BRC repeats.

Following complex assembly by co-incubating His-BRC34, RAD51 and the ssDNA substrate (72mer oligodT) at 37°C for 15 minutes, samples were applied to EM grids and negatively stained for preliminary sample assessment. Negative staining was performed using uranyl acetate and filaments were analysed by Transmission Electron Microscopy (TEM). A Fourier transform of His-BRC34-RAD51-ssDNA filaments was obtained (figure 53) to eliminate low resolution data and proposed a helical pitch of ~100 Å. This value corresponds to the pitch previously seen in extended pre-synaptic filaments of RAD51 on ssDNA, as well as in post-synaptic filaments assembled on dsDNA. Moreover, the filament diameter ranges between 135 Å and 160 Å, which is considerably wider than that of filaments formed on dsDNA substrates, which have a diameter of ~100 Å according to un-published observations from our lab.

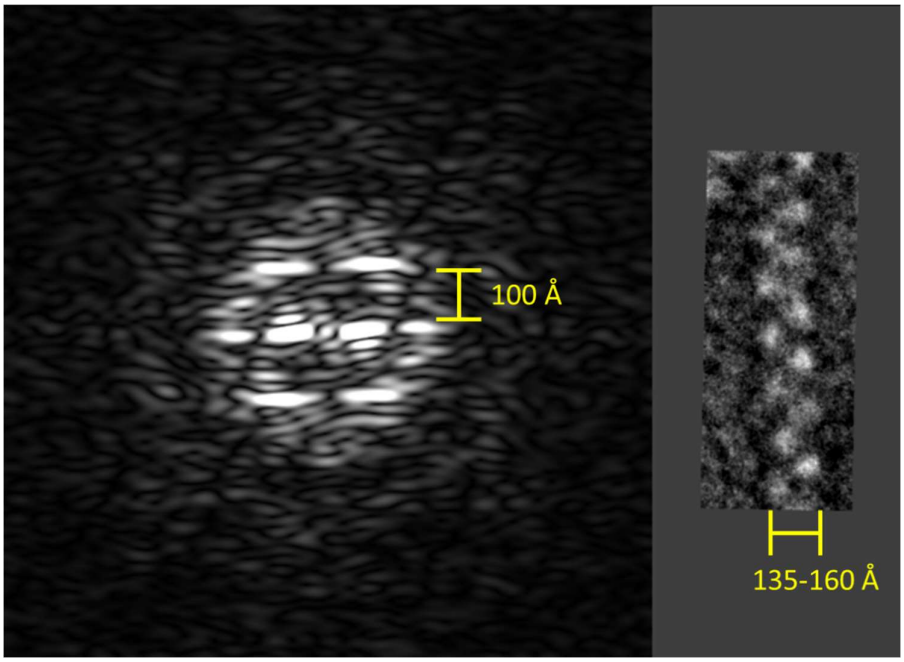

Figure 53: Electron micrograph and Fourier transform obtained by Transmission Electron Microscopy. The filament pitch (~100 Å) is calculated from the distance between the equator and the first layer line in the Fourier transform. Filament diameters range between 135 Å and 160 Å. Image acquisition was performed by Dr. Shaoxia Chen whilst data processing and figure preparation were performed by Dr. Judith Short.

3.4 Helical parameters of a RAD51 nucleoprotein filament assembled following co-incubation with His-BRC34

Following negative staining, we proceeded with cryo-EM to further characterise the pre-synaptic RAD51 filament assembled on the ssDNA substrate (72mer oligodT) in the presence of His-BRC34. Complex assembly was performed as before by co-incubation at 37°C for 15 minutes. A ~105,000 molecule dataset was collected by Dr. Shaoxia Chen (MRC Laboratory of Molecular Biology) and finally processed and refined by Dr. Judith Short in cooperation with Dr. Paul Emsley and Dr. Garib Murshudov (MRC Laboratory of Molecular Biology).

As shown in figure 54, two classes of RAD51 filaments were present in the dataset: one containing two DNA strands (represented by 73,500 molecules), and another containing only one strand (in 31,500 molecules). The RAD51 helical filament represented by the first class encompassing two DNA strands has a pitch of 98.5 Å, whereas the second class lacking the second DNA strand has a pitch of 100.6 Å. These observations suggest that RAD51 stretches the ssDNA molecule within the filament from the normal 34 Å pitch length, posing it ready for homology search in neighbouring DNA molecules. However, annealing to a second DNA strand potentially limits the structural flexibility of the single-stranded DNA originally encased within the nucleoprotein filament, thus leading to a reduction in pitch length in filaments encompassing two DNA strands.

The structure of the RAD51 filament encompassing two DNA strands has a twist, axial rise and diameter of 57°, 15.6 Å and 100 Å, respectively, at a resolution of 3.2Å (figure 60). This structure is thought to represent an intermediate filament state in which the BRC34 peptide is preparing RAD51 for homology search and strand annealing for the subsequent invasion step. Such an intermediate state including a second DNA strand has not been previously observed in sample preparations including only RAD51 and ssDNA in the absence of the BRC34 peptide (unpublished observations by our lab). This suggests that the BRC34 fragment is promoting capture of the second DNA strand by the RAD51-ssDNA nucleoprotein filament, thus guiding the strand invasion step. Interestingly, the second DNA strand (coloured blue in

figure 54) is not in the expected Watson-Crick base-pairing conformation (represented by the fitted purple strand), which would otherwise be observed in a filament encasing a regularly double-stranded DNA molecule.

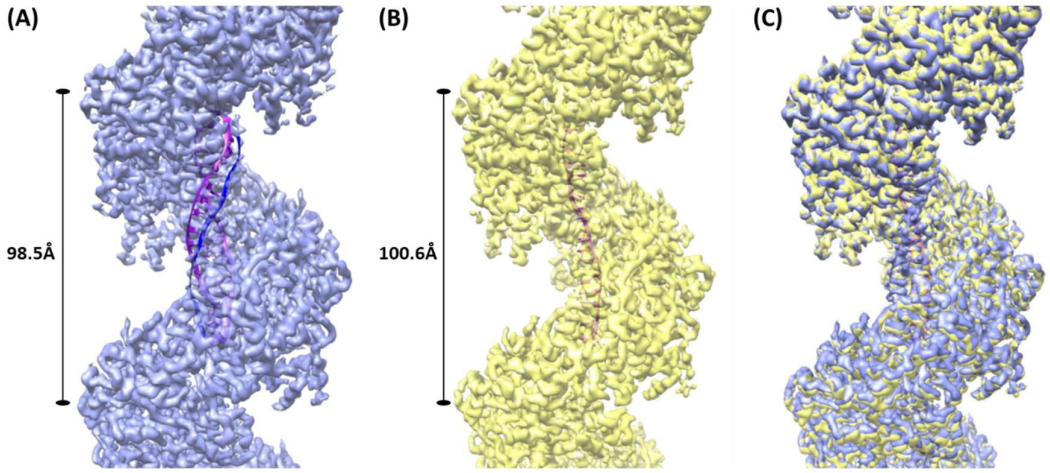

Figure 54: Models obtained for the RAD51-BRC34-ssDNA nucleoprotein filament. Two classes of RAD51 filaments were obtained following dataset processing. One class (~70% of dataset) contains two DNA strands **(A)**, with the blue strand indicating the incoming DNA strand that is attempting base-pairing, whilst the purple strand has been fitted to represent the location of a regular base-paired double-stranded DNA molecule. The other class (~30% of dataset) contains only one DNA strand **(B)**. Pitch lengths of the double-stranded **(A)** and single-stranded **(B)** RAD51 filaments assembled on oligodT in the presence of His-BRC34 are shown. An overlay of the two classes **(C)** indicates lack of any evident structural differences between the two. Data processing and figure preparation were performed by Dr. Judith Short.

3.5 Helical parameters of a filament structure assembled by co-incubating RAD51 and BRC34 in the absence of a DNA substrate

Despite the cryo-EM structure suggesting that the BRC repeat peptide stimulates strand invasion by the RAD51-ssDNA nucleoprotein filament, it revealed no extra density for the His-BRC34 fragment within the filament. For this reason, in an attempt to obtain a structure of BRC34-RAD51, the two proteins were incubated together at 37°C for 15 minutes in the absence of any DNA substrate to trap complex formation and prevent reaction progression to completion. This condition mimics the physiological scenario where the two proteins interact prior to DNA binding. Two different models were obtained following 3D classification and refinement, with ~10% of the dataset belonging to a class that has very distinct features in comparison to previously characterised RAD51 filament structures. In this class, shown in figure 55B, the assembled filament has a pitch of 104 Å and an axial rise of 16.1 Å. Despite the low resolution (~14 Å) of this model, the N-terminal domain of RAD51 seems to be in an elongated conformation in comparison to what has been previously observed. This finding potentially suggests the displacement of the recombinase NTD, with such a conformational shift predicted to occur following BRC repeat binding (Galkin *et al.*, 2005; Subramanyam *et al.*, 2013; Short *et al.*, 2016). Nonetheless, these results are still preliminary, and the model awaits further fitting and analysis.

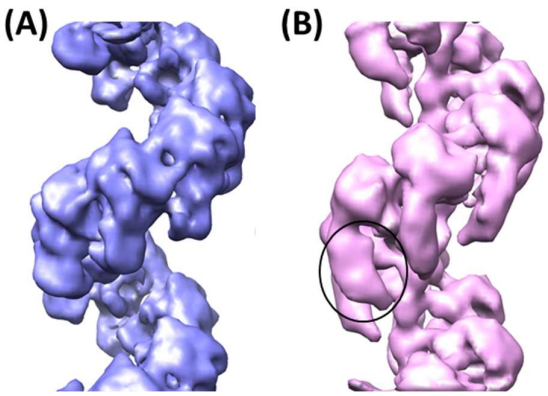

Figure 55: Models obtained for the RAD51-BRC34 structure assembled in the absence of a DNA substrate. 3D classification and refinement of filament segments obtained by co-incubation of RAD51 and His-BRC34 resulted to two preliminary models. **(A)** One class (~90% of dataset) has a twist, rise and pitch of 55.7°, 16.4 Å and 106 Å, respectively, at a resolution of 6.4 Å. **(B)** The other model (remaining ~10% of the dataset) has a twist, rise and pitch of 56.0°, 16.1 Å and 104 Å, respectively, at a resolution of 13.7 Å. This class exhibits an elongated NTD (circled), suggesting displacement of this domain away from the ATPase core of the recombinase. Such a movement is expected to break interactions between adjacent RAD51 protomers in the filament and allow BRC34 binding. Data processing and figure preparation were performed by Dr. Judith Short. NTD, N-terminal domain.

DISCUSSION

RAD51 filament formation is central for homology search, pairing and strand exchange between homologous DNA molecules during the repair of DSBs via homologous recombination. RAD51 activity is known to be regulated by BRCA2 (Yuan *et al.*, 1999; Esashi *et al.*, 2007; Carreira *et al.*, 2009), but the exact mechanism of this regulation has still not been elucidated. A crystal structure of a protein fusion consisting of the BRC4 repeat and the ATPase core of human RAD51 is the only available structure of the recombinase in complex with BRCA2 to date (Pellegrini *et al.*, 2002). This has shown that the BRC repeats interact with RAD51 by mimicking the oligomerisation motif of the protein. The sequence responsible for this structural mimicry is the FxxA motif, which is conserved in seven out of the eight BRC repeats of human BRCA2, and was later confirmed to prevent RAD51 filament assembly (Rajendra and Venkitaraman, 2009). However, the reported structure lacks the flexible N-terminal domain of RAD51, which forms one of the oligomerisation interfaces in assembled filaments, thus rendering the complex monomeric. Moreover, the spatial arrangement of BRC4 in relation to RAD51 might be dictated both by the absence of the NTD and the fusion of the two proteins. Such modifications inadvertently allow peptide flexibilities and/or impose physical constraints in the crystal structure which might not be characteristic of the native complex. Furthermore, no DNA substrate is present in the complex and hence the structure is not necessarily representative of biologically relevant protein-protein interactions that occur during filament assembly on ssDNA. For these reasons, electron cryo-microscopy was used to obtain a structure of a RAD51 nucleoprotein filament in complex with the third and fourth BRC repeats of BRCA2 (BRC34) in order to gain more structural insights regarding the assembly of RAD51 filaments and the mechanism by which BRCA2 regulates this.

Preliminary assessment of the sample was performed by negative staining using uranyl acetate before optimising cryo-grid conditions (figure 53). This indicated the assembly of a nucleoprotein filament structure with an elongated pitch length when compared to the ones formed by pre- and post- synaptic filaments in the absence of the BRC34 fragment (unpublished observations by our lab). However, the use of heavy metal salts for this

technique creates an outline of the particle and obscures any internal information. Moreover, the stain dehydrates and deforms the object, while also increasing background noise, thus providing structures limited to a resolution of about 20 Å (reviewed in Thompson *et al.*, 2016; Lyumkis, 2019).

Despite being able to confirm a physical interaction between recombinant RAD51 and the purified His-BRC34 peptide (figure 52), a cryo-EM structure of the RAD51 nucleoprotein filament in complex with BRC34 could not be obtained under the same biochemical conditions. As previously mentioned, FxxA motifs within BRC repeats have been shown to prevent RAD51 assembly by mimicking and inhibiting the recombinase oligomerisation interface (Pellegrini *et al.*, 2002; Rajendra and Venkitaraman, 2009). Even though the FxxA motifs were mutated to GxxG during construct design to abrogate their inhibitory effects on filament assembly and ensure BRCA2 binding to RAD51, this strategy proved to be inadequate for capturing a complex between RAD51, BRCA2 and ssDNA. This could be due to a variety of reasons. Firstly, the BRC34 fragment is a small peptide with a molecular weight of ~18 kDa. Therefore, unless the peptide is embedded within the filament structure at repetitive segments, obtaining high-resolution structures of molecules smaller than 100 kDa by cryo-EM is intrinsically difficult due to the low signal-to-noise ratio of molecules embedded in vitreous ice. In fact, only three complexes smaller than 100 kDa have been resolved to a resolution of at least 4 Å so far (Herzik, Wu and Lander, 2019). Furthermore, studying nuclear complexes and DNA processes using cryo-EM has always been challenging due to the dynamic nature of the reactions that occur via transient interactions between the proteins and the oligonucleotide substrates (Fernandez-Leiro and Scheres, 2016). Hence, one explanation for the lack BRC34 density in the RAD51 nucleofilament structure obtained might be due to an unstable and/or transient nature of the BRCA2-RAD51 interaction during recombinase loading on DNA for filament assembly. Filament assembly is a dynamic process and hence it can be expected that once BRCA2 delivers a RAD51 protomer or multimer to ssDNA it disengages from the complex. This can therefore imply that BRCA2 molecules act only at the growing ends of a filament, making the sample structurally heterogeneous and adding

another layer of complexity to the transient nature of the assembly. In addition, molecular complexes adopt several different conformations in solution and are frozen in multiple random orientations on the sample grid. Hence, 3D image classification and averaging are used during data analysis to select structurally similar subsets of particles for structure determination. However, structures that are less abundant or ones that are of low-resolution due to their high flexibility and/or disordered configurations might be averaged out, potentially leading to loss of the density corresponding to BRC34. Capturing the transient biological complex might be more readily achievable by mixing or spraying the reaction components directly on the grid immediately before blotting and freezing (Berriman and Unwin, 1994). In this instance, the BRC34-RAD51 protein complex can be pre-assembled and applied onto the grid before subsequent spraying of the oligonucleotide and rapid freezing, thus allowing a snapshot of the assembly in a precisely timed manner before the reaction completes and BRCA2 detaches. However, this technique can also lead to additional sample heterogeneity across the grid due to the reaction only occurring wherever all the components mix (Dillard *et al.*, 2018).

Even if no density is observed for BRC34 in the obtained RAD51 nucleoprotein filament, suggestive inferences can be made regarding the functions of BRCA2 in regulating filament activity during HR-mediated DNA repair. The presence of an additional oligonucleotide strand within the RAD51-ssDNA filament upon inclusion of the BRC34 peptide during complex assembly (figure 54A) was an unanticipated observation. This yielded a double-stranded structure even if the only available DNA substrate was oligodT and hence was not expected to anneal or base-pair with itself. This potentially explains why the typical Watson-Crick base pairing is not observed between the two ssDNA strands encompassed by the RAD51 filament, since there is lack of complementarity between them. Regardless, the lack of complementarity between the two ssDNA strands is probably the factor that enabled capture of this intermediate, by preventing the reaction from going to completion. Interestingly, T-T mismatches have been previously described to form Wobble base-pairs that are stabilised by two Hydrogen bonds (He, Kwok and Lam, 2011). Such pairing enables the bases to become

incorporated in the helix, thus preventing bulging out and subsequent distortion of the sugar phosphate backbone of the DNA helix (Kouchakdjian *et al.*, 1988). A similar attempt at strand invasion, pairing and assembly of a double-stranded structure has never been previously observed in the absence of BRCA2 whilst using a ssDNA substrate and recombinant RAD51 protein (unpublished observations by our lab). This suggests that the BRC repeats have functions in promoting the pairing of the DNA within a RAD51-coated filament and aligning DNA molecules for homologous recombination.

In comparison to the typical 34 Å pitch length of B-DNA, RAD51 encases DNA in a helical filament with a pitch of 100.6 Å in the single-stranded model obtained in the presence of BRC34. This suggests that the BRCA2 peptide encourages ssDNA stretching within the RAD51 nucleoprotein filament, thus preparing it for homology search in neighbouring DNA molecules. Such a pitch length represents a nearly three-fold extension from the B-DNA form and is consistent with previous measurements of active filaments (Short *et al.*, 2016). Notably, the pitch of the double-stranded model obtained is shorter to the one observed in the RAD51-ssDNA structure (98.5 Å versus 100.6 Å), thus suggesting that attempted annealing with the incoming DNA strand minimises filament flexibility and imposes DNA compaction. Our models hence propose that BRCA2 helps RAD51-ssDNA nucleoprotein filaments attain a synaptic complex by stretching the coated ssDNA to allow homology search and subsequent invasion for DNA pairing with a complementary strand. This BRCA2-induced stimulation of the stand invasion step potentially occurs by yet unidentified conformational changes within the RAD51 nucleoprotein filament. As a matter of fact, BRC4 binding has been previously predicted to cause the movement of an α-helix in RAD51, which encompasses residues Ser223-Arg229 and lies close to the DNA-binding L2 loop (Short *et al.*, 2016). This region is hypothesised to move outwards and away from the ssDNA encased in the filament, thus potentially allowing the accommodation of the incoming DNA strand within the pre-synaptic filament. Moreover, ssDNA stretching from a compact filament state into an open conformation requires energy. Although the measured energy difference between the two forms is small and the extended state is thought to be achievable by thermal excitation (Brouwer *et al.*, 2018), BRC repeat

binding to RAD51 might be providing some or all the energy required for the DNA extension process. BRCA2-induced conformational changes within the RAD51 nucleoprotein filament could thus lower the activation energy required for base-pairing with the incoming DNA molecule, making the strand exchange reaction more energetically favourable as a result of improved search for homology within the extended RAD51-ssDNA nucleoprotein filament. Intriguingly, Arg235, a residue situated within the L1 loop found in the ATPase core of RAD51, has been previously speculated to facilitate the capture of the DNA substrate by lowering the energy state of the complementary strand following base-pairing (J. Xu *et al.*, 2017). This remark offers a hypothetical mechanistic model in which BRCA2 could make the steps of DNA extension and strand invasion more energetically favourable, which is supported by un-published observations from our lab demonstrating conformational changes in Arg235 within the ATPase core of the recombinase upon BRC34 binding.

Since no cryo-EM structure could be obtained for BRC34-RAD51-ssDNA, a second attempt was made to study the BRC34-RAD51 interaction in the absence of an oligonucleotide substrate. The two models obtained for the BRC34-RAD51 structure were of low resolution, and thus cannot provide adequate information regarding the protein-protein interaction, the detail of which would be able to offer mechanistic insights into the regulation of RAD51 filament initiation, elongation or DNA pairing by BRCA2 during HR-mediated DNA repair. This interaction is critical for the biological activity of both proteins, as BRCA2 deficiency minimises the ability of RAD51 to form foci following DNA damage (Yu *et al.*, 2000). Notably, in these two models the pitch ranges between ~104-106 Å, which may possibly indicate that BRCA2 defines the spatial distribution of adjacent RAD51 protomers during DNA loading for nucleoprotein filament assembly. Furthermore, the NTD of RAD51 in the model presented in figure 55B seems to have an elongated conformation in comparison to helical reconstruction in figure 55A, suggesting that the BRC repeats might promote an allosteric switch in RAD51 protomers to enable DNA binding as well as homology search, strand invasion and pairing. This BRCA2-induced conformational change of the helical NTD is in line with published data in which BRC4 has been predicted by computational modelling to interact with and encourage

the movement of the N-terminal domain of RAD51 (Subramanyam *et al.*, 2013). In this model reported by Subramanyam *et al.*, 2013, a hydrogen-bond network maintains the interaction between the N-terminal domain of RAD51 and BRC4. These interactions cause movement of the NTD and hence create a cleft between the NTD and the ATPase core of RAD51. This cleft in turn accommodates the C-terminal part of the BRC4 peptide and enables aromatic residues within the BRC repeat to be buried in a hydrophobic cavity of the RAD51 core. This arrangement of BRC4 subsequently enables the peptide to interact with the L1 loop of the adjacent RAD51 protomer. Therefore, this cross-subunit interaction mediated by BRC4 is expected to stabilise the protomer-protomer interface and hence RAD51 filament assembly. In another modelling prediction performed in our lab, BRC4 was predicted to have two binding sites within the RAD51 filament; one permissive and one inhibitory to filament assembly (Short *et al.*, 2016). The LFDE module within BRC4 is described to displace the NTD of RAD51 and is thought to promote filament assembly, as it is not found to perturb the protomer-protomer interface of adjacent RAD51 monomers. This displacement might be thus accountable for the elongated NTD observed in the BRC34-RAD51 structure. In contrast, the FxxA module of BRC4 is hypothesised to clash with the protomer-protomer interface and promote filament disassembly. This interface is buried in active pre-synaptic filaments formed in the presence of AMP-PNP, while being exposed and accessible for BRC repeat binding in the inactive RAD51 filament. Thus, changes in inter-protomer interfaces driven by ATP hydrolysis and the subsequent transition of extended ATP-bound filaments to compact ADP-bound ones, may expose different BRC interaction sites to encourage filament disassembly. In the BRC34 construct used, however, the FxxA motif is mutated and hence RAD51 filament stability should not be destructively affected by this. Intriguingly, conversion of the ‘active’ RecA filament into an ‘inactive’ state involves the rotation of the C-terminal lobe of the bacterial recombinase (Yu *et al.*, 2001). This region corresponds to the NTD of the human RAD51 enzyme, thus suggesting that BRC34, by inducing a similar displacement of the NTD in RAD51, can potentially stimulate activation of the assembled nucleofilament.

On a final note, since efforts to obtain a BRCA2-bound nucleoprotein filament of RAD51 proved fruitless, a few more approaches could be attempted to address this issue. For instance, the C-terminal domain of BRCA2 has been previously shown to stabilise extended RAD51 filaments (Davies and Pellegrini, 2007; Esashi *et al.*, 2007; Haas *et al.*, 2018), and hence including this region might be necessary for obtaining a stable RAD51 nucleoprotein filament in complex with BRCA2. Actually, Esashi *et al.*, 2007 reported that the presence of the BRCA2 C-terminal domain enables the stable interaction between BRC repeats and RAD51 filaments, even at BRC repeat concentrations that are expected to disrupt filament assemblies. Post-translational modifications (PTMs) might also be required to stabilise the BRCA2-RAD51 interaction. PTMs, especially phosphorylation, are induced following DNA damage and are known to regulate the activity of proteins involved in homologous recombination, including RAD51, RAD52, PABL2 and BRCA2 (Yuan *et al.*, 1998; Kitao and Yuan, 2002; Esashi *et al.*, 2005; Sørensen *et al.*, 2005; Davies and Pellegrini, 2007; Ahlskog *et al.*, 2016). However, the recombinant proteins used were expressed in bacteria and are thus very likely lacking such PTMs (Khow and Suntrarachun, 2012). Hence, unless both criteria are met, we might not be able to capture a stable BRCA2-RAD51-ssDNA nucleoprotein filament complex. Lastly, an anti-His antibody could be used to detect the His-BRC34 peptide in the complexes assembled during sample preparation. Antibody labelling, though, can only be used in conjunction with negative staining, and hence such a structure would be limited to a very low resolution that might not be useful for providing new insights (reviewed in Thompson *et al.*, 2016). Furthermore, since antibodies are large molecules, they can obscure important structural information within the assembled filament. Alternatively, the BRC34 peptide could be chemically crosslinked to RAD51, to ensure a stable interaction between the two before proceeding with filament assembly on DNA substrates. However, this technique can have the pitfall of trapping complexes in non-native states that can be non-functional (reviewed in Thompson *et al.*, 2016).

Despite the failed attempts of obtaining a RAD51 nucleoprotein filament structure in complex with BRCA2 BRC repeats, the findings presented in this chapter create new implications and

provide clues regarding the mechanism underlying RAD51-mediated homologous DNA repair and its regulation by BRCA2. In summary, preliminary cryo-EM data suggest that the third and fourth BRC repeats of BRCA2 induce conformational changes within the NTD of the recombinase that in turn encourage homology search and strand invasion by the RAD51-ssDNA nucleoprotein filament, thus enabling the formation of an intermediate synaptic state encompassing a second DNA strand. These observations suggest a model for the BRCA2-catalysed process that directs homologous DNA repair during HR. My work thus implies that mutations within BRCA2 BRC repeats, known to enhance predisposition to ovarian and breast cancers, can impede appropriate homologous DNA strand-pairing by RAD51, therefore preventing accurate DNA repair and ultimately causing genomic instability and tumourigenesis. Nevertheless, further work is required to derive a precise model of how BRCA2 regulates RAD51 dynamics during reactions that lead to DNA repair via HR.

CONCLUDING REMARKS

The research reported in my thesis provides new insight into the mechanisms by which BRCA2 and RAD52 regulate RAD51 activity during homologous DNA repair and replication fork protection.

Firstly, my work has identified a role for human RAD52 as an essential recombination mediator protein in BRCA2-deficient backgrounds. This role supports the chromatin recruitment and DNA assembly of RAD51 for subsequent homology directed DNA repair. These functions in turn sustain the viability of cells that are biallelic mutant for *BRCA2*, but are dispensable for the processes described in cells that are heterozygous or wild-type for *BRCA2*.

Furthermore, my findings reveal that RAD52 confers a fork protective activity at stalled replication forks, where it prevents the excessive degradation of nascent DNA by the MRE11 endonuclease, not only in BRCA2-deficient cells, but also in cells that are heterozygous or wild-type for *BRCA2*. Using a BRCA2 heterozygous cell line as a model, I demonstrate that RAD52 affects RAD51 recruitment to perturbed replication forks, and its depletion enhances the formation of DSBs and cell death following replication stress.

Together, these observations suggest the divergent requirements for BRCA2 and RAD52 in the regulation of RAD51 during HR versus replication fork protection. During homologous DNA repair, RAD52 is dispensable for RAD51 regulation in cells proficient in BRCA2, but becomes an essential HR factor in cells lacking BRCA2. However, during replication protection, RAD52 activity is essential for RAD51 regulation regardless of BRCA2 function. This work therefore clarifies the mechanism by which BRCA2 and RAD52 are synthetic lethal in humans, by indicating that the role of RAD52 in homologous recombination, but not replication fork protection, is critical for supporting the viability of BRCA2-deficient cells. Further research is required to further characterise the emerging roles of RAD52 in human cells and advance our understanding of the contexts in which different functions are essential. Such knowledge will

enable the recognition of settings in which targeting RAD52 could potentially manage genomic instability and tumourigenesis, even beyond the context of HR-deficient cancers.

Finally, I present a high-resolution structure from a RAD51-ssDNA nucleoprotein filament assembled in the presence of BRCA2 BRC repeats, which suggests a BRCA2-catalysed process that enables homology search and strand invasion for HR-mediated DNA repair. The structure obtained is thought to represent an intermediate state induced by BRC repeats in BRCA2 to assist in homologous DNA strand-pairing by RAD51-ssDNA nucleoprotein filaments. Despite this work inferring that BRCA2 BRC repeats encourage RAD51-mediated strand pairing, questions remain regarding the precise mechanism dictating the orderly execution of RAD51 filament assembly, homology search, strand invasion and eventual disassembly upon completion of DNA repair.

Collectively, my thesis elucidates the reactions that lead to homologous DNA repair and replication fork protection, as supported by RAD51 activity and its regulation by BRCA2 and RAD52 in human cells. Disrupting the biological functions of BRCA2 is known to lead to genomic instability, mutagenesis and carcinogenesis, while cells doubly deficient in RAD52 and BRCA2 exhibit reduced proliferative capacity. Although the disruption of RAD2 functions can evidently suppress the proliferation of BRCA1/2 mutant cells, studies should now be extended to *in vivo* settings in order to assess the efficacy of RAD52 inhibitors in HR-deficient tumours, as well as in different genetic and environmental contexts under which inhibition of RAD52 activity can potentially minimise cancer growth given the multiple roles the protein plays in human cells.

CHAPTER 4

Materials and Methods

4.1 Cell culture

All the cell lines were grown at 37°C in a humidified 5% CO_2 atmosphere and maintained by serial passaging using trypsin solution in 1X PBS when 70-80% confluence was reached.

HeLa Kyoto cells were originally obtained from the European Collection of Cell Cultures (ECACC) and contain two wild-type alleles of *BRCA2*. These cells were used as a parental cell line to generate cell lines heterozygous for two clinically relevant *BRCA2* truncating mutations, 6174delT and 3036del4, using CRISPR-Cas9. These two mutations lower the basal levels of the BRCA2 protein, and cause BRCA2 haploinsufficiency upon aldehyde exposure (Tan *et al.*, 2017). Additionally, the HeLa Kyoto cell line was genetically engineered by CRISPR-Cas9 to introduce an N-terminal GFP tag on one of the two BRCA2 alleles, giving rise to the GFP-BRCA2 HeLa Kyoto cells. These were subsequently used as a parental cell line for the introduction of the D2723H mutation in both *BRCA2* alleles, thus creating a cell line homozygous for this point mutation. This mutation prevents the protein interaction between DSS1 and BRCA2 and causes the inappropriate nuclear exclusion and cytoplasmic localisation of BRCA2 (Jeyasekharan *et al.*, 2013). HeLa Kyoto cells and their derivatives were cultured in Dulbecco's modified Eagle's medium (DMEM) supplemented with 10% (v/v) foetal bovine serum (FBS).

The EUFA423 fibroblast cell line was a kind gift from VU University Medical Centre, Netherlands. These cells are derived from a Fanconi anemia (FA) patient with complementation group D1 and are referred to as EUFA- throughout this thesis. The cells have biallelic mutations in BRCA2, where the two mutations (7691insAT in exon 15 and 9900insA in exon 27) lead to two C-terminally truncated versions of the protein. A stable cell line of EUFA423 cells complemented with wild-type, Flag-tagged BRCA2 was previously established

in the lab (Hattori *et al.*, 2011) and are referred to as EUFA+. EUFA423 cells were grown in DMEM supplemented with 10% FBS and 1% penicillin/streptomycin (P/S).

Parental HeLa Kyoto cells containing two wild-type copies of *BRCA2* and the Flag-BRCA2 complemented EUFA423 cell line were used to model cells bearing functional BRCA2 protein.

On the contrary, EUFA- cells and HeLa Kyoto cells containing the biallelic D2723H point mutation in *BRCA2* were used to exemplify BRCA2-deficient cells. Lastly, the +/6174delT and +/3036del4 cell lines were used to represent heterozygous genetic backgrounds of cancer-associated truncating mutations in *BRCA2*.

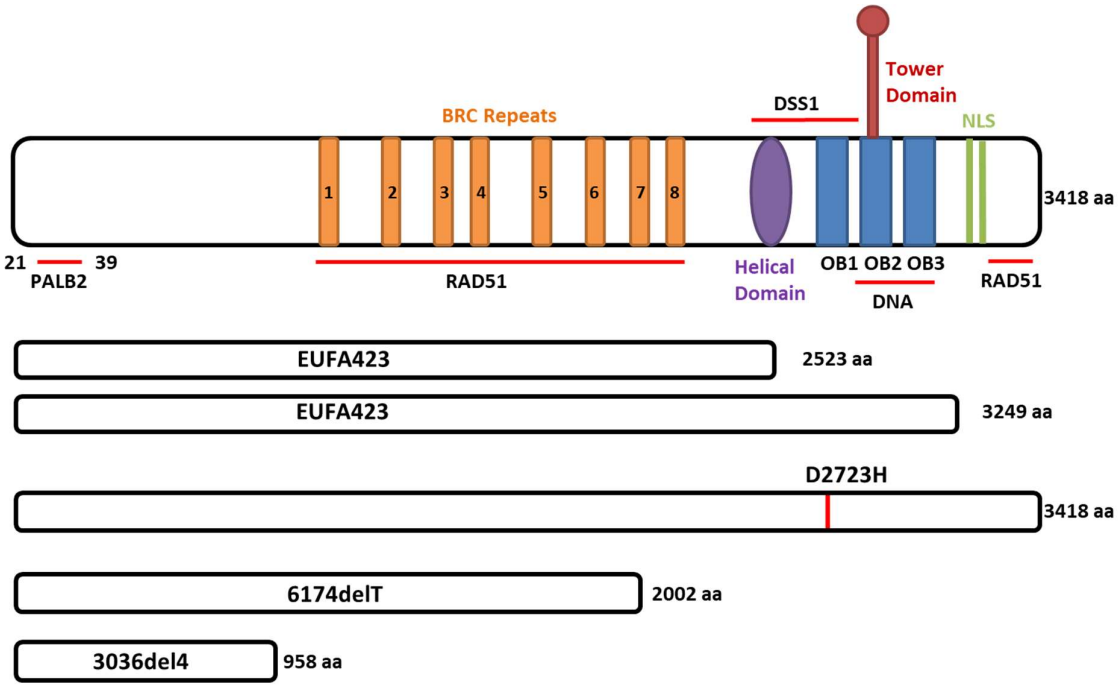

Figure 56: Schematic depicting the wild-type BRCA2 protein and the different mutations found in the cell line models used.

4.2 Constructs

The GFP-RAD52 plasmid was obtained from Kitao et al., 2002 (Harvard School of Public Health, Boston, MA) and cloned by overlap extension PCR to construct an HA-tagged RAD52 insert into the BamHI and XhoI sites. The insert was then sub-cloned into the expression vector pCDNA 3.1 and verified by restriction enzyme digest and sequencing by Source BioScience (Source BioScience, Nottingham, UK). The empty pcDNA3.1 vector was obtained from Christopher Sullivan (Addgene # 17228). All plasmids were cloned into competent BL21 E. coli cells (Bioline Bronze cells, from Bioline, London, UK) and the QIAGEN plasmid purification kit (Qiagen, Hilden, Germany) was used to isolate plasmid DNA as indicated in the manufacturer's instructions. For the transient knockdown of RAD52, a pool of siRNAs targeting human RAD52 was obtained from Dharmacon (GE Healthcare, Buckinghamshire, UK). Stable knockdown of RAD52 was performed using the pTRIPZ inducible vector (HS5087) from Dharmacon with a mature antisense sequence of AAAGCCTTGGACTTGAGGC. This vector carries a constitutive promoter for the expression of puromycin resistance genes, whilst having an additional tetracycline-inducible promoter to enable the controlled expression of the turboRFP reporter and the shRNA downstream.

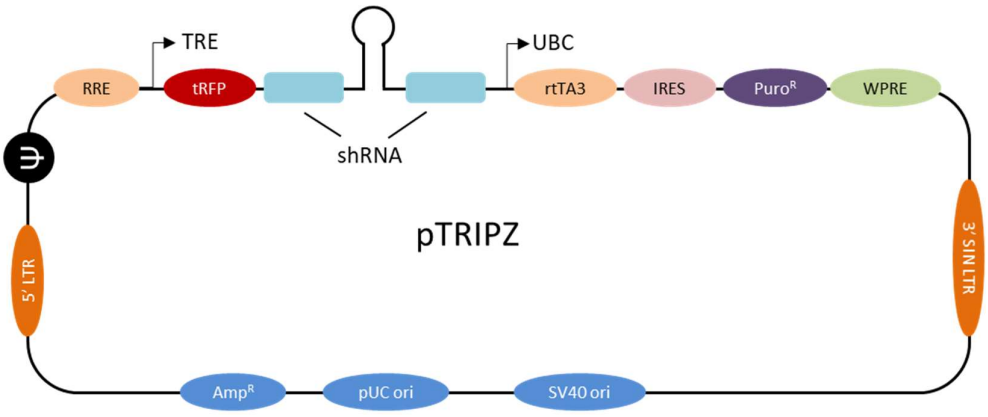

Figure 57: Schematic of the pTRIPZ vector used for shRNA expression. Key: TRE, Tetracycline-inducible promoter; tRFP, turboRFP reporter; shRNA, microRNA for gene knockdown; UBC, Constitutive Ubiquitin C promoter; rtTA3, Reverse tetracycline trans-activator 3; $Puro^R$, Puromycin resistance gene; IRES, Internal ribosomal entry site; 5' LTR, 5' long terminal repeat; 3' SIN LTR, 3' self-inactivating long terminal repeat; Ψ, packaging sequence; RRE, Rev response element; WPRE, Woodchuck hepatitis post-transcriptional regulatory element.

4.3 Cell transfection

RAD52 depletion was performed using a pool of siRNAs (siGENOME from Dharmacon) by reverse transfection using DharmaFECT1 (GE Healthcare, Buckinghamshire, UK). The final siRNA concentration was 25 nM. Transient over-expression of HA-RAD52 was performed at a 3:1 JetPrime:DNA ratio using 1 µg of plasmid, as indicated in the manufacturer's instructions (Polyplus, Reading, UK). For transient siRNA and plasmid co-transfection experiments, DharmaFECT Duo (Dharmacon, CO, USA) was used as indicated in the manufacturer's instructions. The co-transfection was done using siRNA at a concentration of 25 nM and 1 µg of HA-RAD52 plasmid. Following transfection, 48 hours were allowed before cells were harvested for western blot analysis or damaged by IR.

For stable knockdown, lentiviral particles expressing doxycycline-inducible shRNA against human RAD52 (Dharmacon, CO, USA) were used to infect cells at a MOI of 0.3 in serum-free

media. The pTRIPZ inducible vector contains a turboRFP reporter to monitor shRNA induction in cells. TurboRFP is a red fluorescent protein that has excitation and emission maxima of 553 nm and 574 nm, respectively (Merzlyak et al., 2007). Fresh medium was replenished 7 hours later and puromycin selection was initiated 24-48 hours post-transduction. Selection with puromycin was maintained for 9 days. Induction of shRNA expression was performed by addition of 1 µg/ml doxycycline.

4.4 Cell growth

Cells were seeded at a density of 500 cells per well in 12-well plates and growth was monitored over a 7-day period with the IncuCyte ZOOM (Sartorius, Göttingen, Germany) live cell imaging system. Phase-contrast and red fluorescent images were acquired every 3 hours and cell confluence was determined by the IncuCyte software algorithm, which calculates the area covered by cells as a percentage of the total surface area of the well.

4.5 Colony formation assay

Cells were seeded at a density of 500 cells per well in 6-well plates and growth was allowed for 7-10 days. At the end of this period, colonies were washed once with 1X PBS, fixed with 100% methanol for 10 minutes at 4°C, allowed to dry overnight and stained with 0.02% crystal violet (Sigma-Aldrich, St. Luis, USA) solution at room temperature for 10 minutes. The number of colonies was counted using the ColCount™ plate reader (Oxford Optronics, UK).

4.6 Ionising Radiation damage

DNA damage was induced by exposing cultured cells to 5 Gy of ionizing radiation generated by Xstrahl RS225 X-Ray Generator at 195 kV and 10 mA.

4.7 Protein extraction

After the required experimental manipulation, cells were harvested by trypsinisation and washed once with 1X PBS. Following pelleting at 2,300 rpm for 5 minutes at 4 °C, whole cell extracts were obtained by cell lysis in RIPA buffer containing 50 mM HEPES, pH 7.4, 150 mM

NaCl, 0.5% (v/v) NP-40, 1 mM EDTA and 20 mM β-Glycerophosphate, supplemented with 1mM dithiothreitol (DTT) and cOmplete EDTA-free protease inhibitor cocktail (Roche, Basel, Switzerland). The samples were kept on ice for 15 minutes. Supernatant containing total protein extracts was finally collected by centrifugation at 13,000 rpm for 15 minutes at 4 °C.

Sub-cellular fractionation was performed by re-suspending the cell pellet in twice the packed cell volume of CSK buffer (10 mM PIPES, pH 7.0, 100 mM NaCl, 300 mM sucrose, 3 mM $MgCl_2$ and 0.7% Triton X-100, supplemented with cOmplete EDTA-free protease inhibitor cocktail (Roche, Basel, Switzerland) and Phosphatase Inhibitors (Cocktail 2, Sigma-Aldrich, St. Luis, USA). Cells were incubated on ice for 30 minutes before spinning at 13,000 rpm for 10 minutes at 4 °C. The supernatant containing soluble proteins (cytoplasmic and nuclear soluble protein fraction) was obtained and the pellet containing the chromatin-bound protein fraction was washed once with CSK buffer before re-suspending in fresh CSK buffer. The pellets were then sonicated at 30% amplitude four times for 10 seconds each, with 10 seconds in between on ice. Samples were then centrifuged at 13,000 rpm for 5 minutes at 4 °C and the supernatant containing the chromatin-enriched fraction was collected.

Protein concentrations in the extracts were determined using the BCA Protein Assay Kit (Thermo Scientific, MA, USA).

4.8 qPCR

Total RNA was isolated using the RNeasy Kit (Qiagen, Hilden, Germany) and quantified by a NanoDrop ND1000 spectrophotometer (Thermo Scientific, Wilmington, USA). Complementary DNA (cDNA) synthesis was performed using 1 µg total RNA the FastGene Scriptase-II-cDNA synthesis Kit (Nippon Genetics, Dueren, Germany) with oligodT primers according to manufacturer's instructions. Briefly, a mixture of the RNA, primer and dNTP was heated at 65 °C for 5 minutes, and then incubated with FastGene® Scriptase II buffer, DTT and RNase Inhibitor at 42°C for 2 minutes. FastGene® Scriptase II was added to the mix and incubated at 42°C for 50 minutes before enzyme deactivation at 70 °C for 15

minutes. Quantitative PCR (qPCR) reactions were carried out in a final volume of 10 µl using 1 µl of cDNA, 5 µM of appropriate forward and reverse primers (Table 1) and 1X LightCycler® 480 SYBR Green I Master mix (Roche). Results were collected using the Light Cycler 480 (Roche). The first stage was held at 95°C for 5 minutes and subsequent amplification was carried out by 45 cycles of the following three steps: 95°C, 60°C and 72°C for 10 seconds each. Relative mRNA levels in the samples were subsequently determined by normalising to the ribosomal protein lateral stalk subunit P0 (RPLP0) gene using the relative quantification method ($2^{-\Delta\Delta Ct}$), where ΔCt is the difference in Ct between the gene of interest and the housekeeping gene (RPLP0).

Table 1: Primer sequences used for the amplification of target genes for qPCR. Fwd, forward; Rvs, reverse.

Target gene	**Sequence (5'→3')**	
RPLP0	Fwd	GCAGCATCTACAACCCTGAAG
	Rvs	CACTGGCAACATTGCGGAC
RAD52	Fwd	GCTGAAGGATGGTTCATATC
	Rvs	CTTTGTCCAGAATACAGTTTCC

4.9 Western blot

Protein samples were diluted in NuPAGE® 4X LDS sample buffer (Thermo Scientific, Cambridge, UK) and denatured at 100°C for 5 minutes. Sample volumes corresponding to 20 µg of protein were loaded and separated using NuPage® 4-12% Bis-Tris gels (Thermo Scientific, Cambridge, UK) at 200V for 50 minutes. Transfer of the separated proteins to a methanol-activated PVDF membrane (Millipore) was performed by wet transfer in 1X transfer buffer (Thermo Scientific, Cambridge, UK) containing 10% (w/v) methanol at 100V for 2hours or at 10 V for overnight. The membranes were blocked for one hour using 5% (w/v) skimmed

milk (Marvel) in TBS-T (1X TBS, 0.1% Tween-20) prior to overnight incubation with primary antibody at 4°C. Antibodies were diluted in 5% (w/v) BSA in 1X TBS-T and used at the dilutions indicated in table 2. Proteins were then detected by incubation with horseradish peroxidase (HRP) conjugated anti-mouse (1: 10,000, sheep anti-Mouse, GE Healthcare, Buckinghamshire, UK) or anti-rabbit (1: 10,000, Donkey anti-Rabbit, GE Healthcare, Buckinghamshire, UK) secondary antibodies for one hour at room temperature. Enhanced chemiluminescence (ECL) solution (GE Healthcare, Buckinghamshire, UK) was used to visualise proteins using X-ray films.

4.10 Immunofluorescence (IF)

Cells were grown in tissue culture on glass microscope cover slips and fixed at required time-points before and after IR damage. Before fixation, the glass slides were washed once with 1X PBS. The cells were subsequently fixed with 2% formaldehyde (Agar Scientific, Stansted, UK) in 1X PBS for 20 minutes at room temperature. After fixation, cells were washed three times with 1X PBS and formaldehyde was quenched with 50 mM NH_4Cl for 20 minutes at room temperature. Permeabilisation with 0.2% Triton X-100 in 1X PBS was performed for 5 minutes at room temperature. Cells were washed three times with 1X PBS, and subsequently blocked in 1X PBS containing 0.1% Triton X-100, 0.05% Tween-20 and 2% bovine serum albumin (BSA) for 1 hour at room temperature before overnight incubation with primary antibodies at 4°C. The following day, cover slips were washed three times with blocking solution and incubated with fluorophore-conjugated Alexa secondary antibodies, at a 1:500 dilution ratio in blocking solution for 1 hour at room temperature. Cover slips were finally washed three times with 1X PBS and mounted onto microscope glass slides using fluorescence mounting medium (Dako, Cambridgeshire, UK) containing DAPI. Images were acquired using Zeiss 880 Confocal microscope and quantification of the HA-RAD52, RAD51 and RPA foci was done using the ImageJ software. Co-localisation between the protein foci was quantified using the Coloc2 plugin in the Fiji software. Primary antibodies used in this work include RAD51 (Abcam, Cambridge, UK), HA (Roche, Basel, Switzerland), and RPA32 (New England Biolabs, MA, USA), the details and dilutions of which are summarised in table 2.

4.11 Super Resolution Microscopy

For Super resolution imaging by *d*STORM (*direct* stochastic optical reconstruction microscopy), cells were fixed and permeabilised as performed for immunofluorescence. Following incubation with appropriate primary and secondary antibodies, a second fixation step was performed with 2% formaldehyde in 1X PBS for 20 minutes at room temperature to prevent label diffusion. Quenching of formaldehyde was performed as before with 50 mM NH_4Cl for 20 minutes at room temperature and cover slips were stored in 1X PBS until imaged by *d*STORM. Imaging was performed in OxEA buffer containing 20% (v/v) DL-Lactate, 3% OxyFluor (Oxyrase Inc., Mansfield, Ohio, USA) and 50 mM β-mercaptoethanol (MEA, Sigma-Aldrich) in PBS, with the pH adjusted to 8-8.5 with NaOH (Nahidiazar *et al.*, 2016). MEA in the buffer acts as an oxygen scavenger and DL-Lactate as the substrate for Oxyrase. During *d*STORM, the fluorophores are initially transferred to a stable non-fluorescent reduced state, also known as the dark state, by very intense laser excitation. The laser excitation is maintained until individual fluorophores start to blink stochastically, at which point acquisition is initiated. Fluorophore blinking involves the reversible photo-switching between the so-called 'on' and 'off' states. In the 'on' state, a fluorophore gets excited from the ground state (S_0) to the excited singlet state (S_1). This can fall back to the original ground state (S_0), releasing the absorbed energy as fluorescence emission (hv). Alternatively, the excited singlet state (S_1) can enter an excited triplet state (T_1), which can in turn return to the ground state (S_0) or form a long-lived dark state (D). The dark state can return to the original ground state by reacting with oxygen or upon irradiation with UV light. The fluorescence emission pattern enables the precise localisation of single fluorophores with a resolution of ~20 nm. Images were then reconstructed, where each fluorophore is approximated by a Gaussian distribution and drift-corrected.

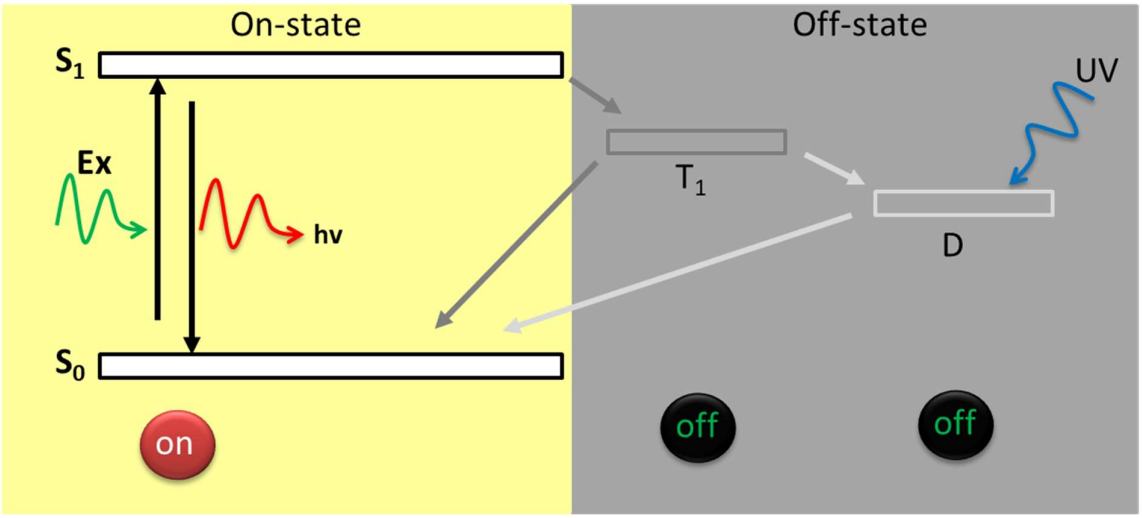

Figure 58: Minimal Jablonski diagram indicating the molecular states essential for *d*STORM. In the bright 'on' state, fluorophores in the ground state **(S_0)** can be excited **(Ex)** to an excited singlet state **(S_1)**. Excited states can subsequently either relax back to the ground state by emitting light **(hv)** or may form a dark triplet state **(T_1)** instead. In the dark triplet state, molecules can return to the ground state or, alternatively, progress to a long-lived dark state **(D)**. Molecules in the dark state **(off-state)** can then return to the ground state by reacting with oxygen or through exposure to near-UV radiation. The blinking of few fluorophores between the on- and off- states whilst the majority of molecules are in the dark 'off' state enables the precise detection and localisation of individual fluorophores. **Adapted from Nahidiazar *et al.*, 2016.**

4.12 Cas9/mClover assay

HR efficiency was tested using the Cas9/mClover assay (Pinder, Salsman and Dellaire, 2015). Briefly, a DSB is introduced within the LaminA gene using a Cas9-gRNA chimeric plasmid targeting the genomic region near the *LMNA* start codon. Repair of this break can be performed using a homologous template plasmid carrying a monomeric green fluorescent protein known as mClover. Hence, DSB repair leads to the incorporation of mClover after the start codon of the *LMNA* gene, making HR-proficient cells fluoresce green. To evaluate HR proficiency, cells were co-transfected with the two plasmids at a 2:1 JetPrime:DNA ratio using 0.5 µg of each plasmid. After 72 hours of transfection, immunofluorescent staining was performed to assess green fluorescence in the cells.

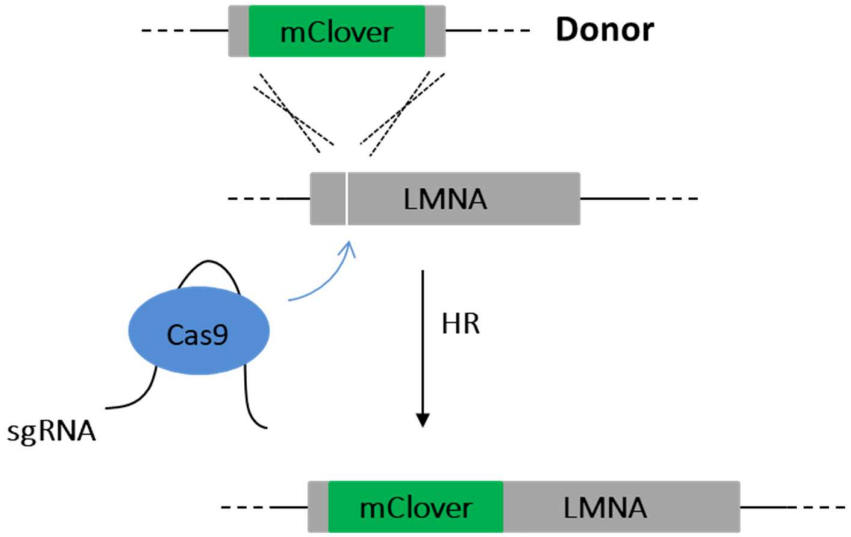

Figure 59: Schematic of the Cas9/mClover assay used to assess HR proficiency in cells. **Adapted from Buisson *et al.*, 2017.**

4.13 DNA Fibre Assay

Cells were labelled with 25µM IdU for 20 minutes before treatment with 4 mM hydroxyurea (HU) for 5 hours with or without 100 µM mirin, as indicated. Following exposure to replication stress by HU, cells were harvested by trypsinisation and resuspended in cold 1X PBS. Cells were then spotted onto glass slides and lysed in lysis buffer (200 mM Tris-HCl, pH 7.4, 50 mM EDTA and 0.5% SDS) for 5 minutes at room temperature. Following cell lysis, DNA combing was performed by tilting the glass slides and allowing the lysed cell suspension to slowly roll down. Slides were then air-dried for at least two hours before fixing in 3:1 methanol/acetic acid for 10 minutes at room temperature. The following day, DNA was denatured in 2.5M HCl for 55 minutes at room temperature and then washed three times, five minutes each, in ice-cold 1X PBS. Blocking was then performed at room temperature for 30 minutes in 1.5% (w/v) blocking reagent for nucleic acid hybridization and detection (Roche, manufacturer code 11096176001) dissolved in 1X PBS, 0.05% Tween-20 at pH 7.5. To detect IdU, slides were incubated with anti-BrdU for 45 minutes at room temperature, followed by secondary and tertiary antibodies for 20 minutes each, with three 5-minute washes with ice-cold 1X PBS in between each antibody incubation. Single-stranded DNA (ssDNA) was detected by incubation with anti-DNA for 45 minutes at room temperature, followed by secondary and tertiary antibodies for 20 minutes each, with three 5-minute washes with ice-cold 1X PBS in between each antibody incubation. Slides were mounted with 90% glycerol in 1X PBS and images of at least 100 DNA fibres per sample were acquired with a Leica SP5 microscope. DNA tract lengths were measured using the Fiji software. Antibodies were diluted in blocking buffer and used at the dilutions indicated in table 2.

4.14 aniPOND (accelerated native isolation of protein on nascent DNA)

Proteins at replication forks were detected by aniPOND as described in Leung et al 2013. Briefly, at least $6x10^7$ cells were labelled with 10 µM 5-ethynyl-2'-deoxyuridine (EdU, Invitrogen) for 10 minutes and, where indicated, treated with 4 mM HU for 3 hours. Cells were subsequently harvested and lysed in ice-cold NEB buffer (20 mM HEPES pH 7.2, 50 mM NaCl,

3 mM $MgCl_2$, 300 mM sucrose and 0.5% IGEPAL CA630) for 15 minutes at 4°C. The buffer solubilises the cytoplasm and permeabilises the nuclei, thus removing all soluble proteins from cells. Biotin was then covalently linked to EdU incorporated in nascent DNA by the click reaction in 1X PBS containing 25 µM biotin–azide, 10 mM (+)-sodium L-ascorbate and 2 mM CuSO4 by rotating for an hour at 4°C. For the negative control, DMSO was included in the click reaction mix instead of biotin-azide. The click reaction mix was then discarded, and the pellet was washed with ice-cold 1X PBS before proceeding to chromatin sonication using a Sonics Vibra-Cell™ ultrasonic processor at an output power of 10W. Each sample was sonicated 12 times for 10 seconds on/10 seconds off in ice-cold B1 buffer (25 mM NaCl, 2 mM EDTA, 50 mM Tris-HCl pH 8.0, 1% IGEPAL CA630 supplemented with cOmplete protease inhibitors). After sonication, solubilized chromatin and bound proteins were retrieved by centrifugation at 13,200 rpm for 10 minutes at 4°C. One volume of ice-cold buffer B2 (150 mM NaCl, 2 mM EDTA, 50 mM Tris-HCl pH 8.0, 0.5% IGEPAL CA630 supplemented with cOmplete protease inhibitors) was added to the supernatant to increase the NaCl concentration to physiological levels. A total input sample (0.25% of total lysate) was obtained and biotinylated chromatin was then captured by overnight rotation with streptavidin beads (Merck Millipore) at 4°C. The following day, beads were washed four times with ice-cold buffer B2 and captured proteins were eluted in 2×Laemmli sample buffer (Biorad, with 5% β-mercaptoethanol) by boiling at 100°C for 15 min. Western blotting was then performed to detect proteins at replication forks, using the antibodies indicated in table 2.

Table 2: Antibodies and the dilutions used in each of the techniques.

Antibody	Supplier Code	Dilution	Species	Technique
BRCA2	Ab-1 (Abnova)	1:500	mouse	Western Blot
PARP	BD556362 (BD Pharmingen)	1:500	mouse	Western Blot
MRE11	NB100-142 (Novus Biologicals)	1:2,000	rabbit	Western Blot
RAD52	ab103067	1:250	rabbit	Western Blot
	sc-365341	1:100	mouse	Western Blot / aniPOND
RAD51	ab133534 (Abcam)	1:2,000 1:1,000 1:250	rabbit	Western Blot / IP IF / *d*STORM aniPOND
PCNA	ab18197 (Abcam)	1:2,000	rabbit	aniPOND
γ-tubulin	GTU-88	1:2,000	mouse	Western Blot

Histone H3	CST4499S (Cell Signalling Technology)	1:2,000	rabbit	Western Blot / aniPOND
HA	12CA5 (Roche)	1:1,000	mouse	Western Blot / IF
6X His	BD631212 (BD Pharmigen)	1:2,000	mouse	Western Blot
β-actin	A5441 (Sigma)	1:2,000	mouse	Western Blot
RPA32	2208S (New England Biolabs)	1:500	rat	IF
BrdU	347580 (BD Pharmingen)	1:5	mouse	DNA Fibre
anti-mouse AF594	A-11062 (Thermo Fisher)	1:50	rabbit	DNA Fibre
anti-rabbit AF594	A-11012 (Thermo Fisher)	1:50	goat	DNA Fibre
ssDNA	MAB3034 (Merck Millipore)	1:50	mouse	DNA Fibre

anti-mouse AF488	A-11059 (Thermo Fisher)	1:100	rabbit	DNA Fibre
anti-rabbit AF488	A-21206 (Thermo Fisher)	1:100	donkey	DNA Fibre

4.15 Neutral comet assay

DNA breakage in terms of DSB gaps was assessed using the neutral comet assay, also known as single cell gel electrophoresis.

Cells were treated as indicated and harvested by trypsinisation. Following collection, cells were centrifuged at 1,500 rpm for 5 minutes, counted and resuspended at a density of 120,000 cells in media. These were then mixed with molten 0.5% (w/v) agarose (in 1X PBS) and laid dropwise on slides pre-coated with 1.5% (w/v) agarose (in 1X PBS). The agarose was allowed to solidify before proceeding to overnight cell lysis at 4°C in buffer containing 2.5 M NaCl, 100 mM EDTA, 10 mM Tris-NaOH, 1% (v/v) Triton-X100 and 10% (v/v) DMSO. The following day, treatment with S1 nuclease was performed for 30 minutes at 20 U/ml and 37°C (Invitrogen, Life Technologies) in S1 nuclease buffer (50 mM NaCl, 30 mM sodium acetate, pH 4.6 and 5% glycerol). Slides were then incubated for 60 minutes in cold electrophoresis buffer (300 mM sodium acetate, 100 mM Tris, acetic acid, pH 8.5) and electrophoresis was performed under non-denaturing conditions for 60 minutes, at 14 V and 20 mA at 4°C. After the run, slides were neutralized by flooding with neutralizing buffer (0.4 M Tris-HCl pH 7.5) three times. Fixation was performed with ice-cold 100% ethanol for 30 minutes and slides were stored at 4°C until processing. Cell DNA was stained with 40 µg/ml ethidium bromide just before image acquisition, and images were acquired using the Zeiss 880 Confocal microscope at 10x magnification. Image analysis was performed by the CaspLab software,

with at least 100 comet heads analysed for each sample. To assess the amount of DNA damage, software-determined values of the DNA percentage in comet tails were used.

4.16 Statistical analysis

Statistical analysis was performed by GraphPad Prism. A p-value equal to or smaller than 0.05 was considered statistically significant and indicated using an asterisk (*$p<0.05$). Increasing statistical significance is indicated with more asterisks (**$p\leq0.01$, ***$p\leq0.001$).

4.17 Protein purification

The sequence of human BRCA2 encoding for the BRC repeats 3 and 4 (BRC34), was cloned into a pET28a vector (Novagen) containing an N-terminal His6 tag. The FxxA motif, which is known to inhibit RAD51 assembly, was mutated to GxxG within each BRC repeat. The constructs were expressed in *E.coli* BL21(DE3)pLysS chemically competent cells. Bacteria were grown on Luria-Bertani media supplemented with kanamycin (30µg/ml) in a shaking incubator at 37°C until $0D_{600}$ reached 0.4-0.8. Once the mid-exponential growth phase was reached, protein expression was induced with 1 mM IPTG and the cultures were grown for two more hours at 37°C. Bacterial cells were harvested by centrifugation at 4,200 rpm for 15 minutes at 4°C and re-suspended in 20 ml of buffer (50 mM Tris pH 7.5, 500 mM NaCl, 0.1% Triton X100 and 0.25 mM EDTA supplemented with cOmplete protease inhibitors). The suspended cells were lysed by incubation with 250 µg/ml lysozyme and 20 µg/ml benzonase for 30 minutes on ice. Soluble proteins were extracted from the cell lysate by centrifugation at 17,000 rpm for an hour at 4°C. The soluble fraction was applied to a HisTrap column, which contains a Ni^{2+} resin that enables the purification of His-tagged proteins due to its high affinity for Histidine residues. Purification was performed using the automated ÄKTA Avant 25 system (GE Healthcare, Buckinghamshire, UK). Following sample application, the column was washed using 10 column volumes of buffer containing 50 mM Tris pH 7.5, 500 mM NaCl, 20 mM imidazole, 10% glycerol and 0.25 mM EDTA. Finally, the protein of interest was eluted using a linear gradient of buffer containing 50 mM Tris pH 7.5, 150 mM NaCl, 450 mM imidazole, 10% glycerol and 0.25 mM EDTA.

Fractions containing the protein were pooled, diluted in buffer containing 50 mM Tris pH 9.0 and 5% glycerol to lower the salt concentration to 20 mM NaCl, and applied to a CaptoQ column which enables separation based on protein charge. Subsequent to sample application the column was washed using 10 column volumes of the binding buffer (50 mM Tris pH 9.0 and 5% glycerol), and elution was performed using a salt gradient of 0-500 mM NaCl in buffer made of 50 mM Tris pH 9.0, 1 M NaCl and 5% glycerol. The construct was finally concentrated using a Vivaspin® centrifugal concentrator (GE Healthcare, Buckinghamshire, UK) with a molecular weight cut-off of 30 kDa. Protein concentration was determined using the NanoOrange™ protein quantitation kit (Thermo Scientific, MA, USA) and found to be 11 µM. The BRC34 protein was aliquoted and stored until use at -80°C.

4.18 Pull-down assays

4.18.1 MagneHis capture

MagneHis™ beads (30 µl, Promega) were incubated with 6.6 µM of His-BRC34 in 50 mM Tris–HCl, pH 7.4, 100 mM NaCl, 0.25 mM EDTA and 0.5% Triton X-100 for 2 hours at 4°C. For the negative control, the beads were incubated with buffer lacking the protein. Following His-BRC34 immobilisation, 500 µg of HeLa Kyoto total protein lysate was added to the beads and incubated by rotating overnight at 4°C. The following day, beads were washed two times, re-suspended in 1X LDS buffer (Invitrogen, Life Technologies) and boiled at 70°C for 10 minutes for subsequent analysis by SDS–PAGE.

4.18.2 Streptavidin capture

Briefly, a biotinylated oligodT made of 72 nucleotides (Sigma-Aldrich, St. Luis, USA) was immobilised on magnetic streptavidin beads (Invitrogen, Life Technologies) at a concentration of 10 µM for 15 minutes at room temperature in buffer containing 5 mM Tris-HCl pH 7.5, 0.5 mM EDTA and 1 M NaCl. Following immobilisation the ssDNA, the beads were washed three times using the same buffer, and 3.3 µM recombinant human RAD51 protein, provided by Dr. Mahmud Shivji, was added and incubated for 15 minutes at room temperature followed by another 15-minute incubation at 37°C using gentle rotation in buffer containing 25 mM Tri-

Acetate pH 7.0, 100 mM NaCl, 2 mM $MgCl_2$, 2 mM AMP-PNP, 1 mM DTT and 0.5% Triton X-100. Purified His-BRC34 was used at a concentration of 1.65 µM and was either added at the same time as RAD51 if co-incubation was performed, or added subsequent to the 30-minute incubation of RAD51 with ssDNA. The reaction components were incubated overnight at 4°C to allow complex assembly. The next day, the supernatant fraction containing any unbound proteins was collected and the streptavidin beads were re-suspended in loading buffer to assess complex formation between recombinant RAD51, His-BRC34 and ssDNA. Samples were boiled at 70°C for 10 minutes and finally analysed by SDS–PAGE.

4.19 Cryo-EM sample preparation

Complex assembly for assessment by Transmission Electron Microscopy (TEM) was performed by co-incubating RAD51 (3.3 µM) with BRC34 (1.65 µM) and biotinylated 72-mer oligo(dT) ssDNA (10 µM) for 15 minutes at 37°C. Assembly was performed in buffer containing 25 mM Tris-Acetate pH 7.0, 100 mM NaCl, 2 mM $MgCl_2$, 2 mM AMP-PNP and 1 mM DTT (Short *et al.*, 2016). Specimen drops of 2 µl were applied to glow-discharged carbon EM grids prepared in-house. Samples were allowed to adsorb on grids for 1 second each, any excess liquid was blotted off, and negatively staining was performed with uranyl acetate for 30'' for analysis. Samples were subsequently checked for nucleoprotein filament presence.

Nucleoprotein filament assembly for Cryo-EM was performed in the same way, apart from doubling the original concentrations used for TEM. Incubation of RAD51 protein (6.6 µM) with BRC34 (3.3 µM) and biotinylated 72-mer oligo(dT) ssDNA (20 µM) was performed for 15 minutes at 37°C, as before.

Specimens were prepared by applying 2 µl of the assembled mixture to commercially available grids. The ones used were coated with a Quantifoil holey carbon film containing 1.2 µm diameter holes with 1.3 µm spacing (R1.2/1.3), mounted on a gold mesh. Following activation by glow-discharge and sample application, the grids were blotted and rapidly

frozen using the FEI Vitrobot™ Mark IV System (Thermo Scientific, MA, USA) at 100% relative humidity and 4°C.

4.20 Cryo-EM data acquisition and image processing

Specimen imaging was performed by Dr. Shaoxia Chen (MRC Laboratory of Molecular Biology) using a Titan-Krios electron cryo-microscope. Low dose images were recorded in counting mode on a Falcon III direct electron detector, using a voltage of 300 keV and delivering 29.36 electrons per $Å^2$ to the specimen in total. The magnification used was 104,478x (59,000x nominal magnification), thus leading to a sampling size of 1.34 Å/pixel since the pixel size of the detector is equivalent to 14 µm. The images were acquired automatically by the EPU software, using a total exposure time of 60s for each image with 40 video frames recorded per second and a dose fraction of 75 electrons per $Å^2$ per second. Objective lens defocus values ranged from -1.5 to -3.0 µm. The specimen was maintained at a temperature of -170°C during grid loading and image recording in the microscope column.

Image processing and fitting were performed by Dr. Judith Short in cooperation with Dr. Paul Emsley and Dr. Garib Murshudov (MRC Laboratory of Molecular Biology). Filaments were selected manually from micrograph images, creating a ~105K molecule dataset from which a 3D starting model was derived using a modification of the Iterative Helical Real Space Reconstruction (IHRSR) approach. The reconstruction was obtained by using a cylinder as the initial model and refining its helical parameters to 57° and 15.6° for the angular and axial increments, respectively. The 3D model was then processed further in RELION3, which was used to perform initial motion correction and contrast transfer function (CTF) estimation. Model resolution was improved by subsequent iterations of 2D classification, 3D refinement and post-processing. CTF refinement, beam tilt estimation, movie refinement with particle polishing and further iterations of 2D and 3D classification followed. A model of 3.2 Å resolution was obtained from 18340 segments, with the resolution confirmed by a local resolution map. Finally, coordinates from the deposited crystal structure of a human RAD51-ATP filament (5NWL, Brouwer *et al.*, 2018b) were fitted in the model using Chimera, COOT,

REFMAC and MOLPROBITY, with >99% of residues found within the preferred and allowed regions of a Ramachandran plot.

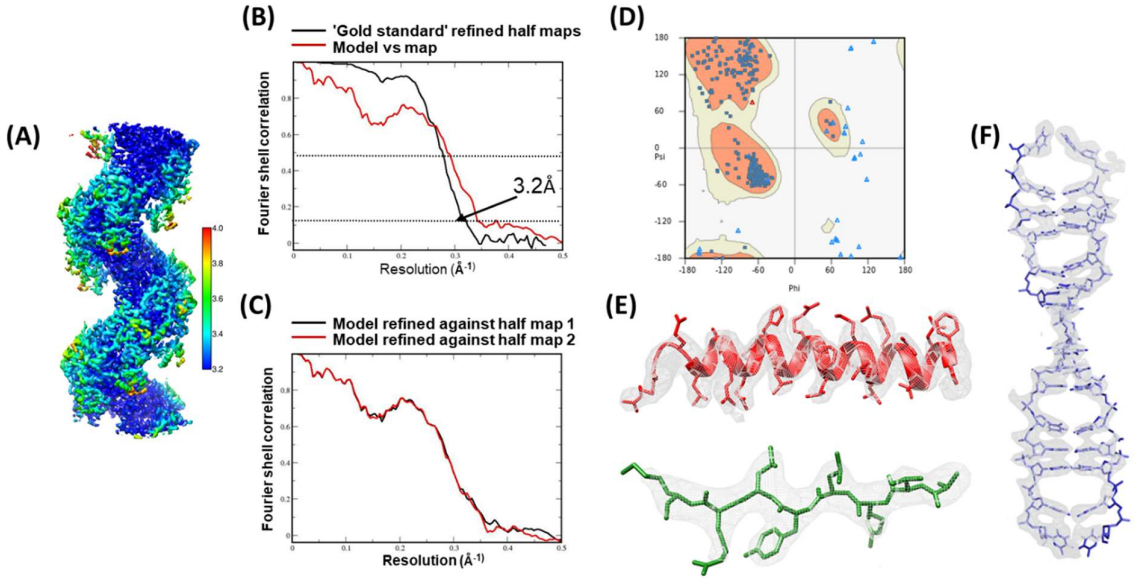

Figure 60: Resolution evaluation of the RAD51-BRC34-dsDNA nucleoprotein filament. (A) Local resolution map of the filament. **(B-C)** Fourier shell correlation plots for 'gold standard' refined half maps and model to map. **(D)** Ramachandran plot of amino acids from the fitted PDB coordinates: 95.13% residues lie in preferred regions, 4.55% are in allowed regions and 0.32% are outliers. Regions of α-helical and β-strand elements **(E)** as well as single-stranded DNA **(F)** are shown fitted to the map density. Data processing and figure preparation were performed by Dr. Judith Short.

BIBLIOGRAPHY

1. Aguilera, A. and García-Muse, T. (2013) 'Causes of Genome Instability', *Annual Review of Genetics*, 47(1), pp. 1–32.
2. Ahlskog, J. K. *et al.* (2016) 'ATM/ATR-mediated phosphorylation of PALB2 promotes RAD51 function', *EMBO Reports*, 17(5), pp. 671–81.
3. Aihara, H. *et al.* (1999) 'The N-terminal Domain of the Human Rad51 Protein Binds DNA : Structure and a DNA Binding Surface as Revealed by NMR', *JMB*, 52(290), pp. 495–504.
4. Alexandrov, L. B. *et al.* (2013) 'Signatures of mutational processes in human cancer', *Nature*, 500(7463), pp. 415–421.
5. Allen, C. *et al.* (2011) 'More forks on the road to replication stress recovery', *J Mol Cell Biol.*, 3, pp. 4–12.
6. Amé, J. C. *et al.* (1999) 'PARP-2, a novel mammalian DNA damage-dependent poly(ADP-ribose) polymerase', *Journal of Biological Chemistry*, 274(25), pp. 17860–17868.
7. Amé, J. C., Spenlehauer, C. and De Murcia, G. (2004) 'The PARP superfamily', *BioEssays*, 26(8), pp. 882–893.
8. Antoniou, A. *et al.* (2003) 'Average Risks of Breast and Ovarian Cancer Associated with BRCA1 or BRCA2 Mutations Detected in Case Series Unselected for Family History: A Combined Analysis of 22 Studies', *The American Journal of Human Genetics*, 72(5), pp. 1117–1130.
9. Aubin, R. J. *et al.* (1983) 'Correlation between endogenous nucleosomal hyper(ADP-ribosyl)ation of histone H1 and the induction of chromatin relaxation.', *The EMBO Journal*, 2(10), pp. 1685–1693.
10. Audebert, M., Salles, B. and Calsou, P. (2004) 'Involvement of poly(ADP-ribose) polymerase-1 and XRCC1/DNA ligase III in an alternative route for DNA double-strand breaks rejoining', *Journal of Biological Chemistry*, 279(53), pp. 55117–55126.
11. Ayoub, N. *et al.* (2009) 'The Carboxyl Terminus of Brca2 Links the Disassembly of Rad51 Complexes to Mitotic Entry', *Current Biology*, 19(13), pp. 1075–1085.
12. Barnes, D. E. and Lindahl, T. (2004) 'Repair and genetic consequences of endogenous DNA base damage in mammalian cells.', *Annual review of genetics*, 38, pp. 445–76.
13. Baumann, P. *et al.* (1997) 'Purification of human Rad51 protein by selective spermidine precipitation', *Mutation Research - DNA Repair*, 384(2), pp. 65–72.
14. Baumann, P., Benson, F. E. and West, S. C. (1996) 'Human Rad51 protein promotes ATP-dependent homologous pairing and strand transfer reactions in vitro', *Cell*, 87(4), pp. 757–766.
15. Baumann, P. and West, S. C. (1997) 'The human Rad51 protein : polarity of strand transfer and stimulation by hRP-A', *The EMBO Journal*, 16(17), pp. 5198–5206.
16. Baumann, P. and West, S. C. (1999) 'Heteroduplex formation by human Rad51 protein: Effects of DNA end-structure, hRP-A and hRad52', *Journal of Molecular Biology*, 291(2), pp. 363–374.
17. Baynton, K. *et al.* (2003) 'WRN interacts physically and functionally with the recombination mediator protein RAD52', *Journal of Biological Chemistry*, 278(38), pp. 36476–36486.
18. Beesley, J. *et al.* (2007) 'Association between single-nucleotide polymorphisms in

hormone metabolism and DNA repair genes and epithelial ovarian cancer: Results from two Australian studies and an additional validation set', *Cancer Epidemiology Biomarkers and Prevention*, 16(12), pp. 2557–2565.
19. Bell, D. W. *et al.* (1999) 'Common nonsense mutations in RAD52', *Cancer Research*, 59(16), pp. 3883–3888.
20. Belt, R. J. *et al.* (1980) 'Studies of hydroxyurea administered by continuous infusion. Toxicity, pharmacokinetics, and cell synchronization', *Cancer*, 46(3), pp. 455–462.
21. Benson, F. E., Baumann, P. and West, S. C. (1998) 'Synergistic actions of Rad51 and Rad52 in recombination and DNA repair.', *Nature*, 391(6665), pp. 401–404.
22. Benson, F. E., Stasiak, A. and West, S. C. (1994) 'Purification and characterization of the human Rad51 protein, an analogue of E. coli RecA.', *The EMBO journal*, 13(23), pp. 5764–5771.
23. Berriman, J. and Unwin, N. (1994) 'Analysis of transient structures by cryo-microscopy combined with rapid mixing of spray droplets', *Ultramicroscopy*, 56(4), pp. 241–252.
24. Berti, M. *et al.* (2013) 'Human RECQ1 promotes restart of replication forks reversed by DNA topoisomerase I inhibition', *Nature Structural and Molecular Biology*, 20(3), pp. 347–354.
25. Bester, A. C. *et al.* (2011) 'Nucleotide deficiency promotes genomic instability in early stages of cancer development', *Cell*, 145(3), pp. 435–446.
26. Bhat, K. P. *et al.* (2018) 'RADX Modulates RAD51 Activity to Control Replication Fork Protection', *Cell Reports*, 24(3), pp. 538–545.
27. Bhat, K. P. and Cortez, D. (2018) 'RPA and RAD51: fork reversal, fork protection, and genome stability', *Nature Structural and Molecular Biology*, 25(June), pp. 1–8.
28. Bhatia, V. *et al.* (2014) 'BRCA2 prevents R-loop accumulation and associates with TREX-2 mRNA export factor PCID2', *Nature*, 511(7509), pp. 362–365.
29. Bhowmick, R., Minocherhomji, S. and Hickson, I. D. (2016) 'RAD52 Facilitates Mitotic DNA Synthesis Following Replication Stress', *Molecular Cell*, 64(6), pp. 1117–1126.
30. Bi, B. *et al.* (2004) 'Human and yeast Rad52 proteins promote DNA strand exchange', *Proceedings of the National Academy of Sciences*, 101(26), pp. 9568–9572.
31. Bork, P., Blomberg, N., and N. M. (1996) 'Internal repeats in the BRCA2 protein sequence', *Nature Genetics*, 13(3), pp. 22–23.
32. Bornhorst, J. A. and Falke, J. J. (2000) 'Purification of Proteins Using Polyhistidine Affinity Tags', *Methods enzymol.*, 326, pp. 245–254.
33. Brandsma, I. and Gent, D. C. Van (2012) 'Pathway choice in DNA double strand break repair : observations of a balancing act', *Genome Integrity*, pp. 1–10.
34. Bridges, C. B. (1922) 'The origin of variations in sexual and sex-limited characters', *The American Naturalist*, 56(642), pp. 51–63.
35. Brouwer, I. *et al.* (2017) 'Human RAD52 Captures and Holds DNA Strands, Increases DNA Flexibility, and Prevents Melting of Duplex DNA: Implications for DNA Recombination', *Cell Reports*. The Author(s), 18(12), pp. 2845–2853.
36. Brouwer, I. *et al.* (2018) 'Two distinct conformational states define the interaction of human RAD51-ATP with single-stranded DNA', *The EMBO Journal*, 37, pp. 1–13.
37. Bryant, H. E. *et al.* (2005) 'Specific killing of BRCA2-deficient tumours with inhibitors of poly(ADP-ribose) polymerase', *Nature*, 434(7035), pp. 913–917.

38. Bryant, H. E. *et al.* (2009) 'PARP is activated at stalled forks to mediate Mre11-dependent replication restart and recombination', *EMBO Journal*, 28(17), pp. 2601–2615.
39. Bugreev, D. V., Mazina, O. M. and Mazin, A. V. (2006) 'Rad54 protein promotes branch migration of Holliday junctions', *Nature*, 442(7102), pp. 590–593.
40. Bugreev, D. V., Rossi, M. J. and Mazin, A. V. (2011) 'Cooperation of RAD51 and RAD54 in regression of a model replication fork', *Nucleic Acids Research*, 39(6), pp. 2153–2164.
41. Buisson, R. *et al.* (2017) 'Coupling of Homologous Recombination and the Checkpoint by ATR', *Molecular Cell*, 65(2), pp. 336–346.
42. Byun, T. S. *et al.* (2005) 'Functional uncoupling of MCM helicase and DNA polymerase activities activates the ATR-dependent checkpoint', *Genes and Development*, 19(9), pp. 1040–1052.
43. Caporale D, S. E. (2014) 'Two different BRCA2 mutations found in a multigenerational family with a history of breast , prostate , and lung cancers', *Advances in Genomics and Genetics*, 2014(4), pp. 87–94.
44. Carreira, A. *et al.* (2009) 'The BRC Repeats of BRCA2 Modulate the DNA-Binding Selectivity of RAD51', *Cel*l, 136(6), pp. 1032–1043.
45. Carreira, A. and Kowalczykowski, S. C. (2011) 'Two classes of BRC repeats in BRCA2 promote RAD51 nucleoprotein filament function by distinct mechanisms.', *Proceedings of the National Academy of Sciences of the United States of America*, 108(26), pp. 10448–53.
46. Ceccaldi, R. *et al.* (2015) 'Homologous-recombination-deficient tumours are dependent on Polθ -mediated repair', *Nature*, 518(7538), pp. 258–262.
47. Chandramouly, G. *et al.* (2015) 'Small-Molecule Disruption of RAD52 Rings as a Mechanism for Precision Medicine in BRCA-Deficient Cancers', *Chemistry and Biology*, 22(11), pp. 1491–1504.
48. Charache, S. *et al.* (1992) 'Hydroxyurea: Effects on hemoglobin F production in patients with sickle cell anemia', *Blood*, 79(10), pp. 2555–2565.
49. Chaudhuri, A. R. *et al.* (2012) 'Topoisomerase I poisoning results in PARP-mediated replication fork reversal', *Nat Struct Mol Biol*, 19(4), pp. 417–423.
50. Chaudhuri, A. R. *et al.* (2016) 'Replication fork stability confers chemoresistance in BRCA-deficient cells', *Nature*, 535(7612), pp. 382–387.
51. Chen, C. *et al.* (1999) 'Expression of BRC Repeats in Breast Cancer Cells Disrupts the BRCA2-Rad51 Complex and Leads to Radiation Hypersensitivity and Loss of G 2 / M Checkpoint Control', *The Journal of biological chemistry*, 274(46), pp. 32931–32935.
52. Chen, Z., Yang, H. and Pavletich, N. P. (2008) 'Mechanism of homologous recombination from the RecA-ssDNA/dsDNA structures', *Nature*, 453(7194), pp. 489–494.
53. Choi, E. *et al.* (2012) 'BRCA2 Fine-Tunes the Spindle Assembly Checkpoint through Reinforcement of BubR1 Acetylation', *Developmental Cell*, 22(2), pp. 295–308.
54. Chou, S. H. and Chin, K. H. (2001) 'Solution structure of a DNA double helix incorporating four consecutive non-Watson-Crick base-pairs', *Journal of Molecular Biology*, 312(4), pp. 769–781.
55. Christmann, M. and Kaina, B. (2013) 'Transcriptional regulation of human DNA repair genes following genotoxic stress: Trigger mechanisms, inducible responses and

genotoxic adaptation', *Nucleic Acids Research*, 41(18), pp. 8403–8420.
56. Chun, J., Buechelmaier, E. S. and Powell, S. N. (2013) 'Rad51 Paralog Complexes BCDX2 and CX3 Act at Different Stages in the BRCA1-BRCA2-Dependent Homologous Recombination Pathway', *Molecular and cellular biology*, 33(2), pp. 387–395.
57. Chung, W. H. *et al.* (2010) 'Defective resection at DNA double-strand breaks leads to de Novo telomere formation and enhances gene targeting', *PLoS Genetics*, 6(5), p. 24-37.
58. Ciccia, A. *et al.* (2009) 'The SIOD disorder protein SMARCAL1 is an RPA-interacting protein involved in replication fork restart', *Genes & Development*, 23(20), pp. 2415–2425.
59. Ciccia, A. and Elledge, S. J. (2010) 'The DNA Damage Response: Making It Safe to Play with Knives', *Molecular Cell*, 40(2), pp. 179–204.
60. Ciccia, A. and Symington, L. S. (2016) 'Stressing Out About RAD52', *Molecular Cell,* 64(6), pp. 1017–1019.
61. Connor, F. *et al.* (1997) 'Tumorigenesis and a DNA repair defect in mice with a truncating BRCA2 mutation', *Nature Genetics*, 17(4), pp. 423–30.
62. Consortium, B. C. L. (1999) 'Cancer risks in BRCA2 mutation carriers', *J. Natl. Cancer Inst.*, 91(15), pp. 1310–1316.
63. Constantinou, A. *et al.* (2002) 'Holliday junction resolution in human cells: Two junction endonucleases with distinct substrate specificities', *EMBO Journal*, 21(20), pp. 5577–5585.
64. Conway, A. B. *et al.* (2004) 'Crystal structure of a Rad51 filament', *Nature structural & molecular biology*, 11(8), pp. 791–796.
65. Costantino, L. *et al.* (2014) 'Break-Induced Replication Repair of Damaged Forks Induces Genomic Duplications in Human Cells', *Science*, 343(January), pp. 88–91.
66. Cramer-Morales, K. *et al.* (2013) *Personalized synthetic lethality induced by targeting RAD52 in leukemias identified by gene mutation and expression profile*, *Blood,* 122(7), pp. 1293–1304.
67. Crook, T. *et al.* (1998) 'p53 mutation with frequent novel codons but not a mutator phenotype in BRCA1- and BRCA2-associated breast tumours', *Oncogene*, (17), pp. 1681–1689.
68. D'Andrea (2010) 'The Fanconi Anemia and Breast Cancer Suceptibility Pathway', *Nature*, 362(20), pp. 1909–1919.
69. Dalgaard, J. Z. (2012) 'Causes and consequences of ribonucleotide incorporation into nuclear DNA', *Trends in Genetics*, 28(12), pp. 592–597.
70. Daniels, M. J. (2004) 'Abnormal Cytokinesis in Cells Deficient in the Breast Cancer Susceptibility Protein BRCA2', *Science*, 306(5697), pp. 876–879.
71. Das, J. *et al.* (2006) 'Non-Canonical Base Pairs and Higher Order Structures in Nucleic Acids: Crystal Structure Database Analysis', *Journal of Biomolecular Structure and Dynamics*, 24(2), pp. 149–161.
72. Davies, A. A. *et al.* (2001) 'Role of BRCA2 in Control of the RAD51 Recombination and DNA Repair Protein', *Mol Cell*, 7, pp. 273–282.
73. Davies, O. R. and Pellegrini, L. (2007) 'Interaction with the BRCA2 C terminus protects RAD51-DNA filaments from disassembly by BRC repeats.', *Nature structural & molecular biology*, 14(6), pp. 475–83.

74. Davies, S. L., North, P. S. and Hickson, I. D. (2007) 'Role for BLM in replication-fork restart and suppression of origin firing after replicative stress', *Nature Structural and Molecular Biology*, 14(7), pp. 677–679.
75. Dexheimer, T. S. (2013) 'DNA Repair Pathways and Mechanisms', *DNA repair of cancer stem cells*, pp. 19–32.
76. Dillard, R. S. *et al.* (2018) 'Biological Applications at the Cutting Edge of Cryo-Electron Microscopy', *Microscopy and microanalysis*, 24(4), pp. 406–419.
77. Dobzhansky, T. (1946) 'Genetics of Natural Populations. Xiii. Recombination and Variability in Populations of Drosophila Pseudoobscura.', *Genetics*, 31(May), pp. 269–290.
78. Donnianni, R. A. and Symington, L. S. (2013) 'Break-induced replication occurs by conservative DNA synthesis', *Proceedings of the National Academy of Sciences*, 110(33), pp. 13475–13480.
79. Doucet-Chabeaud, G. *et al.* (2001) 'Ionising radiation induces the expression of PARP-1 and PARP-2 genes in Arabidopsis', *Molecular Genetics and Genomics*, 265(6), pp. 954–963.
80. Drake, J. W. *et al.* (1998) 'Rates of spontaneous mutation', *Genetics*, 148(4), pp. 1667–1686.
81. Dungrawala, H. *et al.* (2017) 'RADX Promotes Genome Stability and Modulates Chemosensitivity by Regulating RAD51 at Replication Forks', *Molecular Cell*, 67(3), pp. 374-386.
82. Van Dyck, E. *et al.* (1999) 'Binding of double-strand breaks in DNA by human Rad52 protein', *Nature*, 398(6729), pp. 728–731.
83. Dziadkowiec, K. N. *et al.* (2016) 'PARP inhibitors: review of mechanisms of action and BRCA1/2 mutation targeting', *Menopausal Review*, 4(4), pp. 215–219.
84. Easton, D. F., Ford, D. and Bishop, D. T. (1995) 'Breast and ovarian cancer incidence in BRCA1-mutation carriers. Breast Cancer Linkage Consortium.', *American journal of human genetics*, 56, pp. 265–271.
85. Eggler, A. L., Inman, R. B. and Cox, M. M. (2002) 'The Rad51-dependent pairing of long DNA substrates is stabilized by replication protein A', *Journal of Biological Chemistry*, 277(42), pp. 39280–39288.
86. Esashi, F. *et al.* (2005) 'CDK-dependent phosphorylation of BRCA2 as a regulatory mechanism for recombinational repair.', *Nature*, 434(March), pp. 598–604.
87. Esashi, F. *et al.* (2007) 'Stabilization of RAD51 nucleoprotein filaments by the C-terminal region of BRCA2.', *Nature structural & molecular biology*, 14(6), pp. 468–474.
88. Falck, J. *et al.* (2012) 'CDK targeting of NBS1 promotes DNA-end resection, replication restart and homologous recombination', *EMBO reports*, 13(6), pp. 561–568.
89. Farmer, H. *et al.* (2005) 'Targeting the DNA repair defect in BRCA mutant cells as a therapeutic strategy', *Nature*, 434(7035), pp. 917–921.
90. Feng, W. and Jasin, M. (2017) 'BRCA2 suppresses replication stress-induced mitotic and G1 abnormalities through homologous recombination', *Nature Communications*, 8(525), pp. 1–15.
91. Feng, Z. *et al.* (2011) 'Rad52 inactivation is synthetically lethal with BRCA2 deficiency.', *Proceedings of the National Academy of Sciences of the United States of America*, 108(2),

pp. 686–691.
92. Fernandez-Leiro, R. and Scheres, S. H. (2016) 'Unravelling the structures of biological macromolecules by cryo-EM', *Nature*, 537(7620), pp. 339–346.
93. Ford, D. *et al.* (1998) 'Genetic Heterogeneity and Penetrance Analysis of the BRCA1 and BRCA2 Genes in Breast Cancer Families', *The American Journal of Human Genetics*, 62(3), pp. 676–689.
94. Forment, J. V. and O'Connor, M. J. (2018) 'Targeting the replication stress response in cancer', *Pharmacology and Therapeutics*, 188, pp. 155–167.
95. Forrester, H. B. *et al.* (2012) 'DNA Repair Genes: Alternative Transcription and Gene Expression at the Exon Level in Response to the DNA Damaging Agent, Ionizing Radiation', *PLoS ONE*, 7(12), pp. 1–13.
96. Fragkos, M. *et al.* (2015) 'DNA replication origin activation in space and time', *Nature Reviews Molecular Cell Biology*, 16(6), pp. 360–374.
97. Franklin, R. E. and Gosling, R. G. (1953a) 'Evidence for 2-Chain Helix in Crystalline Structure of Sodium Deoxyribonucleate', *Nature*, 172, pp. 156–157.
98. Franklin, R. E. and Gosling, R. G. (1953b) 'The structure of sodium thymonucleate fibres. I. The influence of water content', *Acta Crystallographica*. International Union of Crystallography, 6(8), pp. 673–677.
99. Friedberg, E. C. (2003) 'DNA damage and Repair', *Nature*, 421(January), pp. 436–440.
100. Fujimori, A. *et al.* (2001) 'Rad52 partially substitutes for the Rad51 paralog XRCC3 in maintaining chromosomal integrity in vertebrate cells', *EMBO Journal*, 20(19), pp. 5513–5520.
101. Galkin, V. E. *et al.* (2005) 'BRCA2 BRC motifs bind RAD51 – DNA filaments', *PNAS*, 102(24), pp. 8537–8542.
102. Galkin, V. E. *et al.* (2006) 'The Rad51 / RadA N-Terminal Domain Activates Nucleoprotein Filament ATPase Activity', *Structure*, 14, pp. 983–992.
103. Game, J. C. and Mortimer, R. K. (1974) 'A genetic study of X-ray sensitive mutants in yeast', *Mutation Research - Fundamental and Molecular Mechanisms of Mutagenesis*, 24(3), pp. 281–292.
104. Gasco, M., Shami, S. and Crook, T. (2002) 'The p53 pathway in breast cancer.', *Breast cancer research : BCR*, 4(2), pp. 70–76.
105. Gayther, S. A. *et al.* (1997) 'Variation in risks of breast and ovarian cancer associated with different germline mutations of the BRCA2 gene', *Nature Genetics*, 15, pp. 103–105.
106. Goldgar DE1, Easton DF, Deffenbaugh AM, Monteiro AN, Tavtigian SV, C. F. B. C. I. C. (BIC) S. C. (2004) 'Integrated evaluation of DNA sequence variants of unknown clinical significance: application to BRCA1 and BRCA2.', *American journal of human genetics*, 75(4), pp. 535–544.
107. Gorgoulis, V. *et al.* (2005) 'Activation of the DNA damage checkpoint and genomic instability in human precancerous lesions', *Nature*, pp. 907–913.
108. Grimme, J. M. *et al.* (2010) 'Human Rad52 binds and wraps single-stranded DNA and mediates annealing via two hRad52-ssDNA complexes', *Nucleic Acids Research*, 38(9), pp. 2917–2930.
109. Haas, K. T. *et al.* (2018) 'Suppl: Single-molecule localization microscopy reveals

molecular transactions during RAD51 filament assembly at cellular DNA damage sites', *Nucleic Acids Research*. Oxford University Press, 46(5), pp. 2398–2416.
110. Hahn, S. a *et al.* (2003) 'BRCA2 germline mutations in familial pancreatic carcinoma.', *Journal of the National Cancer Institute*, 95(3), pp. 214–221.
111. Halazonetis, T. D., Gorgoulis, V. G. and Bartek, J. (2008) 'An Oncogene-Induced DNA Damage Model for Cancer Development', *Science*, 319(5868), pp. 1352–1355.
112. Hanada, K. *et al.* (2007) 'The structure-specific endonuclease Mus81 contributes to replication restart by generating double-strand DNA breaks', *Nature Structural and Molecular Biology*, 14(11), pp. 1096–1104.
113. Hanahan, D. and Weinberg, R. A. (2011) 'Hallmarks of Cancer: The Next Generation', *Cell*, 144(5), pp. 646–674.
114. Hartwell, L. H. (1997) 'Integrating Genetic Approaches into the Discovery of Anticancer Drugs', *Science*, 278(5340), pp. 1064–1068.
115. Hashimoto, Y. *et al.* (2010) 'Rad51 protects nascent DNA from Mre11-dependent degradation and promotes continuous DNA synthesis', *Nature Structural and Molecular Biology*, 17(11), pp. 1305–1311.
116. Hashimoto, Y., Puddu, F. and Costanzo, V. (2012) 'RAD51-and MRE11-dependent reassembly of uncoupled CMG helicase complex at collapsed replication forks', *Nature Structural and Molecular Biology*, 19(1), pp. 17–25.
117. Hatanaka, A. *et al.* (2005) 'Similar effects of Brca2 truncation and Rad51 paralog deficiency on immunoglobulin V gene diversification in DT40 cells support an early role for Rad51 paralogs in homologous recombination.', *Molecular and cellular biology*, 25(3), pp. 1124–1134.
118. Hattori, H. *et al.* (2011) 'Context Dependence of Checkpoint Kinase 1 as a Therapeutic Target for Pancreatic Cancers Deficient in the BRCA2 Tumor Suppressor', *Molecular Cancer Therapeutics*, 10(4), pp. 670–678.
119. He, G., Kwok, C. K. and Lam, S. L. (2011) 'Preferential base pairing modes of T·T mismatches', *FEBS Letters*. Federation of European Biochemical Societies, 585(24), pp. 3953–3958.
120. Heijden, T. Van Der *et al.* (2007) 'Real-time assembly and disassembly of human RAD51 filaments on individual DNA molecules', *Nucleic Acids Research*, 35(17), pp. 5646–5657.
121. Hellevik, T. and Martinez-Zubiaurre, I. (2014) 'Radiotherapy and the tumor stroma: The importance of dose and fractionation', *Frontiers in Oncology*, 4, pp. 1–12.
122. Hendrickson, E. A. (1997) 'Cell-Cycle Regulation of Mammalian DNA Double-Strand-Break Repair', *American journal of human genetics*, 61, pp. 795–800.
123. Hengel, S. R. *et al.* (2016) 'Small-molecule inhibitors identify the RAD52-ssDNA interaction as critical for recovery from replication stress and for survival of BRCA2 deficient cells', *eLife*, 5, pp. 1–30.
124. Hengel, S. R., Spies, M. A. and Spies, M. (2017) 'Small-Molecule Inhibitors Targeting DNA Repair and DNA Repair Deficiency in Research and Cancer Therapy', *Cell Chemical Biology*, 24(9), pp. 1101–1119.
125. Her, J. and Bunting, S. F. (2018) 'How cells ensure correct repair of DNA double-strand breaks', *Journal of Biological Chemistry*, 293(27), pp. 10502–10511.
126. Herzik, M. A., Wu, M. and Lander, G. C. (2019) 'High-resolution structure determination

of sub-100 kDa complexes using conventional cryo-EM', *Nature Communications*, 10(1), pp. 1–9.
127. Heyer, W.-D., Ehmsen, K. T. and Liu, J. (2010) 'Regulation of Homologous Recombination in Eukaryotes', *Annual Review of Genetics*, 44(1), pp. 113–139.
128. Higgins, N. P., Kato, K. and Strauss, B. (1976) 'A model for replication repair in mammalian cells', *Journal of Molecular Biology*, 101(3), pp. 417–425.
129. Higgs, M. R. *et al.* (2015) 'BOD1L Is Required to Suppress Deleterious Resection of Stressed Replication Forks', *Molecular Cell*, 59(3), pp. 462–477.
130. Hilario, J. *et al.* (2009) 'Direct imaging of human Rad51 nucleoprotein dynamics on individual DNA molecules', *PNAS*, 106(2), pp. 361–368.
131. Himmels, S. F. and Sartori, A. A. (2016) 'Controlling DNA-end resection: An emerging task for ubiquitin and SUMO', *Frontiers in Genetics*, 7(AUG), pp. 1–7.
132. Hoeijmakers, J. H. J. (2001) 'Genome maintenance mechanisms for preventing cancer', *DNA Repair*, 411, pp. 366–374.
133. Hoffman, E. A. *et al.* (2015) 'Break-seq reveals hydroxyurea-induced chromosome fragility as a result of unscheduled conflict between DNA replication and transcription', *Genome Research*, 25(3), pp. 402–412.
134. Howlett, N. G. *et al.* (2002) 'Biallelic inactivation of BRCA2 in Fanconi anemia.', *Science (New York, N.Y.)*, 297(5581), pp. 606–609.
135. Hromas, R. *et al.* (2017) 'The endonuclease EEPD1 mediates synthetic lethality in RAD52-depleted BRCA1 mutant breast cancer cells', *Breast Cancer Research*. Breast Cancer Research, 19(1), pp. 1–14.
136. Huang, F. *et al.* (2016) 'Targeting BRCA1- and BRCA2-deficient cells with RAD52 small molecule inhibitors', *Nucleic Acids Research*, 44(9), pp. 4189–99.
137. Infante, M. *et al.* (2013) 'The highly prevalent BRCA2 mutation c.2808_2811del (3036delACAA) is located in a mutational hotspot and has multiple origins', *Carcinogenesis*, 34(11), pp. 2505–2511.
138. Ira, G. and Haber, J. E. (2002) 'Characterization of RAD51-Independent Break-Induced Replication That Acts Preferentially with Short Homologous Sequences', *Molecular and cellular biology*, 22(18), pp. 6384–6392.
139. Jackson, D. *et al.* (2002) 'Analysis of the human replication protein A:Rad52 complex: Evidence for crosstalk between RPA32, RPA70, Rad52 and DNA', *Journal of Molecular Biology*, 321(1), pp. 133–148.
140. Jackson, S. P. and Bartek, J. (2010) 'The DNA-damage response in human biology and disease', *Nature*, 461(7267), pp. 1071–1078.
141. Jensen, R B, Carreira, A. and Kowalczykowski, S. C. (2010) 'Purified human BRCA2 stimulates RAD51-mediated recombination.', *Nature*, 467(7316), pp. 678–683.
142. Jewell, R. *et al.* (2011) 'Patterns of expression of DNA repair genes and relapse from melanoma', *Clinical Cancer Research*, 16(March 2009), pp. 5211–5221.
143. Jeyasekharan, A. D. *et al.* (2013) 'A cancer-associated BRCA2 mutation reveals masked nuclear export signals controlling localization', *Nat Struct Mol Biol.*, 20(10), pp. 1191–1198.
144. Jonkers, J. *et al.* (2001) 'Synergistic tumor suppressor activity of BRCA2 and p53 in a conditional mouse model for breast cancer', *Nature Genetics*, 29(4), pp. 418–425.

145. Kagawa, W. *et al.* (2001) 'Homologous Pairing Promoted by the Human Rad52 Protein', *Journal of Biological Chemistry*, 276(37), pp. 35201–35208.
146. Kagawa, W. *et al.* (2002) 'Crystal structure of the homologous-pairing domain from the human Rad52 recombinase in the undecameric form', *Molecular Cell*, 10(2), pp. 359–371.
147. Kagawa, W. *et al.* (2008) 'Identification of a second DNA binding site in the human Rad52 protein', *Journal of Biological Chemistry*, 283(35), pp. 24264–24273.
148. Kagawa, W. *et al.* (2014) 'Functional analyses of the C-terminal half of the Saccharomyces cerevisiae Rad52 protein', *Nucleic Acids Research*, 42(2), pp. 941–951.
149. Kan, Y., Batada, N. N. and Hendrickson, E. A. (2017) 'Human somatic cells deficient for RAD52 are impaired for viral integration and compromised for most aspects of homology-directed repair', *DNA Repair*, 55(April), pp. 64–75.
150. Kang, S. *et al.* (2018) 'Eukaryotic DNA replication : Orchestrated action of multi-subunit protein complexes', *Mutat Res Fund Mol Mech Mutagen,* 809(March 2017), pp. 58–69.
151. Khade, N. V. and Sugiyama, T. (2016) 'Roles of C-Terminal Region of Yeast and Human Rad52 in Rad51-Nucleoprotein Filament Formation and ssDNA Annealing', *Plos One*, 11(6), pp. 1–14.
152. Khow, O. and Suntrarachun, S. (2012) 'Strategies for production of active eukaryotic proteins in bacterial expression system', *Asian Pacific Journal of Tropical Biomedicine*, 2(2), pp. 159–162.
153. Kim, T. M. *et al.* (2014) 'Deletion of BRCA2 exon 27 causes defects in response to both stalled and collapsed replication forks', *Mutation Research - Fundamental and Molecular Mechanisms of Mutagenesis*, 766–767, pp. 66–72.
154. Kitao, H. and Yuan, Z. M. (2002) 'Regulation of ionizing radiation-induced Rad52 nuclear foci formation by c-Abl-mediated phosphorylation', *Journal of Biological Chemistry*, 277(50), pp. 48944–48948.
155. Kojic, M. *et al.* (2012) 'Mutational analysis of Brh2 reveals requirements for compensating mediator functions', *Mol Microbiol.*, 79(1), pp. 180–191.
156. Kojic, M., Milisavljevic, M. and Holloman, W. K. (2018) 'Collaboration in the actions of Brh2 with resolving functions during DNA repair and replication stress in Ustilago maydis', *DNA Repair*, 63(October 2017), pp. 47–55.
157. Kolinjivadi, A. M. *et al.* (2017) 'Smarcal1-Mediated Fork Reversal Triggers Mre11-Dependent Degradation of Nascent DNA in the Absence of Brca2 and Stable Rad51 Nucleofilaments', *Molecular Cell*, 67(5), pp. 867-881.
158. Kouchakdjian, M. *et al.* (1988) 'Pyrimidine · pyrimidine base-pair mismatches in DNA', *Journal of Molecular Biology*, 202(1), pp. 139–155.
159. Krejci, L. *et al.* (2002) 'Interaction with Rad51 Is Indispensable for Recombination Mediator Function of Rad52', *Journal of Biological Chemistry*, 277(42), pp. 40132–40141.
160. Krejci, L. *et al.* (2012) 'Homologous recombination and its regulation', *Nucleic Acids Research*, 40(13), pp. 5795–5818.
161. Kumar, J. K. and Gupta, R. C. (2004) 'Strand exchange activity of human recombination protein Rad52', *Proceedings of the National Academy of Sciences*, 101(26), pp. 9562–9567.

162. Lavery, P. E. and Kowalczykowski, S. C. (1992) 'A postsynaptic role for single-stranded DNA-binding protein in recA protein-promoted DNA strand exchange', *Journal of Biological Chemistry*, 267(13), pp. 9315–9320.
163. Lavin, M. F. *et al.* (2015) 'ATM-dependent phosphorylation of all three members of the MRN complex: From sensor to adaptor', *Biomolecules*, 5(4), pp. 2877–2902.
164. Lee, H. *et al.* (1999) 'Mitotic checkpoint inactivation fosters transformation in cells lacking the breast cancer susceptibility gene, Brca2', *Molecular Cell*, 4(1), pp. 1–10.
165. Lee, M. *et al.* (2011) 'A mitotic function for the high-mobility group protein HMG20b regulated by its interaction with the BRC repeats of the BRCA2 tumor suppressor', *Oncogene*, 30(30), pp. 3360–3369.
166. Lehmann, A. R. (2005) 'Replication of damaged DNA by translesion synthesis in human cells', *FEBS Letters*, 579, pp. 873–876.
167. Lemaçon, D. *et al.* (2017) 'MRE11 and EXO1 nucleases degrade reversed forks and elicit MUS81-dependent fork rescue in BRCA2-deficient cells', *Nature Communications*, 8(1), pp. 1–12.
168. Levy-Lahad, E. *et al.* (1997) 'Founder BRCA1 and BRCA2 mutations in Ashkenazi Jews in Israel: frequency and differential penetrance in ovarian cancer and in breast-ovarian cancer families', *American Journal of Human Genetics*, 60(5), pp. 1059–1067.
169. Liao, H. *et al.* (2018) 'Mechanisms for stalled replication fork stabilization: new targets for synthetic lethality strategies in cancer treatments', *EMBO reports*, 19, pp. 1–18.
170. Lieberman, R. *et al.* (2017) 'Rad52 deficiency decreases development of lung squamous cell carcinomas by enhancing immuno-surveillance', *Oncotarget*, 8(21), pp. 34032–34044.
171. Lindahl, T. (1993) 'Instability and decay of the primary structure of DNA', *Nature*, 362, pp. 709–715.
172. Liu, J. *et al.* (2010) 'Human BRCA2 protein promotes RAD51 filament formation on RPA-covered single-stranded DNA', *Nature Structural & Molecular Biology*, 17(10), pp. 1260–1262.
173. Liu, J. *et al.* (2011) 'Presynaptic filament dynamics in homologous recombination and DNA repair.', *Critical reviews in biochemistry and molecular biology*, 46(3), pp. 240–70.
174. Liu, J. and Heyer, W.-D. (2011) 'Who's who in human recombination: BRCA2 and RAD52', *Proceedings of the National Academy of Sciences*, 108(2), pp. 441–442.
175. Liu, T. and Huang, J. (2016) 'DNA End Resection: Facts and Mechanisms', *Genomics, Proteomics and Bioinformatics*. Beijing Institute of Genomics, Chinese Academy of Sciences and Genetics Society of China, 14(3), pp. 126–130.
176. Liu, Y. and Maizels, N. (2000) 'Coordinated response of mammalian Rad51 and Rad52 to DNA damage.', *EMBO reports*, 1(1), pp. 85–90.
177. Lok, B. H. *et al.* (2013) 'RAD52 inactivation is synthetically lethal with deficiencies in BRCA1 and PALB2 in addition to BRCA2 through RAD51-mediated homologous recombination.', *Oncogene*, 32(30), pp. 3552–8.
178. Lomonosov, M. *et al.* (2003) 'Stabilization of stalled DNA replication forks by the BRCA2 breast cancer susceptibility protein', *Gene therapy*, 17, pp. 3017–3022.
179. Ludwig, T., Chapman, D. L. and Papaioannou, V. E. (1997) 'Targeted mutations of breast cancer susceptibility gene homologs in mice : lethal phenotypes of Brca1, Brca2,

Brca1/Brca2, Brca1/p53, and Brca2/p53 nullizygous embryos', *Genes & Development*, pp. 1226–1241.
180. Lukas, C. *et al.* (2005) 'DNA damage response as a candidate anti-cancer barrier in early human tumorigenesis', *Nature*, 434(7035), pp. 864–70.
181. Lukas, C. *et al.* (2011) '53BP1 nuclear bodies form around DNA lesions generated by mitotic transmission of chromosomes under replication stress', *Nature Cell Biology*, 13(3), pp. 243–253.
182. Luo, J., Solimini, N. L. and Elledge, S. J. (2009) 'Principles of Cancer Therapy: Oncogene and Non-oncogene Addiction', *Cell*, 136(5), pp. 823–837.
183. Lyumkis, D. (2019) 'Challenges and Opportunities in Cryo-EM Single-Particle Analysis', *JBC*, 294, pp. 5181–5197.
184. Ma, C. J. *et al.* (2017) 'Human RAD52 interactions with Replication Protein A and the RAD51 presynaptic complex', *Journal of Biological Chemistry*, 292(28), pp. 11702–11713.
185. Malacaria, E. *et al.* (2019) 'Rad52 prevents excessive replication fork reversal and protects from nascent strand degradation', *Nature Communications*, 10(1), pp. 1–19.
186. Malkova, A. *et al.* (2005) 'RAD51 -Dependent Break-Induced Replication Differs in Kinetics and Checkpoint Responses from RAD51 -Mediated Gene Conversion', *Molecular and cellular biology*, 25(3), pp. 933–944.
187. Malkova, A., Ivanov, E. L. and Haber, J. E. (1996) 'Double-strand break repair in the absence of RAD51 in yeast: a possible role for break-induced DNA replication.', *Proceedings of the National Academy of Sciences*, 93(14), pp. 7131–7136.
188. Marians, K. J., Pasero, P. and Yeeles, J. T. P. (2013) 'Rescuing Stalled or Damaged Replication Forks', *Cold Spring Harbor perspectives in biology*, 5(5), pp. 1–16.
189. Marston, N. J. *et al.* (1999) 'Interaction between the product of the breast cancer susceptibility gene BRCA2 and DSS1, a protein functionally conserved from yeast to mammals.', *Molecular and cellular biology*, 19(7), pp. 4633–4642.
190. Martin, C. *et al.* (2016) 'A second DNA binding site in human BRCA2 promotes homologous recombination', *Nature Cell Biology*, 7, pp. 1–8.
191. Mateos-Gomez, P. A. *et al.* (2015) 'Mammalian polymerase θ promotes alternative NHEJ and suppresses recombination', *Nature*, 518(7538), pp. 254–257.
192. Maxwell, K. N. *et al.* (2017) 'BRCA locus-specific loss of heterozygosity in germline BRCA1 and BRCA2 carriers', *Nature Communications*, 8(1), pp. 1–11.
193. Mazina, O. M. *et al.* (2017) 'Rad52 Inverse Strand Exchange Drives RNA- Article Rad52 Inverse Strand Exchange Drives RNA-Templated DNA Double-Strand Break Repair', *Molecular Cell*, 67(1), pp. 19-29.
194. Mcilwraith, M. J. *et al.* (2000) 'Reconstitution of the Strand Invasion Step of Double-strand Break Repair using Human Rad51 Rad52 and RPA Proteins', *JMB*, 304, pp. 151–164.
195. McIlwraith, M. J. and West, S. C. (2008) 'DNA Repair Synthesis Facilitates RAD52-Mediated Second-End Capture during DSB Repair', *Molecular Cell*, 29(4), pp. 510–516.
196. McVey, M. *et al.* (2016) 'Eukaryotic DNA Polymerases in Homologous Recombination', *Annual Review of Genetics*, 50(1), pp. 393–421.
197. Ménissier de Murcia, J. *et al.* (2003) 'Functional interaction between PARP-1 and PARP-

2 in chromosome stability and embryonic development in mouse', *EMBO Journal*, 22(9), pp. 2255–2263.
198. Menzel, T. *et al.* (2011) 'A genetic screen identifies BRCA2 and PALB2 as key regulators of G2 checkpoint maintenance.', *EMBO reports*, 12(7), pp. 705–12.
199. Mersch, J. *et al.* (2015) 'Cancers associated with BRCA1 and BRCA2 mutations other than breast and ovarian', *Cancer*, 121(2), pp. 269–275.
200. Merzlyak, E. M. *et al.* (2007) 'Bright monomeric red fluorescent protein with an extended fluorescence lifetime', *Nature Methods*, 4(7), pp. 555–557.
201. Mijic, S. *et al.* (2017) 'Replication fork reversal triggers fork degradation in BRCA2-defective cells', *Nature Communications*, 8(1), pp. 1–11.
202. Miki, Y. *et al.* (1994) 'A Strong Candidate for the Breast and Ovarian Cancer Susceptibility Gene BRCA1', *Science*, 266, pp. 5–11.
203. Mimitou PE, S. L. (2010) 'DNA and resection: many nucleases make light work', *DNA Repair*, 8(9), pp. 983–995.
204. Minocherhomji, S. *et al.* (2015) 'Replication stress activates DNA repair synthesis in mitosis', *Nature*, 528, pp. 286–290.
205. Miyazaki, T. *et al.* (2004) 'In vivo assembly and disassembly of Rad51 and Rad52 complexes during double-strand break repair.', *The EMBO journal*, 23(4), pp. 939–949.
206. Mizuta, R. *et al.* (1997) 'RAB22 and RAB163 / mouse BRCA2 : Proteins that specifically interact with the RAD51 protein', *Proc Natl Acad Sci U S A*, 94(June), pp. 6927–6932.
207. Mladenov, E. and Iliakis, G. (2011) 'The Pathways of Double-Strand Break Repair', *DNA Repair - On the Pathways to Fixing DNA Damage and Errors.' IntechOpen.*
208. Mondal, G. *et al.* (2012) 'BRCA2 Localization to the Midbody by Filamin A Regulates CEP55 Signaling and Completion of Cytokinesis', *Developmental Cell*, 23(1), pp. 137–152.
209. Mortensen, U. H. *et al.* (1996) 'DNA strand annealing is promoted by the yeast Rad52 protein.', *Proceedings of the National Academy of Sciences of the United States of America*, 93(October), pp. 10729–10734.
210. Moynahan, M. E., Pierce, A. J. and Jasin, M. (2001) 'BRCA2 is required for homology-directed repair of chromosomal breaks', *Molecular Cell*, 7(2), pp. 263–272.
211. Mueller, A. C., Keaton, M. A. and Dutta, A. (2011) 'DNA replication: Mammalian treslin-topBP1 interaction mirrors yeast Sld3-Dpb11', *Current Biology*, 21(16), pp. R638–R640.
212. Muñoz, I. M. *et al.* (2009) 'Coordination of Structure-Specific Nucleases by Human SLX4/BTBD12 Is Required for DNA Repair', *Molecular Cell*, 35(1), pp. 116–127.
213. Murai, J. *et al.* (2012) 'Differential trapping of PARP1 and PARP2 by clinical PARP inhibitors', *Cancer Res*, 72(21), pp. 5588–5599.
214. Murai, J. *et al.* (2014) 'Stereospecific PARP trapping by BMN 673 and comparison with olaparib and rucaparib', *Molecular Cancer Therapeutics*, 13(2), pp. 433–443.
215. de Murcia, G. *et al.* (1983) 'Poly(ADP-ribose) polymerase auto-modification and interaction with DNA: electron microscopic visualization.', *The EMBO Journal*, 2(4), pp. 543–548.
216. De Murcia, J. M. *et al.* (1997) 'Requirement of poly(ADP-ribose) polymerase in recovery from DNA damage in mice and in cells', *Proceedings of the National Academy of Sciences of the United States of America*, 94(14), pp. 7303–7307.
217. Murfuni, I. *et al.* (2013) 'Survival of the Replication Checkpoint Deficient Cells Requires

MUS81-RAD52 Function', *PLoS Genetics*, 9(10).
218. Muris, D. F. R. *et al.* (1994) 'Cloning of human and mouse genes homologous to RAD52, a yeast gene involved in DNA repair and recombination', *Mutation Research-DNA Repair*, 315(3), pp. 295–305.
219. Nahidiazar, L. *et al.* (2016) 'Optimizing imaging conditions for demanding multi-color super resolution localization microscopy', *PLoS ONE*, 11(7), pp. 1–18.
220. Namsaraev, E. A. and Berg, P. (1998) 'Binding of Rad51p to DNA', *Biological Chemistry*, 273(11), pp. 6177–6182.
221. Neelsen, K. J. *et al.* (2013) 'Oncogenes induce genotoxic stress by mitotic processing of unusual replication intermediates', *Journal of Cell Biology*, 200(6), pp. 699–708.
222. Negrini, S., Gorgoulis, V. G. and Halazonetis, T. D. (2010) 'Genomic instability - an evolving hallmark of cancer', *Nature Reviews Molecular Cell Biology*, 11(3), pp. 220–228.
223. Neuhausen, S. *et al.* (1996) 'Recurrent BRCA2 6174delT mutations in Ashkenazi Jewish women affected by breast cancer', *Nature Genetics*, 14(3), pp. 126–128.
224. New, J. H. *et al.* (1998) 'Rad52 protein stimulates DNA strand exchange by Rad51 and replication protein A.', *Nature*, 391(6665), pp. 407–410.
225. New, J. H. and Kowalczykowski, S. C. (2002) 'Rad52 protein has a second stimulatory role in DNA strand exchange that complements replication protein-A function', *Journal of Biological Chemistry*, 277(29), pp. 26171–26176.
226. Nickoloff, J. A. *et al.* (2017) 'Drugging the Cancers Addicted to DNA Repair', *Journal of the National Cancer Institute*, 109(11), pp. 1–13.
227. Nijman, S. M. B. (2011) 'Synthetic lethality: General principles, utility and detection using genetic screens in human cells', *FEBS Letters*. Federation of European Biochemical Societies, 585(1), pp. 1–6.
228. Nik-Zainal, S. *et al.* (2012) 'Mutational processes molding the genomes of 21 breast cancers', *Cell*, 149(5), pp. 979–993.
229. Niraj, J., Färkkilä, A. and D'Andrea, A. D. (2019) 'The Fanconi Anemia Pathway in Cancer', *Annual Review of Cancer Biology*, 3(1), pp. 457–478.
230. Noordermeer, S. M. and van Attikum, H. (2019) 'PARP Inhibitor Resistance: A Tug-of-War in BRCA-Mutated Cells', *Trends in Cell Biology*. The Authors, 29(10), pp. 820–834.
231. O'Driscoll, M. and Jeggo, P. (2002) 'Immunological disorders and DNA repair', *Mutation Research - Fundamental and Molecular Mechanisms of Mutagenesis*, 509(1–2), pp. 109–126.
232. Oddoux C, Struewing JP, Clayton CM, Neuhausen S, Brody LC, Kaback M, Haas B, Norton L, Borgen P, Jhanwar S, Goldgar D, Ostrer H, O. K. (1996) 'The carrier frequency of the BRCA2 6174delT mutation among Ashkenazi Jewish individuals is approximately 1%.', *Nature Genetics*, 14(3), pp. 188–190.
233. Orthwein, A. *et al.* (2015) 'A mechanism for the suppression of homologous recombination in G1 cells', *Nature*. Nature Publishing Group, 528, pp. 422–426.
234. Özer, Ö. *et al.* (2018) 'Human cancer cells utilize mitotic DNA synthesis to resist replication stress at telomeres regardless of their telomere maintenance mechanism', *Oncotarget*, 9(22), pp. 15836–15846.
235. Özer, Ö. and Hickson, I. D. (2018) 'Pathways for maintenance of telomeres and common fragile sites during DNA replication stress', *Open Biology*, 8(4), pp. 1–11.

236. Park, M. S. *et al.* (1996) 'Physical interaction between human RAD52 and RPA is required for homologous recombination in mammalian cells', *Journal of Biological Chemistry*, 271(31), pp. 18996–19000.
237. Parsons, C. A. *et al.* (2000) 'Precise binding of single-stranded DNA termini by human RAD52 protein', *EMBO Journal*, 19(15), pp. 4175–4181.
238. Patel, K. J. *et al.* (1998) 'Involvement of Brca2 in DNA Repair', *Molecular Cell*, 1(3), pp. 347–357.
239. Payen, C. *et al.* (2008) 'Segmental Duplications Arise from Pol32-Dependent Repair of Broken Forks through Two Alternative Replication-Based Mechanisms', *PLoS Genetics*, 4(9), pp. 1–12.
240. Pellegrini, L. *et al.* (2002) 'Insights into DNA recombination from the structure of a RAD51 – BRCA2 complex', *Nature*, 420, pp. 287–293.
241. Peng, G. *et al.* (2012) 'Human nuclease/helicase DNA2 alleviates replication stress by promoting DNA end resection', *Cancer Research*, 72(11), pp. 2802–2813.
242. Petermann, E. *et al.* (2010) 'Hydroxyurea-Stalled Replication Forks Become Progressively Inactivated and Require Two Different RAD51-Mediated Pathways for Restart and Repair', *Molecular Cell*, 37(4), pp. 492–502.
243. Phelan, C. M. *et al.* (1996) 'Mutation analysis of the BRCA2 gene in 49 site specific breast cancer families', *Nat Genet.*, 13, pp. 120–122.
244. Pinder, J., Salsman, J. and Dellaire, G. (2015) 'Nuclear domain " knock-in " screen for the evaluation and identification of small molecule enhancers of CRISPR-based genome editing', *Nucleic Acids Research*, 43(19), pp. 9379–9392.
245. Piwko, W. *et al.* (2016) 'The MMS22L–TONSL heterodimer directly promotes RAD51-dependent recombination upon replication stress', *The EMBO Journal*, 35(23), pp. 2584–2601.
246. Plate, I. *et al.* (2008) 'Interaction with RPA is necessary for Rad52 repair center formation and for its mediator activity.', *The Journal of biological chemistry*, 283(43), pp. 29077–85.
247. Poirier, G. G. *et al.* (1982) 'Poly (ADP-ribosyl)ation of polynucleosomes causes relaxation of chromatin structure', *Proc Natl Acad Sci U S A*, 79(11), pp. 3423–3427.
248. Pommier, Y., Connor, M. J. O. and Bono, J. De (2016) 'Laying a trap to kill cancer cells : PARP inhibitors and their mechanisms of action', *Science translational medicine*, 17(DECEMBER), pp. 1–8.
249. Prakash, L. (1976) 'Effect of genes controlling radiation sensitivity on chemically induced mutations in Saccharomyces cerevisiae', *Genetics*, 83(2), pp. 285–301.
250. Prakash, S. *et al.* (1980) 'Effects of the Rad52 gene on recombination in Saccharomyces cerevisiae', *Genetics*, 94(1), pp. 31–50.
251. Qing, Y. *et al.* (2011) 'The epistatic relationship between BRCA2 and the other RAD51 mediators in homologous recombination', *PLoS Genetics*, 7(7), pp. 1-14.
252. Quinet, A., Lemaçon, D. and Vindigni, A. (2017) 'Replication Fork Reversal: Players and Guardians', *Molecular Cell*, 68(5), pp. 830–833.
253. Raderschall, E., Golub, E. I. and Haaf, T. (1999) 'Nuclear foci of mammalian recombination proteins are located at single-stranded DNA regions formed after DNA damage', *Proceedings of the National Academy of Sciences of the United States of*

America, 96(5), pp. 1921–1926.
254. Rajendra, E. and Venkitaraman, A. R. (2009) 'Two modules in the BRC repeats of BRCA2 mediate structural and functional interactions with the RAD51 recombinase', *Nucleic Acids Research*, 38(1), pp. 82–96.
255. Reddy, G., Golub, E. I. and Radding, C. M. (1997) 'Human Rad52 protein promotes single-strand DNA annealing followed by branch migration', *Mutation Research - Fundamental and Molecular Mechanisms of Mutagenesis*, 377(1), pp. 53–59.
256. Reymer, A. *et al.* (2009) 'Structure of human Rad51 protein filament from molecular modeling and site-specific linear dichroism spectroscopy', *PNAS*, 106(32), pp. 13248–13253.
257. Rhei, E. *et al.* (1998) 'Molecular Genetic Characterization of BRCA1- and BRCA2-Linked Hereditary Ovarian Cancers', *Cancer Research*, 2, pp. 3193–3197.
258. Rijkers, T. *et al.* (1998) 'Targeted inactivation of mouse RAD52 reduces homologous recombination but not resistance to ionizing radiation.', *Molecular and cellular biology*, 18(11), pp. 6423–6429.
259. Risch, H. A. *et al.* (2001) 'Prevalence and Penetrance of Germline BRCA1 and BRCA2 Mutations in a Population Series of 649 Women with Ovarian Cancer', *American journal of human genetics*, 6, pp. 700–710.
260. Rondinelli, B. *et al.* (2017) 'EZH2 promotes degradation of stalled replication forks by recruiting MUS81 through histone H3 trimethylation', *Nature Cell Biology*, 19(11), pp. 1371–1378.
261. Roy, S. *et al.* (2018) 'p53 orchestrates DNA replication restart homeostasis by suppressing mutagenic RAD52 and POLΘ pathways', *eLife*, 7, pp. 1–23.
262. Ruigrok, R. W. H. *et al.* (1993) 'The inactive form of recA protein : the ' compact ' structure', *The EMBO Journal*, 12(1), pp. 9–16.
263. Saleh-Gohari, N. *et al.* (2005) 'Spontaneous Homologous Recombination Is Induced by Collapsed Replication Forks That Are Caused by Endogenous DNA Single-Strand Breaks', *Molecular and cellular biology*, 25(16), pp. 7158–7169.
264. San Filippo, J., Sung, P. and Klein, H. (2008) 'Mechanism of eukaryotic homologous recombination.', *Annual review of biochemistry*, 77, pp. 229–257.
265. Saotome, M. *et al.* (2018) 'Structural Basis of Homology-Directed DNA Repair Mediated by RAD52', *iScience*, 3, pp. 50–62.
266. Schlacher, K. *et al.* (2011) 'Double-strand break repair-independent role for BRCA2 in blocking stalled replication fork degradation by MRE11', *Cell*., 145(4), pp. 529–542.
267. Schlacher, K. (2017) 'PARPi focus the spotlight on replication fork protection in cancer', *Nature Cell Biology*. Nature Publishing Group, 19(11), pp. 1309–1310.
268. Schreiber, V. *et al.* (2002) 'Poly(ADP-ribose) polymerase-2 (PARP-2) is required for efficient base excision DNA repair in association with PARP-1 and XRCC1', *Journal of Biological Chemistry*, 277(25), pp. 23028–23036.
269. Schreiber, V. *et al.* (2006) 'Poly(ADP-ribose): Novel functions for an old molecule', *Nature Reviews Molecular Cell Biology*, 7(7), pp. 517–528.
270. Schubert, L. *et al.* (2017) 'RADX interacts with single-stranded DNA to promote replication fork stability', *EMBO reports*, 18(11), pp. 1991-2003.
271. Schumacher, A. B. W. and B. (2016) 'p53 in the DNA-Damage-Repair Process', *Cold*

Spring Harbor perspectives in biology, 6(5), pp. 1–15.
272. Seong, C. *et al.* (2008) 'Molecular anatomy of the recombination mediator function of Saccharomyces cerevisiae Rad52', *Journal of Biological Chemistry*, 283(18), pp. 12166–12174.
273. Shahid, T. *et al.* (2014) 'Structure and mechanism of action of the BRCA2 breast cancer tumor suppressor', *Nature Structural & Molecular Biology*, 21(11), pp. 962–968.
274. Shamoo, Y. (2003) 'Structural insights into BRCA2 function', *Current Opinion in Structural Biology*, 13(2), pp. 206–211.
275. Sharan S. K *et al.* (1997) 'Embryonic lethality and radiation hypersensitivity mediated by Rad51 in mice lacking Brca2', *Nature*, pp. 804–810.
276. Sharma, S. *et al.* (2015) 'Homology and enzymatic requirements of microhomology-dependent alternative end joining', *Cell death & disease*. Nature Publishing Group, 6(3), pp. 1–12.
277. Shen, Z. *et al.* (1996) 'Specific Interactions between the Human RAD51 and RAD52 Proteins', *The Journal of biological chemistry*, 271(1), pp. 148–152.
278. Shieh, W. M. *et al.* (1998) 'Poly(ADP-ribose) polymerase null mouse cells synthesize ADP-ribose polymers', *Journal of Biological Chemistry*, 273(46), pp. 30069–30072.
279. Shin, D. S. *et al.* (2003) 'Full-length archaeal Rad51 structure and mutants: Mechanisms for RAD51 assembly and control by BRCA2', *EMBO Journal*, 22(17), pp. 4566–4576.
280. Shinohara, a and Ogawa, T. (1998) 'Stimulation by Rad52 of yeast Rad51-mediated recombination.', *Nature*, 391(6665), pp. 404–407.
281. Shinohara A, Ogawa H, Matsuda Y, Ushio N, Ikeo K, O. T. (1993) 'Cloning of human, mouse and fission yeast recombination genes homologous to RAD51 and recA', *Nature Genetics*, 4, pp. 239–243.
282. Shinohara, A. *et al.* (1998) 'Rad52 forms ring structures and co-operates with RPA in single-strand DNA annealing', *Genes to Cells*, 3(3), pp. 145–156.
283. Shinohara, A., Ogawa, H. and Ogawa, T. (1992) 'Rad51 protein involved in repair and recombination in S. cerevisiae is a RecA-like protein', *Cell*, 69(3), pp. 457–470.
284. Shivji, M. K. K. *et al.* (2006) 'A region of human BRCA2 containing multiple BRC repeats promotes RAD51-mediated strand exchange', *Nucleic Acids Research*, 34(14), pp. 4000–4011.
285. Shivji, M. K. K. *et al.* (2009) 'The BRC repeats of human BRCA2 differentially regulate RAD51 binding on single- versus double-stranded DNA to stimulate strand exchange', *Proceedings of the National Academy of Sciences of the United States of America*, 106(32), pp. 13254–9.
286. Shivji, M. K. K. *et al.* (2018) 'BRCA2 Regulates Transcription Elongation by RNA Polymerase II to Prevent R-Loop Accumulation', *Cell Reports*, 22(4), pp. 1031–1039.
287. Short, J. M. *et al.* (2016) 'High-resolution structure of the presynaptic RAD51 filament on single-stranded DNA by electron cryo-microscopy', *Nucleic Acids Research*, 44(19), pp. 9017–9030.
288. Shukla, A. *et al.* (2005) 'Interaction of hRad51 and hRad52 with MCM complex: A cross-talk between recombination and replication proteins', *Biochemical and Biophysical Research Communications*, 329(4), pp. 1240–1245.
289. Siaud, N. *et al.* (2011) 'Plasticity of BRCA2 Function in Homologous Recombination :

Genetic Interactions of the PALB2 and DNA Binding Domains', *PLoS Genetics*, 7(12), pp. 1–12.
290. Sidorova, J. M. *et al.* (2013) 'Distinct functions of human RECQ helicases WRN and BLM in replication fork recovery and progression after hydroxyurea- induced stalling', *DNA repair*, 12(2), pp. 128–139.
291. Sigurdsson, S. *et al.* (2001) 'Basis for Avid Homologous DNA Strand Exchange by Human Rad51 and RPA', *Journal of Biological Chemistry*, 276(12), pp. 8798–8806.
292. Singleton, M. R. *et al.* (2002) 'Structure of the single-strand annealing domain of human RAD52 protein.', *Proceedings of the National Academy of Sciences of the United States of America*, 99(21), pp. 13492–13497.
293. Sirbu, B. M. *et al.* (2011) 'Analysis of protein dynamics at active , stalled , and collapsed replication forks', *Genes & Development*, 25, pp. 1320–1327.
294. Skoulidis, F. *et al.* (2010) 'Germline Brca2 Heterozygosity Promotes in a Murine Model of Familial Pancreatic Cancer', *Cancer Cell*, 18(5), pp. 499–509.
295. Sørensen, C. S. *et al.* (2005) 'The cell-cycle checkpoint kinase Chk1 is required for mammalian homologous recombination repair', *Nature Cell Biology*, 7(2), pp. 195–201.
296. Sotiriou, S. K. *et al.* (2016) 'Mammalian RAD52 Functions in Break-Induced Replication Repair of Collapsed DNA Replication Forks', *Carcinogenesis*, 34(11), pp. 2505–2511.
297. Spain, B. H. *et al.* (1999) 'Truncated BRCA2 is cytoplasmic: implications for cancer-linked mutations.', *Proceedings of the National Academy of Sciences of the United States of America*, 96(24), pp. 13920–13925.
298. Spies, J. *et al.* (2019) '53BP1 nuclear bodies enforce replication timing at under-replicated DNA to limit heritable DNA damage', *Nature Cell Biology*, 21(4), pp. 487–497.
299. Spírek, M. *et al.* (2018) 'Human RAD51 rapidly forms intrinsically dynamic nucleoprotein filaments modulated by nucleotide binding state', *Nucleic Acids Research*, 46(8), pp. 3967–3980.
300. Spriestersbach, A. *et al.* (2015) 'Purification of His-Tagged Proteins', *Methods enzymol.*, 559, pp. 1–15.
301. Stark, J. M. *et al.* (2004) 'Genetic Steps of Mammalian Homologous Repair with Distinct Mutagenic Consequences', *Molecular and cellular biology*, 24(21), pp. 9305–9316.
302. Stasiak, A. Z. *et al.* (2000) 'The human Rad52 protein exists as a heptameric ring', *Current Biology*, 10(6), pp. 337–340.
303. Stillman, B. (2008) 'DNA polymerases at the replication fork in eukaryotes', *Mol Cell*, 30(3), pp. 259–260.
304. Story RM, Weber IT, S. T. (1992) 'The structure of the E. coli recA protein monomer and polymer.', *Nature*, 355(6360), pp. 318–325.
305. Subramanyam, S. *et al.* (2013) 'Contributions of the RAD51 N-terminal domain to BRCA2-RAD51 interaction', *Nucleic Acids Research*, 41(19), pp. 9020–9032.
306. Sugiyama, T. *et al.* (1998) 'DNA annealing by Rad52 Protein is stimulated by specific interaction with the complex of replication protein A and single-stranded DNA', *Proceedings of the National Academy of Sciences*, 95(11), pp. 6049–6054.
307. Sugiyama, T. *et al.* (2006) 'Rad52-mediated DNA annealing after Rad51-mediated DNA strand exchange promotes second ssDNA capture.', *The EMBO journal*, 25(23), pp. 5539–48.

308. Sullivan-Reed, K. *et al.* (2018) 'Simultaneous Targeting of PARP1 and RAD52 Triggers Dual Synthetic Lethality in BRCA-Deficient Tumor Cells', *Cell Reports*, 23(11), pp. 3127–3136.
309. Sullivan, K. *et al.* (2016) 'Identification of a Small Molecule Inhibitor of RAD52 by Structure-Based Selection', *PLoS ONE*, 11(1), pp. 1–11.
310. Summers, K. C. *et al.* (2011) 'Phosphorylation: The Molecular Switch of Double-Strand Break Repair', *International Journal of Proteomics*, 2011, pp. 1–8.
311. Sung, P. (1995) 'DNA Strand Exchange Mediated by a RAD51-ssDNA Nucleoprotein Filament with Polarity Opposite to That of RecA', *Cell*, 82, pp. 453–461.
312. Sung, P. (1997) 'Function of Yeast Rad52 Protein as a Function of Yeast Rad52 Protein as a Mediator between', *The Journal of biological chemistry*, 272, pp. 28194–28197.
313. Szabo, C. I. and King, M.-C. (1997) 'Population genetics of BRCA1 and BRCA2.', *American journal of human genetics*, 60, pp. 1013–1020.
314. T. Leung, K. H., El Hassan, M. A. and Bremner, R. (2013) 'A rapid and efficient method to purify proteins at replication forks under native conditions', *BioTechniques*, 55(4), pp. 204–206.
315. Taglialatela, A. *et al.* (2017) 'Restoration of Replication Fork Stability in BRCA1- and BRCA2-Deficient Cells by Inactivation of SNF2-Family Fork Remodelers', *Molecular Cell*, 68(2), pp. 414-430.
316. Tan, S. L. W. *et al.* (2017) 'A Class of Environmental and Endogenous Toxins Induces BRCA2 Haploinsufficiency and Genome Instability', *Cell*, 169(6), pp. 1105-1118.
317. Tarsounas, M., Davies, D. and West, S. C. (2003) 'BRCA2-dependent and independent formation of RAD51 nuclear foci.', *Oncogene*, 22(8), pp. 1115–1123.
318. Tavtigian, S. V *et al.* (1996) 'The complete BRCA 2 gene and mutations in chromosome 13q-linked kindreds', *Nat Genet.*, 14, pp. 353–6.
319. Teng, Y. *et al.* (2018) 'ROS-induced R loops trigger a transcription-coupled but BRCA1/2-independent homologous recombination pathway through CSB', *Nature Communications*, 9(1), pp. 4115-4126.
320. Thangavel, S. *et al.* (2015) 'DNA2 drives processing and restart of reversed replication forks in human cells', *Journal of Cell Biology*, 208(5), pp. 545–562.
321. Thompson, D. and Easton, D. (2001) 'Variation in cancer risks, by mutation position, in BRCA2 mutation carriers.', *American journal of human genetics*, 68(2), pp. 410–419.
322. Thompson, R. F. *et al.* (2016) 'An introduction to sample preparation and imaging by cryo-electron microscopy for structural biology', *Methods*, 100, pp. 3–15.
323. Thorslund, T. *et al.* (2010) 'The breast cancer tumor suppressor BRCA2 promotes the specific targeting of RAD51 to single-stranded DNA', *Nature structural & molecular biology*, 17(10), pp. 1263–1265.
324. Thorslund, T., Esashi, F. and West, S. C. (2007) 'Interactions between human BRCA2 protein and the meiosis-specific recombinase DMC1', *EMBO Journal*, 26(12), pp. 2915–2922.
325. Tichy, A. *et al.* (2012) 'PHOSPHATIDYLINOSITOL-3-KINASE RELATED KINASES (PIKKS) IN RADIATION-INDUCED DNA DAMAGE', *MMSL*, 81(4), pp. 177–187.
326. Tomasetti, C., Li, L. and Vogelstein, B. (2017) 'Stem cell divisions, somatic mutations, cancer etiology, and cancer prevention', *Science*, 355(March), pp. 1330–1334.

327. Trenz, K. *et al.* (2006) 'ATM and ATR promote Mre11 dependent restart of collapsed replication forks and prevent accumulation of DNA breaks', *EMBO Journal*, 25(8), pp. 1764–1774.
328. Trucco, C. *et al.* (1998) 'DNA repair defect in poly(ADP-ribose) polymerase-deficient cell lines', *Nucleic Acids Research*, 26(11), pp. 2644–2649.
329. Tuskamoto, M. *et al.* (2003) 'The N-terminal DNA-binding domain of RAd52 promotes RAD51-independent recombination in Saccharomyces cerevisiae', *Current genetics*, 42(4), pp. 185–198.
330. Tutt, A. *et al.* (1999) 'Absence of Brca2 causes genome instability by chromosome breakage and loss associated with centrosome amplification', *Current Biology*, 9(19), pp. 1107–1110.
331. Tutt, A. *et al.* (2001) 'Mutation in Brca2 stimulates error-prone homology-directed repair of DNA double-strand breaks occurring between repeated sequences', *EMBO Journal*, 20(17), pp. 4704–4716.
332. Vaughn, J. P. *et al.* (1996) 'Cell Cycle Control of BRCA2', *Cancer Research*, 56, pp. 4590–4594.
333. Van Veelen, L. R. *et al.* (2005) 'Ionizing radiation-induced foci formation of mammalian Rad51 and Rad54 depends on the Rad51 paralogs, but not on Rad52', *Mutation Research - Fundamental and Molecular Mechanisms of Mutagenesis*, 574, pp. 34–49.
334. Venkitaraman, A. R. (2011) 'Does metabolite deficiency mark oncogenic cell cycles?', *Cell*, 145(3), pp. 337–338.
335. Verma, P. *et al.* (2019) 'RAD52 and SLX4 act nonepistatically to ensure telomere stability during alternative telomere lengthening', *Genes and Development*, 33(3–4), pp. 221–235.
336. Vesela, E. *et al.* (2017) 'Common chemical inductors of replication stress: Focus on cell-based studies', *Biomolecules*, 7(1), pp. 1–36.
337. Wang, A. T. *et al.* (2015) 'A Dominant Mutation in Human RAD51 Reveals Its Function in DNA Interstrand Crosslink Repair Independent of Homologous Recombination', *Molecular Cell*, 59(3), pp. 478–490.
338. Wang, M. *et al.* (2006) 'PARP-1 and Ku compete for repair of DNA double strand breaks by distinct NHEJ pathways', *Nucleic Acids Research*, 34(21), pp. 6170–6182.
339. Watson, J. D. and Crick, F. H. C. (1953) 'Molecular structure of nucleic acids - A structure for Deoxyribose Nucleic Acid', *Nature*, 171, pp. 737–738.
340. Welty, S. *et al.* (2018) 'RAD52 is required for RNA-templated recombination repair in post-mitotic neurons', *Journal of Biological Chemistry*, 293(4), pp. 1353–1362.
341. Whelan, D. R. *et al.* (2018) 'Spatiotemporal dynamics of homologous recombination repair at single collapsed replication forks', *Nature Communications*, 9(1), pp. 3882-3896.
342. Wold, M. S. (1997) 'Replication protein A: A Heterotrimeric, Single-Stranded DNA-Binding Protein Required for Eukaryotic DNA Metabolism', *Annual Review of Biochemistry*, 66, pp. 61–92.
343. Wong, A. K. C. *et al.* (1997) 'RAD51 interacts with the evolutionarily conserved BRC motifs in the human breast cancer susceptibility gene brca2', *Journal of Biological Chemistry*, 272(51), pp. 31941–31944.

344. Wooster *et al.* (1994) 'Localization of a Breast Cancer Susceptibility Gene , BRCA2 , to Chromosome 13q1 2-13', *Science (New York, N.Y.)*, 265(September), pp. 2088–2090.
345. Wooster, R. *et al.* (1995) 'Identification of the breast cancer susceptibility gene BRCA2.', *Nature*, 378(6559), pp. 789–92.
346. Wray, J. *et al.* (2008) 'Distinct RAD51 associations with RAD52 and BCCIP in response to DNA damage and replication stress', *Cancer Research*, 68(8), pp. 2699–2707.
347. Wu, K. *et al.* (2005) 'Functional evaluation and cancer risk assessment of BRCA2 unclassified variants', *Cancer Research*, 65(2), pp. 417–426.
348. Wu, Y. *et al.* (2008) 'Rad51 protein controls Rad52-mediated DNA annealing.', *The Journal of biological chemistry*, 283(21), pp. 14883–92.
349. Xia, B. *et al.* (2006) 'Control of BRCA2 Cellular and Clinical Functions by a Nuclear Partner, PALB2', *Molecular Cell*, 22(6), pp. 719–729.
350. Xu, J. *et al.* (2017) 'Cryo-EM structures of human recombinase RAD51 filaments in the catalysis of DNA strand exchange', *Nat Struct Mol Biol.*, 24(1), pp. 40–46.
351. Xu, S. *et al.* (2017) 'Abro1 maintains genome stability and limits replication stress by protecting replication fork stability', *Genes and Development*, 31(14), pp. 1469–1482.
352. Xue, C. and Greene, E. C. (2018) 'New roles for RAD52 in DNA repair', *Cell Research*, 28, pp. 1127–1128.
353. Yamaguchi-iwai, Y. *et al.* (1998) 'Homologous Recombination , but Not DNA Repair, Is Reduced in Vertebrate Cells Deficient in RAD52', *Molecular and cellular biology*, 18(11), pp. 6430–6435.
354. Yang, H. *et al.* (2002) 'BRCA2 function in DNA binding and recombination from a BRCA2-DSS1-ssDNA structure.', *Science (New York, N.Y.)*, 297(5588), pp. 1837–1848.
355. Yang, H. *et al.* (2005) 'The BRCA2 homologue Brh2 nucleates RAD51 filament formation at a dsDNA-ssDNA junction.', *letters to Nature*, 433(7026), pp. 653–657.
356. Yasuhara, T. *et al.* (2018) 'Human Rad52 Promotes XPG-Mediated R-loop Processing to Initiate Transcription-Associated Homologous Recombination Repair', *Cell*, 175(2), pp. 558-570.
357. Ying, S, Hamdy, F. C. and Helleday, T. (2012) 'Mre11-dependent degradation of stalled DNA replication forks is prevented by BRCA2 and PARP1', *Cancer Research*, 72(11), pp. 2814–2821.
358. Yoshihara, K. *et al.* (1981) 'Mode of enzyme-bound poly(ADP-ribose) synthesis and histone modification by reconstituted poly(ADP-ribose) polymerase-DNA-cellulose complex.', *Journal of Biological Chemistry*, 256(7), pp. 3471–3478.
359. Yoshimura, Y. *et al.* (1993) 'Cloning and sequence of the human RecA-like gene cDNA', *Nucleic Acids Research*, 21(7), pp. 1665.
360. Yu, V. P. C. C. *et al.* (2000) 'Gross chromosomal rearrangements and genetic exchange between nonhomologous chromosomes following BRCA2 inactivation', *Genes and Development*, 14(11), pp. 1400–1406.
361. Yu, X. *et al.* (2001) 'Domain structure and dynamics in the helical filaments formed by RecA and Rad51 on DNA', *PNAS*, 98(15), pp. 8419–8424.
362. Yuan, S. S. F. *et al.* (1999) 'BRCA2 is required for ionizing radiation-induced assembly of Rad51 complex in vivo', *Cancer Research*, 59(15), pp. 3547–3551.
363. Yuan, Z. M. *et al.* (1998) 'Regulation of Rad51 function by c-Abl in response to DNA

damage', *Journal of Biological Chemistry*, 273(7), pp. 3799–3802.
364. Zan, H. *et al.* (2017) 'Rad52 competes with Ku70/Ku86 for binding to S-region DSB ends to modulate antibody class-switch DNA recombination', *Nature Communications*, 8(8), pp. 1–16.
365. Zellweger, R. *et al.* (2015) 'Rad51-mediated replication fork reversal is a global response to genotoxic treatments in human cells', *Journal of Cell Biology*, 208(5), pp. 563–579.
366. Zeman, M. K. and Cimprich, K. A. (2014) 'Causes and consequences of replication stress', *Nature Cell Biology*, 16(1), pp. 2–9.
367. van der Zon, N. L., Kanaar, R. and Wyman, C. (2018) 'Variation in RAD51 details a hub of functions: opportunities to advance cancer diagnosis and therapy', *F1000Research*, 7, pp. 1453-1460.